

DOCTORAL THESIS

Estimation and Conversion of Static Load Models of Aggregated Transmission System Loads

Madis Leinakse

TALLINN UNIVERSITY OF TECHNOLOGY
DOCTORAL THESIS
3/2022

Estimation and Conversion of Static Load Models of Aggregated Transmission System Loads

MADIS LEINAKSE



TALLINN UNIVERSITY OF TECHNOLOGY

School of Engineering

Department of Electrical Power Engineering and Mechatronics

This dissertation was accepted for the defence of the degree of Doctor of Philosophy on
31/01/2022

Supervisor: Professor Jako Kilter, Ph.D.
School of Engineering
Tallinn University of Technology
Tallinn, Estonia

Opponents: Saša Ž. Djokić, Ph.D.
School of Engineering
The University of Edinburgh
Edinburgh, Scotland, United Kingdom

Kazi Nazmul Hasan, Ph.D.
Royal Melbourne Institute of Technology (RMIT)
Melbourne, Australia

Defence of the thesis: 07/03/2022, Tallinn

Declaration:

Hereby I declare that this doctoral thesis, my original investigation and achievement, submitted for the doctoral degree at Tallinn University of Technology, has not been submitted for any academic degree elsewhere.

Madis Leinakse

signature

This research was partially funded by Elering AS, through project "LEP15066 Static and dynamic characteristics of loads of Estonian electrical transmission network". Additional support was provided by City of Tallinn (Jaan Poska Scholarship & City Council Scholarship) and TalTech Development Fund (Mati Jostov Scholarship).

Dora Pluss short term mobility grants of European Regional Development Fund were used for presenting research results at five IEEE conferences.

elering
ÜHENDAME ENERGIAD



Tallinn



European Union
European Regional
Development Fund



Investing
in your future

Copyright: Madis Leinakse, 2022

ISSN 2585-6898 (publication)

ISBN 978-9949-83-792-2 (publication)

ISSN 2585-6901 (PDF)

ISBN 978-9949-83-793-9 (PDF)

Printed by Koopia Niini & Rauam

TALLINNA TEHNIKAÜLIKOOL
DOKTORITÖÖ
3/2022

Ülekandevõrgu sõlmekoormuste staatiliste koormusmudelite määramine ja teisendamine

MADIS LEINAKSE



Contents

List of Publications	7
Author's Contributions to the Publications	8
Introduction	9
Abbreviations.....	15
Symbols.....	16
1 Load Modelling	19
1.1 Introduction	19
1.2 Static Load Models	19
1.2.1 Constant Power, Current and Impedance Characteristic of Load	21
1.2.2 Exponential Load Model	21
1.2.3 Second Order Polynomial (ZIP) Load Model	22
1.2.4 Polynomial Load Model	23
1.3 Methods for Load Model Estimation	24
1.3.1 Component-based Load Modelling.....	24
1.3.2 Measurement-based Load Modelling	24
1.3.3 Combined Load Modelling	25
2 Estimation of Static Load Models of Aggregated Transmission System Loads	27
2.1 Introduction	27
2.2 Acquiring Measurement Data	27
2.2.1 Requirements for Measurement Data.....	28
2.2.2 Measurement Systems	29
2.2.3 Choosing Measurement Locations	30
2.3 Pre-processing Measurement Data	34
2.3.1 DFR Data Preparation	35
2.3.2 Detection of Significant Voltage Events	35
2.3.3 Identification of Unsuitable Events	35
2.4 Estimation of Exponential and ZIP Load Models.....	39
2.4.1 Non-Linear Least Squares Estimation of Load Model Parameters ...	39
2.4.2 Impact of Event Filtering on Estimated Load Model Parameter Values	42
2.4.3 Impact of Measurement Time on Estimated Load Model Parameter Values	47
2.4.4 Impact of Distributed Generation on Estimated Load Model Parameter Values	49
2.5 Post-processing of Estimated Load Models	54
2.5.1 Estimation Error	54
2.5.2 Calculating Representative Value from Set of Values	55
2.6 Conclusion and Discussion.....	56
3 Static Load Model Conversion	57
3.1 Introduction	57
3.2 Measures of Conversion Error	58
3.3 Using Non-linear Least Squares Optimisation for Load Model Conversion...	59
3.4 Analytical Methods for Exponential to ZIP Model Conversion	60

3.4.1	Analytical Method AM1	60
3.4.2	Analytical Method AM2	61
3.4.3	Analytical Method AM3	63
3.5	Analytical Method for ZIP to Exponential Model Conversion	66
3.6	Conversion of Estimated Models and Impact on Event Modelling Error	67
3.7	Impact of Conversion Error on Load Flow Results	70
3.7.1	Conversion Error and Load Modelling Error	70
3.7.2	Case Study: Impact of Conversion Error on Load Flow Results	72
3.7.3	Case Study Results: Impact of Exponential to ZIP Load Model Conversion on Load Flow	75
3.7.4	Case Study Results: Impact of ZIP to Exponential Load Model Conversion on Load Flow	76
3.8	Conclusion and Discussion	78
4	Conclusions and Further Work	81
4.1	Conclusions	81
4.2	Further Work	83
	List of Figures	85
	List of Tables	87
	References	88
	Acknowledgements	99
	Abstract	101
	Kokkuvõte	103
	Appendix 1 - Used Measurement Data	105
	Appendix 2 - Included Publications	107
Publication I	107
Publication II	115
Publication III	123
Publication IV	131
Publication V	139
Publication VI	147
Publication VII	167
Publication VIII	175
	Curriculum Vitae	183
	Elulookirjeldus	188

In the case of the digital version of this dissertation, 16 empty pages have been removed to decrease the need for scrolling. Page numbers of the remaining pages have been corrected to match with the page numbers of the printed version.

List of Publications

The list of author's publications, on the basis of which the thesis has been prepared:

- I M. Leinakse and J. Kilter, "Conversion error of exponential to second order polynomial ZIP load model conversion," in *2018 IEEE International Conference on Environment and Electrical Engineering and 2018 IEEE Industrial and Commercial Power Systems Europe (EEEIC / I&CPS Europe)*, Palermo, Italy, Jun. 2018, pp. 1–5, doi: 10.1109/eeeic.2018.8493667
- II M. Leinakse and J. Kilter, "Conversion error of second order polynomial ZIP to exponential load model conversion," in *Mediterranean Conference on Power Generation, Transmission, Distribution and Energy Conversion (MedPower 2018)*, Dubrovnik, Croatia, 2018, doi: 10.1049/cp.2018.1882
- III M. Leinakse, H. Kiristaja, and J. Kilter, "Identification of intra-day variations of static load characteristics based on measurements in high-voltage transmission network," in *2018 IEEE PES Innovative Smart Grid Technologies Conference Europe (ISGT Europe 2018)*, Sarajevo, Bosnia-Herzegovina, 2018, pp. 1–6, doi: 10.1109/ISGTEurope.2018.8571712
- IV M. Leinakse, P. Tani, and J. Kilter, "Impact of distributed generation on estimation of exponential load models," in *2019 IEEE Power & Energy Society General Meeting (PESGM)*, Atlanta, GA, USA, 2019, pp. 1–5, doi: 10.1109/PESGM40551.2019.8974014
- V M. Leinakse and J. Kilter, "Clustering of transmission system loads based on monthly load class energy consumptions," in *2020 21st International Scientific Conference on Electric Power Engineering (EPE)*, Prague, Czech Republic, Oct. 2020, pp. 1–6, doi: 10.1109/epe51172.2020.9269197
- VI M. Leinakse and J. Kilter, "Exponential to ZIP and ZIP to exponential load model conversion: Methods and error," *IET Generation, Transmission & Distribution*, vol. 15, no. 2, pp. 177–193, 2021, doi: 10.1049/gtd2.12002
- VII M. Leinakse and J. Kilter, "Processing and filtering digital fault recorder events for load model estimation," in *2021 IEEE PES Innovative Smart Grid Technologies Europe (ISGT Europe)*, Espoo, Finland, Oct. 2021, pp. 01–05, doi: 10.1109/isgteurope52324.2021.9640026
- VIII M. Leinakse, G. Andreesen, P. Tani, and J. Kilter, "Estimation of exponential and ZIP load model of aggregated load with distributed generation," in *2021 IEEE 62nd International Scientific Conference on Power and Electrical Engineering of Riga Technical University (RTUCON)*, Riga, Latvia, 2021, to be published

Author's Contributions to the Publications

The author of the thesis is the main author of the previously listed publications I - VIII. He delivered presentations to introduce papers I - V, VII and VIII at the corresponding conferences.

- I** The author derived the presented novel load model conversion methods, implemented the methods, planned & conducted the studies, analysed the results, visualized the data, and wrote the paper.
- II** The author implemented the presented load model conversion methods, planned & conducted the studies, analysed the results, and wrote the paper.
- III** The author proposed the presented post-processing method, implemented the method, planned & conducted the case studies, analysed the measurement data, visualized the data, and wrote most of the paper.
- IV** The author implemented the presented data analysis methods, analysed the measurement data, and wrote the paper.
- V** The author implemented the presented methods, processed the data, conducted the studies, analysed the results, visualized the data, and wrote the paper.
- VI** The author developed the presented novel load model conversion methods, implemented the presented methods, planned & conducted the studies, analysed the results, visualized the data, and wrote the paper.
- VII** The author implemented the presented methods, analysed the results, visualized the data, and wrote the paper.
- VIII** The author derived the proposed method, implemented the presented data analysis methods, analysed the measurement data, and wrote most of the paper.

Introduction

The European Union has the goal of becoming climate-neutral by 2050 [1]. Climate-neutrality is defined by net-zero greenhouse gas emissions. The European Commission's vision includes among the main strategic building blocks energy efficiency (including zero emission buildings), maximising the deployment of renewables and the use of electricity, and developing interconnections [2]. One approach applied for improving energy efficiency is to replace less efficient devices with more efficient ones (for example incandescent lights with LED lights). At the same time there is a technological shift towards using electrical vehicles instead of vehicles with internal combustion engines to decrease the CO_2 emissions and dependence on fossil fuels. The load device replacement by more efficient devices and increasing consumption of electrical transport will slowly transform the load composition. A different composition of loads responds differently to changes of system parameters and leads to different power consumption patterns.

The behaviour of power systems is modelled for increasing situational awareness, optimising operation and planning the development of the system. In order to properly model the behaviour, the load models included in the power system model need to reflect the power consumption and behaviour of the loads to a sufficient level of accuracy. In the case of power system models, typically loads are modelled at the power delivery buses of the system. In the case of transmission systems, the power delivery bus is typically a bus in the substation that supplies the distribution network or a large consumer. The load models describe the total power consumption of the loads connected behind the power delivery bus. Sometimes the models also describe the behaviour of the load. The state of the power system is related to the voltages and frequency of the system. For this reason many load models have the ability to describe the voltage and frequency dependence of the load. The voltage characteristic of the load depends similarly to other properties of the load on the load devices (and distributed generation) connected to the grid. In the short run, the composition of connected devices changes due to switching and operation of the load devices. In the long run, newer devices replace older devices (e.g. more variable speed drives used in appliances) or technology shifts take place that affect consumer habits (e.g. increasing amount of electrical vehicles). In addition, the composition of the load devices connected to the grid depends on the weather, structure of the industry and other factors.

The load models of the power system are often determined by applying a combination of different methods. The power demands of the loads are typically obtained by processing the measurement data (from the metering system or SCADA (Supervisory Control And Data Acquisition)), and future values are forecast if needed. The approaches used for determining the demand may take into account weather, time, and other aspects. Additionally, the behaviour of the load needs to be described for more accurate simulations. The load behaviour in the case of disturbances and system state changes depends on the composition of the devices connected to the grid at the time. There are several approaches to estimating the aggregated response of loads connected to a power delivery point. See Chapter 1 for an overview of the approaches. The load responses can be estimated based on measurement data, literature or by a combined application of both. However, as the load composition depends on many factors, the load models estimated for one grid cannot be directly applied to other grids [3]. This claim is supported by the variability of load characteristics estimated in different countries [4–9].

At the same time as changes on the load side, the capacity of renewable generation (both in distributed and centralised generation form) is increasing. As stated above, maximising the deployment of renewables forms a part of the strategic vision of the Euro-

pean Commission. Furthermore, in the European Union this growth is supported by the Energy Performance of Buildings Directive (2010/31/EU) [10]. According to the Energy Performance of Buildings Directive, all new buildings have been required to be nearly zero-energy buildings (NZEB) from the end of 2020. To achieve NZEB requirements, local photovoltaic generation is often used in new buildings. This increases the amount of Distributed Generation (DG) connected to the distribution network and demand variability [11]. The increasing amount of renewable generation poses new challenges for the grid operation [12]. As the controllability of generation is decreasing, there is a high interest in increasing the flexibility of the demand. Among other methods Conservation Voltage Reduction (CVR) has arisen. [13] defines CVR as the "practice of controlling the voltage levels on the network in order to promote peak load relief and energy demand reduction, considering that loads in the MV (Medium Voltage) networks are predominantly voltage dependent". The achievable load reduction of CVR is strongly related to the voltage characteristics of the loads [11, 14] - typically the loads have a positive voltage dependence (decreasing the voltage decreases the load demand). The voltage sensitivity of the feeder is used in [11] to estimate the available resource for CVR. In addition to the voltage characteristics of the loads, the CVR is affected by the active power generation of DG [11, 14–16] along with the reactive power control method of the DG units [13]. CVR implementation aspects are reviewed in [17].

Motivation and Background

The changes in load composition and the increasing penetration of renewable generation have renewed the interest in load modelling. The load composition changes are slowly altering the behaviour of the aggregated loads, which causes the need for renewing the models. At the same time, the increasing penetration of renewable generation is pushing the power systems closer to the limits: most of the transmission and distribution systems were designed for handling a different power flow (from large thermal power plants towards end consumers), and for that reason may not be optimal for the new situation. In order to be able to utilise the existing system as close to the limits as possible, while sustaining safe and reliable operation, accurate modelling of the system is vital. A good example of the renewed interest is the work of the CIGRE (*Conseil International des Grands Réseaux Electriques* - International Council on Large Electric Systems) working group 4.605, which published a comprehensive report [18] in 2014. The report covers different approaches for load model development and practices of the industry.

The increasing amount of renewables and decreasing amount of dispatchable generation has increased the interest in load flexibility. Increased load flexibility is viewed as one source for balancing the intermittent renewable generation. The static load models discussed in this thesis are related to the topic of CVR, which has come to light with an increased need for demand flexibility. The estimation of aggregated transmission system bus load models could provide insight into assessing the CVR potential of the Estonian power system. However, conducting this assessment is not within the scope of this thesis.

Currently the Estonian power system is connected to the IPS/UPS system (Integrated Power System / Unified Power System of Russia). There is a plan for desynchronising the Estonian system from the IPS/UPS system and synchronising it to the synchronous grid of Continental Europe (also known as Continental Synchronous Area) in 2025. In order to prepare for this shift, investments have been made into the grid, and the future operation of the system is analysed from several aspects. To properly model the system, accurate system models are needed. Among other models of the system, the load models were

taken under review by the Estonian transmission system operator Elering AS. A research project was conducted at Tallinn University of Technology in the years 2015-2017, where the modelling of static and dynamic characteristics of the loads of the transmission system were analysed. This thesis started as a part of the project. Chapter 2 includes the results of some of the case studies conducted for this project.

During the load modelling project there was a need for load model conversion in several stages of the project. When the component-based load modelling approach was applied, the models found in the literature used different equations; some were exponential, others ZIP models. In the case of model aggregation, it was easiest to use the ZIP models, because these can be aggregated by calculating the weighted sum¹. When calculating the weighted sum, the proportions of the power demands of the type loads are used as the weights. This meant that the load models known by exponential models had to be converted to ZIP models for the aggregation. Another potential use scenario was the utilization of software tools, which require different model than was estimated originally. In Estonia, PSS[®] E and PSCAD are widely used. PSS[®] E includes a variation of the ZIP model (see Section 1.2.3 for more details), while PSCAD contains exponential load models (see Section 1.2.2 for more details). As a result of the component-based load modelling ZIP models were derived. The ZIP to exponential load model conversion was needed for acquiring the exponential PSCAD load models. In addition to these two uses, the load model conversion arises when ZIP or exponent models of loads are known, and a simulation software with the other type of load models is adopted. Also, when plotting the load models or comparing the values of different entities, the exponential models are often preferred due to the smaller number of parameters. Thus, when ZIP models are known, they may need to be converted for comparison and plotting.

Main Objectives and Tasks of the Thesis

This thesis has two main goals. Firstly, it aims to develop a methodology for estimating static load models of aggregated transmission system bus loads based on the available measurement data. The available measurement data from the Estonian transmission system is used for testing the methodology. Secondly, it aims to benchmark static load model conversion methods (ZIP to exponential, and exponential to ZIP load model conversion) to assess the accuracy of the methods.

Based on the goals of the research and the literature, several hypotheses were formulated:

- Existing measurement systems and historical measurement data of the transmission system can be used to estimate static load models of aggregated bus loads.
- The clustering of monthly energy consumption, disaggregated by load classes, can be used to group aggregated loads into type groups. The loads can be modelled with acceptable error by the type models.
- The event filtering based on properties of the measured event can improve the precision of the estimated models.
- The measurement time and penetration of distributed generation are assumed to have a significant impact on the estimated aggregated load characteristics.
- The conversion error of conversion methods differs.

¹The standard approach to aggregation of polynomial component models by calculating the weighted sum is described in [19–23].

- A load model conversion with a lower conversion error (defined in Section 3.2) is hypothesised to lead to a smaller mismatch of load flow calculations (load modelling error in load flow).

Based on the hypotheses listed above, the following tasks were formulated for research:

- Assess the usability of existing measurement systems for static load model estimation.
- Implement or develop a method for grouping loads and selecting representative loads (for type model identification and validation of grouping).
- Develop a methodology suitable for processing the available measurement data for estimating the static load models of aggregated loads and assessing the precision of the estimated models.
- Identify how the measurement time and penetration of distributed generation affect the estimated load models.
- Analyse and compare the conversion error of load model conversion methods.
- Assess the impact of load model conversion error on load flow results based on a case study.

Contribution of the Thesis and Dissemination

Theoretical Novelty of the Work

- A novel method for post-processing estimated load model values is proposed. The presented method is based on the estimation error weighted averaging of values. See Chapter 2 for more information.
- The conversion error of load model conversion methods is analysed. No similar studies have previously been conducted. Furthermore, the impact of conversion error on load modelling error in load flow calculations is discussed. No similar discussion and explanation has been found in the literature. See Chapter 3 for more information.
- In Chapter 3, a novel method for exponential to ZIP model conversion (method AM3) is proposed. In the same chapter, an improved conversion method (method AM2) is proposed. Two different variations of method AM2 are presented, one for converting exponential models to constrained² ZIP models and another for converting to unconstrained² ZIP models. The derivation of the analytical method used for ZIP to exponential load model conversion is explained, as this derivation was not found in the literature.

²The difference between a constrained and unconstrained ZIP model is explained in Section 1.2.3. Briefly, the multipliers of ZIP model parameters of the constrained model are limited to the range of 0...1. The unconstrained model does not have this value limitation. In some of the available literature the unconstrained ZIP models are defined as accurate ZIP models, for example in [18, 24].

Practical Originality of the Work

- An approach is presented for clustering aggregated loads based on load class energy consumptions. This method can be used for grouping similar loads, determining representative loads and reducing the number of estimated load models. See Chapter 2 for more information.
- The estimation of static load models of transmission system loads is discussed. Commonly load modelling is discussed in the context of distribution networks.
- The impact of event filtering on estimated load model values is analysed based on a set of Digital Fault Recorder recorded events. See Chapter 2 for more information. No similar analysis has been found in the literature by the author.
- The static load models of Estonian transmission system have never been previously studied. Previous studies have instead focused on other aspects of load modelling (peak load forecasting, weather dependency) or conducted at lower voltage.
- The topic of conversion error is introduced. Conversion error of previously known and proposed conversion methods is analysed and compared. See Chapter 3 for more information. No similar analysis has been found in the literature.
- The impact of conversion error on load flow results is analysed based on a case study. The results of the case study indicate that significant modelling errors can be caused by inaccuracy of converted load models. See Chapter 3 for more information. No similar analysis has been found in the literature.

Dissemination of the Research Work

The research and development work for this dissertation was started in the context of the research project "Static and dynamic characteristics of loads of Estonian electrical transmission network", which was initiated by the Estonian TSO, Elering. The project involved measurement-based and component-based load modelling. The results of the research project were published as technical reports [25–27], and some findings were presented at scientific conferences of IEEE and IET (publications: [I–V]). Four bachelor's theses [28–31] and four master's theses [32–35] were defended on related topics. Some data analysis methods used in the project were applied for ramping behaviour analysis in [36] and [37]. The work on load model conversion methods continued after the end of the project and led to a peer-reviewed journal paper [VI]. In addition, work continued also on measurement-based load modelling and three additional conference papers [VII, VIII], [38] were published.

Thesis Outline

This thesis encompasses four chapters.

Chapter 1 describes the load models used in this dissertation and gives an overview of the fundamentals of load modelling. Due to the wide scope of load modelling, the modelling of voltage dependence of loads is in focus.

Chapter 2 describes a procedure for estimating the static load models for aggregated transmission system bus loads. Measurement data from the Estonian transmission system is used to illustrate the process. The available measurement systems of the transmission system are discussed from the load model estimation perspective. The grouping of loads based on monthly load composition using K-means clustering is presented. Next, the significant event detection and event filtering are discussed based on measured events. The

impact of time of measurement is analysed based on a case study. The impact of distributed generation is also illustrated based on a case study. Finally, a method for post-processing a set of estimated load models is presented and analysed.

Chapter 3 describes how static load models (exponential and ZIP model) can be converted to other static load models (ZIP model or exponential, respectively). The arising conversion error is discussed based on numerical analysis. Impact of conversion error on load flow results is illustrated by using a case study of a small power system.

Chapter 4 summarises the conclusions of the thesis and proposes research directions for future work.

Abbreviations

COMTRADE	COMmon format for TRAnsient Data Exchange for power systems
CHP	Combined Heat and Power
CVR	Conservation Voltage Reduction
DFR	Digital Fault Recorder
DG	Distributed Generation
DSO	Distribution System Operator
EMS	Energy Management System
IPS/UPS	Integrated Power System / Unified Power System of Russia
MAE	Mean Absolute Error
MSE	Mean Square Error
MATLAB	MATrix LABoratory
MV	Medium Voltage
NLS	Non-linear Least Squares
NMAE	Normalized Mean Absolute Error
NMSE	Normalized Mean Square Error
NZEB	Nearly Zero-Energy Building
OLTC	On-Load Tap Changer
p.u.	per unit
PMU	Phasor Measurement Unit
PQM	Power Quality Monitor
PSCAD	Power Systems Computer Aided Design
PSS® E	Power System Simulator for Engineering
r.m.s.	root-mean-square
SCADA	System Control and Data Acquisition
TSO	Transmission System Operator
ZIP	Second order polynomial load model, see Section 1.2.3 for a description

Abbreviations of Institutions and Organisations

CIGRE	<i>Conseil International des Grands Réseaux Electriques</i> - International Council on Large Electric Systems
EPRI	Electric Power Research Institute
IEEE	Institute of Electrical and Electronics Engineers
IET	The Institution of Engineering & Technology

Symbols

I_1	Positive sequence component of current
I_2	Negative sequence component of current
I_0	Zero sequence component of current
K_{Exp}	Exponent of exponential load model (of active power)
$K_{Exp,L}$	Exponent of exponential load model (of active power). Aggregated load excluding DG (all supplied load).
$K_{Exp,T}$	Exponent of exponential load model (of active power). Aggregated load including DG (apparent load of the transformer).
$K_{Exp,Q}$	Exponent of exponential load model (of reactive power)
K_Z	Multiplier in ZIP load model (of active power)
K_I	Multiplier in ZIP load model (of active power)
K_P	Multiplier in ZIP load model (of active power)
$K_{Z,Q}$	Multiplier in ZIP load model (of reactive power)
$K_{I,Q}$	Multiplier in ZIP load model (of reactive power)
K_Q	Multiplier in ZIP load model (of reactive power)
$K_{Z,L}$	Multiplier in ZIP load model (of active power). Aggregated load excluding DG (all supplied load).
$K_{I,L}$	Multiplier in ZIP load model (of active power). Aggregated load excluding DG (all supplied load).
$K_{P,L}$	Multiplier in ZIP load model (of active power). Aggregated load excluding DG (all supplied load).
$K_{Z,T}$	Multiplier in ZIP load model (of active power). Aggregated load including DG (apparent load of the transformer).
$K_{I,T}$	Multiplier in ZIP load model (of active power). Aggregated load including DG (apparent load of the transformer).
$K_{P,T}$	Multiplier in ZIP load model (of active power). Aggregated load including DG (apparent load of the transformer).
P	Active power
P_b	Base value for active power
P_G	Generated active power
P_{IN}	Original load characteristic (input model) to be converted
P_{OUT}	Converted (calculated/fitted) load characteristic
P_L	Active power of aggregated loads
P_n	Nominal value of active power
P_0	Initial (pre-event) value of active power
P_{EXP}	Active power (according to exponential load model)
P_{ZIP}	Active power (according to ZIP load model)
P_{meas}	Active power based on measured values
P_{model}	Active power based on estimated load model

Q	Reactive power
Q_b	Base value for reactive power
Q_G	Generated reactive power
Q_n	Nominal value of reactive power
Q_0	Initial (pre-event) value of reactive power
Q_{EXP}	Reactive power (according to exponential load model)
Q_{ZIP}	Reactive power (according to ZIP load model)
SC	Silhouette Coefficient
SSE	Sum of Squared Euclidean distance
U_1	Positive sequence component of voltage
U_2	Negative sequence component of voltage
U_0	Zero sequence component of voltage
V	Voltage
V_b	Base value for voltage
V_i	Voltage sample with index $i, i \in \{1, 2, \dots, N\}$ ($i, N \in \mathbb{N}$)
V_n	Nominal voltage
V_0	Initial (pre-event) voltage
$\eta(V_i)$	Relative conversion error at voltage V_i
μ	Mean value
μ_{MAE}	Weighted mean value, inverse of MAE used as weight
μ_{MSE}	Weighted mean value, inverse of MSE used as weight
σ	Standard deviation
$\varepsilon(V_i)$	Conversion error at voltage V_i

1 Load Modelling

1.1 Introduction

The power consumption of loads is stochastic in nature [39, 40] and varies in time [41–44]. Additionally, the load depends on weather, social factors, and the operational state of the power system. The impact of weather has been analysed in the literature with respect to temperature [39, 45–49], wind speed [45, 48], hours of sunshine [50] and solar analemma variables (elevation angle and azimuth angle of the sun) [51]. The impact of social events is analysed in [49]. The load sensitivity to system parameters is commonly analysed with respect to voltage and frequency. Possibly one of the earliest studies on voltage and frequency sensitivity of aggregated load is [52]. Similarly to the load itself, the voltage dependence of the load varies in time [4–9, 53–56] due to the changes in load composition. Typically, only some properties of the loads are modelled in power system models. A suitable mathematical model is chosen based on the conducted study and the nature of the modelled load.

System parameter dependent load models can be classified into three groups based on the time-dependence: static (time-independent), dynamic (time-dependent), and composite (model includes static and dynamic components). The use of static load models is justified when the load responds to system parameter changes fast and the steady state is reached very quickly [18, 57]. They are most often used in power flow calculations [18] and voltage stability studies [18, 58]. The dynamic load models are often required for inter-area oscillation [57], voltage stability [57, 59] and long-term stability [57] studies. The most significant load dynamics are the dynamics of motor loads due to the high amount of power consumed by motors. In addition, the behaviour of discharge lamps, protection relays, thermostatically controlled loads, OLTCs of distribution transformers, voltage-controlled capacitor banks and other dynamic aspects of load components need to be considered in stability studies [57].

The industry practice of load model usage was investigated by CIGRE working group C4.605, which conducted a large-scale survey among utilities and system operators. The results of the survey are presented in [18] and [60]. Some results of the survey are shown in Table 1.1. According to [60] (and Table 1.1), 84% of responders used a constant power model for steady state studies. In the case of dynamic simulations, there was no dominant model. Still, the static load models (constant power, current, impedance; exponential and ZIP) were used by over 70% of responders for load modelling in dynamic simulations. Thus, static load models are commonly used in the industry for power system analysis.

This thesis focuses on the static load models, which are used to describe the voltage dependence of the aggregated loads of system buses. An aggregated load of the transmission system is considered to include the total power demand of loads connected to the bus, loads of the downstream networks, and losses of the downstream networks.

1.2 Static Load Models

The static load models describe the load characteristics as functions of voltage (and frequency)³. The equations used are algebraic equations [57, 68]. An example of a static load characteristic is shown in Figure 1.1⁴. Three basic voltage characteristics of load (load behaving as constant power, current, and impedance) are explained in Section 1.2.1.

³In this thesis the focus is on voltage characteristics and for this reason the frequency characteristics of the loads are neglected.

⁴The voltage characteristic shown in Figure 1.1 corresponds to a constant impedance characteristic explained in Section 1.2.1.

Table 1.1: Industry practice of load model usage [60]

	Load Model	Static Studies	Dynamic Studies	
			Active power	Reactive power
Static	Constant power	84%	23%	23%
	Constant current	3%	19%	0%
	Constant impedance	3%	4%	22%
	ZIP model	8%	19%	19%
	Exponential model	2%	7%	9%
Composite	ZIP model with induction motor	-	16%	17%
	Detailed composite model	-	10%	10%

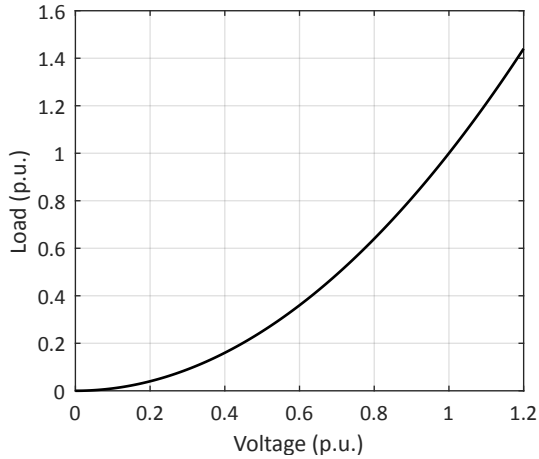


Figure 1.1: A static load characteristic.

The following sections describe three load models for modelling load characteristics: an exponential model in Section 1.2.2, a ZIP model (second order polynomial model) in Section 1.2.3 and a polynomial model in Section 1.2.4. In addition, the respective PSCAD, PSS® E and DigSILENT PowerFactory implementations of the models are discussed.

In Chapter 2 and Chapter 3, the equations are only given for active load, as the mathematical model of active and reactive load is similar. This can be observed when comparing the active and reactive load equations in Section 1.2.2, Section 1.2.3, and Section 1.2.4. Furthermore, the second order polynomial (i.e. ZIP) and exponential load model can be defined using the nominal value of voltage and power [69, 70] or initial values [70, 71]. In this thesis the load models are generalised by using base voltage V_b , base active power P_b and base reactive power Q_b . In the following chapter, Chapter 2, the initial values are used as base values when estimating load models from measurement data. Following this, in Chapter 3, the base values are used for defining load model conversion methods, and the usage of nominal and initial values as base values is discussed.

1.2.1 Constant Power, Current and Impedance Characteristic of Load

The loads with constant power characteristic do not have a voltage dependence and are modelled by a constant power value. The loads with constant current characteristic consume power proportionally to voltage. This characteristic can be represented by a simple algebraic equation in the style⁵ $P = P_b \cdot (V/V_b)$, where P is load at voltage V , when at base voltage V_b the load is P_b . Loads with constant impedance characteristic consume power proportionally to the square of voltage, and can be mathematically described by algebraic equation⁵ $P = P_b \cdot (V/V_b)^2$, where P is load at voltage V , when at base voltage V_b the load is P_b . The voltage characteristics of loads with constant power, current and impedance behaviour are shown in Figure 1.2, where the voltage independence of constant power load, linear dependence of constant current load and square dependence of constant impedance load can clearly be noted.

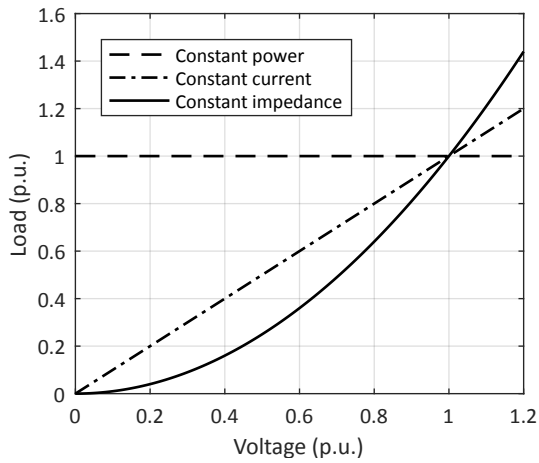


Figure 1.2: Voltage characteristic of constant power, constant current and constant impedance model.

These three load characteristics can be modelled by an exponential load model (described in Section 1.2.2). To use the exponential load model in this way, the exponent K_{Exp} (and/or $K_{Exp,Q}$) is assigned values 0, 1 and 2, respectively. The second order polynomial (ZIP) load model (described in Section 1.2.3) and polynomial load model (described in Section 1.2.4) can be used for modelling combinations of loads with the three described characteristics (constant power, current and impedance). In the case of a polynomial load model, the exponents of the equations are given values 2, 1 and 0. The contributions of the load components with different characteristics are described by the multipliers.

1.2.2 Exponential Load Model

The exponential load model can be described by an exponential equation (1.1), reactive load is represented by a similar equation (1.2).

$$P_{EXP} = P_b \cdot \left(\frac{V}{V_b} \right)^{K_{Exp}} \quad (1.1)$$

⁵In the equations the frequency dependence of the loads has been neglected.

$$Q_{EXP} = Q_b \cdot \left(\frac{V}{V_b} \right)^{K_{Exp,Q}} \quad (1.2)$$

where P_b and Q_b are active and reactive load, respectively, at base voltage V_b . K_{Exp} and $K_{Exp,Q}$ are exponential parameters describing the voltage dependence of the active and reactive load, respectively.

PSCAD load models Fixed Load L-L and Fixed Load L-G

The exponential load model is available in PSCAD software as two different simulation models: Fixed Load L-L and Fixed Load L-G. The main difference between the two models lies in the connection of the load. The L-L version can be used for modelling Δ -connected and L-G for modelling Y-connected loads. When these models operate at voltages within range $V/V_n \in \{0.8...1.2\}$, where V_n is nominal bus voltage, the PSCAD load models Fixed Load L-L and Fixed Load L-G have exponential voltage characteristics⁶ (1.1) and (1.2). In PSCAD, nominal voltage V_n is used as the base voltage V_b . K_{Exp} is denoted in PSCAD by K_{pv} and $K_{Exp,Q}$ is denoted by K_{qv} . At higher ($V/V_n > 1.2$) and lower voltages ($V/V_n < 0.8$), these PSCAD models switch to constant admittance load [72]. The constant admittance load behaves as a constant impedance load described in Section 1.2.1. According to [72], the allowed K_{Exp} and $K_{Exp,Q}$ values are: $-5.0 \leq K_{Exp} \leq 5.0$ and $-5.0 \leq K_{Exp,Q} \leq 5.0$.

1.2.3 Second Order Polynomial (ZIP) Load Model

The second order polynomial load model is described by (1.3) subject to (1.4). Reactive load is represented by similar equations (1.5) and (1.6). The quadratic component of the polynomial equation ($P_b \cdot K_Z \cdot (V/V_b)^2$ and $Q_b \cdot K_{Z,Q} \cdot (V/V_b)^2$) behaves as a load with constant impedance (Z) characteristic, the linear component ($P_b \cdot K_I \cdot (V/V_b)$ and $Q_b \cdot K_{I,Q} \cdot (V/V_b)$) as load with constant current (I) characteristic, and the third component ($P_b \cdot K_P$ and $Q_b \cdot K_Q$) as a load with constant power (P, Q) characteristic. For this reason, this model is also called a ZIP model.

$$P_{ZIP} = P_b \cdot \left[K_Z \cdot \left(\frac{V}{V_b} \right)^2 + K_I \cdot \left(\frac{V}{V_b} \right) + K_P \right] \quad (1.3)$$

$$K_Z + K_I + K_P = 1 \quad (1.4)$$

$$Q_{ZIP} = Q_b \cdot \left[K_{Z,Q} \cdot \left(\frac{V}{V_b} \right)^2 + K_{I,Q} \cdot \left(\frac{V}{V_b} \right) + K_Q \right] \quad (1.5)$$

$$K_{Z,Q} + K_{I,Q} + K_Q = 1 \quad (1.6)$$

where P_b and Q_b are active and reactive load, respectively, at base voltage V_b . K_Z, K_I, K_P and $K_{Z,Q}, K_{I,Q}, K_Q$ are parameters describing the voltage dependence of the active and reactive load, respectively.

⁶In addition to the voltage characteristics, the PSCAD models Fixed Load L-L and L-G also include frequency characteristics, which have been neglected in equations (1.1) and (1.2). For modelling the frequency dependence, a linear model is used in PSCAD.

The values of ZIP model parameters (K_Z , K_I , K_P , $K_{Z,Q}$, $K_{I,Q}$ and K_Q) are sometimes limited to range 0..1. In such a case the ZIP model is called a "constrained ZIP model", and without the constraints the model is considered to be an "accurate ZIP model" [18, 24]. As the term "accurate load model" is used in Chapter 3 of this thesis with another meaning, the terms constrained and unconstrained ZIP load model are used for classifying ZIP models in respect to parameter constraints.

PSS[®]E load model similar to ZIP model

The ZIP load model is included in PSS[®]E as the main load model. Near nominal voltage, the PSS[®]E model corresponds to the generic ZIP model described earlier and can be described by (1.7) and (1.8). Similarly to the generic ZIP model (described by (1.3) and (1.5)), the PSS[®]E model has three distinctive components: $Y\text{Pload}$ and $Y\text{Qload}$ with constant impedance (corresponding to $P_b \cdot K_Z$ and $Q_b \cdot K_{Z,Q}$); $I\text{Pload}$ and $I\text{Qload}$ with constant current (corresponding to $P_b \cdot K_I$ and $Q_b \cdot K_{I,Q}$); $P\text{load}$ and $Q\text{load}$ with constant power (corresponding to $P_b \cdot K_P$ and $Q_b \cdot K_Q$).

$$P = Y\text{Pload} \cdot \left(\frac{V}{V_b}\right)^2 + I\text{Pload} \cdot \left(\frac{V}{V_b}\right) + P\text{load} \quad (1.7)$$

$$Q = Y\text{Qload} \cdot \left(\frac{V}{V_b}\right)^2 + I\text{Qload} \cdot \left(\frac{V}{V_b}\right) + Q\text{load} \quad (1.8)$$

where $Y\text{Pload}$, $I\text{Pload}$, $P\text{load}$ are active load components with different voltage dependence in MW; $Y\text{Qload}$, $I\text{Qload}$, $Q\text{load}$ are reactive load components in Mvar, and V_b corresponds to the nominal voltage of the load bus.

The constant current and constant power components ($I\text{Pload}$, $I\text{Qload}$, $P\text{load}$, $Q\text{load}$) are modelled by elliptical voltage-current (V-I) characteristics at lower voltages [73]. The constant current characteristics ($I\text{Pload}$, $I\text{Qload}$) are replaced by elliptical V-I characteristics at load bus voltages below 0.5 p.u. [73]. The constant power components ($P\text{load}$, $Q\text{load}$) are replaced by elliptical V-I characteristics when the load bus voltage is below the PSS[®]E solution parameter PQBRAK (default value 0.7 p.u.) [73]. The parameter PQBRAK can be assigned a value in solution settings in range $PQBRAK \in (0, 2]$ [73].

1.2.4 Polynomial Load Model

In Chapter 3 of this thesis, a less common polynomial load model is used. It is defined by (1.9) and (1.10), and is included in DiGSILENT PowerFactory as load model *General Load* [74]. The polynomial load model resembles the ZIP load model. The main difference is the ability to configure the exponents of the polynomial components (e_{aP} , e_{bP} , e_{cP} , e_{aQ} , e_{bQ} , e_{cQ}).

$$\begin{cases} P_{GL} = P_o \cdot \left[a_P \cdot \left(\frac{V}{V_o}\right)^{e_{aP}} + b_P \cdot \left(\frac{V}{V_o}\right)^{e_{bP}} + c_P \cdot \left(\frac{V}{V_o}\right)^{e_{cP}} \right] \\ a_P + b_P + c_P = 1 \end{cases} \quad (1.9)$$

$$\begin{cases} Q_{GL} = Q_o \cdot \left[a_Q \cdot \left(\frac{V}{V_o}\right)^{e_{aQ}} + b_Q \cdot \left(\frac{V}{V_o}\right)^{e_{bQ}} + c_Q \cdot \left(\frac{V}{V_o}\right)^{e_{cQ}} \right] \\ a_Q + b_Q + c_Q = 1 \end{cases} \quad (1.10)$$

where P_o and Q_o are active and reactive power of the load at voltage V_o ; a_P, b_P, c_P, a_Q, b_Q and c_Q are coefficients of the polynomial equation; $e_{aP}, e_{bP}, e_{cP}, e_{aQ}, e_{bQ}$ and e_{cQ} are exponents of the polynomial equation. Subscript o stands for *Operating Point* in DIGSILENT PowerFactory, which can be interpreted as the nominal operating point. Thus, V_o, P_o and Q_o can be replaced in the equation by nominal values V_n, P_n and Q_n .

The polynomial load model can accurately describe the ZIP model (Section 1.2.3) and the exponential model (Section 1.2.2). This property of the model is used in Chapter 3, where load model *General Load* is used in DIGSILENT Power Factory for modelling exponential and ZIP load models.

To use this model as a ZIP model, exponents e_{aP}, e_{bP} and e_{cP} (and/or exponents e_{aQ}, e_{bQ} and e_{cQ}) are assigned the values 0, 1 and 2. This way the polynomial equation (1.9) (or (1.10)) becomes a second order polynomial equation, similar to the ZIP model (1.3) (or (1.5)). When this model is used as an exponential load model, the values of two coefficients (among a_P, b_P and c_P ; or among a_Q, b_Q and c_Q for reactive load) are set to 0, and the value of the third is set to 1. The exponent corresponding to the coefficient with value 1 is used as the exponent of the exponential model.

1.3 Methods for Load Model Estimation

In power system models the loads are typically represented by aggregated bus load models. The mathematical equation of the model is chosen based on the modelled aspect of the system, the nature of the aggregated load, and the properties of the load that affect the analysed aspect of the system. The used load model parameter values are identified based on literature, experience, measurements, survey results, or have an unknown source [18, 60]. There are three main approaches for load model derivation: component-based (described in Section 1.3.1), measurement-based (described in Section 1.3.2), and combined (described in Section 1.3.3). The third approach is a combination of the first two approaches.

1.3.1 Component-based Load Modelling

The component-based load model estimation method is a bottom-up approach. Load components comprising the loads are identified. For each component, a load model is determined. A model of the aggregated load is constructed based on the models of the components, taking into account the load power consumptions of the load components.

The approach is illustrated by Figure 1.3 and applied in publications [7, 53, 61]. Each load component (often a type of device) has a load characteristic, which is modelled (approximated) by a load model or combination of several models. Some models of load devices can be found in publications [7, 23, 53, 61–67]. Often, load classes are defined based on customer classification and a load model is constructed for each load class. Finally, based on load class contributions, the aggregated bus load model is constructed by combining the load class models.

1.3.2 Measurement-based Load Modelling

The measurement-based load model estimation method is a top-down approach. Measurement data and data processing techniques are used for load model determination. A comprehensive overview of this approach has been given by EPRI [75, 76] and CIGRE [18]. Both normally occurring [77, 78] and intentionally induced [6, 79] disturbances and events may be used for load model estimation [18].

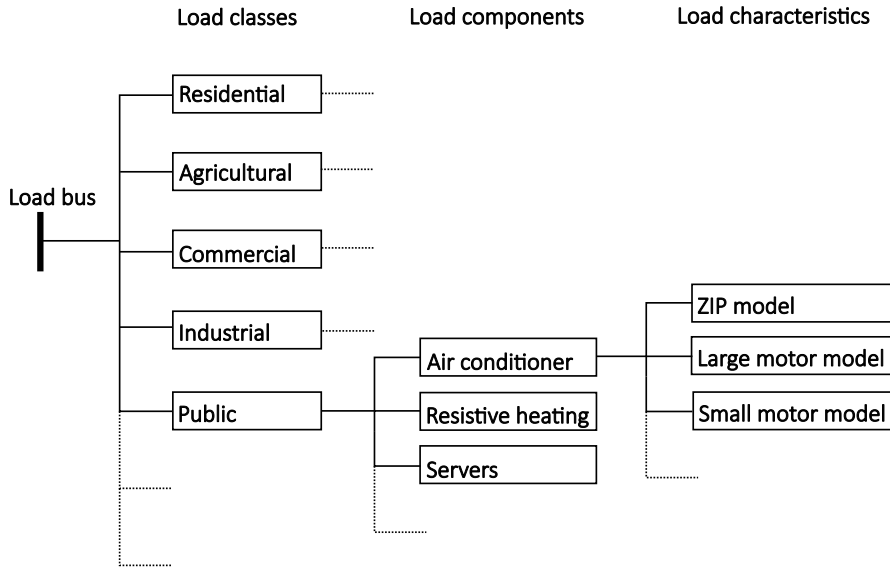


Figure 1.3: Component-based load modelling approach.

Choosing a suitable methodology for measurement data processing depends on the type of estimated load model and properties of the measured data. Typically, the data processing starts from measurement data acquisition. Data acquisition for implementing a measurement-based approach can be performed using Power Quality Monitors (PQM) [18, 76], Digital Fault Recorders (DFR) [18, 58, 76], Phasor Measurement Units (PMU) [18, 56, 76, 78, 80–83], protection relays with data logging capability [18], EMS/SCADA [18, 84], etc. This is followed by data pre-processing, which may include event detection, data filtering, data extraction, and signal smoothing. After the measurement data have been prepared, parameter values for a chosen load model are estimated by using analytical methods, optimisation (minimising error or maximising fitness function) or a stochastic approach. Optimisation through curve-fitting is the most popular among these approaches [76]. Next, the estimated model is validated by comparing the disturbance response of the simulated and measured load. In some cases, several models are fitted to the measured data and the most fitting model is chosen. In some other algorithms, only estimation error is calculated. The typical process of measurement-based load modelling is shown in Figure 1.4.

1.3.3 Combined Load Modelling

The combined approach of measurement- and component-based load modelling is briefly described in [18]. Firstly, the loads are clustered based on the load composition of the maximum summer and winter load. The loads closest to the cluster centres are chosen from each cluster as typical load. Secondly, the data monitors are placed at these buses and the measurement-based load modelling is used for estimating the models of the type loads. Model validation by comparing simulated and measured response of the single load and system is necessary.

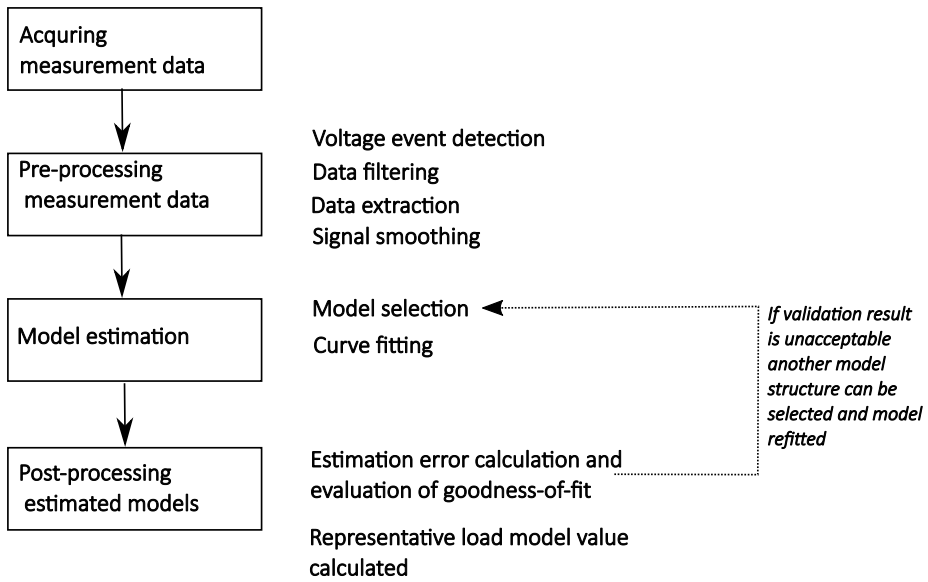


Figure 1.4: Process of measurement-based load modelling.

2 Estimation of Static Load Models of Aggregated Transmission System Loads

2.1 Introduction

This chapter of the thesis was motivated by the interest of a Transmission System Operator (TSO), which arose around the time of publication of [18]. For many years, the Estonian TSO had used the same load models for modelling the aggregated bus loads. This situation was similar to many other TSOs according to [60]. The objective of the research presented in this chapter is to construct a load model estimation methodology that would make use of the existing measurement systems and databases. It analyses which of the existing measurement systems (Digital Fault Recorders (DFRs), Power Quality Monitors (PQMs) and Phasor Measurement Units (PMUs)) could be utilised for updating the models. In order to simplify the task, the focus of the work is on the estimation of static load models (ZIP and exponential model) of 110 kV aggregated bus loads. The static models of aggregated loads of Estonian power system have previously been researched in [85, 86], where the focus is on end consumers and distribution network loads. In this thesis, models of aggregated 110 kV bus loads of transmission system are analysed. In addition to the work presented in this chapter, the author also estimated the load models by using a component-based approach. That work is discussed in technical reports [25–27].

In Section 1.3, three load modelling approaches were presented. The measurement-based modelling approach (Section 1.3.2) was implemented for estimating exponential and ZIP models. The structure of this chapter follows the measurement-based load modelling procedure shown in Figure 2.1. Firstly, in Section 2.2, requirements for the measurement data are presented (Section 2.2.1), the available measurement systems are described (Section 2.2.2), and the selection of measurement locations with higher priority is discussed (Section 2.2.3). Next, the data pre-processing methods used are described (Section 2.3), including the DFR data preparation (2.3.1), voltage event detection method (Section 2.3.2), and unsuitable event identification (Section 2.3.3). After the measurement data acquisition and data preparation methods, the load model estimation method used is presented in Section 2.4.1. The estimation result is affected by the measurement time and distributed generation, which are discussed in Section 2.4.3 and Section 2.4.4, respectively. To quantify the goodness-of-fit of estimated models, some commonly used measures of error are shown in Section 2.5.1. An idea for post-processing estimated load models is presented in Section 2.5.2. The presented method makes use of load model estimation error when the representative load model values are calculated.

The main results of this chapter have been published in [III-V, VII, VIII]The procedure for grouping aggregated loads based on monthly load class compositions is first introduced in [V]. The impact of event filtering on load model estimation is analysed in [VII]. The intra-day variations of load models are analysed in [III]. In [IV, VIII] the impact of distributed generation on estimated exponential load models is analysed based on a case study. The idea for the post-processing method is first presented in [III].

2.2 Acquiring Measurement Data

Different measurement systems are used in the power system for gathering measurement data. Some systems used in the Estonian transmission system are discussed in Section 2.2.2 together with other measurement solutions that were used for conducting the case studies. Depending on the devices used, the technical capabilities of the systems vary, and the properties of the measured data differ. In Section 2.2.1 requirements for measurement

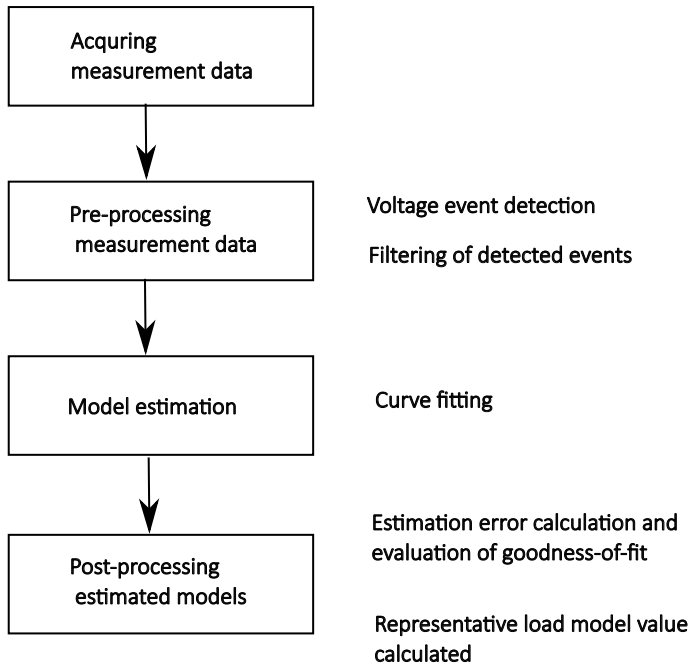


Figure 2.1: Process of load model estimation.

data for load model estimation are described based on the literature. Event filtering based on some of these requirements is discussed in Section 2.3.3, and the impact of these aspects is illustrated in Section 2.4.2

2.2.1 Requirements for Measurement Data

According to [18], suitable events and disturbances for load model determination should have the following characteristics:

1. three-phase event/disturbance with voltage and current unbalance below 10%;
2. takes place either upstream or on an adjacent feeder;
3. sufficient drop in voltage (10% or more);
4. is not a voltage interruption;
5. duration of the event is at least 4 cycles.

Contradicting condition 3, [77] and [87] claim that loads can be modelled using voltage changes of 0.5%. In publication [III], a 0.5% voltage disturbance threshold was used as it was permissible to induce only small voltage disturbances for the case study. In publications [IV, VIII] an on-load tap changer with 1.78% steps was used for inducing voltage changes, and slightly larger disturbances were possible than induced for [III] (compared to condition 3, the disturbances were still far below 10%). Thus, in the case studies performed for this thesis, small voltage changes compared to recommendations of [18] are used. As nearly symmetrical voltage disturbances are less frequent than unbalanced ones, load model estimation from unbalanced events is proposed in [88].

Furthermore, in [18] it is recommended that the recorded data should include at least several cycles of pre-disturbance data and several seconds of post-disturbance data. The sampling rate of the measurement device should be above 100 Hz for estimating parameters of static load models with a high level of confidence [18, 89].

Considering that the voltage sensitivity of the aggregated load is time-dependent [4–9] it is also important for the measurement times to cover different periods of the day. This aspect is illustrated by the case study results in Section 2.4.3.

2.2.2 Measurement Systems

In the literature different measurement systems have been used for estimating exponential and ZIP load models. Some examples are given in Table 2.1. Measurement data from the Estonian transmission system were used for testing the implemented approaches. The Estonian transmission system operator (TSO) uses three types of measurement devices that are capable of offering a relatively high measurement frequency: Digital Fault Recorders (DFR), Power Quality Monitors (PQM), and Phasor Measurement Units (PMU).

Table 2.1: Measurement systems used for load modelling in literature.

Reference	Load Model	Used Measurement System
[42]	Exponential, ZIP	Load monitoring device (0.2...1 Hz sampling rate)
[9]	Exponential, ZIP	1 Hz sampling rate
[8, 84]	ZIP	SCADA
[58]	Exponential	DFR
[90]	Dynamic	DFR
[56, 83]	ZIP	PMU
[81, 91]	Dynamic	PMU
[92]	ZIP, dynamic, composite	PMU

The data recording of DFRs is event based. The measurement events are detected using a set of triggering conditions, which include the rate of current change, an overvoltage limit, an undervoltage limit and the rate of voltage change. The digital fault recorders used by the TSO are typically configured to record 50 ms pre-disturbance (pre-triggering) and 5 seconds post-triggering. Technically, the newer models of the DFR are capable of recording up to 250 ms pre-triggering and 15 seconds post-triggering. From a static load model estimation perspective, this period of time is rather short. 1 kHz sampling rate is used for recording instantaneous values of voltage and current. Sliding window algorithm using discrete Fourier transform can be used for obtaining phasor domain quantities [18] and obtaining power values. The main benefits of a DFR system in the case of the Estonian power system are as follows: large number of installed devices, years of historical database available and good placement of the devices from load model estimation perspective.

At the time of the measurement systems analysis there were some technical issues with the TSO's power quality measurement systems. This meant that some PQM were not available for use. Moreover, the placement of the existing PQM devices was ill-suited to measuring the aggregated 110 kV bus loads. For conducting the case studies of the dissertation, PQM devices of Tallinn University of Technology were used for taking the

measurements of case studies presented in [III, IV, VIII]. Data with a 200 ms time step were used on several occasions, because data with a higher measurement frequency were recorded as short events and there were gaps between the short recordings. This measurement rate (5 Hz) is below the recommended 100 Hz sampling rate of [18], but still provided insightful measurement results.

Similarly to the PQM devices, the placement of the PMUs was found to be unsuitable for estimating the targeted 110 kV bus load models. The devices had been placed with the aim of observing the 330 kV transmission lines, and for this reason were not able to measure the 110 kV bus loads.

2.2.3 Choosing Measurement Locations

The DFR measurements are not available in all the 110 kV substations. In addition, in some substations not all the feeders or transformers are measured. Thus, for those substations, it is not possible to calculate the aggregated load using power balance, and to measure it by this type of device. To model the aggregated loads that are not measured, the load models of similar loads can be applied. In order to take measurements during case studies⁷, PQMs were temporarily placed at chosen locations, voltage disturbances were induced and system responses were recorded. The measurement locations of the PQMs were determined based on analysis of load composition and practical considerations. As a result of the analysis conducted, aggregated loads were classified, and representative loads were chosen for each load group.

Identifying substations with similar load class composition

The distribution network operator provided 33 months (from January 2013 to September 2015) of monthly energy consumption data measured by the metering system. The acquired raw data of 1 substation are plotted in Figure 2.2 as an example. The same data are used for illustrating the used normalisation method in Figure 2.3. The monthly energy consumptions were given for the aggregated transmission system loads by load class accuracy. The demand was given for 5 load classes:

- Class 1: Residential
- Class 2: Agricultural
- Class 3: Commercial
- Class 4: Industrial
- Class 5: Public

These metering data were first processed to obtain a representative annual load class composition for each included aggregated load. The monthly values were averaged for each month of the year and normalised. This way each substation load (object) was described by $12 \cdot 5 = 60$ attributes (12 months, each with values for 5 load classes). An example of a result is plotted in Figure 2.3. The data of the same substation is shown, as was plotted in Figure 2.2.

The grouping of daily load profiles has a similarity to the clustering of aggregated loads by monthly energy consumptions. The daily load profiles have been clustered for customer classification and type profile identification using K-means clustering (Lloyds' algorithm) [93] in [44, 94]. In [95, 96] a more advanced approach of dynamic time warping is

⁷Case studies were presented in [III, IV, VIII]. Measurement data gathered during the case studies was used for plotting the illustrating figures of this chapter.

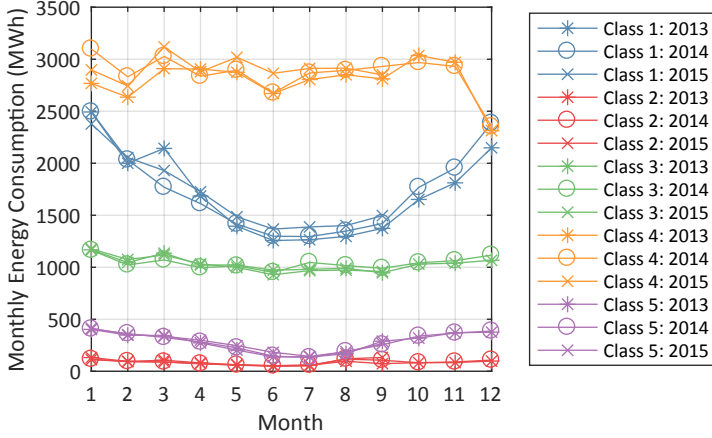


Figure 2.2: Monthly energy consumption of a substation, disaggregated by load classes. Adapted from [V]

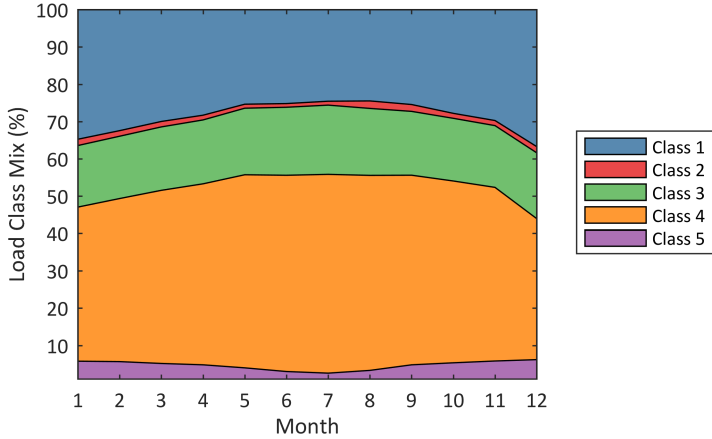


Figure 2.3: Monthly load class compositions of a representative year after normalisation (values stacked). Adapted from [V]

used. Dynamic time warping is similar to the Lloyds' algorithm, and additionally matching of time shifted series is possible. The K-means clustering was used for conducting the grouping of loads.

The K-means algorithm classifies objects into K clusters based on the attributes of the objects. The objective of the algorithm (2.1) is to minimise the total squared Euclidean distance between the objects and centres of the assigned clusters. A detailed explanation of the steps of the algorithm is provided in [94].

$$\min \left(\sum_{i=1}^K \sum_{x \in C_i} d(x, z_i) \right) \quad (2.1)$$

where K is the number of clusters, z_i is the centre of cluster C_i , and $d(x, z_i)$ is the squared Euclidean distance between object x and cluster centre z_i .

The squared Euclidean distance $d(x, z_i)$ between object x with attributes x_1, x_2, \dots, x_n and cluster centre z_1 with attributes $z_{1,1}, z_{1,2}, \dots, z_{1,n}$ is (2.2).

$$d(x, z_1) = (x_1 - z_{1,1})^2 + (x_2 - z_{1,2})^2 + \dots + (x_n - z_{1,n})^2 \quad (2.2)$$

The optimal number of clusters (K) was determined by using a combination of several methods. Firstly, the largest analysed number of clusters was calculated using equation $2 \leq K_{max} \leq \sqrt{m}$, where m is the number of objects. This equation has previously been used in [94]. Secondly, K-means clustering was conducted for $K = 2 \dots K_{max}$. The sum of squared Euclidean distance (SSE) and Silhouette Global Index (SGI) [97] were calculated for the solutions and analysed with respect to K .

In the case of Sum of Squared Euclidean distance (SSE) a lower value is better, as a lower value means that the objects are closer to the cluster centres (clusters are more compact). The SSE decreases as the number of clusters increases. This is illustrated by Figure 2.4. The point on the SSE plot which resembles an elbow is usually where we start to see a diminishing return of increasing K [98]. The first value of K where SSE starts to diminish is chosen [99]. As the curve is rather smooth, based on this logic, the reasonable value of K could be in range 10...15.

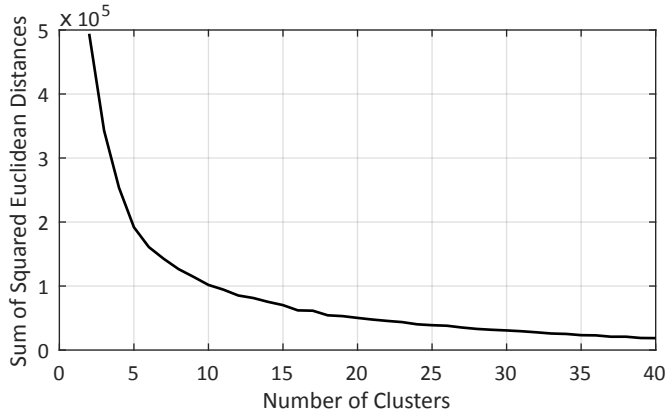


Figure 2.4: Sum of squared Euclidean distance for different number of clusters. Adapted from [V]

One of the most commonly used [94] internal tests for evaluating the results of K-means clustering is the Silhouette Global Index (SGI) [97]. The SGI is based on silhouette values s_i (2.3) of objects i . The silhouette values of the objects are averaged for calculating the local silhouette coefficient S_j (2.4), which are used for calculating the value of silhouette coefficient SC (2.5).

$$s_i = \frac{(b_i - a_i)}{\max(a_i, b_i)} \quad (2.3)$$

where b_i is the minimum mean distance from object i to objects belonging to other clusters, minimised over clusters; a_i is the mean distance between object i and the other objects of the same cluster j .

$$S_j = \frac{1}{n_j} \sum_{i=1}^{n_j} s_i \quad (2.4)$$

where n_j is the number of objects in cluster j .

$$SC = \frac{1}{K} \sum_{j=1}^K S_j \quad (2.5)$$

The following interpretation of silhouette coefficient SC values is proposed in [100]:

- ≤ 0.25 : No substantial structure has been found.
- $0.26 \dots 0.50$: The structure is weak and could be artificial.
- $0.51 \dots 0.70$: A reasonable structure has been found.
- $0.71 \dots 1.00$: A strong structure has been found.

SC values of analysed data are shown in Figure 2.5. From the figure it is clear that a strong structure was not found (all SC values are below 0.71). A reasonable structure (SC value $0.51 \dots 0.70$) was found for several values of SC . The largest value of SC occurred at $K = 2$, which also has the largest value of SSE, and for that reason would not be a good choice. Choosing value 10 would lead to silhouette values s_i shown in Figure 2.6. From this figure it is clear that the number of objects belonging to a cluster varies, cluster 3 includes only a single load.

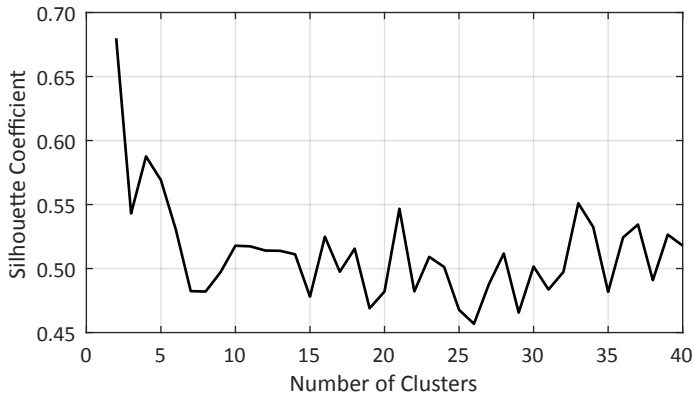


Figure 2.5: Silhouette coefficient for different number of clusters. Adapted from [V]

Selecting representative loads

When choosing representative loads and measurement locations for the case studies, several aspects were considered: placement of existing measurement devices, distance from system buses with voltage control (buses with shunt reactors or on-load tap changer (OLTC)), condition of substation, and load of the substation.

Substations with DFR were analysed based on an Excel file (provided by the TSO) that included information about measured feeders and transformers. This was compared to the network topology (in normal operation), and observable loads were identified. The analysis of PMU and PQM locations indicated that at the time of the analysis, their placement was not suitable for load analysis. This approach led to the identification of loads that can be analysed based on historical data of DFR system.

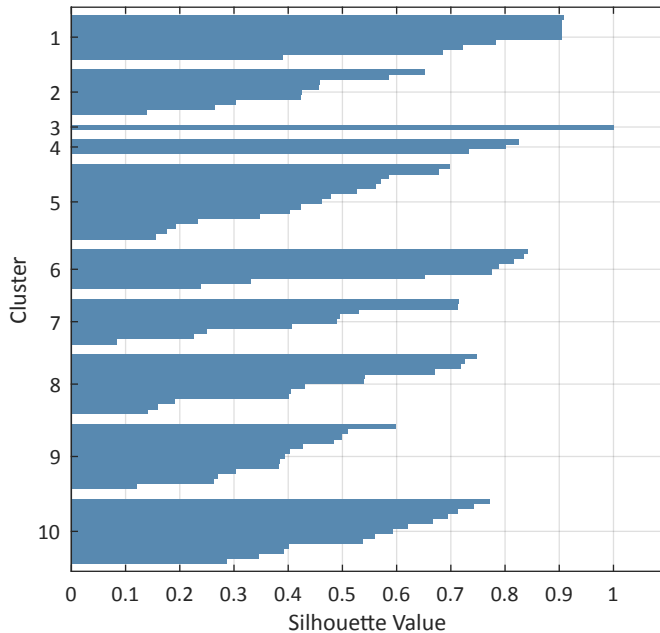


Figure 2.6: Silhouette value of clustering results (92 largest loads). Adapted from [V]

As there were a few mobile PQM devices available, in addition to analysis of DFR data, a few case studies were conducted to acquire data of induced disturbances. Firstly, the substations with the largest power consumption were analysed. The larger loads were assumed to have less stochastic loads, as a set of a larger number of load devices was assumed to behave closer to the statistical mean. Substations located far away were excluded based on practical considerations. A few substations were chosen from the same cluster and some from other clusters to verify the clustering results. Taking measurements in some chosen substations was not possible due to the condition of these substations. These substations were planned to be renewed in the upcoming years and were condition-wise at the end of their life. This meant that connecting measurement devices at the substation would have involved a significantly higher risk: due to the potentially corroded connections, some wires could have come loose and caused a disturbance.

2.3 Pre-processing Measurement Data

Measurement systems can use different databases and file formats for storing the data. For processing the gathered data, several different approaches had to be used and data import interfaces had to be programmed. In the case of DFR data, measurement data of each triggered event are stored in a separate file (in proprietary format). The use of proprietary format and recording of instantaneous values posed the need for several data preparation steps discussed in Section 2.3.1. In the case of the continuous measurements of PQM, the voltage events had to be detected first. A simple method implemented for this purpose is presented in Section 2.3.2.

2.3.1 DFR Data Preparation

A set of MATLAB scripts was developed for handling the DFR measurement data files. The software of the DFR manufacturer included a command-prompt-based API for converting the proprietary format files to COMTRADE (COMmon format for TRANsient Data Exchange for power systems). This was combined in MATLAB with file search codes to convert the historical data into easily readable COMTRADE format and to enable automatic processing of the data. However, the converted files only included part of the information included in the proprietary file format. For this reason, scripts were developed for reading and processing the header section of the partially readable proprietary files. This way it was possible to identify the device ID, event date, and substation name. These properties of the event were used for renaming the event files with unique names. Measured instantaneous voltage and current values were acquired from the COMTRADE files. The r.m.s. (root-mean-square) values of current, voltage, and power were calculated. To enable the analysis presented in Section 2.3.2 and Section 2.4.2 the positive, negative and zero sequence components of the voltage and current were calculated.

2.3.2 Detection of Significant Voltage Events

The voltage disturbances can be detected in the measurement data based on the relative voltage difference ΔV (2.6) of two sliding windows. The calculated values of ΔV are compared to the event threshold; if it is exceeded, the event is flagged. This method has been used for voltage event detection in [77, 101].

$$\Delta V = \left| \frac{\frac{\Sigma V_{old}}{n} - \frac{\Sigma V_{new}}{n}}{\frac{\Sigma V_{old}}{n}} \right| \cdot 100\% \quad (2.6)$$

where ΣV_{old} and ΣV_{new} are the sum of n old and n new samples, respectively, and n is the length of the averaging window.

In [77] and [87] it is claimed that small voltage changes of 0.5% can be used for load modelling. In [77, 79, 87] voltage changes 0.5%...2% have been used. For this reason, 0.5% was chosen as the event threshold in the case study presented in Section 2.4.3. In the study presented in Section 2.4.4 the events were detected based on threshold $\Delta V \geq 1.5\%$ as OLTC with 1.78% step was used for inducing voltage changes. This meant the smallest induced changes were over 1.5%, and were correctly detected by this threshold setting.

In [101] a window length of 20 seconds was used. Depending on the measurement data used, the author of this thesis used n value corresponding to 10 or 40 seconds, which is close to the previously mentioned 20 seconds.

2.3.3 Identification of Unsuitable Events

In Section 2.2.1 several requirements for suitable events were listed. In the case of the DFR data, naturally occurring voltage disturbances are recorded. This means that the recorded events include responses to different disturbances and only a small proportion of the recorded events fulfil all the listed requirements. To illustrate the properties of DFR recorded events, the value distributions of one substation are plotted.

Firstly, in [102] current and voltage unbalance below 10% is suggested as one condition for a suitable event. To analyse the unbalance, the maximum value of negative and zero sequence unbalance ratio is calculated for each DFR recorded event. According to the definition of [103] the negative sequence unbalance ratio of voltage u_2 (2.7) is the ratio between negative sequence component U_2 and the positive sequence component U_1 . The

zero sequence unbalance ratio of voltage u_0 (2.8) is the ratio of zero sequence component U_0 , and the positive sequence component U_1 . The current unbalance ratios are calculated similarly by (2.9) and (2.10).

$$u_2 = \frac{U_2}{U_1} \cdot 100\% \quad (2.7)$$

$$u_0 = \frac{U_0}{U_1} \cdot 100\% \quad (2.8)$$

$$i_2 = \frac{I_2}{I_1} \cdot 100\% \quad (2.9)$$

$$i_0 = \frac{I_0}{I_1} \cdot 100\% \quad (2.10)$$

The symmetrical components of the voltages and currents that are used in (2.7), (2.8), (2.9) and (2.10) can be calculated from the voltage and current phasors ($U_a, U_b, U_c, I_a, I_b, I_c$) using (2.11) and (2.12), respectively.

$$\begin{bmatrix} U_1 \\ U_2 \\ U_0 \end{bmatrix} = \begin{bmatrix} 1 & a & a^2 \\ 1 & a^2 & a \\ 1 & 1 & 1 \end{bmatrix} \begin{bmatrix} U_a \\ U_b \\ U_c \end{bmatrix} \quad (2.11)$$

$$\begin{bmatrix} I_1 \\ I_2 \\ I_0 \end{bmatrix} = \begin{bmatrix} 1 & a & a^2 \\ 1 & a^2 & a \\ 1 & 1 & 1 \end{bmatrix} \begin{bmatrix} I_a \\ I_b \\ I_c \end{bmatrix} \quad (2.12)$$

Where $a = 1 \angle 120^\circ$

According to Figure 2.7 the negative sequence ratio of voltage tends to have slightly higher values than zero sequence ratio. Still, in general both of these stay below 5%. Thus, the values of voltage unbalance ratios are mostly below 10%, which was proposed in the literature as the limit value. The current unbalance ratios display significantly higher values. A large number of events have unbalance ratio values over 100%. Thus, limiting the current unbalance to 10% would exclude a large number of recorded events. The number of remaining events is shown in Table 2.2.

Table 2.2: Number of events with unbalance ratio below threshold value (in total 1843 events recorded at the substation).

Unbalance Ratio	<1%	<5%	<10%	<20%
Negative sequence ratio of voltage	1224	1678	1778	1798
Zero sequence ratio of voltage	1685	1800	1803	1807
Negative sequence ratio of current	9	385	415	441
Zero sequence ratio of current	14	561	579	604

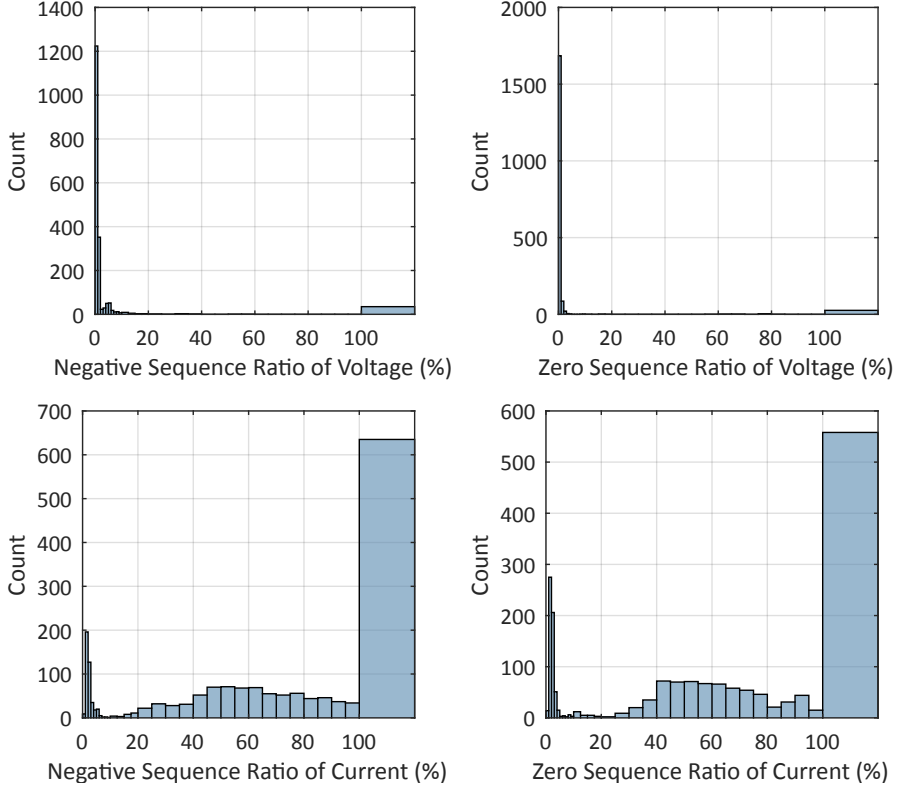


Figure 2.7: Voltage and current unbalance ratios of DFR recorded events of one substation. Maximum value of each event is plotted. Values above the maximum value of tick are included in the last bar.

In Section 2.2.1 the second requirement for suitable event is for the location of the event (upstream or on an adjacent feeder in respect to the measured load). To exclude load change induced voltage changes, [77] uses the direction of voltage and power change. When the active power of the load changes due to a voltage change, the direction of the changes should match. [77] presents this condition as $sign(\Delta V) \cdot sign(\Delta P) > 0$. The same approach can be implemented in several ways. Calculation $\Delta V \cdot \Delta P > 0$ could be used to remove the sign functions, and acquire an identical result. In addition, the opposing direction of voltage and load change would lead to an estimation of negative value of active power exponent K_{Exp} . According to the survey results [60], the minimum values used of active power parameter K_{Exp} are 0. Furthermore, in [61] only a few loads displayed a K_{Exp} value of -0.01. Thus, estimation of true negative values of K_{Exp} should be unlikely, and the detection of negative K_{Exp} value could be used for achieving similar results to equation $\Delta V \cdot \Delta P > 0$ and $sign(\Delta V) \cdot sign(\Delta P) > 0$.

In Section 2.2.1 the third requirement is for the voltage change (10% or more proposed in [102]). Significantly smaller changes of 0.5% are proposed in [77] and [87]. The difference between the maximum and minimum value of measured voltage was calculated to quantify the DFR recorded events. Based on Figure 2.8 most of the events have voltage differences below 0.05 p.u. and some are interruptions (voltage differences above 1 p.u.).

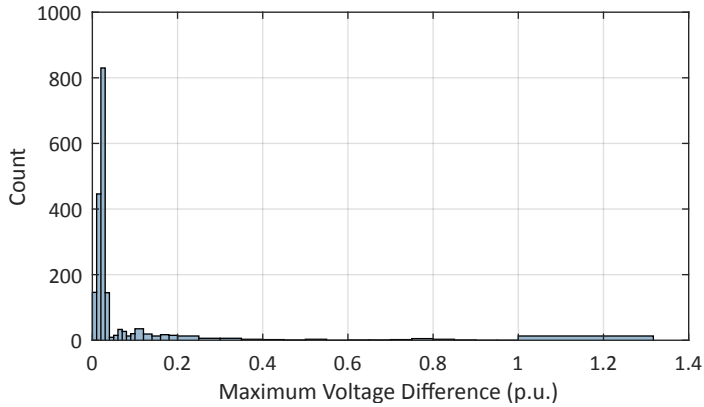


Figure 2.8: Difference between minimum and maximum value of voltage during the event.

Table 2.3: Number of events with maximum voltage difference below threshold value (in total 1843 events recorded at the substation).

	<0.5%	<1%	<2%	<3%	<5%	<10%	<20%
Voltage difference below threshold	26	146	592	1422	1576	1684	1783

A suitable event should not be an interruption. An interruption is defined in [104] by an r.m.s. voltage drop below 5%, [103] mentions a threshold of 5% or 10%. In the context of load modelling, a significantly higher threshold should be used. This is because at voltages below 85% load devices start self-disconnecting from the grid [18]. For this reason, residual voltages of events below 80% were detected and the corresponding events were flagged as unsuitable. According to Figure 2.9 most of the recorded events have minimum values of voltage above 0.8 p.u., and only a limited number of events have lowest voltage in range 0.1...0.8 p.u.

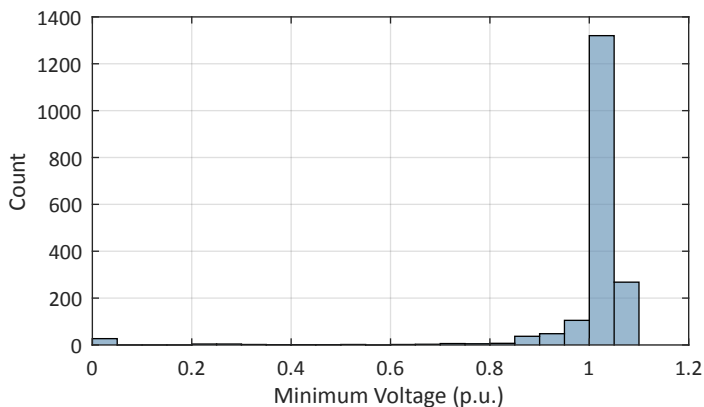


Figure 2.9: Minimum value of voltage during the event.

Event Filtering

These previously introduced approaches for unsuitable event detection were implemented as 9 different filters:

- F1 - K_{Exp} value is negative (voltage and active power change have an opposing direction)
- F2 - negative sequence ratio of voltage is over 10%
- F3 - zero sequence ratio of voltage is over 10%
- F4 - negative sequence ratio of current is over 10%
- F5 - zero sequence ratio of current is over 10%
- F6 - voltage variation during event is below 5%
- F7 - r.m.s. voltage drops below 80% of nominal
- F8 - value of K_{Exp} is at a boundary value
- F9 - value of $K_{Exp,Q}$ is at a boundary value

To analyse how many common events are detected by the filters, Table 2.4 was constructed. The diagonal elements of the table indicate how many events would be flagged if a filter were be used. The other elements represent the common events of 2 filters.

According to Table 2.4 the largest number of events is flagged as unsuitable by filter F6 (voltage variation during event) and F9 ($K_{Exp,Q}$ at boundary), while around 90% of the detections are common events. A large number of events is also detected by F4 (neg. seq. ratio of current), F5 (zero seq. ratio of current) and F8 (K_{Exp} at boundary). The voltage unbalance based filters F2 and F3 detect the lowest number of events. The events detected by F2 can also be detected by F4 and F5. The F3 detected events by F4, F5, and F7. Thus, when current unbalance filters F4 or F5 are applied, there is no need to apply voltage unbalance filters F2 or F3. Similarly, filter F7 detected events can be fully detected by applying F4 (negative sequence current ratio), or mostly detected by F2 and F5. When applying filters F1...F9, only 3 events⁸ out of 1843 recorded events are left. Without filter F9, this number increases to 24. This result supports the hypothesis that among the numerous recorded events only a limited number fulfil the requirements stated in the literature (listed in Section 2.2.1). The impact of event filtering on the probability distribution function of the estimated load model parameters is presented in Section 2.4.2.

2.4 Estimation of Exponential and ZIP Load Models

2.4.1 Non-Linear Least Squares Estimation of Load Model Parameters

The exponential load models (described in Section 1.2.2) and ZIP load models (described in Section 1.2.3) can be estimated using the Non-linear Least Squares (NLS) estimation. For example, it has been used in [77, 105]. A performance comparison of NLS, Genetic Algorithm (GA) and Simulated Annealing (SA) is provided in [105], and it is shown that GA and SA do not provide a significant benefit over NLS.

⁸When additionally the durations of these 3 events were to be analysed, only 1 of the 3 events left after filtering would have a duration over 4 cycles. Thus, the situation would be even worse.

Table 2.4: Number of unsuitable events detected by a filter^a (diagonal elements) and common events for two filters (non-diagonal elements). [VII]

	F1	F2	F3	F4	F5	F6	F7	F8	F9
F1	842								
F2	19	65							
F3	11	40	40						
F4	728	65	40	1428					
F5	602	64	40	1257	1264				
F6	769	11	11	1193	1070	1576			
F7	18	56	40	58	55	11	58		
F8	682	18	10	1266	1144	1155	13	1279	
F9	736	11	7	1183	1025	1421	11	1105	1557

^a Explanation of event filter F1...F9 in text.

The objective of the NLS algorithm is to minimise the sum of squared estimation error (2.13). The estimation error is the mismatch between the estimated load model P_{model} , and the measured load P_{meas} . In the context of this thesis, for load model estimation, the initial voltage V_0 , active power P_0 , and reactive power Q_0 were used as the base values V_b , P_b , and Q_b , respectively. The following equations are given for active load models, reactive load models can be estimated using similar equations.

$$\min \frac{1}{N} \sum_{i=1}^N (P_{modeli} - P_{measi})^2 \quad (2.13)$$

To estimate the exponential load model (Section 1.2.2), the following load model equation (2.14)⁹, and boundary conditions (2.15) are used for (2.13):

$$P_{modeli} = P_{EXP} = P_0 (V_i/V_0)^{K_{Exp}} \quad (2.14)$$

$$-10.0 \leq K_{Exp} \leq 10.0 \quad (2.15)$$

The boundary values -10 and 10 were chosen based on load model parameter values published in the literature. In [24] device models of [20, 62–67, 106] are statistically analysed, and it is found that with 95.5% probability that the load model parameter values of devices are: $-0.643 \leq K_{Exp} \leq 0.959$ and $-1.800 \leq K_{Exp,Q} \leq 2.384$. Furthermore, when load models of aggregated system loads are estimated, even higher K_{Exp} and Exp, Q may occur. This is apparent from the values shown in Table 2.5, where K_{Exp} is in range 0.18...1.51, and $K_{Exp,Q}$ values 2.96...6.00. Based on these findings, the limits were set to -10 and 10. In some situations, even larger values may actually occur. In the case of active power, high penetration level of DG increases the voltage sensitivity (and exponent) of the net load. This is discussed in Section 2.4.4 of the thesis. In the case of $K_{Exp,Q}$ extremely high values have been shown to be possible in the presence of compensating capacitor [107]. In such cases the estimated exponential models may be unreliable for modelling the load behaviour, and other types of model should be considered.

⁹Corresponding to (1.1) and (1.2).

Table 2.5: Exponential load model parameter value ranges in literature.

Reference	K_{Exp}	$K_{Exp,Q}$
[4]	0.18...1.51	2.96...6.00
[108]	0.44...1.1	3.2...5.22
[6]	1.16...1.76	3.46...4.10

Similarly, to estimate the ZIP load model (Section 1.2.3), the following load model equation (2.16)¹⁰, and boundary conditions (2.17)¹¹ are used for (2.13):

$$P_{modeli} = P_{ZIP} = P_0(K_Z(V_i/V_0)^2 + K_I(V_i/V_0) + K_P) \quad (2.16)$$

$$\begin{cases} K_Z + K_I + K_P = 1 \\ -10.0 \leq K_Z \leq 10.0 \\ -10.0 \leq K_I \leq 10.0 \\ -10.0 \leq K_P \leq 10.0 \end{cases} \quad (2.17)$$

In [24] device models of [20, 62–67, 106] are statistically analysed, and it is found that with 95.5% probability the ZIP load model parameter values of the devices are:

- $-0.602 \leq K_Z \leq 1.814$
- $-2.482 \leq K_I \leq 2.184$
- $-1.219 \leq K_P \leq 3.127$
- $-5.600 \leq K_Z, Q \leq 6.080$
- $-8.597 \leq K_I, Q \leq 6.241$
- $-1.595 \leq K_Q \leq 4.741$

Based on Table 2.6 the ZIP models of aggregated system loads presented in the analysed literature are in the ranges:

- $-0.11 \leq K_Z \leq 0.26$
- $0.38 \leq K_I \leq 0.86$
- $0.13 \leq K_P \leq 0.65$
- $-0.75 \leq K_Z, Q \leq 1.74$
- $-0.06 \leq K_I, Q \leq 1.75$
- $-0.26 \leq K_Q \leq 0.27$

¹⁰Corresponding to (1.3) and (1.5).

¹¹The first boundary condition corresponds to (1.4) and (1.6).

All these values are within the range of -10...10. For this reason values -10 and 10 were chosen as the boundary values for ZIP model estimation. The highest voltage sensitivity that could be modelled in this way would correspond to model $K_Z = 10$, $K_I = 0$, $K_P = -9$. According to (3.26) (introduced in Section 3.5), this would be approximately comparable to an exponential model with $K_{Exp} = 20$ (2.18).

$$K_{Exp} \approx \frac{2 \cdot 10 + 1 \cdot 0 + 0 \cdot (-9)}{10 + 0 - 9} = 20 \quad (2.18)$$

Table 2.6: ZIP load model parameter value ranges in literature.

Reference	K_Z	K_I	K_P	$K_{Z,Q}$	$K_{I,Q}$	K_Q
[108]	-0.11...0.26	0.38...0.86	0.13...0.65	-0.75...1.74	-0.06...1.75	-0.26...0.27

An example of an estimated load model is shown in Figure 2.10 where the measured power is fitted to an exponential and ZIP load model. The modelled load follows the voltage, as the model equation only takes into account the voltage sensitivity of the load.

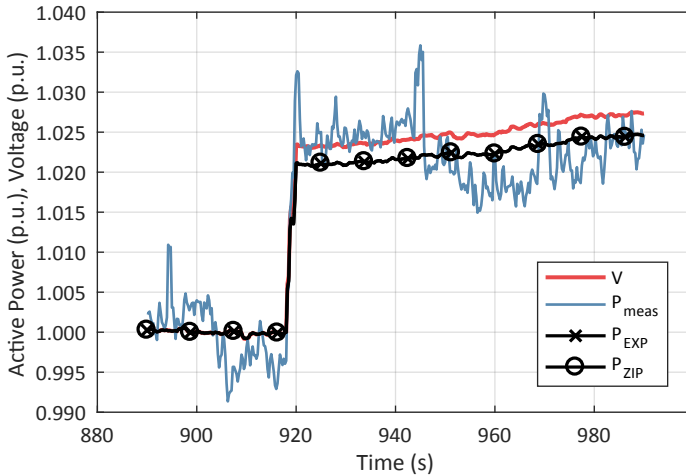


Figure 2.10: Measured and simulated load (estimated by exponential and ZIP model).

2.4.2 Impact of Event Filtering on Estimated Load Model Parameter Values

In the analysed DFR dataset there are 1843 events from 3 years. In Section 2.3.3 some properties of the recorded events were plotted and analysed. Furthermore, event filtering was applied to detect events that would comply with the requirements set in the literature. In this subsection the impact of filtering on estimated load models is analysed. To enable the analysis exponential load models were estimated for all the events that are in the dataset. The histograms of the estimated K_{Exp} and $K_{Exp,Q}$ values are shown in Figure 2.11.

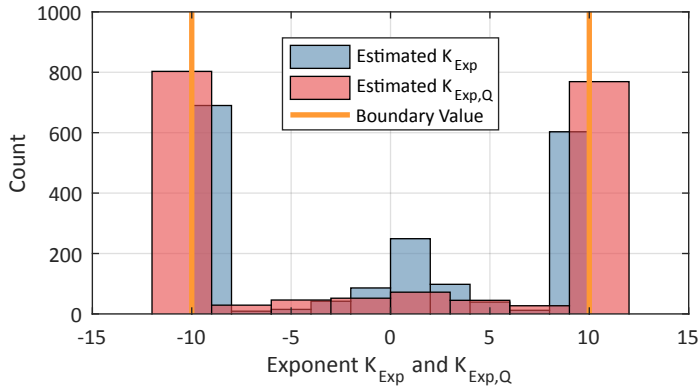


Figure 2.11: Estimated exponential parameter K_{Exp} and $K_{Exp,Q}$ when load models are estimated for all measured events, blue lines mark the boundary values used in estimation. Adapted from [VII]

In Figure 2.11 there are high bars at exponent value -10 and 10, which are caused by the boundary condition used (2.15). Previously, filters F8 and F9 were defined for detecting the boundary values of K_{Exp} and $K_{Exp,Q}$, respectively. When these filters are applied to the estimated load models, Figure 2.12 is acquired.

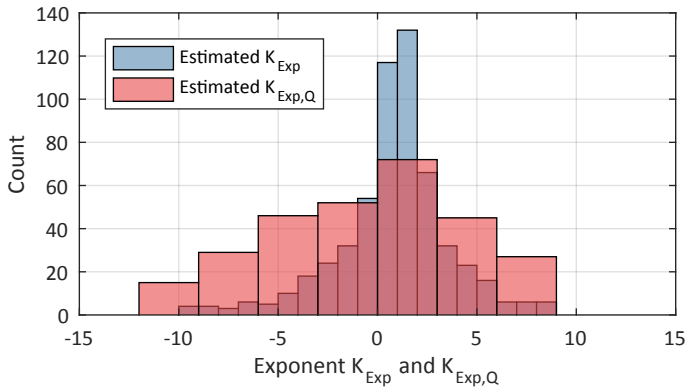


Figure 2.12: Estimated exponential parameter K_{Exp} and $K_{Exp,Q}$ when load models are estimated for all measured events and results at boundary values are removed. Adapted from [VII]

As the histogram (Figure 2.12) resembles normal distribution, the estimated load model parameter values were fitted to normal distribution (with 95% confidence). The mean μ and the standard deviation σ were calculated, and the values shown in Table 2.7 were acquired. The corresponding estimated Probability Density Functions (PDF) are shown in Figure 2.13 and Figure 2.14.

The estimated K_{Exp} and $K_{Exp,Q}$ values of the events detected by the filters F1...F9 are shown in Figure 2.15. The histogram of filter F1 (Figure 2.15a) indicates that the usage of the filter may cause additional offset error. When the negative values of K_{Exp} are removed, indicated by filter F1 as bad values, the symmetry of the estimated K_{Exp} values decreases and the mean value increases. Furthermore, after this change, the distribution of the values is no longer normal distribution. This change of mean value can be viewed as offset error. To avoid this error, filter F1 may need to be omitted when the mean value of the estimated load models is used. From Figure 2.15b, Figure 2.15c and Figure 2.15g it is clear that the events with the K_{Exp} and $K_{Exp,Q}$ values corresponding to the boundary values are not detected by filter F2, F3 and F7.

Table 2.7: Mean value μ and standard deviation σ of normal distribution fit (with 95% confidence), MSE weighted mean value μ_{MSE} and MAE weighted mean value μ_{MAE} based on all measured events, except boundary values. [VII]

Exp. Model	Average	Std. Dev.,	MAE Weight.	MSE Weight.
Parameter	μ	σ	Avg., μ_{MSE}	Avg., μ_{MAE}
K_{Exp}	0.792	2.854	0.927	0.782
$K_{Exp,Q}$	-0.448	4.857	0.176	1.034

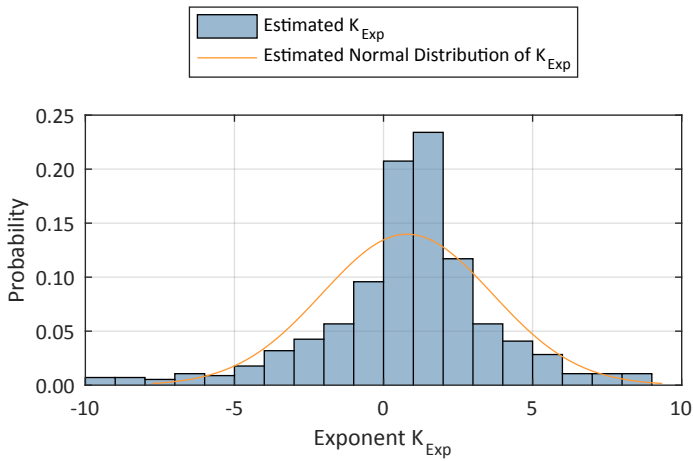


Figure 2.13: Estimated exponential parameter K_{Exp} when load models are estimated for all measured events and results at boundary values are removed. Adapted from [VII]

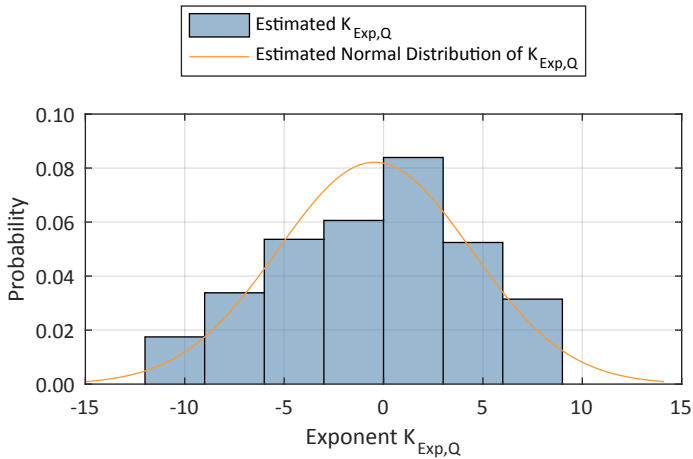


Figure 2.14: Estimated exponential parameter $K_{Exp,Q}$ when load models are estimated for all measured events and results at boundary values are removed. Adapted from [VII]

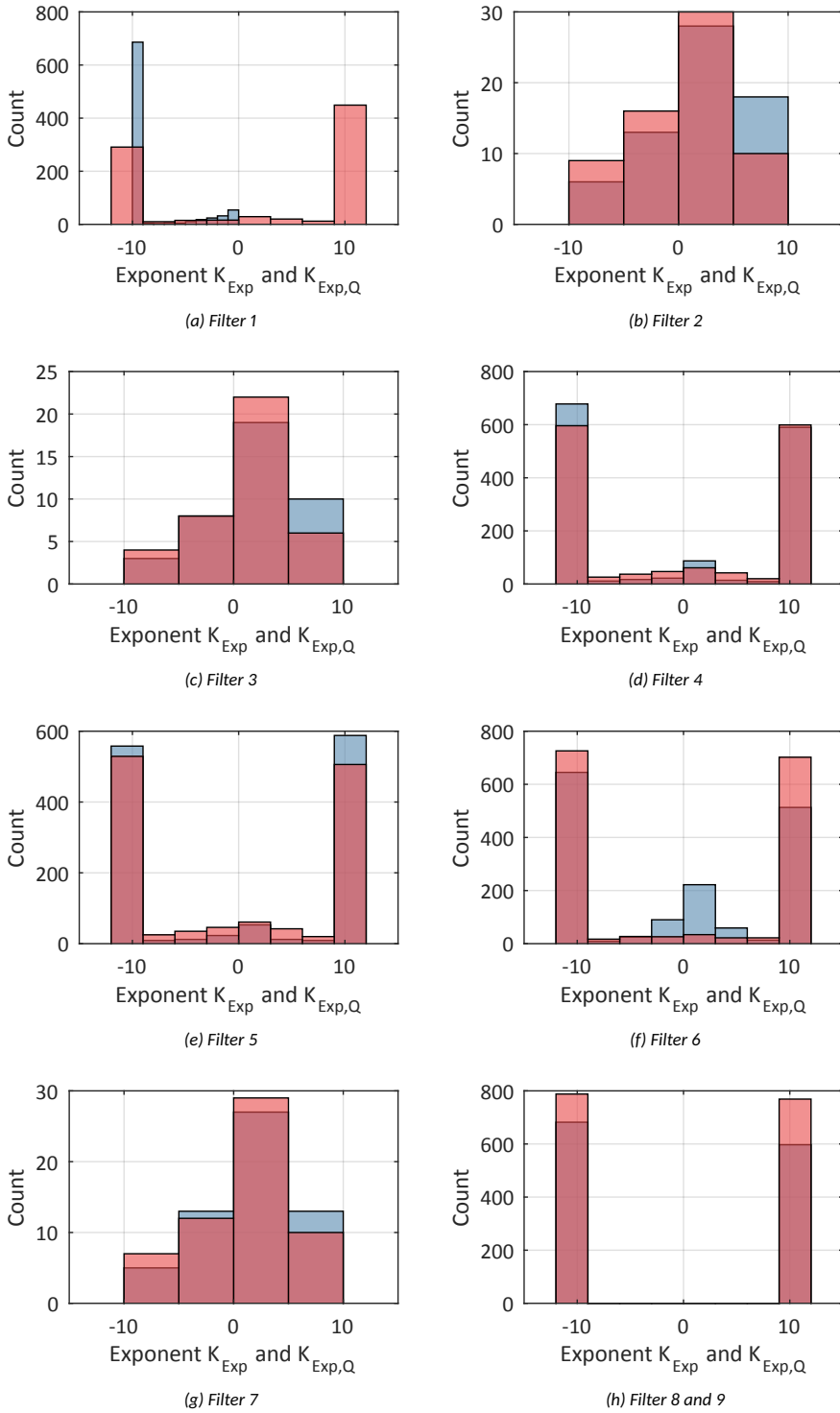


Figure 2.15: Estimated K_{Exp} and $K_{Exp,Q}$ of events flagged by different event filters.

Estimated Load Models After Event Filtering

Filters F2...F9¹² were applied on the load models estimated from the DFR data. After filtering the estimated K_{Exp} values corresponded to Figure 2.16 and $K_{Exp,Q}$ values to Figure 2.17.

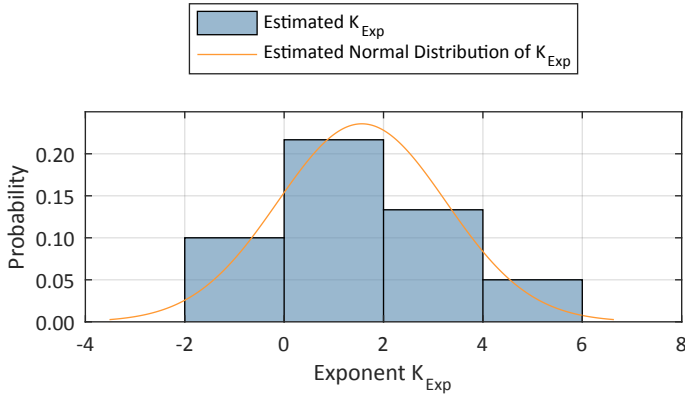


Figure 2.16: Estimated exponential parameter K_{Exp} when load models are estimated for filtered events.

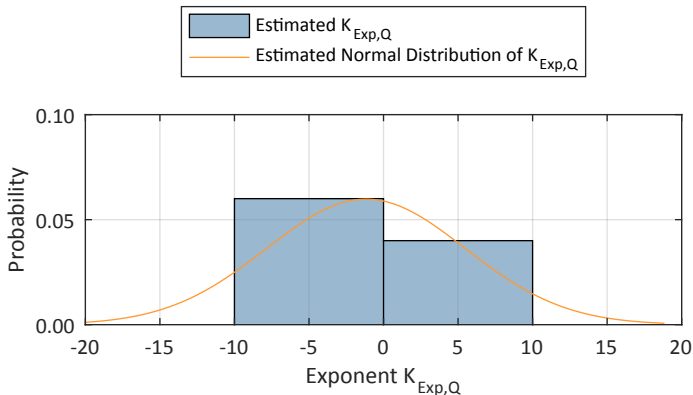


Figure 2.17: Estimated exponential parameter $K_{Exp,Q}$ when load models are estimated for filtered events.

The mean value of K_{Exp} (Table 2.8) increased from 0.792 (Table 2.7) to 1.018 as a result of applying filters F2...F8. The standard deviation (with 95% confidence) decreased from 2.854 to 2.498. This decrease in standard deviation indicates that the filtering could have improved the accuracy of the estimated value of K_{Exp} . In comparison, [109] obtained average values of K_{Exp} in the range 0.79...1.62 with standard deviations of 0.56...1.34. Compared to these values the obtained mean value is in the same range, but the standard deviation is significantly larger.

The mean value of exponent $K_{Exp,Q}$ changed according to Table 2.7 and Table 2.8 from -0.448 to -0.078, while the standard deviation increased from 4.857 to 5.148. In [109], the $K_{Exp,Q}$ mean values are in the range 2.69...5.73 with standard deviation 1.99...2.50. Compared to these values, the standard deviation of the values is around 2 times larger. Thus, compared to the results presented in the literature, this load model estimation approach may be less accurate. Some possible reasons for this difference could be the load

¹²F1 was omitted to avoid possible skewing of the mean value.

behaviour difference: higher variability of voltage sensitivity of the measured load compared the loads analysed in the literature. Alternatively, it could be caused by the difference of voltage level, time of measurement (e.g. typical loads from the 1990s and 2000s are different from the loads in the 2010s and 2020s).

Table 2.8: Mean value μ and standard deviation σ of normal distribution fit (with 95% confidence), MSE weighted mean value μ_{MSE} and MAE weighted mean value μ_{MAE} based on filtered events [VII]

Exp. Model	Average	Std. Dev.,	MAE Weight.	MSE Weight.
Parameter	μ	σ	Avg., μ_{MSE}	Avg., μ_{MAE}
K_{Exp}	1.018	2.498	0.889	0.763
$K_{Exp,Q}$	-0.078	5.148	0.272	0.964

2.4.3 Impact of Measurement Time on Estimated Load Model Parameter Values

In publication [III] a case study was presented. In the study small voltage disturbances were induced at different times of the day using shunt reactors of the system, and load models were estimated for 2 different substations. Voltage changes were induced at 3 different times of the day: night (around 3 am), day (around 2 pm) and evening (around 7 pm). Temperature in these periods was near 0°C. In addition, in the first substation an additional test was carried out on another day with significantly colder weather (the temperature at the time of the measurement was around -10°C). The number of recorded voltage disturbances with relative voltage difference (2.6) over 0.5% is shown in Table 2.9.

Table 2.9: Number of voltage disturbances. [III]

Substation	Cold Day	Day	Evening	Night
1	5	11	8	10
2	-	11	8	10

The estimated exponential load models corresponding to the detected voltage changes are plotted in Figure 2.18. There is significant variation for the estimated values, which was probably caused by the stochastic changes of the load. The values pose the question "How can we find a representative value?" Some potential methods for this are discussed in Section 2.5.

In order to acquire a representative value for each time period (cold day, day, evening, night), the mean and error weighted mean (Section 2.5) value were calculated. The calculated values are shown in Table 2.10 and Table 2.11. Based on Table 2.10, on a cold day the K_{Exp} is higher compared to a warmer day. Thus, the K_{Exp} value has a temperature dependence, which is most likely caused by heating loads. To detect cooling loads, measurements from a significantly warmer day would be needed. The lowest K_{Exp} values occur for the nighttime measurements, and highest during the evenings. According to Table 2.5, the daytime values of K_{Exp} depend the most on the post-processing method used. The differences are up to 20%. At the other times of the day the differences are within 10% of the calculated value.

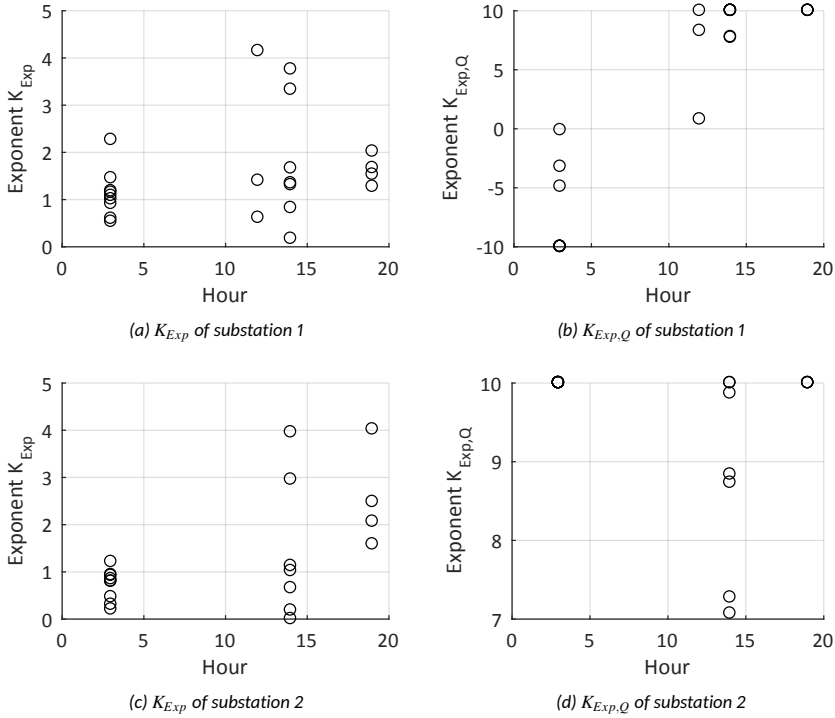


Figure 2.18: Exponential load model parameters estimated at 2 substations at different times of the day.

Table 2.10: Impact of post-processing method on calculated value of exponent K_{Exp} . [III]

Substation	Time Period	MSE	NMSE	MAE	NMAE	Mean	Median
		Weight.	Weight.	Weight.	Weight.		
1	Cold day	1.53	1.58	1.95	1.97	2.06	1.40
	Day	1.44	1.46	1.60	1.61	1.77	1.35
	Evening	1.58	1.58	1.59	1.59	1.62	1.60
	Night	1.06	1.06	1.09	1.09	1.13	1.08
2	Day	1.04	1.05	1.23	1.23	1.42	1.02
	Evening	2.48	2.43	2.56	2.53	2.54	2.27
	Night	0.81	0.81	0.77	0.77	0.72	0.80

The reactive load model parameter $K_{Exp,Q}$ is in many cases on the boundary value 10. A different situation is seen for the daytime values of $K_{Exp,Q}$, which are mostly close to 9. This could have been caused by the higher reactive power consumption that decreased the relative stochastic changes of the reactive loads. An exceptional situation is the night-time value of substation 1, which is highly dependent on the post-processing method and obtained negative values.

Table 2.11: Impact of post-processing method on calculated value of exponent $K_{Exp,Q}$. [III]

Substation	Time Period	MSE	NMSE	MAE	NMAE	Mean	Median
		Weight. Avg.	Weight. Avg.	Weight. Avg.	Weight. Avg.		
1	Cold day	8.54	8.66	8.65	8.81	6.37	8.30
	Day	8.81	9.00	9.04	9.13	9.36	10.00
	Evening	10.00	10.00	10.00	10.00	10.00	10.00
	Night	-3.07	-2.85	-5.67	-5.67	-7.58	-10.00
2	Day	8.82	8.84	8.83	8.83	8.83	8.84
	Evening	10.00	10.00	10.00	10.00	10.00	10.00
	Night	10.00	10.00	10.00	10.00	10.00	10.00

2.4.4 Impact of Distributed Generation on Estimated Load Model Parameter Values

In [110–112] aggregated bus loads that include wind turbines are modelled by composite models. The composite models include a static load model and an induction machine model (or several machine models), which are connected in parallel. Several composite models are discussed and compared in [110]. Parameter estimation methods for composite models are presented and analysed in [111, 112].

Figure 2.19 illustrates how the static voltage characteristic of an aggregated composite load (combined response of a DG modelled as negative load and voltage sensitive load with voltage characteristic $K_{Exp,L} = 2$, corresponding ZIP model: $K_Z = 1$, $K_I = 0$, $K_P = 0$). The rise of the voltage characteristic (voltage sensitivity of the load) increases with increasing penetration of DG.

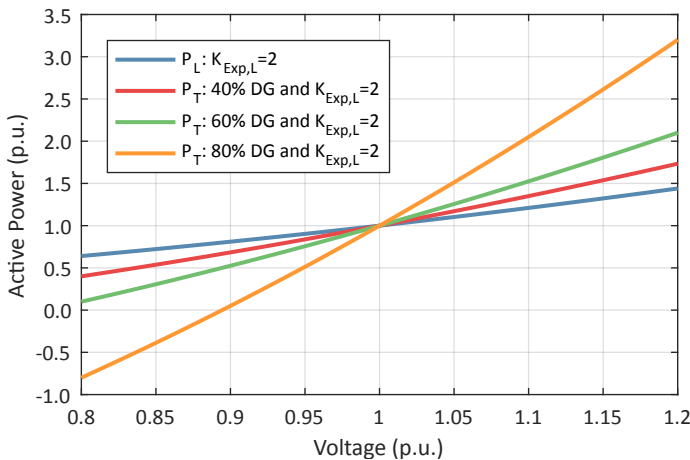


Figure 2.19: Normalised voltage characteristic P_L of exponential load model with exponent $K_{Exp,L} = 2$. Aggregated load: P_L with DG 40% of P_{L0} , 80% of P_{L0} and 120% of P_{L0} .

In [11] aggregated loads including distributed generation are estimated by an exponential load model using voltage changes induced by a smart transformer. The voltage sensitivity of the exponential model is assumed to be equal to the exponent (2.19), similarly to [113].

$$\frac{dP/P_b}{dV/V_b} = K_{Exp} \quad (2.19)$$

In [11] (2.20) is derived by assuming the Distributed Generation (DG) to be operating at a unity power factor ($Q_G = 0$), and the power generated by the DG (P_G) to be smaller than the load of the feeder P_L ($P_G < P_L$).

$$K_{Exp,T} = K_{Exp,L} \cdot \frac{P_L}{P_L - P_G} \quad (2.20)$$

Based on (2.20) it is possible to derive (2.21), which describes the voltage sensitivity of the load $K_{Exp,L}$ based on apparent voltage sensitivity K_{Exp} of the feeder, load power P_L and generated power P_G .

$$K_{Exp,L} = K_{Exp,T} \cdot \frac{P_L - P_G}{P_L} \quad (2.21)$$

When the penetration level of DG corresponding to the fraction P_G/P_L is denoted by factor β , (2.20) and (2.21) can be derived to correspond to (2.22) and (2.23), respectively.

$$K_{Exp,T} = K_{Exp,L} \cdot \frac{1}{1 - \beta} \quad (2.22)$$

$$K_{Exp,L} = K_{Exp,T} \cdot (1 - \beta) \quad (2.23)$$

The voltage sensitivity of the ZIP load model is (2.24).

$$\frac{dP/P_b}{dV/V_b} = 2 \cdot K_Z + K_I \quad (2.24)$$

Equation (2.20) was derived based on the voltage sensitivity of the exponential model. Applying the same factors on voltage sensitivity of ZIP load model (2.24), equation (2.25) with multiple solutions is acquired.

$$2 \cdot K_{Z,T} + K_{I,T} = \frac{P_L}{P_L - P_G} \cdot (2 \cdot K_{Z,L} + K_{I,L}) \quad (2.25)$$

One solution to (2.25) is (2.26). Using DG penetration level β , it can also be written as (2.27). Similarly, (2.28) and (2.29) can be acquired.

$$\begin{cases} K_{Z,T} = \frac{P_L}{P_L - P_G} \cdot K_{Z,L} \\ K_{I,T} = \frac{P_L}{P_L - P_G} \cdot K_{I,L} \\ K_{P,T} = 1 - K_{I,T} - K_{Z,T} \end{cases} \quad (2.26)$$

$$\begin{cases} K_{Z,T} = \frac{1}{1 - \beta} \cdot K_{Z,L} \\ K_{I,T} = \frac{1}{1 - \beta} \cdot K_{I,L} \\ K_{P,T} = 1 - K_{I,T} - K_{Z,T} \end{cases} \quad (2.27)$$

$$\begin{cases} K_{Z,L} = \frac{P_L - P_G}{P_L} \cdot K_{Z,T} \\ K_{I,L} = \frac{P_L - P_G}{P_L} \cdot K_{I,T} \\ K_{P,L} = 1 - K_{I,L} - K_{Z,L} \end{cases} \quad (2.28)$$

$$\begin{cases} K_{Z,L} = (1 - \beta) \cdot K_{Z,T} \\ K_{I,L} = (1 - \beta) \cdot K_{I,T} \\ K_{P,L} = 1 - K_{I,L} - K_{Z,L} \end{cases} \quad (2.29)$$

Figure 2.20 illustrates how the apparent voltage sensitivity K_{Exp} (2.20) of the feeder depends on the penetration level of the DG. The load is assumed to have exponent $K_{Exp,L} = 2$. It is clear that the DG increases the voltage sensitivity of the load and DG aggregate, the apparent load of the feeder.

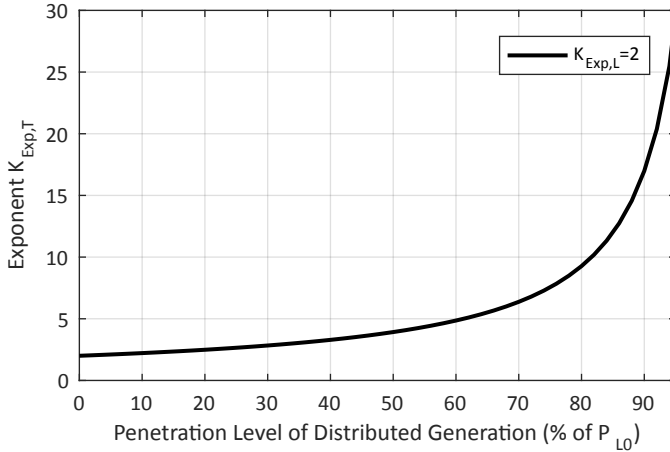
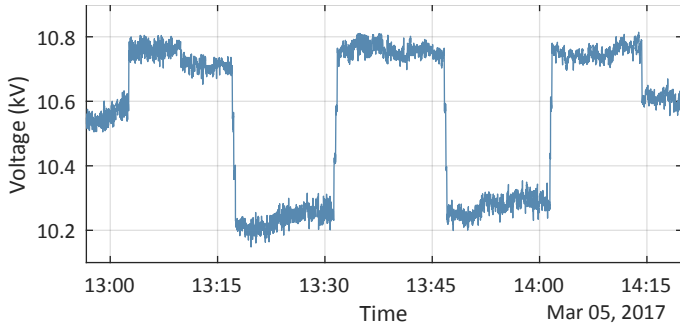
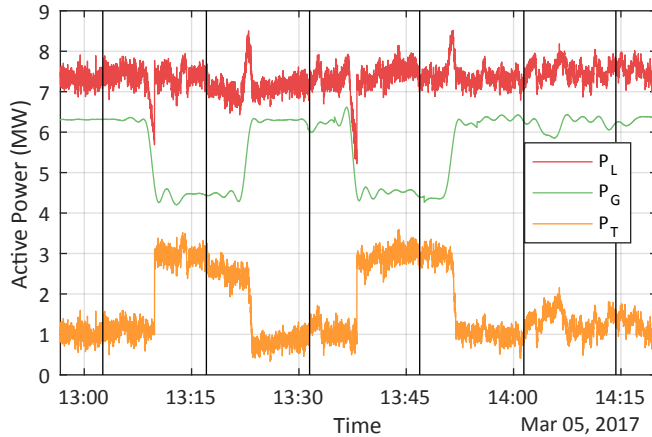


Figure 2.20: Impact of penetration level of DG on exponential voltage characteristic of aggregated load model (based on (2.20)).

In order to validate how closely (2.20), (2.21), (2.26) and (2.28) match the measurement data a case study was conducted in a medium voltage distribution network. The case study is presented and discussed in [IV] and [VIII]. During the measurement period of the case study the average load of the customers connected to the feeder was 7.4 MW. There is 6.7 MW of DG connected to the feeder: 2 wind turbines (2.3 MW and 2.0 MW), and a 2.4 MW combined heat and power plant (CHP). The DG units are operated in fixed $\cos\phi$ mode. Measurement data were collected using PQM and SCADA system. The voltage changes shown in Figure 2.21a were induced by OLTC switching. The first and last OLTC position change were 1 tap, the other changes were 3 taps. The generated power in Figure 2.21b was acquired from the SCADA system. Rapid generator output power P_{Gen} changes were caused by the unplanned starting and stopping of a wind turbine that might have been caused by a combination of bad configuration of the control system and voltage changes.



(a) Measured voltage



(b) Measured and calculated power data. Calculated load power P_L , total power output of the distributed generation according to SCADA system P_G , and measured transformer load P_T (net load). Voltage events marked by vertical lines.

Figure 2.21: Measured and calculated values during the case study of distributed generation impact. Adapted from [VIII]

When the load model parameters (exponential model parameter $K_{Exp,L}$) were estimated based on calculated total load (supplied by the DG units and the transformer), the values were in the range 0.74...1.24 (see Table 2.12). The static load model of the aggregated transformer load (sum of DG and load) displayed significantly higher values in the range 1.30...2.92 (lower level of P_{Gen}) and range 5.11...8.15 (higher level of P_{Gen}). The net load model parameter values are given in Table 2.13. This was an expected result considering Figure 2.19 and Figure 2.20.

Using (2.20) and (2.21) the apparent transformer load model parameter $K_{Exp,T}$ was calculated from $K_{Exp,L}$ and vice versa. The calculated values are shown with estimated values in Figure 2.22. In the figure, the estimated $K_{Exp,T}$ and $K_{Exp,L}$ values of the first two events and the 4th event closely match with the calculated values. However, the 3rd, 5th and 6th event display significant differences for the transformer load exponent $K_{Exp,T}$. When the estimated exponential models and modelling error in Table 2.13 is compared to the calculated models in Table 2.14, it is clear that there is a significant difference in the same parameter values, as noted in Figure 2.22. However, the modelling errors (MSE and MAE) are similar for all the event-based models. Thus, the calculated exponent values have an accuracy similar to the estimated values, despite the value difference.

Table 2.12: Estimated load models of connected load

Event	ZIP Model					Exponential Model			
	$K_{Z,L}$	$K_{I,L}$	$K_{P,L}$	MSE		$K_{Exp,L}$	MSE		
				$(\cdot 10^{-3})$	MAE		$(\cdot 10^{-5})$	MAE	
1	0.38	-0.02	0.65	0.19	0.010	0.74	17	0.011	
2	-8.32	17.66	-8.33	32.43	0.122	1.24	10	0.008	
3	4.71	-8.77	5.06	7.85	0.074	0.79	14	0.009	
4	10.49	-20.00	10.51	40.50	0.170	0.62	9.9	0.008	
5	1.32	-2.05	1.73	0.30	0.014	0.65	8.1	0.008	
6	2.07	-3.09	2.02	0.17	0.011	1.03	4.7	0.006	

Table 2.13: Estimated load models of transformer load (net load)

Event	ZIP Model					Exponential Model			
	$K_{Z,T}$	$K_{I,T}$	$K_{P,T}$	MSE		$K_{Exp,T}$	MSE		
				$(\cdot 10^{-2})$	MAE		$(\cdot 10^{-3})$	MAE	
1	4.31	-3.40	0.09	1.87	0.10	5.11	19	0.105	
2	-8.69	20.00	-10.31	4.82	0.16	2.92	1.9	0.034	
3	-5.36	20.00	-13.64	10.03	0.26	8.11	14	0.093	
4	10.83	-20.00	10.17	3.76	0.16	1.30	1.3	0.030	
5	-2.46	13.61	-10.15	6.67	0.20	7.64	11	0.084	
6	4.61	-1.44	-2.17	0.47	0.05	8.15	3.5	0.046	

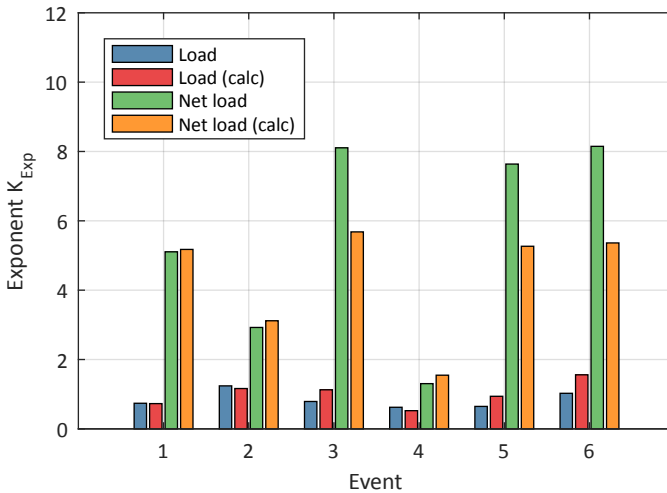


Figure 2.22: Actual load model (exponent $K_{Exp,L}$) and apparent net load (exponent $K_{Exp,T}$) of the feeding transformer.

Table 2.14: Transformer load modelling by calculated load model (based on DG penetration and the model of the connected load)

Event	ZIP Model					Exponential Model		
	$K_{Z,T}$	$K_{I,T}$	$K_{P,T}$	MSE	MAE	$K_{Exp,T}$	MSE	MAE
1	2.56	-0.01	-1.55	0.020	0.11	5.18	0.019	0.11
2	-21.12	44.77	-22.65	0.286	0.36	3.12	0.002	0.03
3	35.52	-66.44	31.92	1.156	0.76	5.68	0.018	0.10
4	26.08	-49.73	24.65	0.160	0.35	1.55	0.001	0.03
5	13.47	-22.17	9.70	0.019	0.11	5.27	0.015	0.10
6	14.64	-23.69	10.05	0.004	0.05	5.36	0.004	0.05

In the case study the DG units were installed close to the 10 kV substation. This means that the voltage profile of the medium voltage feeder was not affected by the generation. This situation is similar to the parallel operation of DG units and feeder with loads. The DG has an impact on the load of the transformer, but not on the operation points of the loads. When the DG is further from the substation, somewhere on the feeder, it would have an impact on the voltage profile of the feeder, losses of the feeder (analysed in [14]) and load bus voltages. The impact of DG on feeder voltages is discussed in [114].

2.5 Post-processing of Estimated Load Models

In the case study presented in [III] the intra-day variability of load models was analysed based on relatively small induced voltage disturbances (mostly $\leq 3\%$). The small load deviations caused by these voltage changes are of a comparable size to the stochastic changes of the load. In order to quantify the fit of the estimated models (match between the measured response and estimated response), several commonly used error measures presented in Section 2.5.1 were adopted. A method is presented in Section 2.5.2 for post-processing a set of estimated load model parameter values based on the estimation errors.

2.5.1 Estimation Error

The estimation error quantifies the mismatch between the load calculated using the estimated load model P_{model} , and the measured load P_{meas} . For calculating load P_{model} the measured voltage values are used and the load is calculated based on the equation of P_{EXP} (1.1), Q_{EXP} (1.2), P_{ZIP} (1.3) or Q_{ZIP} (1.5). In the context of this thesis the load models were estimated by using the initial voltage V_0 , active power P_0 , and reactive power Q_0 as the base values V_b , P_b , and Q_b , respectively. When calculating the value P_{model} , a similar use of base value is applied as during the estimation. The following equations are given for active load models, reactive load models can be calculated using similar equations.

Four different measures of error are used in Section 2.4.2, Section 2.4.3 and Section 2.5.2 for calculating a representative value from a set of estimated load models:

- Mean Absolute Error (MAE) (2.30)
- Normalised Mean Absolute Error (NMAE) (2.31)
- Mean Square Error (MSE) (2.32)
- Normalised Mean Square Error (NMSE) (2.33)

The measurement samples are denoted in the following equations by P_{meas_i} and modelled values P_{model_i} , where i is the index of the sample from $1 \dots N$. N is the total number of samples.

$$MAE = \frac{1}{N} \sum_{i=1}^N |P_{model_i} - P_{meas_i}| \quad (2.30)$$

$$NMAE = \frac{1}{N} \sum_{i=1}^N \left| \frac{P_{model_i} - P_{meas_i}}{P_{meas_i}} \right| \quad (2.31)$$

$$MSE = \frac{1}{N} \sum_{i=1}^N (P_{model_i} - P_{meas_i})^2 \quad (2.32)$$

$$NMSE = \frac{1}{N} \sum_{i=1}^N \left(\frac{P_{model_i} - P_{meas_i}}{P_{meas_i}} \right)^2 \quad (2.33)$$

2.5.2 Calculating Representative Value from Set of Values

Typically, several load model parameter sets are estimated when measurement-based load modelling is applied. One load model is estimated for each processed event (analysis window). To find a representative model, commonly, the average value is calculated for each parameter of the used model. This approach has been used for example in [9, 42, 70, 77, 105, 109, 115]. The outliers of estimated load model parameter values can significantly affect the results when the number of averaged samples is relatively small. This has also been pointed out in [89]. In contrast to the common averaging approach, [116] uses a multi-curve identification process. In this approach the measurement data of several events is used to estimate a load model. Considering the stochastic nature of the load, the accuracy of the estimated load models varies. For this reason, it is reasonable to give a higher weight to more accurate models when the representative load model is calculated.

When M load model parameter values K_i have been estimated, and for each a weight w_i (describing estimation accuracy) is given, the weighted average value can be calculated by (2.34).

$$K = \frac{\sum_{i=1}^M (w_i \cdot K_i)}{\sum_{i=1}^M w_i} \quad (2.34)$$

The accuracy of estimated load models is often quantified by a measure of error (e.g. by MAE (2.30), NMAE (2.31), MSE (2.32), or NMSE (2.33)). If the accuracy of the estimated load model parameter values K_i is assumed to be inversely proportional to the modelling error γ_i , the weight w_i in (2.34) can be replaced by $1/\gamma_i$. In this thesis, MAE (2.30), NMAE (2.31), MSE (2.32), or NMSE (2.33) are used as the value of γ_i when using (2.35).

$$K = \frac{\sum_{i=1}^M \frac{K_i}{\gamma_i}}{\sum_{i=1}^M \frac{1}{\gamma_i}} \quad (2.35)$$

The estimation error weighted averaging was used in Section 2.4.2 and Section 2.4.3 for post-processing the estimated load models. The results in Section 2.4.2 indicate that, compared to averaging, the MAE and MSE weighted averaging are less affected by the event filtering (selection of events). This could indicate a greater robustness. The results in Section 2.4.3 indicate a 10...20% difference caused by the selection of measure of error. Due to the significant uncertainty and unknown true value, it is difficult to assess which of the calculated values has the best accuracy.

2.6 Conclusion and Discussion

There are different measurement systems used in the transmission system for acquiring measurement data (Section 2.2.2). However, only some of these systems are usable for load model estimation. The placement of the devices and availability of the measurement data determines the observability of the aggregated loads. To choose representative loads, and grouping similar loads into clusters, K-means clustering was introduced in Section 2.2.3. The aggregated loads were grouped into 10 groups based on monthly load class compositions. In Section 2.3.3 and Section 2.4.2 the historical DFR data of a substation were processed to illustrate the impact of event filtering and to detect unsuitable events (from a load model estimation viewpoint). When all the event requirements stated in Section 2.2.1 were applied on the analysed DFR dataset in the strictest way, only 1 event was left from recorded 1843 events. When the dataset was used for estimating static load models in Section 2.4.2 the large values of standard deviation indicated a result with low reliability. As an alternative to the commonly used averaging, estimation error weighted averaging was proposed in Section 2.5, and the method was applied on load models estimated in Section 2.4.2 and 2.4.3. The error weighted averaging proved to be less sensitive to event filtering than normal averaging. In the conducted case studies the true value of the load was unknown, and for this reason it was not possible to determine the post-processing method that would provide the most accurate results. In Section 2.5.2 MAE (2.30), NMAE (2.31), MSE (2.32), and NMSE (2.33) were used as the measures of goodness-of-fit. Other measures of error could be tested for γ_i in (2.35). The impact of DG on the estimation of aggregated load model was discussed in Section 2.4.4 for the simplest case when the DG unit and the load are connected close to the aggregated bus and the feeder losses are not affected by the DG output. The simple analytical equations used for predicting the apparent voltage sensitivity of the load was found to work well under such circumstances. Other network configurations could be analysed.

3 Static Load Model Conversion

3.1 Introduction

The use of several different load models sometimes leads to model conversion: parameter values of one type of load model are known, and the parameter values of another type need to be acquired. In this chapter methods for exponential load model to ZIP (second order polynomial) load model conversion, and ZIP model to exponential load model conversion, are developed and presented.

In Section 3.3, load model conversion using Non-linear Least Squares (NLS) is discussed. This approach can be used for either conversion direction, and can handle a variety of application needs. Thus, it is the most flexible approach for conducting the conversion. In Section 3.4 several analytical methods for exponential to ZIP load model are presented. These methods are denoted in Table 3.1 by AM1, AM2, AM3, similarly to [I] and [VI]. Among those methods there are some that are suitable for converting exponential models to constrained¹³ ZIP models, and some which can lead to unconstrained¹³ models. In Section 3.5 an analytical method for ZIP to exponential load model conversion is presented. This method is widely used, and is included to give a better comparability of the methods.

Table 3.1: Analysed conversion methods and the available conversions.

Method	Section	From Exponential to		From ZIP to Exponential
		ZIP (constr.)*	ZIP (unconstr.)*	
NLS	3.3	Yes	Yes	Yes
AM1	3.4.1	Yes	No	No
AM2	3.4.2	Yes	Yes	No
AM3	3.4.3	No	Yes	No
Analytical (ZIP to exp)	3.5	No	No	Yes

* "Yes" in only unconstrained column means that using the method can in some cases lead to unconstrained¹³ ZIP models. When "Yes" is in both exponential to ZIP columns, the user can choose if they wish to apply constraints to the output models or not.

There is typically a mismatch between the original model and the converted model. In order to quantify the difference, in Section 3.2 the measures of error are defined, which are used for comparing the performance of the methods. The estimated load models presented in Section 2.4.4 are converted in Section 3.6 to provide a numerical example of load model conversion. To illustrate how the conversion error affects the results of load flow calculations, the results of a case study are introduced in Section 3.7.

The included conversion methods for exponential to ZIP load model conversion were first presented in [I] and [VI]. The developed analytical methods provide lower conversion error than the analytical method described in the literature¹⁴. The methods for ZIP

¹³In some literature unconstrained ZIP models are defined as accurate ZIP models, for example in [18, 24]. As the term "accurate load model" is used in this thesis with another meaning, the terms constrained and unconstrained ZIP load model are used for classifying ZIP models in respect to parameter constraints. The difference between a constrained and unconstrained ZIP model is explained in Section 1.2.3. Briefly, the multipliers of ZIP model parameters of the constrained model are limited to the range of 0...1. The unconstrained model does not have this value limitation.

¹⁴Analytical conversion method described in [117] was implemented as the method AM1 for comparison. The implementation is described in Section 3.4.1. Comparison to the developed analyti-

to exponential load model were presented and analysed in [II, VI]. Different aspects of conversion error were analysed in [I, II, VI]. Furthermore, in [VI] the impact of conversion error on load flow calculation results was discussed and illustrated by a case study. The author found no similar analysis in the literature.

3.2 Measures of Conversion Error

In this thesis, in the case of load model conversion, a mathematical model of a voltage characteristic of a load is converted to another mathematical model. Depending on the mathematical models used, voltage characteristic and conversion method, the original and the converted model may have a mismatch. This mismatch is considered to be the load model conversion error, and the original model describing the voltage characteristic is assumed to be accurate. To illustrate the conversion error of static load models, two static voltage characteristics and the mismatch of the characteristics are shown in Figure 3.1.

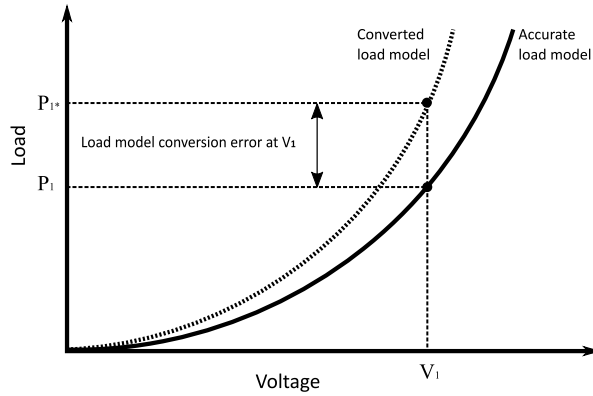


Figure 3.1: Load model conversion error (model mismatch) at voltage V_i when accurate load model is converted to a converted load model. Due to the conversion error, the converted model indicates load P_{1^*} at V_i instead of P_1 .

To quantify the previously described mismatch of load models (original and converted), several measures of error can be used. The original load characteristic (input model) P_{IN} is assumed to be accurate. The difference between converted (calculated/fitted) characteristic P_{OUT} and input characteristic P_{IN} is considered to be the conversion error. In the context of this thesis, depending on the conversion direction and the converted model, P_{IN} and P_{OUT} can be P_{EXP} (1.1), Q_{EXP} (1.2), P_{ZIP} (1.3) or Q_{ZIP} (1.5).

The difference $\varepsilon(V_i)$ (3.1) of the original (accurate) load characteristic P_{IN} and converted load characteristic P_{OUT} at voltage V_i is considered to be the conversion error at voltage V_i .

$$\varepsilon(V_i) = P_{IN}(V_i) - P_{OUT}(V_i) \quad (3.1)$$

Similarly, the relative difference $\eta(V_i)$ (3.2) of the original (accurate) load characteristic P_{IN} and converted load characteristic P_{OUT} at voltage V_i is considered to be the relative conversion error at voltage V_i .

$$\eta(V_i) = \frac{P_{IN}(V_i) - P_{OUT}(V_i)}{P_{IN}(V_i)} \quad (3.2)$$

cal method AM2 is provided in Section 3.4.2. Furthermore, Section 3.4.3 indicates that developed method AM3 provides even lower conversion error than AM1 and AM2.

Conversion error $\varepsilon(V_i)$ describes the conversion error at a specific voltage V_i . To compare the performance of conversion methods across a voltage range $V_i \in \{V_1, V_2 \dots V_N\}$ ($i, N \in \mathbb{N}$) the Mean Absolute Error (MAE) (3.3) can be used.

$$MAE = \frac{1}{N} \sum_{i=1}^N |\varepsilon(V_i)| = \frac{1}{N} \sum_{i=1}^N |P_{IN}(V_i) - P_{OUT}(V_i)| \quad (3.3)$$

Similarly, the relative conversion error $\eta(V_i)$ describes the conversion error at a specific voltage V_i . To quantify the relative conversion error across a voltage range $V_i \in \{V_1, V_2 \dots V_N\}$ ($i, N \in \mathbb{N}$) the Normalised Mean Absolute Error (NMAE) (3.4) can be used.

$$NMAE = \frac{1}{N} \sum_{i=1}^N |\eta(V_i)| = \frac{1}{N} \sum_{i=1}^N \left| \frac{P_{IN}(V_i) - P_{OUT}(V_i)}{P_{IN}(V_i)} \right| \quad (3.4)$$

In the thesis and related publications, voltage range 0.8...1.2 p.u. is used as MAE and NMAE calculation range $V_1 \dots V_N$.¹⁵

3.3 Using Non-linear Least Squares Optimisation for Load Model Conversion

In Chapter 2 load models were estimated from measurement data using an NLS fitting (Section 2.4.1). For estimation, a load model was fitted to measured values, and the goal was to minimise the difference between measured and modelled values. The load model conversion is also a curve fitting problem: one curve (original load model) is known, and another curve (converted load model) is fitted with the goal of minimising the difference between the two curves. This optimisation problem can be written as a NLS optimisation problem, which has the objective of minimising the sum of squared errors (3.5). In the case of NLS, the error $\psi(V_i)$ is minimised across voltage range $V_i \in \{V_1 \dots V_N\}$ ($i, N \in \mathbb{N}$).

$$\min \sum_{i=1}^N [\psi(V_i)]^2 \quad (3.5)$$

Error $\psi(V_i)$ can be replaced by absolute conversion error $\varepsilon(V_i)$ (3.1) formulating (3.6) for minimising absolute error, and by relative conversion error $\eta(V_i)$ (3.2) formulating (3.7) for relative conversion error minimisation. The input model is denoted by P_{IN} and the output model by P_{OUT} . In the context of this thesis, depending on the conversion direction and the converted model, P_{IN} and P_{OUT} can be P_{EXP} (1.1), Q_{EXP} (1.2), P_{ZIP} (1.3) or Q_{ZIP} (1.5).

$$\min \sum_{i=1}^N [\varepsilon(V_i)]^2 = \sum_{i=1}^N [P_{IN}(V_i) - P_{OUT}(V_i)]^2 \quad (3.6)$$

¹⁵The voltage range was motivated by the PSCAD implementation of the exponential load model described in Section 1.2.2. In PSCAD calculations, the exponential model is replaced by a constant impedance model when the load bus voltage is not within range 0.8...1.2 p.u. The PSS®E main load model (similar to ZIP model) uses another approach for modelling load at low voltages. The PSS®E approach is described in Section 1.2.3. Common to both software, at low voltages, the configured exponential or ZIP model is not used for calculations.

$$\min \sum_{i=1}^N [\eta(V_i)]^2 = \sum_{i=1}^N \left[\frac{P_{IN}(V_i) - P_{OUT}(V_i)}{P_{IN}(V_i)} \right]^2 \quad (3.7)$$

In the case of exponential to ZIP model conversion, the NLS optimisation problem, (3.6) or (3.7), is subject to $K_Z + K_I + K_P = 1$ (1.4). To restrict the approximated ZIP models to constrained models, additionally: $0 \leq K_Z \leq 1$, $0 \leq K_I \leq 1$ and $0 \leq K_P \leq 1$.

3.4 Analytical Methods for Exponential to ZIP Model Conversion

3.4.1 Analytical Method AM1

The method proposed in [117]

An analytical method for converting exponential load models to ZIP models is described in [117] without any reference to other publications. The analytical method AM1 is an improved version of the method. The method proposed in [117] is case based: depending on the exponent K_{Exp} value a ZIP model is chosen or a set of equations is used for acquiring the ZIP model parameter values.

Exponential models with small exponent K_{Exp} values (K_{Exp} is less than 0.5) are converted to a constant power model. The constant power component K_P of ZIP model is set to 1, thus $K_Z = K_I = 0$. When the exponent K_{Exp} is less than 1 (and larger than 0.5), the constant current model is used: K_I is set to 1, thus $K_Z = K_P = 0$. Exponential models with exponent greater than 2 are converted to constant impedance model: constant impedance component K_Z of ZIP model is set to 1, thus $K_I = K_P = 0$. When the value of K_{Exp} is between 1 and 2, the following equation system is solved:

$$\begin{cases} K_Z + K_I = 1 \\ 2 \cdot K_Z + K_I = K_{Exp} \end{cases} \quad (3.8)$$

The used analytical method AM1

The previous description of the conversion method leaves the exponential to ZIP model conversion undefined for situations when $K_{Exp} = 0.5$, $K_{Exp} = 1$, and $K_{Exp} = 2$. This is caused by the use of strict inequality relations, which do not include the limits. Moreover, solving the equation system (3.8) each time a conversion is conducted is impractical.

At $K_{Exp} = 0.5$, both the constant power and constant current load model would be around 0.5 powers off from the value with lowest error. Thus, adding equal to term to either causes an error. The previously undefined model ($K_{Exp} = 0.5$) was assigned a constant current model by (3.10). The second undefined model ($K_{Exp} = 1$) behaves as a constant current model, so it was assigned to (3.10). The third undefined model $K_{Exp} = 2$ would behave as a constant impedance, thus it was assigned to (3.12). The equation system (3.8) has a solution (3.11). $K_Z = K_{Exp} - 1$ can be derived by subtracting the first equation of (3.8) from the second equation of (3.8). Next, the equation $K_I = 2 - K_{Exp}$ can be found by replacing K_Z in the first equation of (3.8) by $K_Z = K_{Exp} - 1$.

After making the described improvements, the conversion method can be presented by the following set of case-based equations:

$$K_{Exp} < 0.5 \rightarrow \begin{cases} K_Z = 0 \\ K_I = 0 \\ K_P = 1 \end{cases} \quad (3.9)$$

$$0.5 \leq K_{Exp} \leq 1.0 \rightarrow \begin{cases} K_Z = 0 \\ K_I = 1 \\ K_P = 0 \end{cases} \quad (3.10)$$

$$1.0 < K_{Exp} < 2.0 \rightarrow \begin{cases} K_Z = K_{Exp} - 1 \\ K_I = 2 - K_{Exp} \\ K_P = 0 \end{cases} \quad (3.11)$$

$$K_{Exp} \geq 2.0 \rightarrow \begin{cases} K_Z = 1 \\ K_I = 0 \\ K_P = 0 \end{cases} \quad (3.12)$$

3.4.2 Analytical Method AM2

For conversion to constrained ZIP model: analytical method AM2 (constrained)

When analysing the conversion error of method described in Section 3.4.1 it was found that the method has an error peak at $K_{Exp} = 0.5$. Around that point, the load models were converted based on (3.9) and (3.10). Near base voltage $K_{Exp} \approx 2 \cdot K_Z + K_I$. Furthermore, when K_Z is chosen to be $K_Z = 0$, the previous equation becomes $K_{Exp} \approx K_I$, while $K_P = 1 - K_I$. When these two equations (3.14) are used for calculating ZIP models between the constant power and constant current model, the conversion error is significantly decreased, as can be seen in Figure 3.2.

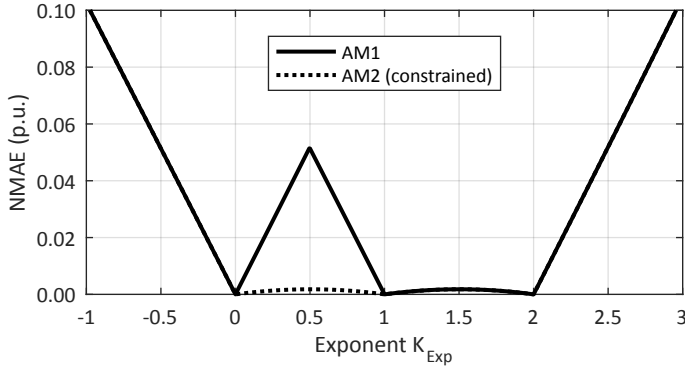


Figure 3.2: Exponential to ZIP load model conversion error when analytical method AM1 and analytical method AM2 (constrained) are used for converting exponential load models with low K_{Exp} values. NMAE is used for quantifying the conversion error.

The conversion method described in Section 3.4.1 is limited to the constrained ZIP model: all solutions of the equation system (3.9)-(3.12) limit ZIP model parameters K_Z , K_I , K_P to 0..1. The equations (3.13)-(3.16) have a similar property. The converted models differ from the models converted by the method AM1 described in Section 3.4.1 only when $0 \leq K_{Exp} < 1$.

$$K_{Exp} \leq 0 \rightarrow \begin{cases} K_Z = 0 \\ K_I = 0 \\ K_P = 1 \end{cases} \quad (3.13)$$

$$0 \leq K_{Exp} \leq 1 \rightarrow \begin{cases} K_Z = 0 \\ K_I = K_{Exp} \\ K_P = 1 - K_{Exp} \end{cases} \quad (3.14)$$

$$1 < K_{Exp} < 2 \rightarrow \begin{cases} K_Z = K_{Exp} - 1 \\ K_I = 2 - K_{Exp} \\ K_P = 0 \end{cases} \quad (3.15)$$

$$K_{Exp} \geq 2 \rightarrow \begin{cases} K_Z = 1 \\ K_I = 0 \\ K_P = 0 \end{cases} \quad (3.16)$$

For conversion to unconstrained ZIP model: analytical method AM2 (unconstrained)

Equation (3.13) models loads inversely proportional to voltage by constant power model. Experimentally it was found that these models can be more accurately converted by (3.17). Moreover, the load models with high voltage dependence (K_{Exp} over 2) were estimated in the case of method AM1 and previously described implementation of AM2 (with constrained ZIP model output) as constant impedances after conversion in the case of (3.16). To increase the conversion accuracy of models with high voltage dependence, the limits of (3.15) were relaxed, and (3.18) was acquired.

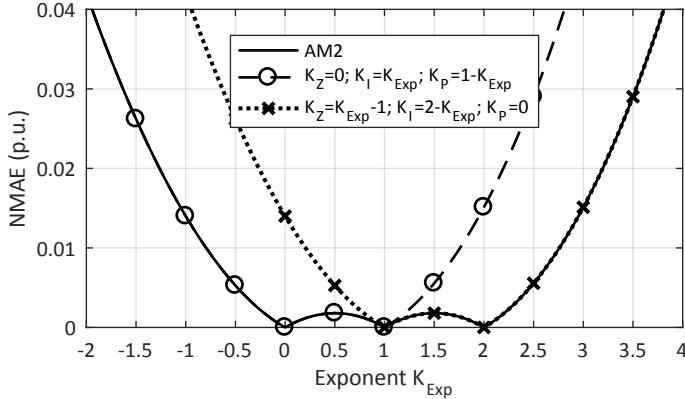


Figure 3.3: Analytical method AM2 (unconstrained) uses Equation (3.17) and (3.18) for different range of K_{Exp} values. When either equation is used for the whole K_{Exp} range, the NMAE would be higher than the error of method AM2 (unconstrained) for part of the K_{Exp} range.

These modifications lead to accurate load models when $K_{Exp} < 0$ or $K_{Exp} > 2$.

$$K_{Exp} \leq 1 \rightarrow \begin{cases} K_Z = 0 \\ K_I = K_{Exp} \\ K_P = 1 - K_{Exp} \end{cases} \quad (3.17)$$

$$K_{Exp} > 1 \rightarrow \begin{cases} K_Z = K_{Exp} - 1 \\ K_I = 2 - K_{Exp} \\ K_P = 0 \end{cases} \quad (3.18)$$

The NMAE of analytical method AM1 and AM2 (unconstrained ZIP models) is illustrated by Figure 3.4. When $K_{Exp} = 0$ or $1.0 \leq K_{Exp} \leq 2.0$, the conversion results of method AM2 (unconstrained) and the method AM1, described in Section 3.4.1 are the same. For the rest of the K_{Exp} values, the NMAE of AM2 (unconstrained) is lower, and the method provides a more accurate conversion.

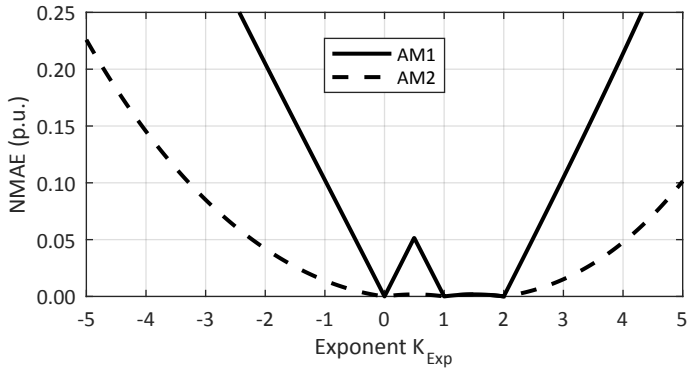


Figure 3.4: NMAE of analytical method AM1 and AM2 (unconstrained).

3.4.3 Analytical Method AM3

The analysis of load model conversion error of NLS methods (methods presented in Section 3.3) indicated that there are typically three intersections of input and output characteristic. The three intersections are indicated in Figure 3.5 by 0 conversion error. The first of the intersections is located at a voltage below base voltage (in Figure 3.5 at 0.84 p.u.), the second at the base values (initial or nominal voltage and load, in Figure 3.5 1 p.u.), and the third at a voltage above the base value (in Figure 3.5 at 1.15 p.u.). This aspect of conversion was used for deriving an additional conversion method AM3 described in this section.

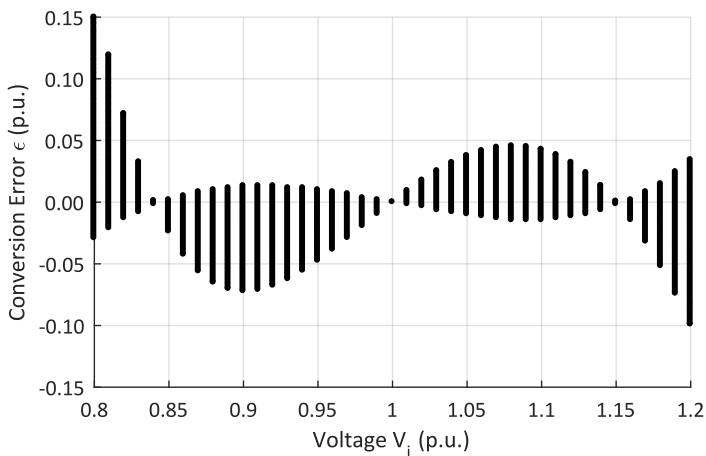


Figure 3.5: Voltage dependence of conversion error of non-linear least squares conversion based on absolute error minimisation. Method NLS abs.

At the intersection point of the converted exponential and acquired ZIP model, the equations (1.3) and (1.1) are equal

$$P_b \cdot \left[K_Z \cdot \left(\frac{V}{V_b} \right)^2 + K_I \cdot \left(\frac{V}{V_b} \right) + K_P \right] = P_b \cdot \left(\frac{V}{V_b} \right)^{K_{Exp}} \quad (3.19)$$

Dividing (3.19) by P_b leads to

$$K_Z \cdot \left(\frac{V}{V_b} \right)^2 + K_I \cdot \left(\frac{V}{V_b} \right) + K_P = \left(\frac{V}{V_b} \right)^{K_{Exp}} \quad (3.20)$$

Replacing K_P in (3.20) by $1 - K_Z - K_I$ and simplifying the equations leads to derivation of

$$K_Z \cdot \left(\frac{V}{V_b} + 1 \right) + K_I = \frac{\left(\frac{V}{V_b} \right)^{K_{Exp}} - 1}{\left(\frac{V}{V_b} \right) - 1} \quad (3.21)$$

Previously it was mentioned that the characteristics intersect at two voltages (in addition to nominal/initial), denoted here as V_1 and V_2 . Thus, it is possible to formulate an equation system based on equation (3.21)

$$\begin{cases} K_Z \cdot \left(\frac{V_1}{V_b} + 1 \right) + K_I = \frac{\left(\frac{V_1}{V_b} \right)^{K_{Exp}} - 1}{\frac{V_1}{V_b} - 1} \\ K_Z \cdot \left(\frac{V_2}{V_b} + 1 \right) + K_I = \frac{\left(\frac{V_2}{V_b} \right)^{K_{Exp}} - 1}{\frac{V_2}{V_b} - 1} \end{cases} \quad (3.22)$$

A solution to the equation system (3.22) is (3.23). The third parameter K_P can be calculated using (3.24) from the values of K_Z and K_I .

$$\begin{bmatrix} K_Z \\ K_I \end{bmatrix} = \frac{V_b}{V_1 - V_2} \cdot \begin{bmatrix} 1 & -1 \\ -\frac{V_2}{V_b} - 1 & \frac{V_1}{V_b} + 1 \end{bmatrix} \begin{bmatrix} \frac{\left(\frac{V_1}{V_b} \right)^{K_{Exp}} - 1}{\frac{V_1}{V_b} - 1} \\ \frac{\left(\frac{V_2}{V_b} \right)^{K_{Exp}} - 1}{\frac{V_2}{V_b} - 1} \end{bmatrix} \quad (3.23)$$

$$K_P = 1 - K_Z - K_I \quad (3.24)$$

Equations (3.23) and (3.24) can also be written as equation system (3.25).

$$\begin{cases}
K_Z = \frac{V_b}{V_1 - V_2} \cdot \left[\frac{\left(\frac{V_1}{V_b}\right)^{K_{Exp}} - 1}{\frac{V_1}{V_b} - 1} - \frac{\left(\frac{V_2}{V_b}\right)^{K_{Exp}} - 1}{\frac{V_2}{V_b} - 1} \right] \\
K_I = \frac{V_b}{V_1 - V_2} \cdot \left[\left(-\frac{V_2}{V_b} - 1\right) \cdot \frac{\left(\frac{V_1}{V_b}\right)^{K_{Exp}} - 1}{\frac{V_1}{V_b} - 1} + \left(\frac{V_1}{V_b} + 1\right) \cdot \frac{\left(\frac{V_2}{V_b}\right)^{K_{Exp}} - 1}{\frac{V_2}{V_b} - 1} \right] \\
K_P = 1 - K_Z - K_I
\end{cases} \quad (3.25)$$

Figure 3.6 indicates that the derived analytical method AM3 provides the lowest conversion error at voltage V_1 , base voltage and at voltage V_2 . At these voltages, the conversion error is zero. This is an expected result taking into account the assumptions of the derivation (3 intersections of characteristics, at V_1 , V_b and V_2).

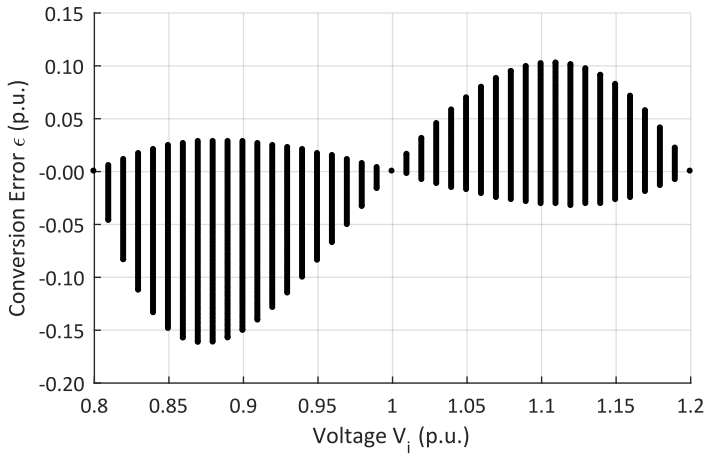


Figure 3.6: Voltage dependence of conversion error of AM3, when 0.8 and 1.2 p.u. are used as V_1/V_b and V_2/V_b .

An interesting result is the NMAE of the method AM3 illustrated by Figure 3.7. The conversion error of the method is significantly lower than the error of analytical method AM2 (both the constrained and unconstrained version). At exponent K_{Exp} values from 0.5 to 2.5 the error is comparable to the non-linear least squares methods.

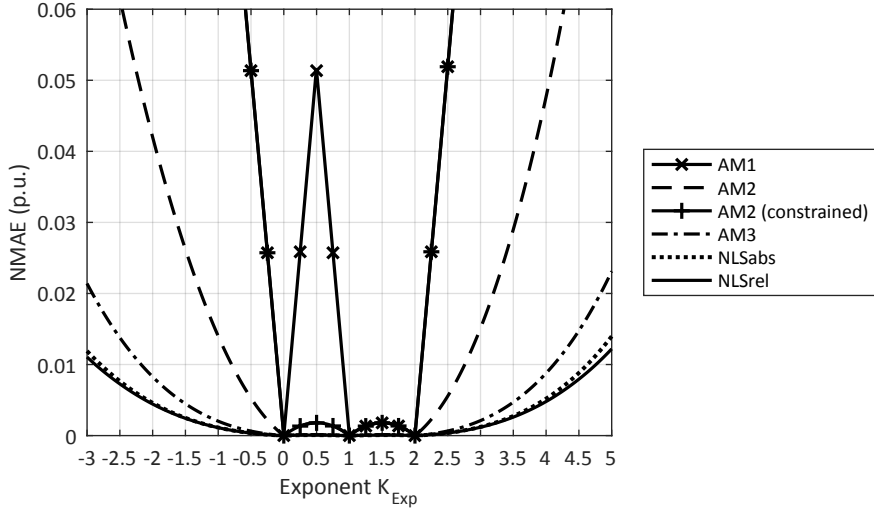


Figure 3.7: NMAE of developed analytical methods compared to non-linear least squares conversions (NLSrel, NLSabs).

3.5 Analytical Method for ZIP to Exponential Model Conversion

For converting ZIP models to exponential models, there is a well-known equation (3.26), which has been used in [18, 53, 60]. Based on the following derivation, the equation will work with both non-normalised and normalised ZIP model parameters.¹⁶ The origin of this method is unclear.

$$K_{Exp} \approx \frac{2 \cdot K_Z + 1 \cdot K_I + 0 \cdot K_P}{K_Z + K_I + K_P} \quad (3.26)$$

Probably the method has been derived based on the approximate derivatives of exponential and ZIP load model equation. An explanation of one way to derive this equation will now follow.

We assume the exponential model to have equation (3.27)¹⁷ and ZIP model to have equation (3.28)¹⁸. Here $P_b \cdot K_Z$, $P_b \cdot K_I$ and $P_b \cdot K_P$ represent non-normalised ZIP model parameters, and are similar to $Yload$, $Iload$ and $Pload$ of PSS®E load model presented in Section 1.2.3 and described by (1.7).

$$P_{EXP} = P_b \cdot \left(\frac{V}{V_b} \right)^{K_{Exp}} \quad (3.27)$$

¹⁶Non-normalised parameters are used in PSS®E load model presented in Section 1.2.3 and described by (1.7), and could be represented by $P_b \cdot K_Z$, $P_b \cdot K_I$ and $P_b \cdot K_P$. Normalised parameters correspond to the parameters defined in case of (1.3) in Section 1.2.3, where the multiplier P_b was in front of the brackets. In the case of non-normalised parameters, the sum of parameters corresponds to the load at base voltage V_b . The sum of normalised parameters is 1 and they describe the fraction of P_b .

¹⁷Corresponds to (1.1) presented in Section 1.2.2.

¹⁸Combination of (1.7) and (1.3) that were presented in Section 1.2.3.

$$P_{ZIP} = P_b \cdot K_Z \cdot \left(\frac{V}{V_b}\right)^2 + P_b \cdot K_I \cdot \left(\frac{V}{V_b}\right) + P_b \cdot K_P \quad (3.28)$$

The partial derivatives of these equations with respect to voltage are:

$$\frac{\partial P_{Exp}}{\partial(V/V_b)} = P_b \cdot K_{Exp} \cdot \left(\frac{V}{V_b}\right)^{K_{Exp}-1} \quad (3.29)$$

$$\frac{\partial P_{ZIP}}{\partial(V/V_b)} = P_b \cdot 2 \cdot K_Z \cdot \left(\frac{V}{V_b}\right) + P_b \cdot K_I + 0 \cdot P_b \cdot K_P \quad (3.30)$$

When the voltage is assumed to be $\left(\frac{V}{V_b}\right) \approx 1$, the partial derivatives can be approximated by (3.31) and (3.32).

$$\frac{\partial P_{Exp}}{\partial(V/V_b)} \approx P_b \cdot K_{Exp} \quad (3.31)$$

$$\frac{\partial P_{ZIP}}{\partial(V/V_b)} \approx P_b \cdot 2 \cdot K_Z + P_b \cdot K_I + 0 \cdot P_b \cdot K_P \quad (3.32)$$

Setting these two approximately equal, and knowing that $P_b \cdot K_Z + P_b \cdot K_I + P_b \cdot K_P = P_b$, because $K_Z + K_I + K_P = 1$.

$$P_b \cdot K_{Exp} \approx P_b \cdot 2 \cdot K_Z + P_b \cdot K_I + 0 \cdot P_b \cdot K_P \quad (3.33)$$

$$K_{Exp} = \frac{P_b \cdot 2 \cdot K_Z + P_b \cdot K_I + 0 \cdot P_b \cdot K_P}{P_b} = \frac{P_b \cdot 2 \cdot K_Z + P_b \cdot K_I + 0 \cdot P_b \cdot K_P}{P_b \cdot K_Z + P_b \cdot K_I + P_b \cdot K_P} \quad (3.34)$$

This last equation matches (3.26) if $P_b \cdot K_Z$, $P_b \cdot K_I$ and $P_b \cdot K_P$ were to be denoted by K_Z , K_I , K_P . Here the multiplications are used to more clearly express the relation of this equation to non-normalised and normalised ZIP model parameter values. In the case of normalised parameters, base powers P_b would cancel out and simply equation $K_{Exp} \approx 2 \cdot K_Z + K_I$ can be used for conducting the conversion.

3.6 Conversion of Estimated Models and Impact on Event Modelling

Error

In Section 2.4.4 a case study, where six voltage disturbances were induced by OLTC switching, was introduced. The study was conducted in a network with high penetration of DG. For each event two exponential and two ZIP load models were estimated. The load models fitted to the responses of the supplied load were presented in Table 2.12. Denotations $K_{Exp,L}$, $K_{Z,L}$, $K_{I,L}$ and $K_{P,L}$ were used for the load model parameters. The models corresponding to the responses of the apparent transformer load were presented in Table 2.13. These values were denoted by $K_{Exp,T}$, $K_{Z,T}$, $K_{I,T}$ and $K_{P,T}$. The load models of Table 2.12 and Table 2.13 were converted by least squares estimation (denoted by NLSa, described in Section 3.3), analytical method presented in Section 3.4.1 (denoted by AM1, used for exponential to ZIP conversion) and analytical method from Section 3.5 (denoted AM, used for ZIP to exponential conversion).

The estimated and converted exponential models are presented in Table 3.2 for comparison. This table indicates that there is a significant mismatch between the estimated and converted models. Furthermore, results of the conversion methods differ as well. In the case study the voltages were in the range 0.95...1.05 p.u.. Thus, the estimated ZIP model (that was converted to exponential model) and estimated exponential model should be most accurate in that voltage range. The analytical method AM was derived by using the derivatives of exponential and ZIP model. Furthermore, the voltage was assumed to be equal to the base voltage V_b . Thus, the model converted by analytical method AM should have the highest accuracy near the base voltage V_b , corresponding to the pre-event voltage of each event in this study. Furthermore, the least squares method was applied for model conversion by using the same voltage range (0.8...1.2 p.u.) as is used in the rest of the thesis. In addition to the voltage range difference, in estimation and conversion process the voltage value distribution differs as well: it is even in conversion and not even in measurement data. These differences cause the least squares to find significantly different results in estimation and conversion situation.

Table 3.2: Estimated exponential load model and exponential models acquired by conversion of estimated ZIP models. $K_{Exp,L}$ - exponent for total supplied load. $K_{Exp,T}$ - exponent for apparent transformer load.

Event	Estimated		Converted by AM		Converted by NLSa	
	$K_{Exp,L}$	$K_{Exp,T}$	$K_{Exp,L}$	$K_{Exp,T}$	$K_{Exp,L}$	$K_{Exp,T}$
1	0.74	5.11	0.73	5.21	0.73	4.65
2	1.24	2.92	1.01	2.62	0.92	2.21
3	0.79	8.11	0.65	9.28	0.66	6.22
4	0.62	1.30	0.98	1.66	1.14	2.01
5	0.65	7.64	0.60	8.70	0.60	6.11
6	1.03	8.15	1.06	7.78	1.09	6.04

In Table 3.2 the estimated and converted exponential load models differ significantly. In order to determine how well they describe the measured load responses, simulated load was calculated based on measured voltage and compared to the measured load. The obtained simulation error is presented in Table 3.3 and Table 3.4. Based on these tables, the modelling accuracy of the estimated and converted models is mostly similar. The models acquired by the least squares conversion tend to be least accurate.

Table 3.3: Event modelling error. Total supplied load. Estimated exponential load model and exponential models acquired by conversion of estimated ZIP models.

Event	Estimated		Converted by AM		Converted by NLSa	
	MSE	MAE	MSE	MAE	MSE	MAE
	($\cdot 10^{-3}$)		($\cdot 10^{-3}$)		($\cdot 10^{-3}$)	
1	0.17	0.011	0.17	0.011	0.17	0.011
2	0.10	0.008	0.11	0.009	0.11	0.008
3	0.14	0.009	0.15	0.009	0.17	0.010
4	0.10	0.008	0.17	0.011	0.10	0.008
5	0.08	0.008	0.08	0.008	0.08	0.008
6	0.05	0.006	0.05	0.006	0.05	0.006

In the case study (introduced in Section 2.4.4) the ZIP models were less accurate than exponential models at describing the load behaviour. Surprisingly, when the estimated ZIP models were converted to exponential models, in several cases, the accuracy improved. For example in Table 3.4 the 2nd and the 3rd event.

Table 3.4: Event modelling error. Apparent load of the transformer. Estimated exponential load model and exponential models acquired by conversion of estimated ZIP models.

Event	Estimated		Converted by AM		Converted by NLSa	
	MSE ($\cdot 10^{-3}$)	MAE	MSE ($\cdot 10^{-3}$)	MAE	MSE ($\cdot 10^{-3}$)	MAE
1	18.55	0.105	18.55	0.105	18.81	0.108
2	1.94	0.034	1.96	0.035	2.46	0.037
3	14.23	0.093	15.25	0.096	16.91	0.100
4	1.34	0.030	1.41	0.031	1.35	0.030
5	10.61	0.084	11.51	0.087	15.32	0.102
6	3.46	0.046	3.47	0.046	3.77	0.048

The estimated and converted ZIP models are presented in Table 3.5. Similarly to the previously described exponential models, the converted ZIP models differ from the estimated ZIP models. Still, in the case of supplied load models (with index L), the converted models have some similarity in values. Analytical method AM1 leads to constrained ZIP models. The models provided by the least squares fitting can be considered to be close to constrained model in the case of supplied load, compared to the models of apparent transformer load.

Table 3.5: Estimated ZIP load model and ZIP models acquired by conversion of estimated exponential models.

Event	Estimated			Converted by AM1			Converted by NLSa		
	$K_{Z,L}$	$K_{I,L}$	$K_{P,L}$	$K_{Z,L}$	$K_{I,L}$	$K_{P,L}$	$K_{Z,L}$	$K_{I,L}$	$K_{P,L}$
1	0.38	-0.02	0.65	0.00	1.00	0.00	-0.10	0.93	0.16
2	-8.32	17.66	-8.33	0.24	0.76	0.00	0.15	0.94	-0.09
3	4.71	-8.77	5.06	0.00	1.00	0.00	-0.08	0.96	0.13
4	10.49	-20.00	10.51	0.00	1.00	0.00	-0.12	0.86	0.26
5	1.32	-2.05	1.73	0.00	1.00	0.00	-0.11	0.88	0.24
6	2.07	-3.09	2.02	0.03	0.97	0.00	0.01	1.00	-0.01
Event	$K_{Z,T}$	$K_{I,T}$	$K_{P,T}$	$K_{Z,T}$	$K_{I,T}$	$K_{P,T}$	$K_{Z,T}$	$K_{I,T}$	$K_{P,T}$
1	4.31	-3.40	0.09	1.00	0.00	0.00	10.64	-15.92	6.28
2	-8.69	20.00	-10.31	1.00	0.00	0.00	2.81	-2.68	0.87
3	-5.36	20.00	-13.64	1.00	0.00	0.00	30.96	-52.37	22.40
4	10.83	-20.00	10.17	0.30	0.70	0.00	0.20	0.90	-0.10
5	-2.46	13.61	-10.15	1.00	0.00	0.00	26.94	-45.06	19.13
6	4.61	-1.44	-2.17	1.00	0.00	0.00	31.35	-53.07	22.72

The event modelling error of ZIP models (of Table 3.5) is displayed in Table 3.6 and Table 3.7. According to the tables, the least accurate are the estimated ZIP models. This indicates that the implemented ZIP model estimation algorithm may be unable to find the best solution, and could be improved further. The most accurate are the ZIP models obtained by least squares conversion of exponential models.

Table 3.6: Event modelling error. Total supplied load. Estimated ZIP load model and ZIP models acquired by conversion of estimated exponential models.

Event	Estimated		Converted by AM		Converted by NLSa	
	MSE ($\cdot 10^{-3}$)	MAE	MSE ($\cdot 10^{-3}$)	MAE	MSE ($\cdot 10^{-3}$)	MAE
1	0.19	0.010	0.18	0.011	0.17	0.011
2	32.43	0.122	0.10	0.008	0.10	0.008
3	7.85	0.074	0.16	0.010	0.14	0.009
4	40.50	0.170	0.18	0.011	0.10	0.008
5	0.30	0.014	0.14	0.009	0.08	0.008
6	0.17	0.011	0.05	0.006	0.05	0.006

Table 3.7: Event modelling error. Apparent load of the transformer. Estimated ZIP load model and ZIP models acquired by conversion of estimated exponential models.

Event	Estimated		Converted by AM		Converted by NLSa	
	MSE ($\cdot 10^{-3}$)	MAE	MSE ($\cdot 10^{-3}$)	MAE	MSE ($\cdot 10^{-3}$)	MAE
1	18.65	0.105	20.11	0.110	18.56	0.106
2	48.16	0.155	2.16	0.037	1.94	0.034
3	100.26	0.257	36.04	0.149	15.01	0.096
4	37.60	0.161	1.34	0.030	1.34	0.030
5	66.69	0.202	30.89	0.139	11.23	0.086
6	4.71	0.053	7.39	0.067	3.70	0.048

3.7 Impact of Conversion Error on Load Flow Results

3.7.1 Conversion Error and Load Modelling Error

In Section 3.2 the load model conversion error was defined by the difference of load characteristics at a specific voltage. That approach is useful when the load bus voltage is not affected by the load characteristic or the impact of the load characteristic replacement is negligible. In that case, the load model conversion error matches the load modelling error in load flow, as shown in Figure 3.8.

Actually, the load bus voltage is also dependent on the power consumption of the load. This means that converting and replacing a load characteristic in a power system model can lead to a different load operation point. In the load flow results both load bus voltage and consumed power would differ compared to the original results. This situation is illustrated by Figure 3.9, where the load model conversion error and load flow error differ significantly. Moreover, as the load operates at two different voltages (V_1 and V_2),

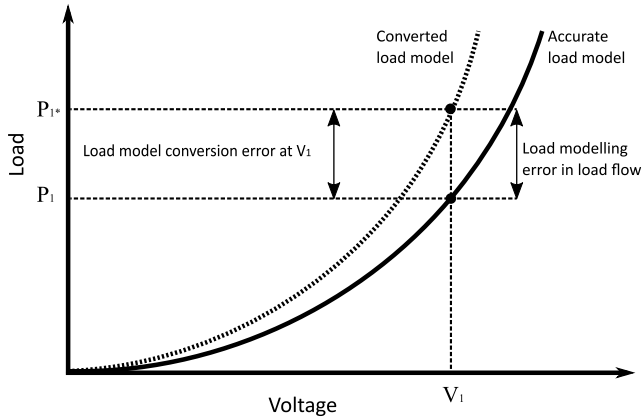


Figure 3.8: Conversion error and load modelling error in load flow results when the load bus voltage is not affected by the load characteristic. With an accurate load model the load operates at voltage V_1 and consumes P_1 . With converted load model the load operates at voltage V_1 and consumes P_1^* . Adapted from [VI]

the related load model conversion error can be calculated at 2 different voltages, and different values would be obtained. Neither would match with the load modelling error in load flow. To illustrate the described situation, a conducted case study is described and analysed from Section 3.7.2.

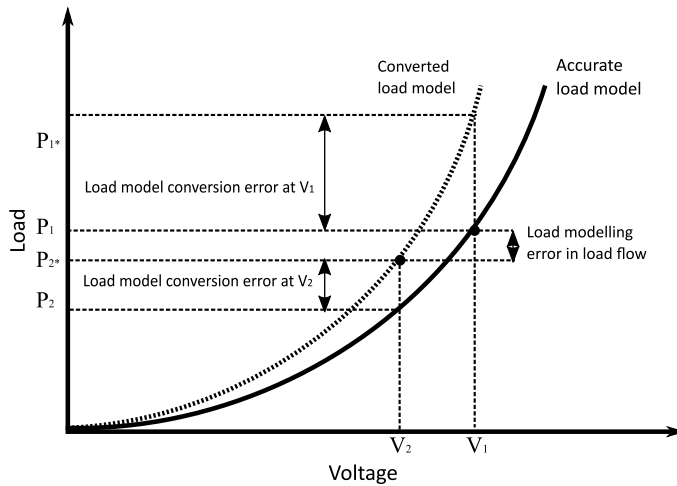


Figure 3.9: Conversion error and load modelling error in load flow when change of load characteristics causes the load bus voltage to change. With an accurate load model the load operates at voltage V_1 and consumes P_1 . With converted load model the load operates at voltage V_2 and consumes P_2^* . Adapted from [VI]

3.7.2 Case Study: Impact of Conversion Error on Load Flow Results

In the case of conversion between exponential and ZIP load model, typically, a conversion error is involved. The aim of the case study is to analyse how conversion error affects the results of load flow calculations. To achieve this goal, load flow is calculated for the same Nine-bus power system model using different load models. The analysed cases are listed in Table 3.8. For conducting the calculations, DlgSILENT Power Factory was used. This software was chosen because the polynomial load model of DlgSILENT Power Factory (described in detail in Section 1.2.4) can accurately model exponential and ZIP load models¹⁹.

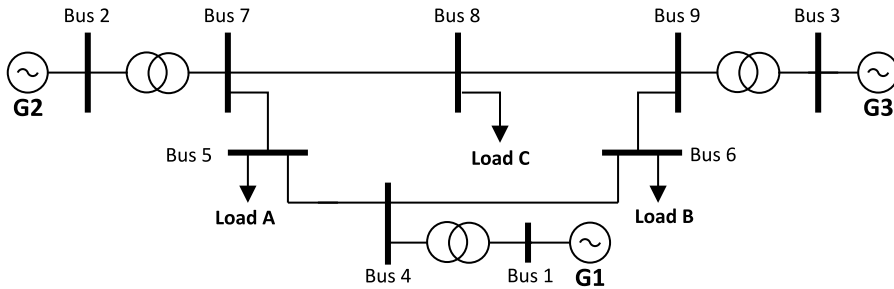


Figure 3.10: Nine-bus power system. Adapted from [VI]

Simulated Cases

Firstly, Case 1 (in Table 3.8) was calculated to verify if the load flow results of the Nine-bus power system model correspond to the documentation of DlgSILENT Power Factory [118] and the source of the model [119]. The load flow results matched the documentation.

After the validation of the Nine-bus model (Case 1), the voltages of the generators were increased to increase load bus voltages for amplifying the effect of the load modelling error, while still keeping the system at a realistic voltage. This was done in Case 2, where original constant power load models were used. After the modifications, the generator bus voltages increased from 1.025...1.040 p.u. to 1.088...1.090 p.u. This was achieved by increasing the slack generator (G1) voltage reference from 1.040 to 1.090 p.u. and adjusting the reactive power references of generators G2 and G3. Generators G1 and G2 operate in the model at a fixed active and reactive power output. The same generator modelling approach is used in all the cases (Case 1 to 8). The load bus voltages increased as a result from 0.996...1.016 p.u. to 1.061...1.084 p.u. (loads modelled by constant power loads in Case 2).

Chosen Load Models and Converted Load Models

Exponential load models were chosen and implemented in Case 3 to analyse the impact of exponential to ZIP load model conversion error. For choosing the models, the results of an international survey [60] were used. Load B was assigned the mean value of the World (Table VI and Table VIII in [60]). Load A models were assigned the highest values of the World load model range (Table VI and VIII in [60]). Load C was assigned negative values that have equal absolute value as highest exponents of Load A and B. The chosen exponential models (Table 3.10) were assumed to be accurate voltage characteristics when analysing the results of Case 4 and Case 5, where ZIP models were used that were acquired by converting the exponential models chosen for Case 3.

¹⁹Section 1.2.4 describes how this can be achieved.

Table 3.8: Cases modelled for case study.

Case	Generator References	Load Models	Comment
1	Original	Constant power	Loads without voltage dependence
2	Modified*	Constant power	Loads without voltage dependence
3	Modified*	Exponential	Chosen exponential models
4	Modified*	ZIP	Exponential models** converted by the most accurate method
5	Modified*	ZIP	Exponential models** converted by the least accurate method
6	Modified*	ZIP	Chosen ZIP load models
7	Modified*	Exponential	ZIP models*** converted by the most accurate method
8	Modified*	Exponential	ZIP models*** converted by the least accurate method

* Generator reference values were increased to increase the voltages of the generator buses to raise the voltage in the modelled system.

** Input load models (exponential) are the same as used in Case 3.

*** Input load models (ZIP) are the same as used in Case 6.

Table 3.9: Load and generator voltages and powers in the original Nine-bus system model, and after increasing generator bus voltages (after modification).

		Original Nine-bus Model			After Modification			
	Bus	P [MW]	Q [Mvar]	V [p.u.]	P [MW]	Q [Mvar]	V [p.u.]	
Generators	G1	1	71.60	26.78	1.040	71.06	12.32	1.090
	G2	2	163.00	6.70	1.025	163.00	1.00	1.088
	G3	3	85.00	-10.90	1.025	85.00	-15.00	1.089
Loads	A	5	125.00	50.00	0.996	125.00	50.00	1.061
	B	6	90.00	30.00	1.013	90.00	30.00	1.077
	C	8	100.00	35.00	1.016	100.00	35.00	1.084

Another set of load models was chosen for Case 6, a set of ZIP models (Table 3.10) that was used for analysing the impact of ZIP to exponential load model conversion error on load flow results. The ZIP models were chosen with voltage sensitivities comparable to the models presented in [61] and high conversion error. The chosen ZIP load models (used in Case 6) were assumed to be accurate voltage characteristics when analysing the results of Case 7 and 8. The load models of Case 7 and 8 were acquired by converting the ZIP models chosen for Case 6.

Table 3.10: Chosen exponential and ZIP load models. [VI]

Load	Exponential		ZIP					
	K_{Exp}	$K_{Exp,Q}$	$K_{Z,P}$	$K_{I,P}$	K_P	$K_{Z,Q}$	$K_{I,Q}$	K_Q
A	1.33	2.47	5.68	-9.89	5.21	-5.77	9.86	-3.09
B	0.67	1.35	-4.70	9.49	-3.79	-11.39	24.48	-12.09
C	-1.35	-2.47	-4.18	9.98	-4.80	-5.66	8.93	-2.27

The chosen exponential load models were converted to ZIP models using the conversion methods presented in Section 3.3 and 3.4. The NMAE of the conversions (Table 3.11) indicates that analytical method AM1 provided the lowest accuracy (highest values of NMAE) and the highest accuracy (lowest values of NMAE) was provided by NLS minimisation of relative error (NLSrel). These results correspond well to Figure 3.7.

Table 3.11: NMAE when chosen exponential models converted to ZIP models. [VI]

Load	AM1		AM2		AM3		NLSrel	
	P	Q	P	Q	P	Q	P	Q
A	0.16%	4.88%	0.16%	0.51%	0.01%	0.06%	0.01%	0.03%
B	3.39%	0.16%	0.16%	0.16%	0.01%	0.01%	0.01%	0.01%
C	13.82%	25.36%	2.22%	6.03%	0.36%	1.34%	0.20%	0.71%

The most accurate converted model (converted by NLSrel) was used in Case 4, and the least accurate model (converted by AM1) in Case 5.

Table 3.12: Chosen exponential load models and ZIP models acquired by model conversion (using method AM1 and NLSrel). [VI]

Conversion method	Load	ZIP Model of P			ZIP Model of Q		
		$K_{Z,P}$	$K_{I,P}$	K_P	$K_{Z,Q}$	$K_{I,Q}$	K_Q
AM1	A	0.33	0.67	0.00	1.00	0.00	0.00
	B	0.00	1.00	0.00	0.35	0.65	0.00
	C	0.00	0.00	1.00	0.00	0.00	1.00
NLSrel	A	0.22	0.89	-0.11	1.81	-1.14	0.33
	B	-0.11	0.89	0.22	0.24	0.87	-0.11
	C	1.62	-4.63	4.01	4.37	-11.37	7.99

Similarly, the chosen ZIP models were converted to exponential models by the conversion methods presented in Section 3.3 and Section 3.5. The conversion error of the two methods was similar to that shown by Table 3.13. The acquired load models shown in Table 3.14 were used in Case 7 and 8.

Table 3.13: NMAE when chosen ZIP models converted to exponential models using analytical method (AM) and NLSrel. [VI]

Load	AM		NLSrel	
	P	Q	P	Q
A	6.82%	14.82%	6.72%	14.99%
B	7.43%	30.94%	7.38%	29.16%
C	8.07%	20.28%	7.87%	20.56%

Table 3.14: Converted exponential models from AM and NLSrel. [VI]

Load	AM		NLSrel	
	K_{Exp}	$K_{Exp,Q}$	K_{Exp}	$K_{Exp,Q}$
A	1.48	-1.69	1.25	-1.99
B	0.09	1.69	0.15	2.94
C	1.61	-2.39	1.91	-3.00

3.7.3 Case Study Results: Impact of Exponential to ZIP Load Model Conversion on Load Flow

Simulation Case 3 was calculated using the chosen exponential model presented in Table 3.10. The results of that case are considered to be accurate in the context of this analysis. Next, Case 4 and Case 5 were calculated with load models that were acquired by converting the chosen exponential models to ZIP models. Case 4 used the most accurate converted models (converted by NLSrel). In contrast, Case 5 used the least accurate models (converted by AM1). The used ZIP model parameter values are presented in Table 3.12.

Replacement of the load models had an effect on the load flow results, as can be seen in Table 3.15. The less accurate ZIP models (converted by AM1) increased the power output of the slack generator (G1) significantly, active power output increased by 14% and reactive power 51%. A large change of Load C was observed, active power increased by 12% and reactive power 23%. The load changes decreased voltages in the system (bus voltages decreased 1...2%). This can create a false sense of security: modelled voltages are lower, thus the margin in respect to upper voltage limit is increased. The more accurate NLSrel conversion led to almost no change of active power output of slack generator (G1) and a 3% decrease in reactive power. Bus voltages of the system increased up to 0.1%, which is a small change compared to the system modelled with load models from AM1.

The conversion error was defined for a specific voltage. In the case of the conducted simulations, there are several voltages which occur: voltages of the simulation with the exponential load models (Case 3) and voltages of the simulations with the converted load models (Case 4 and 5). This means that the load model conversion error depends on the voltage chosen for the analysis. Table 3.16 illustrates this situation. The load modelling error in load flow is in column V_{LF} . The conversion error at Case 3 (chosen exponential models) voltages is in columns V_{Exp} , and the conversion error at Case 4 and Case 5 voltages is shown in column V_{NLSrel} and V_{AM1} , respectively.

Table 3.15: Relative error η of simulation with ZIP models acquired by using conversion methods AM1 and NLSrel. [VI]

Conv. Meth.	Bus	Voltage		P Gen.	Q Gen.	P Load	Q Load
		Magn.	Angle				
AM1	1	-	-	14.35%	50.57%	-	-
	2	-1.68%	-6.70%	0.00%	0.00%	-	-
	3	-1.61%	-15.89%	0.00%	0.00%	-	-
	5	-0.76%	13.46%	-	-	-0.99%	-3.90%
	6	-0.87%	16.67%	-	-	1.44%	-1.12%
	8	-1.97%	-100.00%	-	-	12.07%	23.20%
NLSrel	1	-	-	-0.30%	-2.62%	-	-
	2	0.09%	0.00%	0.00%	0.00%	-	-
	3	0.00%	0.23%	0.00%	0.00%	-	-
	5	0.04%	-0.26%	-	-	0.05%	0.14%
	6	0.04%	-0.58%	-	-	0.03%	0.06%
	8	0.10%	2.97%	-	-	-0.37%	-1.16%

In the case of NLSrel converted load models, the V_{Exp} and V_{ZIP} values are approximately equal. This is explained by the nearly unchanged bus voltages (magnitudes of load bus voltages changed up to 0.04...0.1%). In this case the load flow error is on a similar scale to the conversion error. The AM1 case is more interesting. Load C displays an equal error in V_{Exp} and V_{LF} columns. This is caused by the model used - load is modelled by a constant power model (because the constrained ZIP model is not able to model negative voltage dependencies more accurately). For columns V_{Exp} and V_{LF} the chosen exponential load model is calculated at voltage V_{Exp} , and the AM1 converted load model consumes nominal power. However, for column V_{ZIP} the exponential model is calculated at voltage V_{ZIP} , while the AM1 converted model still consumes nominal power, leading to a different calculated error value.

3.7.4 Case Study Results: Impact of ZIP to Exponential Load Model Conversion on Load Flow

Simulation Case 6 was calculated using the chosen ZIP model presented in Table 3.10. The results of Case 6 are considered to be accurate in the context of this analysis. Next, Case 7 and Case 8 were calculated with load models that were acquired by converting the chosen ZIP models to exponential models. Case 7 used the non-linear least squares conversion (NLSrel). Case 8 used the analytical method (AM). As previously stated, the load model conversion error of the methods was similar (shown in Table 3.13). The parameter values for the exponential model used are presented in Table 3.14.

Compared to the exponential to ZIP load model conversion cases, significantly larger load flow changes were observed. The slack generator active power output decreased by several per cent (2...4%) and reactive power output changed the direction and decreased 10..20 times. Active power change was larger using the AM converted load models, and reactive power change for the NLSrel converted models. The load bus voltages decreased by 2.2...3.5%. This is a significant change of voltages, and if the ZIP models used were accurate, such a decrease in calculated voltages could lead to a false sense of security.

Table 3.16: Relative conversion error η of AM1 and NLSrel converted models at different voltages. [VI]

Load	P/Q	AM1 Load Model			NLSrel Load Model		
		V_{Exp}	V_{AM1}	V_{LF}	V_{Exp}	V_{NLSrel}	V_{LF}
A	P	0.03%	0.02%	-0.99%	0.00%	0.00%	0.05%
	Q	-2.43%	-2.08%	-3.90%	0.03%	0.03%	0.12%
B	P	2.34%	2.04%	1.45%	-0.10%	-0.10%	-0.07%
	Q	0.06%	0.04%	-1.13%	0.09%	0.09%	0.16%
C	P	12.07%	9.11%	12.07%	-0.27%	-0.27%	-0.41%
	Q	23.19%	17.29%	23.19%	-1.06%	-1.07%	-1.31%

Voltages based on:

V_{Exp} - load flow with exponential models;

V_{AM1} - load flow with ZIP models from AM1;

V_{NLSrel} - load flow with ZIP models from NLSrel;

V_{LF} - load flow corresponding to model.

Table 3.17: Relative error η of simulation with exponential models acquired by using analytical conversion (AM) and method NLSrel. [VI]

Conv. Meth.	Bus	Voltage Magn.	Voltage Angle	P Gen.	Q Gen.	P Load	Q Load
AM	1	-	-	-3.72%	-105.02%	-	-
	2	-3.20%	19.51%	0.00%	0.00%	-	-
	3	-3.19%	40.34%	0.00%	0.00%	-	-
	5	-2.23%	-6.49%	-	-	-7.39%	13.90%
	6	-2.23%	1.53%	-	-	5.60%	9.21%
	8	-3.51%	-12.00%	-	-	2.05%	45.21%
NLSrel	1	-	-	-2.06%	-108.23%	-	-
	2	-3.12%	13.97%	0.00%	0.00%	-	-
	3	-3.19%	21.01%	0.00%	0.00%	-	-
	5	-2.16%	-5.44%	-	-	-8.81%	11.31%
	6	-2.45%	3.94%	-	-	6.08%	20.03%
	8	-3.47%	0.40%	-	-	5.15%	36.68%

The conversion error describes the mismatch of load characteristics at a specific voltage. In simulation Case 7 and Case 8, the load bus voltages changed significantly (decreased 2.2...3.5%) due to the load model replacement.²⁰ In these simulations, several

²⁰The chosen ZIP load models (used in Case 6) were replaced by exponential models acquired by conversion (in Case 7 and Case 8).

voltage values occur for the loads: voltages of the simulation with the chosen ZIP load models (Case 6) and voltages of the simulations with the converted load models (Case 7 and Case 8). Table 3.18 displays the load model errors for different voltages. The load modelling error in load flow is shown in columns V_{LF} . The conversion error at Case 6 (chosen ZIP models) voltages is shown in columns V_{ZIP} . The conversion error at Case 7 and Case 8 voltages is shown in column V_{NLSrel} and V_{AM} , respectively. The table indicates that the larger conversion errors (NMAE was in Table 3.13 in the range 7...31%) led to load and bus voltage changes. Even if the buses would have been directly supplied from a slack bus (or generators with fixed voltage), and the load bus voltage remained unchanged, the active loads would have been misrepresented by 2...12% and reactive loads by 7...33% (indicated by V_{ZIP} column of the table). Thus, the load model conversion error in the model conversion stage can translate into large changes in load flow calculations and methods with higher accuracy should be preferred.

Table 3.18: Relative conversion error η of AM and NLSrel converted models at different voltages. [VI]

Load	P/Q	AM Load Model			NLSrel Load Model		
		V_{ZIP}	V_{AM}	V_{LF}	V_{ZIP}	V_{NLSrel}	V_{LF}
A	P	-4.27%	-2.53%	-7.41%	-6.29%	-4.16%	-8.81%
	Q	9.63%	5.03%	13.89%	6.60%	2.92%	11.33%
B	P	5.77%	3.36%	5.56%	6.46%	3.68%	6.07%
	Q	13.47%	7.94%	9.22%	29.20%	18.63%	20.10%
C	P	8.14%	4.26%	2.07%	12.48%	7.36%	5.13%
	Q	33.30%	13.68%	45.21%	23.03%	7.32%	36.78%

Voltages based on:

V_{ZIP} - load flow with chosen ZIP models;

V_{AM} - load flow with exponential models from AM;

V_{NLSrel} - load flow with exponential models from NLSrel;

V_{LF} - load flow corresponding to model.

3.8 Conclusion and Discussion

The load model conversion error (defined in Section 3.2) describes the mismatch between the original and converted load model. The values of the error were analysed by using numerical analysis in publications [I], [II] and [VI]. In Section 3.4, load model conversion error analysis results were used for developing new conversion methods that were presented in publication [I] and [VI]. The new exponential to ZIP model conversion methods displayed higher accuracy than the known method. There might exist other, better, methods for conducting the conversions. The same measures of error and similar numerical analysis can be applied for benchmarking new methods against the methods presented in this dissertation. Thus, one value of the conducted work is also the establishment of an approach usable for benchmarking (static) load model conversion methods.

In Section 3.6 load models estimated in Section 2.4.4 were converted (ZIP models to exponential, exponential models to ZIP), and compared to the corresponding estimated models. It was found that the estimated and converted models typically differ. When

the estimated and converted models were used for simulating the load responses of the case study, the simulation errors (MAE and MSE) were with comparable magnitude. The simulation was conducted by using a simple mathematical model and all the network interactions were neglected (for example load had no impact on voltage).

When load flow calculations are conducted, the conversion error describes only one part of the error caused by the mismatch of the load characteristics. Additionally, the load model error also causes a shift in the state of the modelled system. This leads to voltage changes in the system that, depending on the situation, can amplify or dampen the effect of the conversion error. This was discussed in Section 3.7.1 and illustrated by a case study in Section 3.7.2, Section 3.7.3 and Section 3.7.4. The case study was first presented in publication [VI]. In the case study, significant changes of system state were observed in the case of load model replacement by converted load models. In several cases, compared to the original model (assumed to be accurate) the bus voltages of the system decreased, which might cause false sense of security. The voltages calculated to be within allowable limits using converted load models could give a false indication of the allowable mode of operation. With accurate models the simulation would indicate a voltage issue and a different mode of operation could be chosen. The conducted simulations indicated that the conversion error is an enabler of load flow error, but the values are not an exact match. In future research it may be possible to analyse how the values of the two are related one to another in greater detail.

4 Conclusions and Further Work

4.1 Conclusions

The first objective of this thesis was to develop a methodology for estimating static load models of aggregated transmission system bus loads based on the available measurement data. The available measurement data from the Estonian transmission system was used for testing the methodology. The usability of existing measurement systems from the static load model estimation aspect was analysed. The placement of phasor measurement units and power quality monitors was found to be unsuitable for load modelling (at the time of the analysis). The digital fault recorder (DFR) system was found to cover most of the aggregated transmission system loads. In addition, several years of historical data was found to be available for the DFRs. For this reason the DFR data was chosen for processing.

In order to decrease the number of type models and assign models for unmeasured loads, K-means clustering was implemented for grouping loads into type groups. In the literature load composition at the time of peak loads or the load profiles has been used for clustering. These types of data was not available for the system, and for this reason clustering was implemented based on the monthly load class composition. The 92 substations with the largest loads were clustered into 10 groups with silhouette coefficient indicating a reasonable structure. Due to the insufficient amount of measurement data with high certainty, it was not possible to validate the grouping results in respect to load modelling.

The developed load modelling methodology includes event filtering based on the key indicators of recorded events, and post-processing acquired values using the proposed method of error weighted averaging. The event filtering was implemented because the DFR measurements are event based (measurement started by triggering conditions and ended based on a timer), and most of the events were hypothesised to be unsuitable for load model estimation. The analysis of event filtering results indicated that only a negligible number of events recorded by the DFRs comply with the suitable event requirements (presented in literature). The event filtering was shown to decrease the standard deviation of estimated active load model values (indicating an increase in model precision). Even after the filtering, the standard deviation of the estimated values indicated low precision of estimated values.

The impact of measurement time, weather and penetration of DG (within aggregated load) was illustrated based on the case studies. During the nighttime the voltage sensitivity of the active loads was found to be lowest, and was highest during the evenings. On a colder day, the sensitivity was higher, possibly due to the heating loads. The DG was shown to increase the voltage sensitivity of the aggregated loads. Finally, a method for post-processing a set of estimated load models was presented and analysed. The method was found to be less sensitive to event filtering than the commonly used averaging of values. This could indicate a higher robustness (smaller sensitivity to outliers). However, for conclusive results, a more detailed analysis is needed.

The second objective of this thesis was to benchmark static load model conversion methods (ZIP to exponential, and exponential to ZIP load model conversion) to assess the accuracy of the methods. Firstly, measures of conversion error were defined for comparing different methods using numerical analysis. Derivation of several new methods was explained. The conversion error of the methods was compared to the known and benchmark methods (NLS minimisation of error). A similar benchmarking approach can be applied for assessing the accuracy of methods emerging in the future. The new exponential to ZIP model conversion methods displayed higher accuracy than the known

method and comparable error to NLS minimisation of conversion error. The difference and relation between conversion error and load modelling error in load flow calculations was discussed and illustrated by a case study. In the case study the selection of exponential to ZIP load model conversion method was shown to have a significant impact on the load flow results. In the case of ZIP to exponential load model conversion the load flow differences were larger and similar to both methods.

4.2 Further Work

The measurement systems evolve in time. Thus, after some years it would be reasonable to once again analyse the availability of measurement data in the Estonian transmission system. In addition to assessing the measurement systems and making use of the new available data, it would be reasonable to validate and renew the load models periodically. The devices connected to the power system are slowly replaced by devices based on newer technologies (e.g. incandescent lights replaced by LEDs, newer home appliances using variable speed drives instead of direct drives), which slowly change the aggregated load responses to disturbances.

Furthermore, the estimated static load models of the aggregated transmission system bus loads could be used for assessing the conservation voltage reduction potential of the Estonian power system. This assessment was, however, not in the scope of this thesis. The first reason for not assessing the CVR potential in this thesis is related to the numerical results: it was not possible to determine all the bus load models with sufficient confidence. A measurement campaign would need to be organised to validate and improve the clustering results and estimated models of the loads. In the conducted research project the resources were sufficient for conducting a few pilot studies, but not for a full scale measurement campaign. Secondly, the voltage drop on lower voltage levels would need to be analysed in order to determine how low voltage can be applied without automatic voltage regulation interfering and customer voltages remaining at acceptable level.

A method for post-processing the estimated load model values was presented in Chapter 2. Several ways for implementing the method were presented. However, due to the limited amount of measurement data available, it was difficult to assess which implementation provides the highest load model estimation accuracy and precision. This evaluation could be conducted in the future based on measurement data that enables precise estimation of correct load model.

Numerous methods were presented in Chapter 3 for converting load models. It should be possible to develop methods for handling other load models and to use a similar conversion error analysis for mapping the conversion error of these methods. Also, there might exist some other more accurate ways for conducting these ZIP to exponential and exponential to ZIP load model conversions.

The case study presented in Chapter 3 indicated that replacing load models in load flow by converted load models can cause significant voltage changes. Additional modelling studies can be conducted to analyse in more detail the interaction between the system and load modelling error. Studies of real power systems with validated load models should be analysed in order to properly assess if the models chosen for the illustrative study were realistic or if in a real power system model the load models are more suitable for conversion (lower conversion errors occur and the load flow results are less affected).

List of Figures

1.1	A static load characteristic.	20
1.2	Voltage characteristic of constant power, constant current and constant impedance model.	21
1.3	Component-based load modelling approach.	25
1.4	Process of measurement-based load modelling.	26
2.1	Process of load model estimation.	28
2.2	Monthly energy consumption of a substation, disaggregated by load classes. Adapted from [V].....	31
2.3	Monthly load class compositions of a representative year after normalisation (values stacked). Adapted from [V]	31
2.4	Sum of squared Euclidean distance for different number of clusters. Adapted from [V].....	32
2.5	Silhouette coefficient for different number of clusters. Adapted from [V] ...	33
2.6	Silhouette value of clustering results (92 largest loads). Adapted from [V] ..	34
2.7	Voltage and current unbalance ratios of DFR recorded events of one substation. Maximum value of each event is plotted. Values above the maximum value of tick are included in the last bar.	37
2.8	Difference between minimum and maximum value of voltage during the event.	38
2.9	Minimum value of voltage during the event.	38
2.10	Measured and simulated load (estimated by exponential and ZIP model). ..	42
2.11	Estimated exponential parameter K_{Exp} and $K_{Exp,Q}$ when load models are estimated for all measured events, blue lines mark the boundary values used in estimation. Adapted from [VII]	43
2.12	Estimated exponential parameter K_{Exp} and $K_{Exp,Q}$ when load models are estimated for all measured events and results at boundary values are removed. Adapted from [VII]	43
2.13	Estimated exponential parameter K_{Exp} when load models are estimated for all measured events and results at boundary values are removed. Adapted from [VII]	44
2.14	Estimated exponential parameter $K_{Exp,Q}$ when load models are estimated for all measured events and results at boundary values are removed. Adapted from [VII]	44
2.15	Estimated K_{Exp} and $K_{Exp,Q}$ of events flagged by different event filters.	45
2.16	Estimated exponential parameter K_{Exp} when load models are estimated for filtered events.	46
2.17	Estimated exponential parameter $K_{Exp,Q}$ when load models are estimated for filtered events.	46
2.18	Exponential load model parameters estimated at 2 substations at different times of the day.	48
2.19	Normalised voltage characteristic P_L of exponential load model with exponent $K_{Exp,L} = 2$. Aggregated load: P_L with DG 40% of P_{L0} , 80% of P_{L0} and 120% of P_{L0}	49
2.20	Impact of penetration level of DG on exponential voltage characteristic of aggregated load model (based on (2.20)).	51
2.21	Measured and calculated values during the case study of distributed generation impact. Adapted from [VIII]	52

2.22	Actual load model (exponent $K_{Exp,L}$) and apparent net load (exponent $K_{Exp,T}$) of the feeding transformer.	53
3.1	Load model conversion error (model mismatch) at voltage V_1 when accurate load model is converted to a converted load model. Due to the conversion error, the converted model indicates load P_{1*} at V_1 instead of P_1	58
3.2	Exponential to ZIP load model conversion error when analytical method AM1 and analytical method AM2 (constrained) are used for converting exponential load models with low K_{Exp} values. NMAE is used for quantifying the conversion error.	61
3.3	Analytical method AM2 (unconstrained) uses Equation (3.17) and (3.18) for different range of K_{Exp} values. When either equation is used for the whole K_{Exp} range, the NMAE would be higher than the error of method AM2 (unconstrained) for part of the K_{Exp} range.	62
3.4	NMAE of analytical method AM1 and AM2 (unconstrained).	63
3.5	Voltage dependence of conversion error of non-linear least squares conversion based on absolute error minimisation. Method NLS abs.	63
3.6	Voltage dependence of conversion error of AM3, when 0.8 and 1.2 p.u. are used as V_1/V_b and V_2/V_b	65
3.7	NMAE of developed analytical methods compared to non-linear least squares conversions (NLSrel, NLSabs).	66
3.8	Conversion error and load modelling error in load flow results when the load bus voltage is not affected by the load characteristic. With an accurate load model the load operates at voltage V_1 and consumes P_1 . With converted load model the load operates at voltage V_1 and consumes P_{1*} . Adapted from [VI]	71
3.9	Conversion error and load modelling error in load flow when change of load characteristics causes the load bus voltage to change. With an accurate load model the load operates at voltage V_1 and consumes P_1 . With converted load model the load operates at voltage V_2 and consumes P_{2*} . Adapted from [VI]	71
3.10	Nine-bus power system. Adapted from [VI]	72

List of Tables

1.1	Industry practice of load model usage [60]	20
2.1	Measurement systems used for load modelling in literature.	29
2.2	Number of events with unbalance ratio below threshold value (in total 1843 events recorded at the substation).	36
2.3	Number of events with maximum voltage difference below threshold value (in total 1843 events recorded at the substation).	38
2.4	Number of unsuitable events detected by a filter ^a (diagonal elements) and common events for two filters (non-diagonal elements). [VII]	40
2.5	Exponential load model parameter value ranges in literature.	41
2.6	ZIP load model parameter value ranges in literature.	42
2.7	Mean value μ and standard deviation σ of normal distribution fit (with 95% confidence), MSE weighted mean value μ_{MSE} and MAE weighted mean value μ_{MAE} based on all measured events, except boundary values. [VII]	44
2.8	Mean value μ and standard deviation σ of normal distribution fit (with 95% confidence), MSE weighted mean value μ_{MSE} and MAE weighted mean value μ_{MAE} based on filtered events [VII].....	47
2.9	Number of voltage disturbances. [III]	47
2.10	Impact of post-processing method on calculated value of exponent K_{Exp} . [III]	48
2.11	Impact of post-processing method on calculated value of exponent $K_{Exp,Q}$. [III]	49
2.12	Estimated load models of connected load	53
2.13	Estimated load models of transformer load (net load)	53
2.14	Transformer load modelling by calculated load model (based on DG penetration and the model of the connected load	54
3.1	Analysed conversion methods and the available conversions.....	57
3.2	Estimated exponential load model and exponential models acquired by conversion of estimated ZIP models. $K_{Exp,L}$ - exponent for total supplied load. $K_{Exp,T}$ - exponent for apparent transformer load.	68
3.3	Event modelling error. Total supplied load. Estimated exponential load model and exponential models acquired by conversion of estimated ZIP models.	68
3.4	Event modelling error. Apparent load of the transformer. Estimated exponential load model and exponential models acquired by conversion of estimated ZIP models.	69
3.5	Estimated ZIP load model and ZIP models acquired by conversion of estimated exponential models.....	69
3.6	Event modelling error. Total supplied load. Estimated ZIP load model and ZIP models acquired by conversion of estimated exponential models.....	70
3.7	Event modelling error. Apparent load of the transformer. Estimated ZIP load model and ZIP models acquired by conversion of estimated exponential models.	70
3.8	Cases modelled for case study.	73
3.9	Load and generator voltages and powers in the original Nine-bus system model, and after increasing generator bus voltages (after modification). ...	73
3.10	Chosen exponential and ZIP load models. [VI].....	74
3.11	NMAE when chosen exponential models converted to ZIP models. [VI]	74

3.12	Chosen exponential load models and ZIP models acquired by model conversion (using method AM1 and NLSrel). [VI]	74
3.13	NMAE when chosen ZIP models converted to exponential models using analytical method (AM) and NLSrel. [VI]	75
3.14	Converted exponential models from AM and NLSrel. [VI]	75
3.15	Relative error η of simulation with ZIP models acquired by using conversion methods AM1 and NLSrel. [VI]	76
3.16	Relative conversion error η of AM1 and NLSrel converted models at different voltages. [VI]	77
3.17	Relative error η of simulation with exponential models acquired by using analytical conversion (AM) and method NLSrel. [VI]	77
3.18	Relative conversion error η of AM and NLSrel converted models at different voltages. [VI]	78
4.1	Measurement data used in the thesis.	105

References

- [1] European Commission. 2050 long-term strategy. [Online]. Available: https://ec.europa.eu/clima/policies/strategies/2050_en
- [2] European Commission. (2019, Jul.) Going climate-neutral by 2050: A strategic long-term vision for a prosperous, modern, competitive and climate-neutral EU economy.
- [3] A. Arif, Z. Wang, J. Wang, B. Mather, H. Bashualdo, and D. Zhao, "Load modeling – a review," *IEEE Transactions on Smart Grid*, vol. 9, no. 6, pp. 5986–5999, Nov. 2018, doi: 10.1109/tsg.2017.2700436.
- [4] E. Vaahedi, M. A. Fl-Kady, J. A. Libaque-Esaine, and V. F. Carvalho, "Load models for large-scale stability studies from end-user consumption," *IEEE Transactions on Power Systems*, vol. 2, no. 4, pp. 864–870, 1987, doi: 10.1109/tpwrs.1987.4335264.
- [5] M. L. Coker and H. Kgasoane, "Load modeling," in *1999 IEEE Africon. 5th Africon Conference in Africa (Cat. No.99CH36342)*, vol. 2, Cape Town, South Africa, 1999, pp. 663–668, doi: 10.1109/afrcon.1999.821844.
- [6] L. M. Korunović, D. P. Stojanović, and J. V. Milanović, "Identification of static load characteristics based on measurements in medium-voltage distribution network," *IET Generation, Transmission & Distribution*, vol. 2, no. 2, pp. 227–234, 2008, doi: 10.1049/iet-gtd:20070091.
- [7] A. J. Collin, J. L. Acosta, B. P. Hayes, and S. Z. Djokic, "Component-based aggregate load models for combined power flow and harmonic analysis," in *7th Mediterranean Conference and Exhibition on Power Generation, Transmission, Distribution and Energy Conversion (MedPower 2010)*, Agia Napa, Cyprus, 2010, pp. 1–10, doi: 10.1049/cp.2010.0901.
- [8] C. A. Baone, S. Veda, Y. Pan, W. Premerlani, J. Dai, and A. Johnson, "Measurement based static load model identification," in *2015 IEEE Power & Energy Society General Meeting*, Denver, CO, USA, Jul. 2015, pp. 1–5, doi: 10.1109/pesgm.2015.7285681.
- [9] J. Marchgraber, E. Xypolytou, I. Lupandina, W. Gawlik, and M. Stifter, "Measurement-based determination of static load models in a low voltage grid," in *2016 IEEE PES Innovative Smart Grid Technologies Conference Europe (ISGT-Europe)*, Ljubljana, Slovenia, Oct. 2016, pp. 1–6, doi: 10.1109/isgteurope.2016.7856297.
- [10] European Commission. Nearly zero-energy buildings. [Online]. Available: <https://ec.europa.eu/energy/en/topics/energy-efficiency/buildings/nearly-zero-energy-buildings>
- [11] G. D. Carne, G. Buticchi, M. Liserre, and C. Vournas, "Load control using sensitivity identification by means of smart transformer," *IEEE Transactions on Smart Grid*, vol. 9, no. 4, pp. 2606–2615, Jul. 2018, doi: 10.1109/tsg.2016.2614846.
- [12] Z. Wang, J. Wang, B. Chen, M. M. Begovic, and Y. He, "MPC-based voltage/var optimization for distribution circuits with distributed generators and exponential load models," *IEEE Transactions on Smart Grid*, vol. 5, no. 5, pp. 2412–2420, Sep. 2014, doi: 10.1109/tsg.2014.2329842.

- [13] D. A. Quijano and A. P. Feltrin, "Assessment of conservation voltage reduction effects in networks with distributed generators," in *2015 IEEE PES Innovative Smart Grid Technologies Latin America (ISGT LATAM)*, Montevideo, Uruguay, Oct. 2015, pp. 393–398, doi: 10.1109/isgt-la.2015.7381188.
- [14] T. Lawanson, R. Karandeh, V. Cecchi, and A. Kling, "Impacts of distributed energy resources and load models on conservation voltage reduction," in *2018 Clemson University Power Systems Conference (PSC)*, Charleston, SC, USA, Sep. 2018, pp. 1–6, doi: 10.1109/psc.2018.8664059.
- [15] T. Masuta, S. Asano, and N. H. Viet, "Applicability of conservation voltage reduction to distribution networks with photovoltaic generation considering various load characteristics," in *2017 IEEE International Conference on Industrial and Information Systems (ICIIS)*, Peradeniya, Sri Lanka, Dec. 2017, pp. 1–6, doi: 10.1109/iciinfs.2017.8300333.
- [16] B. Hayes and K. Tomsovic, "Conservation voltage reduction in secondary distribution networks with distributed generation and electric vehicle charging loads," in *2018 5th International Conference on Electric Power and Energy Conversion Systems (EPECS)*, Kitakyushu, Japan, Apr. 2018, pp. 1–6, doi: 10.1109/epecs.2018.8443502.
- [17] Z. Wang and J. Wang, "Review on implementation and assessment of conservation voltage reduction," *IEEE Transactions on Power Systems*, vol. 29, no. 3, pp. 1306–1315, May 2014, doi: 10.1109/tpwrs.2013.2288518.
- [18] "Modelling and aggregation of loads in flexible power networks," CIGRE, Tech. Rep., Feb. 2014, reference: 566.
- [19] W. W. Price, K. A. Wirgau, A. Murdoch, J. V. Mitsche, E. Vaahedi, and M. El-Kady, "Load modeling for power flow and transient stability computer studies," *IEEE Transactions on Power Systems*, vol. 3, no. 1, pp. 180–187, 1988, doi: 10.1109/59.43196.
- [20] L. M. Hajagos and B. Danai, "Laboratory measurements and models of modern loads and their effect on voltage stability studies," *IEEE Transactions on Power Systems*, vol. 13, no. 2, pp. 584–592, May 1998, doi: 10.1109/59.667386.
- [21] J. A. Fuentes, A. Molina-García, and E. Gómez, "A measurement approach for obtaining static load model parameters in real time at the distribution level," *European Transactions on Electrical Power*, vol. 17, no. 2, pp. 173–190, 2007, doi: 10.1002/etep.135.
- [22] M. Sedighzadeh and A. Rezazadeh, "Load modeling for power flow and transient stability computer studies at BAKHTAR network," *International Journal of Energy and Power Engineering*, vol. 1, no. 12, pp. 1809–1816, 2007. [Online]. Available: <https://publications.waset.org/vol/12>
- [23] C. Cresswell, "Steady state load models for power system analysis," Ph.D. dissertation, Institute for Energy Systems, The University of Edinburgh., Edinburgh, UK, 2009.
- [24] L. M. Korunovic, S. Sterpu, S. Djokic, K. Yamashita, S. M. Villanueva, and J. V. Milanovic, "Processing of load parameters based on existing load models," in *2012 3rd IEEE PES Innovative Smart Grid Technologies Europe (ISGT Europe)*, Oct. 2012, doi: 10.1109/isgteurope.2012.6465741.

- [25] Ü. Treufeldt, M. Leinakse, U. Salumäe, T. Sarnet, M. Meldorf, J. Kilter, A. Reinson, and I. Drovtar, "Eesti elektrisüsteemi ülekandevõrgu koormuste staatilised ja dünaamilised karakteristikud. Uurimistöö 1.1-4/2015/227 / Lep 15066 I etapi lõpparuanne," Tallinn University of Technology, Tech. Rep., 2015, (In Estonian).
- [26] Ü. Treufeldt, M. Leinakse, U. Salumäe, T. Sarnet, M. Meldorf, J. Kilter, A. Reinson, I. Matjas, and K. Krusell, "Eesti elektrisüsteemi ülekandevõrgu koormuste staatilised ja dünaamilised karakteristikud. Uurimistöö 1.1-4/2015/227 / Lep 15066 II etapi lõpparuanne," Tallinn University of Technology, Tech. Rep., 2016, (In Estonian).
- [27] Ü. Treufeldt, M. Meldorf, M. Leinakse, T. Sarnet, U. Salumäe, J. Kilter, and A. Reinson, "Eesti elektrisüsteemi ülekandevõrgu koormuste staatilised ja dünaamilised karakteristikud. Uurimistöö 1.1-4/2015/227 / Lep 15066 lõpparuanne," Tallinn University of Technology, Tech. Rep., 2017, (In Estonian).
- [28] S. Rõigas, "Äri ja avaliku teeninduse sektori agregeeritud koormuste modelleerimine tarkvaras PSCAD (Modelling of aggregated commercial and public services loads with PSCAD)," B.Sc. thesis, Dept. Electrical Power Engineering and Mechatronics, Tallinn University of Technology, Tallinn, Estonia, 2017, (In Estonian).
- [29] H. Kapp, "Koormuste modelleerimise erinevused tarkvarades PSCAD ja PSS/E (Comparative load modelling with PSCAD and PSS/E)," B.Sc. thesis, Dept. Electrical Power Engineering and Mechatronics, Tallinn University of Technology, Tallinn, Estonia, 2017, (In Estonian).
- [30] H. Kiristaja, "Koormuse staatiliste pingekarakteristikute ööpäeva-sisese muutlikkuse katseline määramine (Identification of intra-day variations of static load characteristics)," B.Sc. thesis, Dept. Electrical Power Engineering and Mechatronics, Tallinn University of Technology, Tallinn, Estonia, 2018, (In Estonian).
- [31] T. Pihlak, "Kiirete pingemuutuste esinemissageduse määramine pidevmõõteandmetes (Determining frequency of rapid voltage changes in continuous measurement data)," B.Sc. thesis, Dept. Electrical Power Engineering and Mechatronics, Tallinn University of Technology, Tallinn, Estonia, 2020, (In Estonian).
- [32] R. Aavik, "Asünkroonmootorite modelleerimine PSCAD tarkvara võrguarvutustes (Modelling of induction motors in PSCAD network calculations)," M.Sc. thesis, Dept. Electrical Power Engineering and Mechatronics, Tallinn University of Technology, Tallinn, Estonia, 2017, (In Estonian).
- [33] E. Karin, "Kodutarbijate tüüpkoormusseadmete pingekarakteristikute modelleerimine tarkvaraga PSCAD (Modelling of voltage characteristics of domestic load components in PSCAD)," M.Sc. thesis, Dept. Electrical Power Engineering and Mechatronics, Tallinn University of Technology, Tallinn, Estonia, 2017, (In Estonian).
- [34] S. Sorts, "Eesti elektrisüsteemi põhivõrgu koormusklasside sagedussõltuvuste uurimine (Researching frequency dependence of Estonian electrical system load classes)," M.Sc. thesis, Dept. Electrical Power Engineering and Mechatronics, Tallinn University of Technology, Tallinn, Estonia, 2017, (In Estonian).
- [35] P. Tani, "Hajatootjate mõju agregeeritud sõlmekoormustele (Influence of distributed generation on the aggregated load models of the bus loads)," M.Sc. thesis, Dept. Electrical Power Engineering and Mechatronics, Tallinn University of Technology, Tallinn, Estonia, 2017, (In Estonian).

- [36] S. Mishra, M. Leinakse, and I. Palu, "Wind power variation identification using ramping behavior analysis," *Energy Procedia*, vol. 141, pp. 565–571, 2017, doi: 10.1016/j.egypro.2017.11.075.
- [37] S. Mishra, M. Leinakse, I. Palu, and J. Kilter, "Ramping behaviour analysis of wind farms," in *2018 IEEE International Conference on Environment and Electrical Engineering and 2018 IEEE Industrial and Commercial Power Systems Europe (EEEIC / I&CPS Europe)*, Palermo, Italy, Jun. 2018, pp. 1–5, doi: 10.1109/eeeic.2018.8493720.
- [38] M. Leinakse, "Modelling aggregated load with distributed generation by exponential load model," in *2021 IEEE 62nd International Scientific Conference on Power and Electrical Engineering of Riga Technical University (RTUCon)*, Riga, Latvia, 2021, to be published.
- [39] V. Panuska, "Short-term forecasting of electric power system load from a weather-dependent model," *IFAC Proceedings Volumes*, vol. 10, no. 1, pp. 414–418, 1977, doi: [https://doi.org/10.1016/S1474-6670\(17\)67097-6](https://doi.org/10.1016/S1474-6670(17)67097-6). IFAC Symposium on Automatic Control and Protection of Electric Power Systems, Melbourne, Australia, 21-25 February.
- [40] M. Meldorf, T. Täht, and J. Kilter, "Stochasticity of electrical network load," *Oil Shale*, vol. 24, no. 2 Special, pp. 225–236, 2007.
- [41] M. Meldorf and J. Kilter, "Type models of electrical network load," *Oil Shale*, vol. 26, no. 3 Special, pp. 243–253, 2009.
- [42] X. Tang, K. N. Hasan, J. V. Milanovic, K. Bailey, and S. J. Stott, "Estimation and validation of characteristic load profile through smart grid trials in a medium voltage distribution network," *IEEE Transactions on Power Systems*, vol. 33, no. 2, pp. 1848–1859, Mar. 2018, doi: 10.1109/tpwrs.2017.2740563.
- [43] K. N. Hasan, K. M. Muttaqi, P. Borboa, J. Scira, Z. Zhang, and M. Leishman, "Measurement-based electric vehicle load profile and its impact on power system operation," in *2019 9th International Conference on Power and Energy Systems (ICPES)*, Dec. 2019, doi: 10.1109/icpes47639.2019.9105651.
- [44] J. E. Parra, F. L. Quilumba, and H. N. Arcos, "Customers' demand clustering analysis — a case study using smart meter data," in *2016 IEEE PES Transmission & Distribution Conference and Exposition-Latin America (PES T&D-LA)*, Morelia, Mexico, Sep. 2016, pp. 1–7, doi: 10.1109/tdc-la.2016.7805685.
- [45] S. Ruzic, A. Vuckovic, and N. Nikolic, "Weather sensitive method for short term load forecasting in electric power utility of serbia," *IEEE Transactions on Power Systems*, vol. 18, no. 4, pp. 1581–1586, Nov. 2003, doi: 10.1109/tpwrs.2003.811172.
- [46] M. Meldorf, Ü. Treufeldt, and J. Kilter, "Temperature dependency of electrical network load," *Oil Shale*, vol. 24, no. 2 Special, pp. 237–247, 2007.
- [47] L. M. Korunović, A. S. Jović, and S. Z. Djokic, "Measurement-based evaluation of static load characteristics of demands in administrative buildings," *International Journal of Electrical Power & Energy Systems*, vol. 118, p. 105782, jun 2020, doi: 10.1016/j.ijepes.2019.105782.

- [48] A. S. Jović, L. M. Korunović, and S. Z. Djokic, "Application of meteorological variables for the estimation of static load model parameters," *Energies*, vol. 14, no. 16, p. 4874, aug 2021, doi: 10.3390/en14164874.
- [49] M. S. Owayedh, A. A. Al-Bassam, and Z. R. Khan, "Identification of temperature and social events effects on weekly demand behavior," in *2000 Power Engineering Society Summer Meeting*, Seattle, WA, USA, 2000, doi: 10.1109/pess.2000.867364.
- [50] C. Ziser, Z. Dong, and T. K. Saha, "Investigation of weather dependency and load diversity on queensland electricity demand," in *Australasian Universities Power Engineering Conference*, Hobart, Tasmania, Australia, 2005.
- [51] A. Paisios, A. Ferguson, and S. Z. Djokic, "Solar analemma for assessing variations in electricity demands at mv buses," in *Mediterranean Conference on Power Generation, Transmission, Distribution and Energy Conversion (MedPower 2016)*, Belgrade, Serbia, 2016, doi: 10.1049/cp.2016.1006.
- [52] H. A. Bauman, O. W. Manz, J. E. McCormack, and H. B. Seeley, "System load swings," *Transactions of the American Institute of Electrical Engineers*, vol. 60, no. 6, pp. 541–547, Jun. 1941, doi: 10.1109/t-aiee.1941.5058372.
- [53] A. J. Collin, G. Tsagarakis, A. E. Kiprakis, and S. McLaughlin, "Development of low-voltage load models for the residential load sector," *IEEE Transactions on Power Systems*, vol. 29, no. 5, pp. 2180–2188, Sep. 2014, doi: 10.1109/tpwrs.2014.2301949.
- [54] J. Xu, B. Xie, S. Liao, Y. Sun, D. Ke, J. Yang, P. Li, L. Yu, Q. Xu, and X. Ma, "Online assessment of conservation voltage reduction effects with micro-perturbation," *IEEE Transactions on Smart Grid*, vol. 12, no. 3, pp. 2224–2238, May 2021, doi: 10.1109/tsg.2020.3043957.
- [55] Y. Wang, C. Lu, P. Wu, X. Zhang, Y. Su, C. Xiong, and B. Zhao, "Online realization of an ambient signal based load modeling algorithm and its application in field measurement data," *IEEE Transactions on Industrial Electronics*, pp. 1–1, 2021, doi: 10.1109/tie.2021.3102428.
- [56] S. M. H. Rizvi, S. K. Sadanandan, and A. K. Srivastava, "Real-time ZIP load parameter tracking using adaptive window and variable elimination with realistic synthetic synchrophasor data," in *2020 IEEE Industry Applications Society Annual Meeting*, Oct. 2020, doi: 10.1109/ias44978.2020.9334878.
- [57] P. Kundur, *Power System Stability and Control*, N. J. Balu and M. G. Lauby, Eds. McGraw-Hill, Inc., Jan. 1994. ISBN 978-0-07-035958-1
- [58] A. Y. Abdelaziz, M. A. L. Badr, and A. H. Younes, "Dynamic load modeling of an Egyptian primary distribution system using neural networks," *International Journal of Electrical Power & Energy Systems*, vol. 29, no. 9, pp. 637–649, Nov. 2007, doi: 10.1016/j.ijepes.2006.09.006.
- [59] A. Borghetti, R. Caldon, A. Mari, and C. A. Nucci, "On dynamic load models for voltage stability studies," *IEEE Transactions on Power Systems*, vol. 12, no. 1, pp. 293–303, 1997, doi: 10.1109/59.574950.

- [60] J. V. Milanovic, K. Yamashita, S. M. Villanueva, S. Z. Djokic, and L. M. Korunovic, "International industry practice on power system load modeling," *IEEE Transactions on Power Systems*, vol. 28, no. 3, pp. 3038–3046, Aug. 2013, doi: 10.1109/tpwrs.2012.2231969.
- [61] L. Korunovic, J. V. Milanovic, S. Z. Djokic, K. Yamashita, S. Martinez-Villanueva, and S. Sterpu, "Recommended parameter values and ranges of most frequently used static load models," *IEEE Transactions on Power Systems*, pp. 1–1, 2018, doi: 10.1109/tpwrs.2018.2834725.
- [62] C. Cresswell, S. Z. Djokic, and S. Munshi, "Analytical modelling of adjustable speed drive loads for power system studies," in *Power Tech 2007*, Lausanne, Switzerland, 2007, doi: 10.1109/PCT.2007.4538607.
- [63] C. Cresswell and S. Z. Djokic, "Steady state models of low-energy consumption light sources," in *16th Power Systems Computation Conference PSCC 2008*, Glasgow, Scotland, UK, 2008.
- [64] C. Cresswell and S. Z. Djokic, "Representation of directly connected and drive-controlled induction motors. part 1: Single-phase load models," in *2008 18th International Conference on Electrical Machines*, Vilamoura, Portugal, 2008, doi: 10.1109/ICELMACH.2008.4800118.
- [65] C. Cresswell and S. Z. Djokic, "Representation of directly connected and drive-controlled induction motors. part 2: Three-phase load models," in *2008 18th International Conference on Electrical Machines*, Vilamoura, Portugal, 2008, doi: 10.1109/ICELMACH.2008.4800119.
- [66] S. Z. Djokic, C. E. Cresswell, and A. J. Collin, "The future of residential lighting: shift from incandescent to CFL to LED light sources," in *2009 IES Annual Conference*, Seattle, WA, USA, 2009.
- [67] S. Z. Djokic, C. E. Cresswell, and A. J. Collin, "Comparison of electrical characteristics of low-power and high-power CFL and LED light sources," in *2009 IES Annual Conference*, Seattle, WA, USA, 2009.
- [68] M. Ghandhari, *Stability of Power Systems: An Introduction*. Royal Institute of Technology (KTH), Electric Power Systems, 2013.
- [69] M. Kheradmandi and R. Feuillet, "Using voltage control for reducing standing phase angle in power system restoration," *Electric Power Systems Research*, vol. 146, pp. 9–16, May 2017, doi: 10.1016/j.epsr.2017.01.006.
- [70] L. M. Korunovic and D. P. Stojanovic, "The effects of normalization of static load characteristics," in *2009 IEEE Bucharest PowerTech*, Bucharest, Romania, Jun. 2009, pp. 227–234, doi: 10.1109/ptc.2009.5281826.
- [71] "Bibliography on load models for power flow and dynamic performance simulation," *IEEE Transactions on Power Systems*, vol. 10, no. 1, pp. 523–538, 1995, doi: 10.1109/59.373979.
- [72] *PSCAD User's Guide v4.6.0*, Manitoba HVDC Research Centre, Manitoba, Canada, 2015.

- [73] *PSS® E 34 Program Operation Manual*, Siemens Industry, Inc., Siemens Power Technologies International, Schenectady, NY, USA, 2015.
- [74] *DIGSILENT PowerFactory 2017: Technical Reference Documentation General Load (ElmLod, TypLod)*, Digsilent GmbH, Gomaringen, Germany, 2017.
- [75] "Advanced load modeling, 1007318," EPRI, Tech. Rep., 2002.
- [76] "Measurement-based load modeling, 1014402," EPRI, Tech. Rep., 2006.
- [77] S. A. Arefifar and W. Xu, "Online tracking of voltage-dependent load parameters using ULTC created disturbances," *IEEE Transactions on Power Systems*, vol. 28, no. 1, pp. 130–139, Feb. 2013, doi: 10.1109/tpwrs.2012.2199336.
- [78] S. Guo, Y. Jiang, and D. Chen, "Recent developments in load model parameter identification via ambient PMU signal," *Journal of Physics: Conference Series*, vol. 1983, no. 1, p. 012071, Jul 2021, doi: 10.1088/1742-6596/1983/1/012071.
- [79] H. Guo, K. Rudion, H. Abildgaard, and Z. A. Styczynski, "Parameter estimation of dynamic load model using field measurement data performed by OLTC operation," in *2012 IEEE Power and Energy Society General Meeting*, San Diego, CA, USA, Jul. 2012, pp. 1–7, doi: 10.1109/pesgm.2012.6345563.
- [80] X. Zhang, C. Lu, J. Lin, Y. Wang, J. Wang, H. Huang, and Y. Su, "Experimental measurement of PMU error distribution and its impact on load model identification," in *2016 IEEE Power and Energy Society General Meeting (PESGM)*, Jul. 2016, doi: 10.1109/pesgm.2016.7741069.
- [81] X. Wang, "Estimating dynamic load parameters from ambient PMU measurements," in *2017 IEEE Power & Energy Society General Meeting*, Jul. 2017, doi: 10.1109/pesgm.2017.8273913.
- [82] X. Zhang, C. Lu, J. Lin, and Y. Wang, "Experimental test of PMU measurement errors and the impact on load model parameter identification," *IET Generation, Transmission & Distribution*, vol. 14, no. 20, pp. 4593–4604, Sep 2020, doi: 10.1049/iet-gtd.2020.0297.
- [83] K. Fungyai, N. Sangmeg, A. Pichetjamroen, S. Dechanupaprittha, and N. Somaketarin, "Determination of ZIP load model parameters based on synchrophasor data by genetic algorithm," in *2020 8th International Electrical Engineering Congress (IEECON)*, Mar. 2020, doi: 10.1109/ieecon48109.2020.229509.
- [84] A. Gulakhmadov, A. Tavlintsev, A. Pankratov, A. Suvorov, A. Kovaleva, I. Lipnitskiy, M. Safaraliev, S. Semenenko, P. Gubin, S. Dmitriev, and K. Rasulzoda, "A statistical-based approach to load model parameter identification," *IEEE Access*, vol. 9, pp. 66 915–66 928, 2021, doi: 10.1109/access.2021.3076690.
- [85] T. Vinnal, "Eesti ettevõtete elektritarbimise uurimine ja soovituste väljatöötamine tarbimise optimeerimiseks," Ph.D. dissertation, Dept. Electrical Engineering, Tallinn University of Technology, Tallinn, Estonia, 2011.
- [86] T. Vinnal, "Aruanne nr 19062. Toitepinge kvaliteet Eesti 0,4 kV madalpingevõrkudes ja tarbijapagaldiste liitumispunktides," Tallinn University of Technology, Tech. Rep., 2013, (In Estonian).

- [87] W. Freitas and L. C. P. da Silva, "A discussion about load modeling by using voltage variations," in *2012 IEEE 15th International Conference on Harmonics and Quality of Power*, Hong Kong, China, Jun. 2012, pp. 40–44, doi: 10.1109/ichqp.2012.6381271.
- [88] V. Vignesh, S. Chakrabarti, and S. C. Srivastava, "Load modeling under unbalanced disturbances," *IEEE Transactions on Power Systems*, vol. 31, no. 2, pp. 1661–1662, Mar. 2016, doi: 10.1109/tpwrs.2015.2412695.
- [89] K. N. Hasan and J. V. Milanovic, "Interim profile modelling study," The University of Manchester & Electricity North West Limited, UK, Tech. Rep., 2015.
- [90] S. Sheng, K. K. Li, W. L. Chan, Z. Xiangjun, and L. Xinran, "Using substation automation information for electric power load modeling and predictive maintenance of circuit breaker," in *INDIN '05. 2005 3rd IEEE International Conference on Industrial Informatics*, Perth, WA, Australia, 2005, doi: 10.1109/indin.2005.1560435.
- [91] K. Q. Hua, A. Vahidnia, Y. Mishra, and G. Ledwich, "PMU measurement based dynamic load modeling using SVC devices in online environment," in *2015 IEEE PES Asia-Pacific Power and Energy Engineering Conference (APPEEC)*, Brisbane, QLD, Australia, Nov. 2015, pp. 1–5, doi: 10.1109/appeec.2015.7381020.
- [92] Y. Ge, A. J. Flueck, D.-K. Kim, J.-B. Ahn, J.-D. Lee, and D.-Y. Kwon, "An event-oriented method for online load modeling based on synchrophasor data," *IEEE Transactions on Smart Grid*, vol. 6, no. 4, pp. 2060–2068, Jul. 2015, doi: 10.1109/tsg.2015.2405920.
- [93] S. Lloyd, "Least squares quantization in PCM," *IEEE Transactions on Information Theory*, vol. 28, no. 2, pp. 129–137, Mar. 1982, doi: 10.1109/tit.1982.1056489.
- [94] G. Grigoras, F. Scarlatache, and G. Cartina, "Load estimation for distribution systems using clustering techniques," in *2012 13th International Conference on Optimization of Electrical and Electronic Equipment (OPTIM)*, Brasov, Romania, May 2012, pp. 301–306, doi: 10.1109/optim.2012.6231789.
- [95] M. Grabner, Z. Bregar, Š. Ivanjko, and L. Valenčič, "Improved model for the spatial load forecasting of the Slovenian distribution network," *CIREN - Open Access Proceedings Journal*, vol. 2017, no. 1, pp. 2354–2357, Oct. 2017, doi: 10.1049/oap-cired.2017.1020.
- [96] M. Grabner, A. Souvent, B. Blazic, and A. Kosir, "Statistical load time series analysis for the demand side management," in *2018 IEEE PES Innovative Smart Grid Technologies Conference Europe (ISGT-Europe)*, Sarajevo, Bosnia-Herzegovina, Oct. 2018, pp. 1–6, doi: 10.1109/isgteurope.2018.8571845.
- [97] P. J. Rousseeuw, "Silhouettes: A graphical aid to the interpretation and validation of cluster analysis," *Journal of Computational and Applied Mathematics*, vol. 20, pp. 53–65, Nov. 1987, doi: 10.1016/0377-0427(87)90125-7.
- [98] R. Gove. (2017) Using the elbow method to determine the optimal number of clusters for k-means clustering. [Online]. Available: <https://bl.ocks.org/rpgove/0060ff3b656618e9136b>
- [99] K. Mahendru. (2019) How to determine the optimal K for K-means? [Online]. Available: <https://medium.com/analytics-vidhya/how-to-determine-the-optimal-k-for-k-means-708505d204eb>

- [100] L. Kaufman and P. J. Rousseeuw, Eds., *Finding Groups in Data*. John Wiley & Sons, Inc., Mar. 1990.
- [101] I. R. Navarro, "Dynamic power system load – estimation of parameters from operational data," Ph.D. dissertation, Dept. Industrial Electrical Engineering and Automation, Lund Univ., Lund, Sweden, 2005.
- [102] Z. Y. Dong, A. Borghetti, K. Yamashita, A. Gaikwad, P. Pourbeik, and J. Milanovic, "CI-GRE WG C4.065 recommendations on measurement based and component based load modelling practice," in *CIGRE SC C4 Colloquium: Fusion of Lightning Research and Practice for Power System in the Future*, Hakodate, Japan, Oct. 2012.
- [103] *European standard EN 61000-4-30:2015. Electromagnetic compatibility (EMC) - Part 4-30: Testing and measurement techniques - Power quality measurement methods*, European Committee for Electrotechnical Standardization Std.
- [104] *European standard EN 50160:2010+A1+A2+A3:2019. Voltage characteristics of electricity supplied by public electricity networks*, European Committee for Electrotechnical Standardization Std.
- [105] Y. Zhu and J. V. Milanovic, "Automatic identification of power system load models based on field measurements," *IEEE Transactions on Power Systems*, vol. 33, no. 3, pp. 3162–3171, May 2018, doi: 10.1109/tpwrs.2017.2763752.
- [106] L. Korunović and D. Stojanović, "Load model parameters in low and medium voltage distribution networks," *Elektroprivreda*, vol. 55, no. 2, pp. 46–56, 2002, (in Serbian).
- [107] J. V. Milanović, "On unreliability of exponential load models," *Electric Power Systems Research*, vol. 49, no. 1, pp. 1–9, Feb. 1999, doi: 10.1016/S0378-7796(98)00047-9.
- [108] W.-S. Kao, C.-J. Lin, C.-T. Huang, Y.-T. Chen, and C.-Y. Chiou, "Comparison of simulated power system dynamics applying various load models with actual recorded data," *IEEE Transactions on Power Systems*, vol. 9, no. 1, pp. 248–254, 1994, doi: 10.1109/59.317604.
- [109] K. N. Hasan, J. V. Milanovic, P. Turner, and V. Turnham, "A step-by-step data processing guideline for load model development based on field measurements," in *2015 IEEE Eindhoven PowerTech*, Eindhoven, Netherlands, Jun. 2015, pp. 1–6, doi: 10.1109/ptc.2015.7232307.
- [110] W. Jili, H. Renmu, and M. Jin, "Load modeling considering distributed generation," in *2007 IEEE Lausanne Power Tech*, Lausanne, Switzerland, Jul. 2007, pp. 1072–1077, doi: 10.1109/pct.2007.4538464.
- [111] J. Qian, X. Li, and J. Hui, "Impact of wind generation on load modeling of distribution network," in *2009 International Conference on Sustainable Power Generation and Supply*, Nanjing, China, Apr. 2009, pp. 1–5, doi: 10.1109/supergen.2009.5348295.
- [112] L. Rodriguez-Garcia, S. Perez-Londono, and J. Mora-Florez, "A methodology for composite load modeling in power systems considering distributed generation," in *2012 Sixth IEEE/PES Transmission and Distribution: Latin America Conference and Exposition (T&D-LA)*, Montevideo, Uruguay, Sep. 2012, pp. 1–7, doi: 10.1109/tdc-la.2012.6319122.

- [113] T. V. Cutsem and C. Vournas, *Voltage Stability of Electric Power Systems*. Kluwer, 1998.
- [114] R. A. Walling, R. Saint, R. C. Dugan, J. Burke, and L. A. Kojovic, "Summary of distributed resources impact on power delivery systems," *IEEE Transactions on Power Delivery*, vol. 23, no. 3, pp. 1636–1644, Jul. 2008, doi: 10.1109/tpwrd.2007.909115.
- [115] Y. Ge, A. J. Flueck, D.-K. Kim, J.-B. Ahn, J.-D. Lee, and D.-Y. Kwon, "Power system real-time event detection and associated data archival reduction based on synchrophasors," *IEEE Transactions on Smart Grid*, vol. 6, no. 4, pp. 2088–2097, Jul. 2015, doi: 10.1109/tsg.2014.2383693.
- [116] D. Han, J. Ma, R. mu He, and Z. yang Dong, "A real application of measurement-based load modeling in large-scale power grids and its validation," *IEEE Transactions on Power Systems*, vol. 24, no. 4, pp. 1756–1764, Nov. 2009, doi: 10.1109/tpwrs.2009.2030298.
- [117] J. Zhang, Y. Sun, J. Xu, S. Liu, J. Xin, Q. Lei, and H. Dong, "Electric load model based on aggregation algorithm," in *2009 Asia-Pacific Power and Energy Engineering Conference*, Wuhan, China, Mar. 2009, pp. 1–4, doi: 10.1109/appeec.2009.4918324.
- [118] *DIGSILENT PowerFactory 2017: Nine-bus System*, DIGSILENT GmbH, Gomaringen, Germany, 2017.
- [119] P. M. Anderson, *Power System Control and Stability*, 2nd ed. Piscataway, N.J: Iowa State University Press, 2003. ISBN 0-471-23862-7
- [120] J. C. Lansey. (2021) Beautiful and distinguishable line colors + colormap. MATLAB Central File Exchange:. [Online]. Available: <https://www.mathworks.com/matlabcentral/fileexchange/42673-beautiful-and-distinguishable-line-colors-colormap>
- [121] C. Brewer and M. Harrower. Colorbrewer. The Pennsylvania State University. [Online]. Available: <http://colorbrewer2.org>
- [122] M. Leinakse and J. Kilter, "Conversion error of exponential to second order polynomial ZIP load model conversion," in *2018 IEEE International Conference on Environment and Electrical Engineering and 2018 IEEE Industrial and Commercial Power Systems Europe (EEEIC / I&CPS Europe)*, Palermo, Italy, Jun. 2018, pp. 1–5, doi: 10.1109/eeeic.2018.8493667.
- [123] M. Leinakse and J. Kilter, "Conversion error of second order polynomial ZIP to exponential load model conversion," in *Mediterranean Conference on Power Generation, Transmission, Distribution and Energy Conversion (MedPower 2018)*, Dubrovnik, Croatia, 2018, doi: 10.1049/cp.2018.1882.
- [124] M. Leinakse, H. Kiristaja, and J. Kilter, "Identification of intra-day variations of static load characteristics based on measurements in high-voltage transmission network," in *2018 IEEE PES Innovative Smart Grid Technologies Conference Europe (ISGT Europe 2018)*, Sarajevo, Bosnia-Herzegovina, 2018, pp. 1–6, doi: 10.1109/ISGTEurope.2018.8571712.
- [125] M. Leinakse, P. Tani, and J. Kilter, "Impact of distributed generation on estimation of exponential load models," in *2019 IEEE Power & Energy Society General Meeting (PESGM)*, Atlanta, GA, USA, 2019, pp. 1–5, doi: 10.1109/PESGM40551.2019.8974014.

- [126] M. Leinakse and J. Kilter, "Clustering of transmission system loads based on monthly load class energy consumptions," in *2020 21st International Scientific Conference on Electric Power Engineering (EPE)*, Prague, Czech Republic, Oct. 2020, pp. 1–6, doi: 10.1109/epe51172.2020.9269197.
- [127] M. Leinakse and J. Kilter, "Exponential to ZIP and ZIP to exponential load model conversion: Methods and error," *IET Generation, Transmission & Distribution*, vol. 15, no. 2, pp. 177–193, 2021, doi: 10.1049/gtd2.12002.
- [128] M. Leinakse and J. Kilter, "Processing and filtering digital fault recorder events for load model estimation," in *2021 IEEE PES Innovative Smart Grid Technologies Europe (ISGT Europe)*, Espoo, Finland, Oct. 2021, pp. 01–05, doi: 10.1109/isgteurope52324.2021.9640026.
- [129] M. Leinakse, G. Andreesen, P. Tani, and J. Kilter, "Estimation of exponential and ZIP load model of aggregated load with distributed generation," in *2021 IEEE 62nd International Scientific Conference on Power and Electrical Engineering of Riga Technical University (RTUCON)*, Riga, Latvia, 2021, to be published.
- [130] M. Leinakse, T. Sarnet, T. Kangro, and J. Kilter, "First results on load model estimation using digital fault recorder measurements," in *16th International Symposium "Topical Problems in the Field of Electrical and Power Engineering" and "Doctoral School of Energy and Geotechnology III"*, Pärnu, Estonia, 2017, pp. 101–105.
- [131] M. Leinakse, H. Kapp, and J. Kilter, "Preliminary study on comparative load modelling in PSS/E and PSCAD," in *17th International Symposium "Topical Problems in the Field of Electrical and Power Engineering" and "Doctoral School of Energy and Geotechnology III"*, Kuressaare, Estonia, 2018, pp. 197–199.
- [132] I. Palu, M. Leinakse, Ü. Treufeldt, M. Meldorf, T. Sarnet, J. Šuvalova, K. Kull, U. Salumäe, A. Avingu, and T. Trummal, "Reaktiivvõimsuse kompenseerimine Eesti elektrisüsteemis. Iep 17056 lõpparuanne," Tallinn University of Technology, Tech. Rep., 2018, (In Estonian).
- [133] M. Leinakse, "Thoughts on conversion of static load models," in *18th International Symposium "Topical Problems in the Field of Electrical and Power Engineering" and "Doctoral School of Energy and Geotechnology III"*, Toila, Estonia, 2019, pp. 187–188.
- [134] M. Leinakse, "Thoughts on impact of distributed generation on estimation of exponential load models," in *19th International Symposium "Topical Problems in the Field of Electrical and Power Engineering" and "Doctoral School of Energy and Geotechnology III"*, Tartu, Estonia, 2020, pp. 161–162.
- [135] S. Mishra, C. Bordin, M. Leinakse, F. Wen, R. Howlett, and I. Palu, *Handbook of Smart Energy Systems*. Springer Nature, 2022, ch. Scope and overview of virtual power plants with integrated energy systems, to be published.

Acknowledgements

This dissertation is dedicated to Evi, Malju, Jaan, Leo and Linda. You have always had an important place in my life and memories. I am deeply sorry for taking too long to complete these studies, knowing that in many ways now is simply too late. Hopefully, I will be able to explain some part of this to you, my dear granny.

Looking back at the past years, there are a few people who were always there for me when I needed them the most. I would like to express my deepest gratitude to my family, near and far. All of this was only possible thanks to your support. Hopefully, in the future I will be able to be there for you more often than in the past ten years. Maybe even spend more time with Riley and Ellie than on these past years.

This brings me to you, my dear friends. More often than I would like to admit, you listened to my moaning, groaning and whining, without any complaints. Also, for once too many I probably bailed on you by some old, sorry I have to get this thing done now (yesterday) at work/school. Furthermore, you even came along with many crazy ideas and helped to prove that sometimes seemingly impossible is possible. Thank you for the fun times, for not giving up on me, and being there when I needed you.

During my PhD studies, I met several times a man, who is driven by curiosity and fascinated by power systems. At one point he might have even claimed that PhD studies should be an enjoyable journey and doing science should be fun. Without his grant applications and support completing this research would not had been possible. Thank you Jako, for believing in me at times, when I had lost hope.

In addition to the previously mentioned people, there were many others who enabled me to conduct this work. Many employees of Elektrilevi and Elering contributed to this work by providing insight, completing different tasks and sharing measurement data. Thank you for taking the time to support me in this work! Several BSc and MSc students conducted research related to this dissertation. Saamuel, Henry, Hendrik, Tanel, Rasmus, Enn, Sander, Pärtel, thank you for your contributions!

In science we stand upon the shoulders of giants. In the light of that thought I would like to list some of the researchers, who were especially inspirational, and some publications, which had a high impact on my research. I am thankful for the authors of these works for their contributions to science. The first publications I read on load modelling were technical reports of CIGRE [18] and EPRI [75, 76]. The authors of these technical reports have done a tremendous work gathering and organising the included information. I have enjoyed reading the well written publications of Lidija Korunović, Adam Collin, Jovica Milanović and Saša Djokić. In addition, a tutorial of Giovanni De Carne conducted at ISGT Europe 2018 gave me an inspiration for the work described in Section 2.4.4. The color selection of the included figures of the dissertation was inspired by the colormaps published in [120]. These colormaps are based on the theory of [121].

Financial support of Elering AS, European Development Fund, Development Foundation of Tallinn University of Technology; City of Tallinn has been greatly appreciated and without the support, this dissertation would not be what it is.

Abstract

Estimation and Conversion of Static Load Models of Aggregated Transmission System Loads

The load composition and behaviour of the devices connected to the power system changes in time. This leads to a need for renewing the load models used for modelling the behaviour of the system. Additionally, the increasing amount of renewable generation is pushing the power systems closer to their limits. In order to utilise the existing system as close to the limits as possible, while sustaining safe and reliable operation, accurate modelling of the system (including load modelling) is vital. However, the load is dependent on weather, the habits of consumers, and inhibits stochastic changes. This means the load models estimated for one power system may not be suitable for modelling another system. Currently preparations are underway to desynchronise the Estonian and Baltic power system from the IPS/UPS system and synchronise to the Continental Synchronous Area in 2025. In order to accurately model the system, the load models of the system were taken under review in research project "Static and dynamic characteristics of loads of Estonian electrical transmission network". This project was conducted at Tallinn University of Technology for the Estonian transmission system operator Elering AS. This thesis was started as a part of the project. Among other tasks of the project, a combined load modelling methodology needed to be developed and implemented to take use of the existing measurement data and systems.

The first objective of this thesis was to develop a methodology for estimating static load models of aggregated transmission system bus loads based on the available measurement data. The developed load modelling methodology combines the K-means clustering of loads (based on monthly load class composition), event filtering based on the key indicators of the recorded event, and post-processing acquired values using the proposed method of error weighted averaging. This combination of data processing methods is a novel approach for load model estimation. The usability of existing measurement systems from the static load model estimation aspect was analysed. The placement of phasor measurement units and power quality monitors was found to be unsuitable for load modelling (at the time of the analysis). The digital fault recorder (DFR) system was found to cover most of the aggregated transmission system loads. In addition, several years of historical data were found to be available for the DFRs. A data processing methodology was developed and implemented for processing the historical data of the DFRs. In order to decrease the number of type models and assign models for unmeasured loads, the K-means clustering was implemented for grouping loads into type groups. In the literature load composition at the time of peak loads or the load profiles has been used for clustering. These types of data were not available for the system, and for this reason clustering was implemented based on the monthly load class composition.

The analysis of event filtering results indicated that only a negligible number of events recorded by the DFRs comply with the suitable event requirements (presented in the literature). The event filtering was shown to decrease the standard deviation of estimated active load model values (indicating an increase in model precision). In addition, the impact of measurement time, outside temperature, and penetration of distributed generation (connected to the load bus and not affecting the feeder losses) was analysed and discussed based on measurement data acquired from case studies. These factors were shown to have a significant impact on the estimation results.

In addition to the developed combined load modelling approach, component-based modelling was conducted as a part of the research project "Static and dynamic charac-

teristics of loads of Estonian electrical transmission network". In the project load models had to be estimated for PSS® E (uses ZIP model) and PSCAD software (uses exponential load model) based on component models found in the literature. This caused the need for conducting load model conversions (ZIP to exponential, and exponential to ZIP model conversion). When choosing the methods for conducting the conversions, it was found that there is a lack of information on the accuracy of conversion methods. In order to choose the best method, the conversion error of known methods was analysed and compared.

The second objective of this thesis was to benchmark static load model conversion methods (ZIP to exponential, and exponential to ZIP load model conversion) to assess the accuracy of the methods. Numerical analysis of generated load models was used for quantifying and comparing the conversion error of known and developed methods. The developed methods for exponential to ZIP load model conversion were shown to have better accuracy than the known method. Furthermore, the impact of conversion error on load modelling error in load flow calculations was analysed based on a case study. The results of the case study indicated that significant power flow calculation errors can be caused by the inaccuracy of load model conversion. Static load model conversion error and comparison of accuracy of conversion methods is a novel research topic.

Keywords

Clustering, Conversion error, Exponential model, Data mining, Distributed generation, Load modelling, Static load models, ZIP model

Kokkuvõte

Ülekandevõrgu sõlmekoormuste staatiliste koormusmodelite määramine ja teisendamine

Elektrisüsteemiga ühendatud tarbimisseadmete koosseis ja käitumine muutub ajas. Tulevalt süsteemiga ühendatud koormuse muutumisest on tarvis süsteemi modelleerimisel kasutatavaid koormusmudeleid uuendada. Lisaks on kasvanud hajatootjate hulk, mis kohati põhjustab süsteemi opereerimist süsteemi piiridele varasemast lähemal. Selleks, et opereerida süsteemi piiridele lähemal ilma töökindluses oluliselt kaotamata on tarvilik süsteemi varasemast täpsemalt modelleerida. Paraku sõltuvad koormused nii ilmastikutingimustest, tarbijate harjumustest kui ka teistest teguritest. Seetõttu ei ole sageli võimalik ühe ülekandevõrgu tarbijate jaoks määratud mudeleid teises võrgus rakendada. Eestis, Lätis ja Leedus on ettevalmistamisel IPS/UPS süsteemist desünkroniseerimine ja sünkroniseerimine Mandri-Euroopa sünkroonalaga. Elektrisüsteemi täpsemaks modelleerimiseks uuriti projektis "Eesti elektrisüsteemi ülekandevõrgu koormuste staatilised ja dünaamilised karakteristikud" ülekandevõrgu sõlmekoormuste mudeleid. Projekti partneriteks olid Tallinna Tehnikaülikool ja Elering AS. Selle lõputöö koostamine algas nimetatud projekti raames. Projekti käigus tekkis tarvidus mudelite kombineeritud määramise meetodika välja töötamiseks ja rakendamiseks.

Doktoritöö esimeseks eesmärgiks oli ülekandevõrgu agregeeritud sõlmekoormuste mudelite määramise meetodika välja töötamine. Välja töötatud meetodika kombineerib K-keskmise klasterdamismeetodit (kasutades sisendina ekvivalentaasta kuude koormuskoosseise), mõõtesündmuste filtreerimist (tuginedes sündmuse põhinäitajatele) ja järeltöötlust kasutades veaga kaalutud keskmistamist. Selline andmetöötlusmeetodite kombinatsioon on uudne. Mõõtesüsteemide kasutatavuse analüüsil tuvastati, et olemasolevate faasimõõteseadmete ja elektrikvaliteedi analüsaatorite paigutus on koormusmodelite määramise seisukohalt ebasobiv. Samas, häiringusalvestite mõõdetavate suuruste kaudu oli võimalik tuvastada enamiku sõlmekoormuste tarbimine. Lisaks sisaldas häiringusalvestite andmebaas mitmete aastate jagu mõõteandmeid. Nende andmete töötlemiseks töötati välja meetodika ning rakendati MATLAB tarkvaras. Tüüpmodelite arvu vähendamiseks ning mitte mõõdetavatele sõlmekoormuste mudelite määramiseks võeti kasutusele K-keskmise klasterdamismeetod, mille abil on võimalik koormusi grupeerida. Kirjanduses kasutatakse grupeerimiseks koormusprofile ja tipukoormuse aegseid koormuskoosseise. Paraku vastavad andmed ei olnud saadaval ja seetõttu rakendati klasterdamist lähtudes ekvivalentaasta kuude koormusklassi koosseisudest.

Mõõtesündmuste filtreerimise tulemuste põhjal vastavad ainult üksikud mõõdetud sündmused kirjanduses esitatud sobiva mõõtesündmuse tingimustele. Kasutatud andmekogumi puhul vähendas filtreerimine määratud väärtuste standardhälvet. Lisaks käsitletakse töös mõõteaja, välistemperatuuri ja hajatootjate mõju sõlmekoormuse mudeli määramise tulemustele lähtudes teostatud juhtumiuringutest. Tulemuste põhjal on nendel teguritel oluline mõju koormusmodelite määramise tulemustele.

Lisaks kombineeritud koormusmodelite määramise meetodikale rakendati projektis "Eesti elektrisüsteemi ülekandevõrgu koormuste staatilised ja dünaamilised karakteristikud" komponentidepõhise koormusmodelite määramise meetodikat. Projekti raames oli tarvis määrata mudelid nii PSS® E (kasutab koormuse ZIP mudelit) kui ka PSCAD tarkvara (kasutab koormuse eksponentmudelit) tuginedes kirjanduses kirjeldatud mudelitele. Komponentidepõhise koormusmodelite määramise meetodika rakendamisel tekkis vajadus eksponent- ja ZIP mudeli vaheliste teisenduste teostamiseks. Teisenduste teostamiseks meetodi valimisel ilmnis, et kirjandusest ei ole võimalik leida infot teisendusmee-

todite täpsuse kohta. Info hankimiseks oli tarvis analüüsida ja võrrelda teadaolevate teisendusmeetodite täpsust.

Doktoritöö teiseks eesmärgiks oli staatiliste koormusmodelite teisendusmeetodite (ZIP ja eksponentmudeli vahelise teisenduse) täpsuse hindamine. Täpsuse hindamiseks kasutati numbrilist analüüsi. Eksponentmudelite ZIP mudeliteks teisendamisel kasutatavate meetodite teisendusvigade analüüsi ilmnisid seaduspärad, millest lähtudes töötati välja uued meetodid. Tuvastati, et uued meetodid on täpsemad kui teadaolev analüütiline teisendusmeetod. Lisaks analüüsiti koormusmodelite teisendusvea mõju püsiseisundi arvutuse tulemustele kasutades tuntud võrgumudelit. Tuvastati, et koormusmodelite teisendamine võib oluliselt mõjutada arvutustulemusi. Koormusmodelite teisendamise täpsus ja meetodite täpsuse võrdlemine on uued teematikad elektrisüsteemide modelleerimise valdkonnas.

Märksõnad

Andmekaeve, Eksponentmudel, Hajatootmine, Klasterdamine, Koormuste modelleerimine, Staatilised koormuskarakteristikud, Staatilised koormusmodelid, ZIP mudel, Teisendusviga

Appendix 1 - Used Measurement Data

In Chapter 2 different sets of measurement data are used for illustrating different aspects of load model estimation. In Table 4.1 the main properties of the used datasets are listed.

Table 4.1: Measurement data used in the thesis.

Number of Measured Substations	Duration	Type of Data	Used in	Other Details
92	January 2013 to September 2015	Metering data	Section 2.2.3	Monthly energy consumption of substations, disaggregated by 5 load classes
1	January 2018 to December 2020	DFR	Section 2.3, Section 2.4.2	
1	December 2016 (1.5 hours)	PQM	Section 2.4.1	
1	February 2017 (1 hour)	PQM	Section 2.4.3	
2	April 2017 (3x 1...1.5 hours)	PQM	Section 2.4.3	One of the substations was measured also in February 2017
1	March 2017 (1.5 hours)	PQM, SCADA	Section 2.4.4	

Appendix 2 - Included Publications

Publication I

M. Leinakse and J. Kilter, "Conversion error of exponential to second order polynomial ZIP load model conversion," in *2018 IEEE International Conference on Environment and Electrical Engineering and 2018 IEEE Industrial and Commercial Power Systems Europe (EEEIC / I&CPS Europe)*, Palermo, Italy, Jun. 2018, pp. 1–5, doi: 10.1109/eeeic.2018.8493667

©2018 IEEE. Reprinted with permission.

Conversion Error of Exponential to Second Order Polynomial ZIP Load Model Conversion

Madis Leinakse, Jako Kilter

Department of Electrical Power Engineering and Mechatronics

Tallinn University of Technology

Tallinn, Estonia

madis.leinakse@ttu.ee, jako.kilter@ttu.ee

Abstract—This paper presents two novel analytical methods for exponential to second order polynomial (i.e. ZIP) load model conversion. The load model conversion error of the proposed methods and three known methods is compared based on the results of conducted numerical analysis. The conversion accuracy of the proposed analytical methods was found to be better than the accuracy of previously known analytical conversion method. In some cases, the conversion error of proposed methods was comparable to non-linear least squares conversion results. It is also shown that the load model conversion error depends on the used conversion method, exponential load model parameter values and the voltage used for error calculation.

Keywords—conversion error; exponential model; load modeling; static load models; ZIP model;

I. INTRODUCTION

According to the survey results presented in [1], several software packages are in use for steady state and time-domain simulations of power systems. The load models of the software packages differ in some cases, e.g. PSS/E uses a ZIP model based model [2], while PSCAD uses exponential model based model [3] as the main load model. The main load model of PSCAD and PSS/E are described in more detail in section II.

The need for load model conversion arises if two software packages have a different load model and the system model of one software is taken as a basis for constructing model for the second software. If the raw data used for load model estimation is available, the load model conversion may in some cases be replaced by re-estimation of load models. A second use case for exponential to ZIP model conversion is the application of component-based load modelling. If the known component models are in exponent format, the conversion to ZIP model is useful for simplifying load model aggregation. ZIP models can be accurately aggregated using weighted sum of ZIP models, as was done in [4].

In case of load model conversion, the main goal is to minimise the conversion error to preserve the original load characteristics and to limit the additional modelling inaccuracy of the power system model. For minimising the error between measured and simulated values, non-linear least squares (NLS) algorithms have been widely used due to their robustness

and easy implementation [5]. The squared error minimisation approach to load model conversion is presented in section III-D. NLS conversion was implemented in this study to obtain a comparison basis for the analytical methods.

Describing methods for load model conversion from exponential to second order polynomial is an uncommon topic in load modelling papers. Still, an analytical method for conversion from exponential to ZIP model has been described in [6]. Analytical solution of that method is presented in section III-A. The method was used in the cited paper without considering the load model conversion error.

This paper consists of five sections. In section II, the exponential load model, PSCAD load model, second order polynomial load model (ZIP) and PSS/E main load model are described. Next, in section III, five methods for exponential to ZIP model conversion are presented. The load model conversion error of the presented methods is analysed in section IV. Finally, the main results of the study are summarized in section V.

II. LOAD MODELS

In the following sections of the paper, equations are given only for the real load component. The reactive component of the load has mathematically similar equations.

A. Exponential Load Model and PSCAD Model Fixed Load

The exponential load model describes the voltage characteristic of the load by an exponential equation (1).

$$P_{EXP} = P_n (V/V_n)^{K_{Exp}} \quad (1)$$

where P_n is the real power of the load at nominal voltage V_n .

PSCAD load models Fixed Load L-L and Fixed Load L-G are both based on exponential load model. Within voltage range $V/V_0 \in \{0.8...1.2\}$, where V_0 is nominal voltage, the PSCAD load models Fixed Load L-L and Fixed Load L-G have exponential voltage characteristic (2).

$$P = P_0 (V/V_0)^{K_{pv}} \quad (2)$$

where P_0 is the real power of the load at nominal voltage V_0 .

In case of lower and higher voltages, the PSCAD load models behave as constant admittance load [3], similar to an exponential load model with exponent value $K_{pv} = 2$. According to [3], the allowed K_{pv} values are: $-5.0 \leq K_{pv} \leq 5.0$.

This paper was funded by the European Union via the European Regional Development Fund.

B. Second Order Polynomial (ZIP) Load Model and PSS/E Load Model

The ZIP load model describes the voltage characteristic of the load by a second order polynomial equation (3).

$$\begin{cases} P_{ZIP} = P_n(K_Z(V/V_n)^2 + K_I(V/V_n) + K_P) \\ K_Z + K_I + K_P = 1 \end{cases} \quad (3)$$

where P_n is the real power of the load at nominal voltage V_n ; K_Z , K_I , K_P are power components with constant resistance, constant current and constant power, respectively.

The PSS/E main load model is based on the ZIP model. Near nominal voltage, the PSS/E model can be described by (4).

$$P = Y\text{Pload}(V/V_b)^2 + I\text{Pload}(V/V_b) + P\text{load} \quad (4)$$

where $Y\text{Pload}$, $I\text{Pload}$, $P\text{load}$ are in MW and represent components of the load, and V_b corresponds to the nominal voltage of the load bus.

Similarly to the generic ZIP model (3), the PSS/E model has three distinctive components: $Y\text{Pload}$ with constant impedance; $I\text{Pload}$ with constant current; $P\text{load}$ with constant power. At lower voltages, the constant current and constant power components are modelled by elliptical voltage-current (V-I) characteristics [2]. The constant current characteristic is changed to elliptical V-I characteristic at bus voltages below 0.5 p.u. [2]. The constant power component is switched to elliptical V-I characteristic if bus voltage is below the PSS/E solution parameter PQBRAK value [2]. The solution parameter PQBRAK has setting values range $PQBRAK \in (0, 2]$ [2] and a default value of 0.7 p.u [2]. The value of the parameter PQBRAK can be changed by the user in solution settings.

III. METHODS FOR EXPONENTIAL TO ZIP MODEL CONVERSION

According to section II-A, in voltage range 0.8...1.2 p.u. the voltage characteristic of PSCAD load model is (2), which is equivalent to (1). Thus, conversion methods used for converting exponential load models can be used for converting parameters of PSCAD model Fixed Load if the voltage is within the aforementioned voltage range. If the value of parameter PQBRAK in PSS/E is 0.8 p.u. or lower, the PSS/E load model in voltage range 0.8...1.2 p.u is (4), which differs from (3) mainly by the component parameters $Y\text{Pload}$, $I\text{Pload}$ and $P\text{load}$. The values of these parameters can be easily found by dividing the values of K_Z , K_I and K_P with P_n .

To summarise, methods suitable for converting from exponential model (1) to ZIP model (3), can be applied for PSCAD model Fixed Load to PSS/E main load model conversion, keeping in mind the load model switching aspect of the software tools, setting $V_0 = V_b$ and $P_0 = Y\text{Pload} + I\text{Pload} + P\text{load}$.

The exponential load models can be converted to ZIP models by analytical methods, described in sections III-A, III-B and III-C, or by non-linear squares optimisation, described in section III-D.

A. Analytical Method AM1

In [6] the exponential models are converted to second order polynomial models using a set rules and equations. The suitable equation or set of parameter values is chosen based on the value of the exponent K_{Exp} .

For exponent K_{Exp} values below 0.5, a constant power model is used (5). A constant current model is used if the exponent K_{Exp} value is below 1 (6) and a constant admittance model is used if the value of exponent K_{Exp} is larger than 2 (8). In exponent K_{Exp} value range 1...2, the values of ZIP model parameters are calculated using (7), which is the analytical solution of the equation system presented in [6].

$$K_{Exp} < 0.5 \rightarrow \begin{cases} K_Z = 0 \\ K_I = 0 \\ K_P = 1 \end{cases} \quad (5)$$

$$0.5 \leq K_{Exp} < 1.0 \rightarrow \begin{cases} K_Z = 0 \\ K_I = 1 \\ K_P = 0 \end{cases} \quad (6)$$

$$1.0 \leq K_{Exp} < 2.0 \rightarrow \begin{cases} K_Z = K_{Exp} - 1 \\ K_I = 2 - K_{Exp} \\ K_P = 0 \end{cases} \quad (7)$$

$$K_{Exp} \geq 2.0 \rightarrow \begin{cases} K_Z = 1 \\ K_I = 0 \\ K_P = 0 \end{cases} \quad (8)$$

B. Proposed Analytical Method AM2

When load model conversion method AM1, described in section III-A, was analysed, it was found that the method can be improved. Method AM1 displayed high conversion error if $K_{Exp} < 0$ and had a local error maximum at $K_{Exp} = 0.5$. Firstly, it was found that if $0 < K_{Exp} < 1$, (9) is more accurate than (5) and (6). Numerical analysis indicated that for $K_{Exp} < 0$, (9) has lower conversion error than (5) and (8). As a result, (9) was applied to $K_{Exp} < 1$.

The $1.0 \leq K_{Exp} < 2.0$ range in (7) was extended to $K_{Exp} \geq 1$ in (10), because if $K_{Exp} > 2$, the voltage sensitivity of the load is larger than $K_Z = 1$ and the result of (10) is closer to the exponential input characteristic K_{Exp} than ZIP characteristic $K_Z = 1$.

In case of $K_{Exp} = 0$ and $1.0 \leq K_{Exp} \leq 2.0$, the conversion results of method AM1 and proposed method AM2 are equivalent.

$$K_{Exp} < 1 \rightarrow \begin{cases} K_Z = 0 \\ K_I = K_{Exp} \\ K_P = 1 - K_{Exp} \end{cases} \quad (9)$$

$$K_{Exp} \geq 1 \rightarrow \begin{cases} K_Z = K_{Exp} - 1 \\ K_I = 2 - K_{Exp} \\ K_P = 0 \end{cases} \quad (10)$$

C. Proposed Analytical Method AM3

The exponential (1) and polynomial (3) load model are equivalent at nominal voltage V_n , because if $V/V_n = 1$, then $P = P_n$. At intersections of the load characteristics, the load equations have equivalent values $P_{ZIP} = P_{EXP}$:

$$K_Z(V/V_n)^2 + K_I(V/V_n) + K_P = (V/V_n)^{K_{Exp}} \quad (11)$$

Replacing K_P in (11) with $1 - K_Z - K_I$ and simplifying the equations leads to derivation of (12).

$$K_Z(V/V_n + 1) + K_I = \frac{(V/V_n)^{K_{Exp}} - 1}{V/V_n - 1} \quad (12)$$

Equation (12) includes two unknowns: K_Z and K_I . Thus, the equation has $0 \dots \infty$ solutions. To limit the number of solutions to $0 \dots 1$, it is assumed that 2 intersections of polynomial and exponential characteristic exist at voltages V_1 and V_2 . Using the assumption, (13) is derived.

$$\begin{cases} K_Z(V_1 + 1) + K_I = \frac{(V_1)^{K_{Exp}} - 1}{V_1 - 1} \\ K_Z(V_2 + 1) + K_I = \frac{(V_2)^{K_{Exp}} - 1}{V_2 - 1} \end{cases} \quad (13)$$

where V_1 and V_2 are in p.u., normalised with nominal voltage V_n .

The solution of equation system (13) is (14). The value of K_P can be found from values of K_Z and K_I using equation (15).

$$\begin{bmatrix} K_Z \\ K_I \end{bmatrix} = \frac{1}{V_1 - V_2} \begin{bmatrix} 1 & -1 \\ -V_2 - 1 & V_1 + 1 \end{bmatrix} \begin{bmatrix} \frac{V_1^{K_{Exp}} - 1}{V_1 - 1} \\ \frac{V_2^{K_{Exp}} - 1}{V_2 - 1} \end{bmatrix} \quad (14)$$

$$K_P = 1 - K_Z - K_I \quad (15)$$

D. Conversion by Non-linear Least Squares Optimisation

In case of load model conversion, the goal is to minimise the difference between the input model and output model. This optimisation problem can be written as a non-linear least squares optimisation problem, which has the goal to minimise the sum of squared errors.

$$\min J = \sum_{i=1}^N [\epsilon_i]^2 \quad (16)$$

If the error ϵ_i in (16) is represented by conversion error ϵ_i (19), the model conversion problem can be formulated by (17). In section IV, the optimisation of absolute error is noted by **NLS abs**.

$$\min J = \sum_{i=1}^N (P_{EXP}(V_i) - P_{ZIP}(V_i))^2 \quad (17)$$

If instead of conversion error ϵ_i , the relative conversion error η_i (20) is used as ϵ_i in (16), the objective function (18) is obtained. In section IV, the non-linear squares optimisation of relative error is noted by **NLS rel**.

$$\min J = \sum_{i=1}^N \left(\frac{P_{EXP}(V_i) - P_{ZIP}(V_i)}{P_{EXP}(V_i)} \right)^2 \quad (18)$$

IV. CONVERSION ERROR ANALYSIS

A. Measures of Conversion Error

In case of exponential to ZIP model conversion, the exponential voltage characteristic of the load P_{EXP} (1) is assumed to be accurate. The difference ϵ_i (19) between the accurate voltage-power characteristic P_{EXP} (1) and converted characteristic P_{ZIP} (3) at voltage V_i is considered to be conversion error at voltage V_i . The relative conversion error at voltage V_i is η_i . In some figures, the relative error is given in percentages, in those instances, the value of η_i has been multiplied by 100.

$$\epsilon_i = P_{EXP}(V_i) - P_{ZIP}(V_i) \quad (19)$$

$$\eta_i = \frac{P_{EXP}(V_i) - P_{ZIP}(V_i)}{P_{EXP}(V_i)} \quad (20)$$

The values of ϵ_i and η_i are used for analysing the direction of the conversion error. In analysis steps, where the maximum conversion error is more important than the direction, the absolute values of ϵ_i and η_i are used. To quantify the conversion error across a voltage range $V_1 \dots V_N$, the Mean Absolute Error (MAE) (21) and Mean Absolute Percentage Error (MAPE) (22) are used. MAE describes the mean magnitude of conversion error ϵ_i and MAPE the mean absolute value of relative conversion error η_i .

$$MAE = \frac{1}{N} \sum_{i=1}^N |P_{EXP}(V_i) - P_{ZIP}(V_i)| \quad (21)$$

$$MAPE = \frac{100\%}{N} \sum_{i=1}^N \left| \frac{P_{EXP}(V_i) - P_{ZIP}(V_i)}{P_{EXP}(V_i)} \right| \quad (22)$$

In this paper, voltage range 0.8...1.2 p.u. was used as MAE and MAPE calculation range $V_1 \dots V_N$. This range corresponds to voltages where described PSCAD load models behave as exponential model and the PSS/E load model corresponds to a ZIP model (assuming the value of PQBRAK to be 0.8 p.u. or lower).

B. Input Models and Notation of Methods

The set of exponential load models for load model conversion error analysis was calculated using 0.01 step size and value range -5...5. This led to a dataset of 1001 exponent values with even distribution. The analysed range is equivalent to the allowed range of PSCAD load model exponent values.

Exponential load models were converted to second order polynomial load models by using 5 different methods:

- **AM1**: analytical method described in section III-A
- **AM2**: proposed method described in section III-B
- **AM3**: proposed method described in section III-C
- **NLS abs**: optimisation of squared conversion error described by (17) in section III-D
- **NLS rel**: optimisation of squared relative error described by (18) in section III-D

C. Mean and Maximum Absolute Conversion Error of Compared Methods

The value of MAE (21) and MAPE (22) was calculated for each load model conversion using voltage range from 0.8 to 1.2 p.u. The same voltage range was used for load model conversion. In total, 1001 MAPE and MAE values were obtained for each conversion method. The results were plotted in Fig. 1 and Fig. 2.

According to the two figures, the mean conversion error (MAE and MAPE) of negative K_{Exp} value is typically larger than the error of positive K_{Exp} value with equivalent absolute value. The model conversion error is approximately symmetrical for $K_{Exp} = 1$. An exception to the described trend is analytical method AM1 at $K_{Exp} = (0..1)$. AM1 has a local peak at $K_{Exp} = 0.5$, at the boundary of (5) and (6).

The complexity of analytical methods AM1 and AM2 is mathematically similar. However, the proposed method AM2 offers lower conversion error than method AM1. For this reason, the use of method AM1 is not recommended and proposed method AM2 should be used instead. For more accurate conversion results, proposed method AM3 or optimisation methods should be used. The higher conversion accuracy (and lower conversion error) of proposed method AM3 and optimisation methods, NLS abs and NLS rel, becomes more apparent at low and high K_{Exp} values.

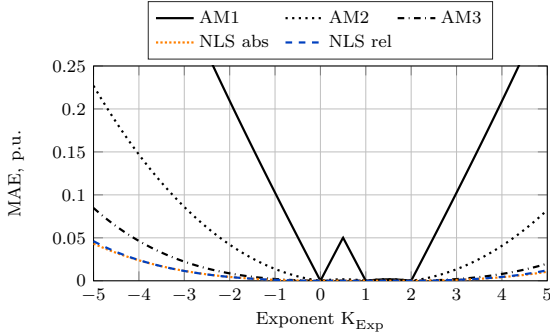


Fig. 1. Impact of input model exponent K_{Exp} on the mean absolute error (MAE) of conversion.

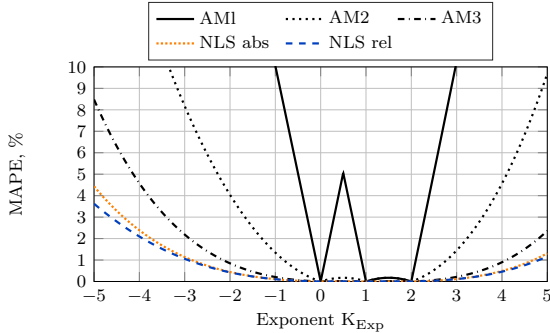


Fig. 2. Impact of input model exponent K_{Exp} on the mean absolute percentage error (MAPE) of conversion.

TABLE I
CONVERSION ERROR OF EXPONENTIAL MODELS WITH $K_{Exp} = -5$ AND $K_{Exp} = 5$: MEAN ABSOLUTE ERROR (MAE) AND MEAN ABSOLUTE PERCENTAGE ERROR (MAPE)

Conversion method	$K_{Exp} = -5$		$K_{Exp} = 5$	
	MAE (p.u.)	MAPE (%)	MAE (p.u.)	MAPE (%)
AM1	0.581	52.284	0.322	32.300
AM2	0.227	21.674	0.082	9.691
AM3	0.085	8.482	0.020	2.235
NLS abs	0.043	4.438	0.011	1.312
NLS rel	0.046	3.363	0.012	1.164

According to Table I, the MAE and MAPE of method AM2 are up to 10 times larger than the error values of optimisation methods, at $K_{Exp} = -5$ and $K_{Exp} = 5$. The MAE and MAPE of AM3 are approximately two times larger than the values of NLS abs and NLS rel at the same K_{Exp} values.

The MAE and MAPE of proposed method AM3 were larger than the values of NLS abs and NLS rel in Fig. 1, Fig. 2 and in Table I. The maximum absolute value of conversion error (19) and relative conversion error (20) shown in Fig. 3 and Fig. 4 display a different result. The maximum absolute errors of AM3 are at the same level as NLS abs and NLS rel. The maximum absolute value of AM3 conversion error in Fig. 3 is on same level as NLS abs and the maximum absolute relative conversion error in Fig. 4 is between NLS abs and NLS rel.

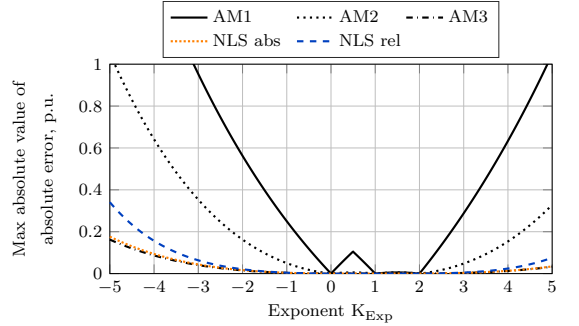


Fig. 3. Impact of input load model exponent value K_{Exp} on the max absolute value of absolute error of conversion.

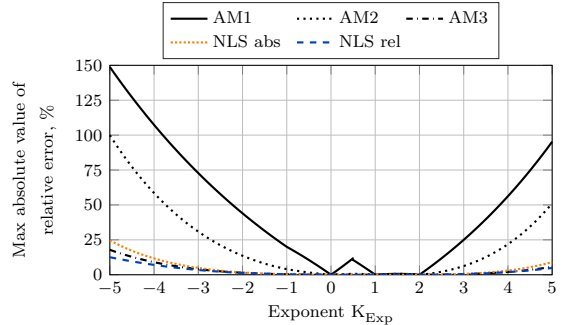


Fig. 4. Impact of input load model exponent value K_{Exp} on the max absolute value of relative error of conversion.

D. Methods NLS abs and NLS rel: Voltage Dependence of Conversion Error

The exponential load models were converted to ZIP models using voltage range from 0.8 to 1.2 p.u. Conversion error (19) and relative conversion error (20) were calculated for NLS abs and NLS rel, respectively. The conversion error of method NLS abs is plotted for selected K_{Exp} values in Fig. 5 and relative conversion error of NLS rel in Fig. 6. According to the figures, the conversion error and relative conversion error of optimisation based methods have a voltage dependence.

According to Fig. 5, the direction of conversion error for analysed K_{Exp} values is related to the sign of K_{Exp} . The errors of negative K_{Exp} values are in opposite direction to the positive K_{Exp} values. The smallest conversion error, zero, occurs at 3 points: at nominal voltage $V = 1$ p.u. (where power is nominal) and two additional voltages, $V = 0.83$ p.u. and $V = 1.16$ p.u. At these points, the exponential and polynomial line intersect. In section III-C, 2 intersection points V_1 and V_2 were used for deriving (13), which was a key step in AM3 derivation. The results in Fig. 5 justify the assumption. The intersections occur within the optimisation region, between voltages 0.8 and 1.2 p.u. In addition, the intersection points of different K_{Exp} values are close, indicating a low sensitivity to value of K_{Exp} , if K_{Exp} is within the analysed region $-5 \geq K_{Exp} \geq 5$.

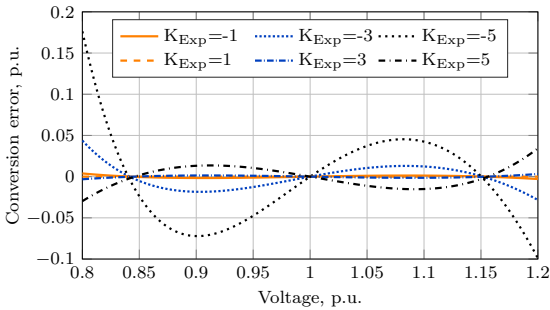


Fig. 5. Method NLS abs: impact of voltage and input model exponent K_{Exp} on conversion error.

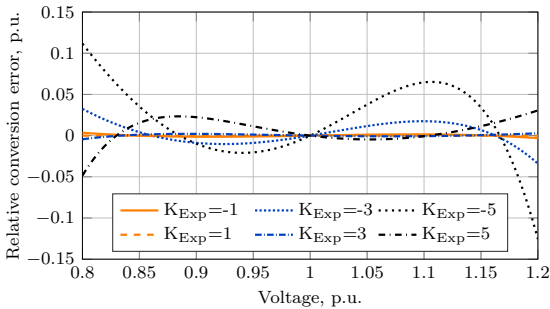


Fig. 6. Method NLS rel: impact of voltage and input model exponent K_{Exp} on relative conversion error.

Similarly to Fig. 5, in Fig. 6 the direction of the relative conversion error is related to the sign of K_{Exp} . However, the intersection points of characteristics in Fig. 6 depend on the value of K_{Exp} . The larger the K_{Exp} value, the more to the left the intersection points are located.

E. Proposed Method AM3: Voltage Dependence of Conversion Error

Conversion error (19) and relative conversion error (20) of proposed method AM3 have voltage dependency according to Fig. 7 and Fig. 8. Similarly to Fig. 5 and Fig. 6, the direction of the error depends on the sign of K_{Exp} . In case of positive K_{Exp} values, the error is positive below nominal voltage and negative at higher voltages. This means that the second order polynomial characteristic of AM3 has lower load values than exponential input characteristic below nominal voltage and higher values above nominal voltage, if $K_{Exp} > 0$. For $K_{Exp} < 0$, the opposite applies.

The conversion error is zero at the intersection points of exponential input characteristic and second order polynomial output characteristic. In Fig. 7 and Fig. 8, the intersection points are located at 0.8 p.u., 1.0 p.u. and 1.2 p.u. Thus, using the range boundary values 0.8 p.u. and 1.2 p.u. as V_1 and V_2 in (14), the lowest conversion error will occur at the voltage boundaries. This is an expected result, for deriving (13) equivalence of exponential and ZIP characteristic at V_1 and V_2 was used.

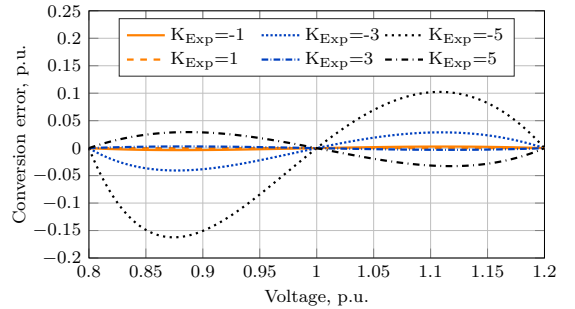


Fig. 7. Proposed method AM3: impact of voltage and input model exponent K_{Exp} on conversion error.

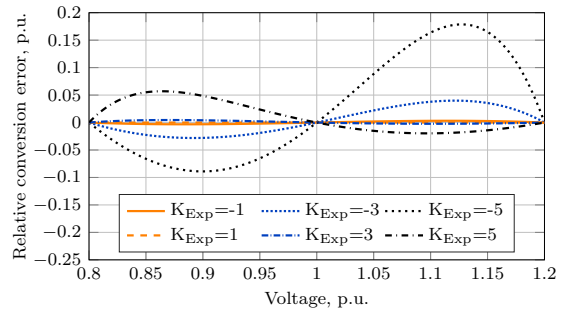


Fig. 8. Proposed method AM3: impact of voltage and input model exponent K_{Exp} on relative conversion error.

Comparison of the intersection points at Fig. 7 and Fig. 8 with intersection points of Fig. 5 and Fig. 6 suggests that the MAE and MAPE of AM3 could be decreased by changing voltage V_1 and V_2 to values within the desired accurate conversion range. The selection of best V_1 and V_2 value was not in the scope of this study.

F. Proposed Method AM2: Voltage Dependence of Conversion Error

The conversion error (19) and relative conversion error (20) of proposed method AM2 in Fig. 9 and Fig. 10 are lowest near 1 p.u. voltage, where the load is close to nominal. Zero error occurs in case of $K_{Exp} = 1$. At $K_{Exp} = 1$, the error-less conversion is possible, because the exponential model is equivalent to the constant current component of the ZIP model. Similar error-less conversion takes place for $K_{Exp} = 0$ and $K_{Exp} = 2$. These three K_{Exp} values are exceptions, for other K_{Exp} values, a conversion error occurs with method AM2.

In Fig. 5, Fig. 6, Fig. 7 and Fig. 8, the conversion error was zero in 3 points, indicating 3 intersections of exponential input characteristic and second order polynomial output characteristic. The conversion errors in Fig. 9 and Fig. 10 have positive values across voltage range 0.8...1.2 p.u. and zero error only at nominal voltage 1 p.u. The positive sign of error, (19) and (20), indicates that the ZIP characteristic calculated by AM2 typically underestimates the load compared to the exponential input characteristic.

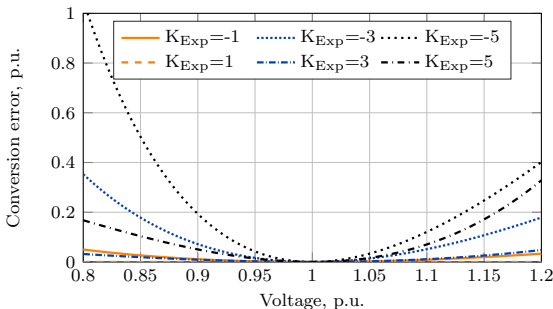


Fig. 9. Proposed method AM2: impact of voltage and input model exponent K_{Exp} on conversion error.

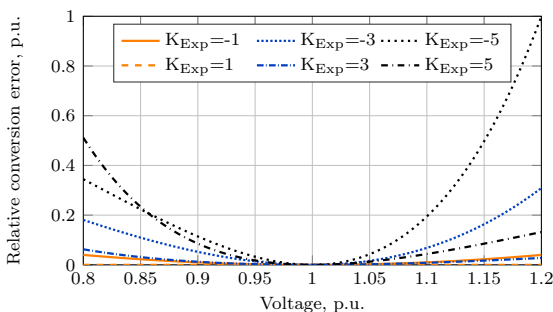


Fig. 10. Proposed method AM2: impact of voltage and input model exponent K_{Exp} on relative conversion error.

V. CONCLUSION

The main load models of PSCAD and PSS/E are at near nominal voltages similar to exponential and second order polynomial (ZIP) load model, respectively. Thus, the methods suitable for exponential to ZIP model conversion can be used for PSCAD load model to PSS/E load model conversion. In this study, three analytical conversion methods for exponential to second order polynomial model were described, the load model conversion error was evaluated and a comparison was made based on absolute error and relative error minimisation solutions.

Firstly, it was shown that the conversion error depends on the conversion method. The analytical method AM1 described in section III-A had the highest conversion error and is not recommended for use. Proposed method AM2 presented in section III-B should be used instead, if a simple conversion method is needed. Method AM2 has similar mathematical complexity and causes significantly lower conversion error than the non-recommended method AM1. More accurate conversion results can be obtained using proposed analytical method AM3, presented in section III-C, or by the use of non-linear least squares optimisation.

The analysis of conversion error indicated that the conversion error depends on the value of input load model exponent K_{Exp} . In case of all methods, the conversion error is smallest at exponent values 0, 1 and 2. At these values, the exponent and second order polynomial model have equivalent characteristics. The conversion error is larger for negative exponent values, when compared to positive exponents with same absolute value. It was found that the mean absolute error (MAE) and mean absolute percentage error (MAPE) of conversion are nearly symmetrical to exponent value 1.

It was shown that the conversion error is voltage dependent and the direction of error depends on the sign of K_{Exp} in case of optimisation based conversion methods and proposed method AM3, the method presented in section III-C. The conversion error indicated that the ZIP characteristics found by optimisation results have typically 3 intersections with the exponential characteristic.

REFERENCES

- [1] J. V. Milanovic, K. Yamashita, S. M. Villanueva, S. Z. Djokic, and L. M. Korunovic, "International industry practice on power system load modeling," *IEEE Trans. Power Systems*, vol. 28, no. 3, pp. 3038-3046, Aug. 2013.
- [2] *PSS/E 34 Program Operation Manual*. Siemens Power Technologies International, Schenectady, NY, USA, 2015.
- [3] *PSCAD User's Guide v4.6.0*. Manitoba HVDC Research Centre, Manitoba, Canada, 2015.
- [4] A. J. Collin, G. Tsagarakis, A. E. Kiprakis, and S. McLaughlin, "Development of low-voltage load models for the residential load sector," *IEEE Trans. Power Systems*, vol. 29, no. 5, pp. 2180-2188, Sept. 2014.
- [5] *Measurement-based load modeling*. EPRI, Palo Alto, CA, USA, 1014402, 2006.
- [6] J. Zhang, Y. Sun, J. Xu, S. Liu, J. Xin, Q. Lei, and H. Dong, "Electric load model based on aggregation algorithm," *2009 Asia-Pacific Power and Energy Engineering Conf.*, Wuhan, China, 2009, pp. 1-4.

Publication II

M. Leinakse and J. Kilter, "Conversion error of second order polynomial ZIP to exponential load model conversion," in *Mediterranean Conference on Power Generation, Transmission, Distribution and Energy Conversion (Med-Power 2018)*, Dubrovnik, Croatia, 2018, doi: 10.1049/cp.2018.1882

Reproduced by permission of the Institution of Engineering & Technology

Conversion Error of Second Order Polynomial ZIP to Exponential Load Model Conversion

Madis Leinakse¹* Jako Kilter¹

¹ Department of Electrical Power Engineering and Mechatronics, Tallinn University of Technology, Tallinn, Estonia

* E-mail: madis.leinakse@taltech.ee

Abstract: This paper analyses the conversion error that occurs when second order polynomial (i.e. ZIP) load model is converted to exponential load model. Two conversion methods are used: an analytical method and a non-linear least squares based method. The conversion error of both methods is described and compared based on numerical analysis. It is shown that the load model conversion error depends on the input load model parameter values, used method, chosen voltage and the voltage sensitivity of the characteristic.

Keywords: CONVERSION ERROR, EXPONENTIAL MODEL, LOAD MODELLING, STATIC LOAD MODELS, ZIP MODEL

1 Introduction

Many software packages are available for conducting steady state and time-domain studies of electrical power systems and are in active use according to [1]. Usually these software tools include load model(s) for describing the voltage characteristic of the load. Several different models are in use, for example the main load model of PSS/E is based on a second order polynomial equation [2–4], while PSCAD offers an exponential model [3–5].

The active use of several models causes in some cases the need for load model conversion. The conversion of ZIP to exponential model has been used for comparing load models [1] and plotting load model changes in time [6]. In addition, the load model conversion may be required if ZIP models of loads are known from component-based modelling or validated power system model, and a software is taken into use with exponential load models [3].

Generally, the exponential model obtained as a result of a load model conversion is not equivalent to the original ZIP model. In this paper, the often neglected aspect of load model conversion error is analysed and the accuracy difference of analytical and non-linear least squares conversion is shown. Several conversion methods for opposite conversion direction, exponential to ZIP model conversion, were presented, compared and analysed in [4].

This paper consists of five sections. In section 2, the second order polynomial (ZIP) and exponential load model are described. The methods for converting from ZIP model to exponential model, and measures of conversion error, are presented in section 3. An evaluation of model conversion error is given in section 4 based on the results of numerical analysis. The main findings of the work are summarised in section 5.

2 Load Models

This paper focuses on the load model conversion from generic ZIP load model to exponential load model. The specifics of PSS/E and PSCAD load model that have to be taken into account when converting the models of these software packages have been discussed in [3, 4].

In case of ZIP and exponential load model, the models can be defined using the nominal value [4, 7] or initial value [7–9] of voltage and power. In this paper, the nominal value based load model definitions are used. The conversion error analysis results of the paper also apply to models normalised based on initial values, if both the input

and output model use the same base value. Conversion of models with base value mismatch is discussed in section 3.2.

2.1 Second Order Polynomial (ZIP) Load Model

The second order polynomial load model, also known as a ZIP model, can be described by (1) subject to (2). Reactive load is represented by a similar equation.

$$P_{ZIP} = P_n \cdot [K_Z \cdot (V/V_n)^2 + K_I \cdot (V/V_n) + K_P] \quad (1)$$

$$K_Z + K_I + K_P = 1 \quad (2)$$

where V_n corresponds to the nominal voltage of the load bus. P_n is the real power of the load at nominal voltage V_n . K_Z , K_I , K_P describe the contribution of load components with constant resistance, constant current and constant power, respectively.

The values of K_Z , K_I and K_P may in some cases be limited to range 0...1, such ZIP model is called a "constrained ZIP model" [10]. Without these constraints the model is considered to be an "accurate ZIP model" [10].

2.2 Exponential Load Model

The exponential load model can be described by (3), reactive load is represented by a similar equation.

$$P_{EXP} = P_n \cdot (V/V_n)^{K_{Exp}} \quad (3)$$

where P_n is the real power of the load at nominal voltage V_n , and K_{Exp} is an exponent describing the voltage characteristic of the real power of load.

3 Load Model Conversion Methods and Error

3.1 Analytical Method for ZIP to Exponential Model Conversion

For conversion from ZIP model to exponential model, [1] and [6] have used equation (4), reactive load exponent can be calculated similarly. In section 4, load model conversion by this method is noted by keyword **Analytical**.

$$K_{Exp} \approx \frac{2 \cdot K_Z + 1 \cdot K_I + 0 \cdot K_P}{K_Z + K_I + K_P} \quad (4)$$

3.2 Using Non-linear Least Squares Optimisation for Conversion

The goal of load model conversion is to minimise the conversion error. This aim can be written as a non-linear least squares optimisation problem (5).

$$\min \sum_{i=1}^N (\psi_i)^2 \quad (5)$$

If the conversion error ψ_i in (5) is represented by absolute conversion error ε_i (8), the model conversion problem can be formulated by (6). The reactive load models can be converted similarly. In section 4, load model conversion by minimisation of squared absolute error is noted by **NLS abs**.

$$\min \sum_{i=1}^N (P_{ZIP}(V_i) - P_{EXP}(V_i))^2 \quad (6)$$

where V_i is normalised voltage V/V_n , P_{ZIP} is (1) and P_{EXP} is (3).

If the base power and voltage of known ZIP model and desired exponential model differ, the differences can be taken into account by using different value of P_n and V_n in the equation of P_{ZIP} (1) and P_{EXP} (3).

However, if P_{ZIP} and P_{EXP} use the same normalisation bases, P_n and V_n , the optimisation problem (6) can be simplified to equation (7).

$$\min \sum_{i=1}^N \left([K_Z \cdot (V_i)^2 + K_I \cdot (V_i) + K_P] - (V_i)^{K_{Exp}} \right)^2 \quad (7)$$

3.3 Measures of Conversion Error

In case of ZIP to exponential model conversion, the voltage characteristic of the ZIP model P_{ZIP} (1) is assumed to be accurate. The difference ε_i (8) between the accurate voltage-power characteristic P_{ZIP} (1) and converted characteristic P_{EXP} (3) at voltage V_i is considered to be conversion error at voltage V_i .

$$\varepsilon_i = P_{ZIP}(V_i) - P_{EXP}(V_i) \quad (8)$$

To quantify the conversion error across voltage range $V_i \in \{V_1 \dots V_N\}$ ($i, N \in \mathbb{N}$) the Mean Absolute Error (MAE) (9) is used. MAE describes the mean magnitude of conversion error ε_i .

$$MAE = \frac{1}{N} \sum_{i=1}^N |P_{ZIP}(V_i) - P_{EXP}(V_i)| \quad (9)$$

In this paper, voltage range 0.8...1.2 p.u. was used as MAE calculation range $V_1 \dots V_N$, similarly to [3, 4, 11].

4 Conversion Error Analysis

4.1 Input Models and Notation of Methods

To obtain ZIP model parameter sets, two random vectors with values -25...25 were generated with uniform distribution. A third vector was calculated so that the sum of ZIP model parameters would be 1 (2). As a result, a set of nearly 30000 models was obtained, which was found to be sufficient for analysis of the conversion error.

ZIP to exponential load model conversion was done using 2 different methods:

- **Analytical:** analytical method described in section 3.1
- **NLS abs:** conversion method based on minimisation of squared absolute error described in section 3.2

The exponent K_{Exp} values obtained by the use of the aforementioned methods differ significantly, as shown by Fig. 1. The smallest result difference occurs near $K_{Exp} = 0.5$ and largest at high absolute values of K_{Exp} . Typical differences are close to 1 unit.

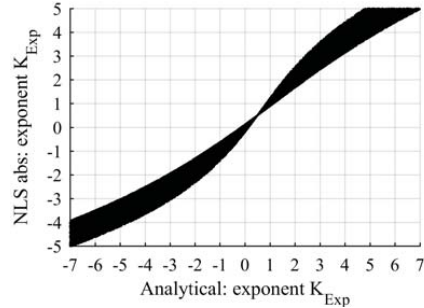


Fig. 1: Calculated exponent K_{Exp} values of Analytical and NLS abs method.

4.2 Mean Absolute Error of Conversion

Fig. 2 displays the mean absolute error (MAE) (9) of ZIP to exponential model conversion. ZIP models with analytical K_{Exp} values $-8 \leq K_{Exp} \leq 8$ are shown. According to Fig. 2, the conversion error displays a significant variation for all K_{Exp} values, difference of MAE for a specific K_{Exp} value is 0.2...0.3 p.u. Thus, it is not possible to assign a specific MAE value for each calculated K_{Exp} value. However, it is possible to notice that the lowest maximum values of MAE occur in K_{Exp} range -1...3. The error for negative K_{Exp} values (compared to K_{Exp} values with equal absolute value) are larger.

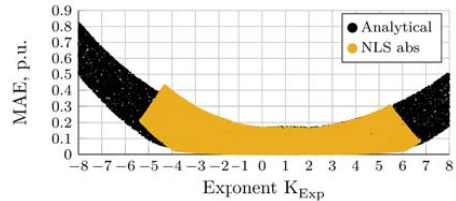


Fig. 2: Relation between the calculated model exponent value K_{Exp} and the mean absolute error (MAE) of the load characteristic.

The MAE value difference of analytical and NLS abs method ΔMAE (10) is plotted in Fig. 3. ZIP models with NLS abs determined K_{Exp} values $-5 \leq K_{Exp} \leq 5$ are shown.

$$\Delta MAE = MAE_{Analytical} - MAE_{NLSabs} \quad (10)$$

The mostly positive ΔMAE values in Fig. 3 indicate that the conversion accuracy of NLS abs method is higher than the accuracy of analytical method. Also, it is possible to notice that the lowest difference occurs for K_{Exp} values in range -1...2 where ΔMAE is below 0.02 p.u. Outside that K_{Exp} range, the use of NLS abs over analytical method may provide significant increase in conversion accuracy.

4.3 Voltage Dependence of Conversion Error

The load model conversion error ε (8) depends on voltage. The voltage dependence of conversion error of analytical method is shown in Fig. 4 and Fig. 7, and NLS abs in Fig. 5 and Fig. 8. ZIP models with NLS abs determined K_{Exp} values $-5 \leq K_{Exp} \leq 5$ are shown. According to the mentioned figures, the conversion error of both analysed methods, NLS abs and analytical, is lowest near nominal voltage. This is an expected result, as near nominal voltage, the

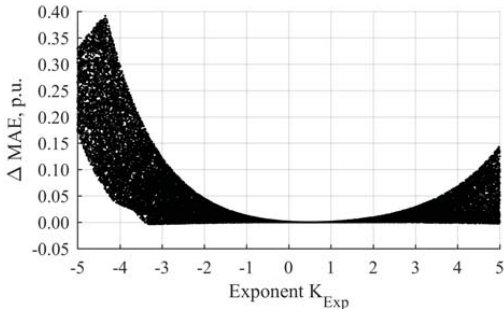


Fig. 3: Relation between the exponent value K_{Exp} of NLS abs method and mean absolute error decrease ΔMAE compared to analytical method.

load is close to nominal as well, independent of load model parameter values. The analytical method, Fig. 4, displays largest conversion errors at lower voltages while the NLS abs method, Fig. 5, at higher voltages. Thus, the voltage dependence of the analysed conversion methods differs.

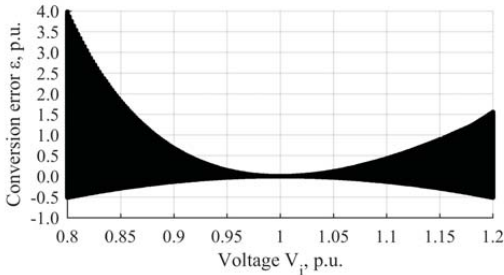


Fig. 4: Voltage dependence of analytical conversion method. Accurate ZIP models.

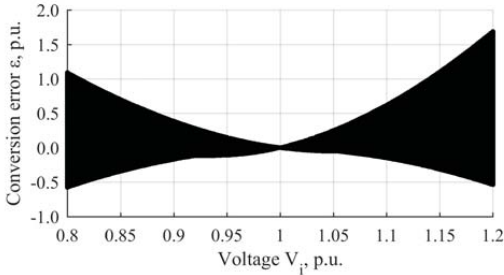


Fig. 5: Voltage dependence of NLS abs conversion method. Accurate ZIP models.

To analyse the difference between Fig. 4 and Fig. 5, $\Delta \varepsilon_i$ is plotted in Fig. 6. $\Delta \varepsilon_i$ is the difference between the absolute conversion error of analytical and NLS abs conversion method, defined by (11). The absolute values of conversion error are used to detect which conversion result is closer to the accurate voltage-power characteristic at voltage V_i .

$$\Delta \varepsilon_i = |\varepsilon_{i,Analytical}| - |\varepsilon_{i,NLSabs}| \quad (11)$$

Fig. 6 indicates that the gains of using NLS abs method instead of analytical method can be significant at voltages further from the nominal voltage ($V_i = 1$ p.u.). The gains are higher for lower voltages, compared to higher: $\Delta \varepsilon_i$ values at 0.8 p.u. are higher than at 1.2 p.u.

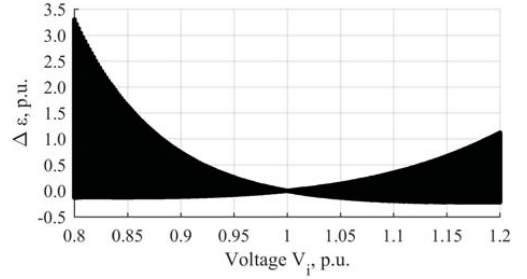


Fig. 6: Relation between voltage V_i and conversion error decrease $\Delta \varepsilon$ when NLS abs is used instead of analytical method.

Voltage dependence of constrained ZIP model conversion error is shown in Fig. 7 and Fig. 8. The conversion error for both methods, analytical and NLS abs, is unidirectional, indicating that the estimated exponential characteristic runs above the ZIP characteristic (in V-P plane) and the load is overestimated by up to 0.02 p.u. if voltage is near 0.8 p.u.

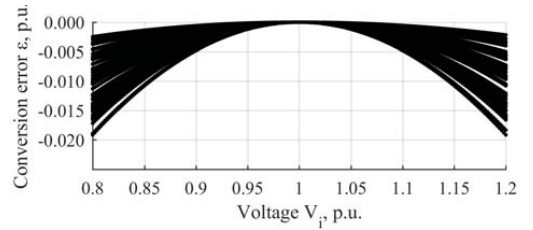


Fig. 7: Voltage dependence of analytical conversion method. Constrained ZIP models.

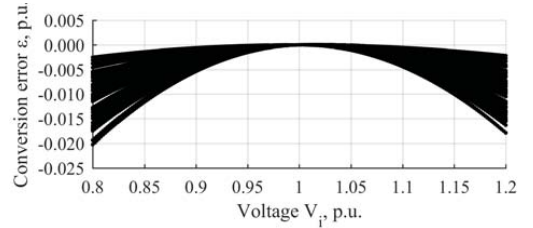


Fig. 8: Voltage dependence of NLS abs conversion method. Constrained ZIP models.

4.4 Impact of ZIP Model Parameter Values on Conversion Error

Fig. 9 describes the impact of ZIP model parameter values K_Z, K_I, K_P on the mean absolute error (MAE) (9) of conversion. ZIP models with NLS abs determined exponent K_{Exp} values $-5 \leq K_{Exp} \leq 5$ are shown.

The highest conversion error (maximum value in Fig. 9) occurs if ZIP load model parameter K_Z has a large negative value while K_I has a large positive value. In such cases, based on the ΔMAE plots, the NLS abs method is able to decrease the MAE value by about half, compared to the analytical method. However, from the figure it is apparent that the gain of using NLS abs method is not directly linked to the values of ZIP load model parameters K_Z, K_I, K_P , as for each value of K_Z, K_I and K_P , a range of ΔMAE values were found.

In Fig. 9, the conversion error of constrained ZIP models with $0 \leq K_Z, K_I, K_P \leq 1$, which corresponds to $0 \leq K_{Exp} \leq 2$, is negligibly small compared to the errors of models with more relaxed

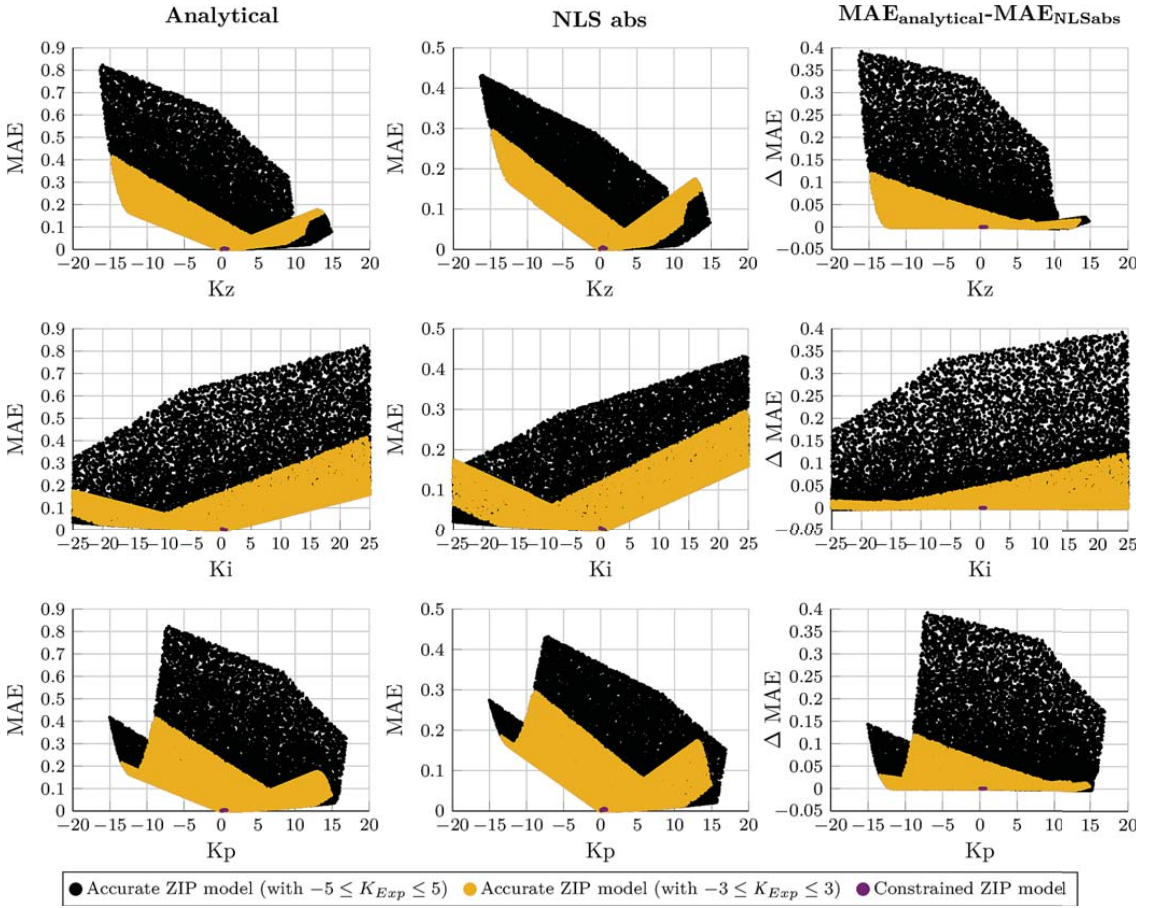


Fig. 9: Mean absolute error (MAE) dependence on ZIP model parameters K_Z , K_I and K_P .

constraints. Fig. 10 illustrates the dependence between MAE, exponent K_{Exp} and constraints of ZIP model parameters K_Z , K_I and K_P . The model conversion was conducted using NLS abs method. Based on Fig. 10, the larger the ZIP model parameter value limits, the larger the variability of mean absolute error of conversion and the larger the maximum values of MAE.

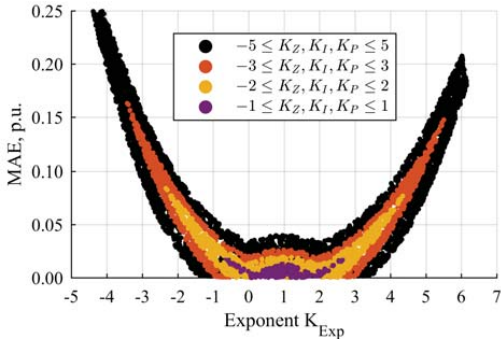


Fig. 10: Impact of ZIP model parameter constraints on the mean absolute error (MAE) of conversion. Calculation method NLS abs. Plotted subsets filtered based on ZIP load model parameter ranges -1..1, -2...2, -3..3 and -5..5.

5 Conclusion

In this paper, two methods for second order polynomial (i.e. ZIP) to exponential load model conversion were described. The first presented conversion technique was an analytical method and the second a non-linear least squares based approach. The conversion error of the methods was analysed with respect to voltage, input and output load model parameter values based on numerical analysis.

The difference between the value of exponential parameter K_{Exp} determined by the conversion methods was smallest near $K_{Exp} = 0.5$. A typical difference of K_{Exp} value estimated by the methods was within 0...2 units. The lowest conversion error difference occurred for K_{Exp} values in range -1...2, where the mean absolute error difference ΔMAE is below 0.02 p.u. Outside that K_{Exp} range, the use of non-linear least squares over analytical approach may provide significant increase in conversion accuracy.

It was shown that the conversion error of both analysed methods is lowest near the nominal voltage, which was an expected result. The conversion error of analytical method was largest at lowest voltages, while the NLS abs method at highest voltages. Still, mostly the exponential models obtained by the use of NLS abs method displayed a higher accuracy across the whole analysed voltage range.

When the impact of input load model parameter values on conversion error was analysed, the impact of model parameter constraints was found to be significant. The variability and maximum value of the mean absolute conversion error (MAE) increased when the

model parameter value constraints were increased. The highest conversion error occurred if K_Z had a large negative value and K_I a large positive value. In such cases, the NLS abs method was able to decrease the MAE value by half, compared to the analytical method.

6 References

- 1 Milanovic, J.V., Yamashita, K., Villanueva, S.M., *et al.*: 'International industry practice on power system load modeling', *IEEE Trans. Power Syst.*, 2013, 28, (3), pp. 3038–3046
- 2 Siemens Power Technologies International, 'PSS/E 34 Program Operation Manual' (Siemens Power Technologies International, 2015)
- 3 Leinakse, M., Kapp, H., Kilter, J.: 'Preliminary study on comparative load modelling in PSS/E and PSCAD', 17th International Symposium "Topical Problems in the Field of Electrical and Power Engineering" and "Doctoral School of Energy and Geotechnology III", Kuressaare, Estonia, 2018, pp. 197–199
- 4 Leinakse, M., Kilter, J.: 'Conversion error of exponential to second order polynomial ZIP load model conversion', 2018 IEEE International Conference on Environment and Electrical Engineering and 2018 IEEE Industrial and Commercial Power Systems Europe (EEEIC / I&CPS Europe), Palermo, Italy, 2018, pp. 1–5
- 5 Manitoba HVDC Research Centre, 'PSCAD User's Guide v4.6.0' (Manitoba HVDC Research Centre, 2015)
- 6 Collin, A.J., Tsagarakis, G., Kiprakis, A.E., *et al.*: 'Development of low-voltage load models for the residential load sector', *IEEE Trans. Power Syst.*, 2014, 29, (5), pp. 2180–2188
- 7 Korunovic, L.M., Stojanovic, D.P.: 'The effects of normalization of static load characteristics', 2009 IEEE Bucharest PowerTech, Bucharest, Romania, 2009, pp. 227–234
- 8 Leinakse, M., Kiristaja, H., Kilter, J.: 'Identification of intra-day variations of static load characteristics based on measurements in high-voltage transmission network', 2018 IEEE PES Innovative Smart Grid Technologies Conference Europe (ISGT-Europe), Sarajevo, Bosnia and Herzegovina, 2018, pp. 1–6
- 9 Leinakse, M., Tani, P., Kilter, J.: 'Impact of Distributed Generation on Estimation of Exponential Load Models', 2019 IEEE Power & Energy Society General Meeting (PESGM), Atlanta, GA, USA, 2019, pp. 1–5, In press.
- 10 CIGRE Working Group C4.605, 'Modelling and aggregation of loads in flexible power networks' (CIGRE, 2014)
- 11 Leinakse, M.: 'Thoughts on Conversion of Static Load Models', 18th International Symposium "Topical Problems in the Field of Electrical and Power Engineering" and "Doctoral School of Energy and Geotechnology III", Toila, Estonia, 2019, pp. 187–188

Publication III

M. Leinakse, H. Kiristaja, and J. Kilter, "Identification of intra-day variations of static load characteristics based on measurements in high-voltage transmission network," in *2018 IEEE PES Innovative Smart Grid Technologies Conference Europe (ISGT Europe 2018)*, Sarajevo, Bosnia-Herzegovina, 2018, pp. 1–6, doi: 10.1109/ISGTEurope.2018.8571712

©2018 IEEE. Reprinted with permission.

Identification of Intra-Day Variations of Static Load Characteristics Based on Measurements in High-Voltage Transmission Network

Madis Leinakse, Hendrik Kiristaja, Jako Kilter
Department of Electrical Power Engineering and Mechatronics
Tallinn University of Technology
Tallinn, Estonia
madis.leinakse@ttu.ee

Abstract—This paper discusses the aspects of measurement-based load model identification of aggregated transmission system bus loads. A novel post-processing method for calculating a single load model parameter value from a set of event-based values is presented. The proposed method offers a way to combine the estimated load model parameters with the results of data validation. This approach may provide better results than commonly used average value calculation if the number of samples is relatively small. A measurement-based case study was conducted to test the load model identification methods. Shunt reactors were used for inducing voltage disturbances instead of commonly used OLTC (on-load tap changer) switching. The static load model variability with respect to day periods (day, evening and night) is analysed.

Index Terms—exponential model, load modelling, static load models, ZIP model

I. INTRODUCTION

Three different methodologies are in use for load modelling: component-based, measurement-based and the combination of the two. In case of the component-based approach, the aggregation of load component models is used to identify the model of the aggregated load. This approach has been used for example in [1]. To apply this method, statistics of load component power consumptions and load component models are needed. Obtaining the required data is challenging or often even impossible due to data ownership issues, especially for higher voltage levels [2]–[4]. The second load modelling method, measurement-based approach, uses measurement data for load model estimation. Measurement-based load modelling typically involves taking measurements (with sampling rate of 1 Hz or higher), pre-processing the measurement data, estimating the load model, validating the load model and post-processing the results. In some cases, data analysis stages may be repeated if obtained result is not within desired boundaries. To identify the voltage sensitivity of load by measurement based load modelling, voltage changes are needed.

The voltage changes may be either naturally occurring [5], [6] or induced [2], [7] for measurement purposes. Due to the difficulties associated with the usage of component-based method and the increasing number of measurement devices available in power systems, the measurement-based

approach is preferable in many cases [4], [8]. The complexity of measurement-based load model identification is related to the variability of load: the aggregated load changes in time [9], is affected by weather [10] and has stochastic nature [11]. In this paper, the measurement-based load modelling is used due to the lack of load component data and to assess the suitability of available measurement systems for load modelling.

Hourly and daily variability of load characteristics has been discussed in [1], [2], [12]–[15]. In these papers, the load characteristics of case studies or in some cases customer categories are presented. The voltage characteristics of aggregate load depend on load composition. The load composition is dependent on the structure of the industrial sector, habits of end users, weather and many other factors. Therefore, load model parameters estimated for a specific grid should not be directly applied to other grids [16]. In articles [1], [2], [12]–[15], the load characteristics estimated in Austria, Canada, Serbia, South Africa, UK and other countries have been discussed. The intra-day variability and load model parameter values identified were contradicting. For this reason, and due to missing data for countries similar to Estonia, a pilot case study was conducted for improving the understanding of the behaviour of the aggregated loads of Estonian transmission system. The results of the case study are presented in this paper.

The introduction section of the paper is followed by three main sections. In section II, used load model estimation methodology is explained together with a novel method for estimated load model post-processing. The conducted case study is described in section III. In addition, section III illustrates the impact of load model post-processing on the identified load models and presents the results of the case study. The conclusions of the paper are summarised in section IV.

II. METHODOLOGY

A. Inducing Voltage Disturbances

Often, the on-load tap-changer (OLTC) of transformer is used for inducing voltage disturbances, OLTC has been used

for example in [2], [5] and [7]. Another option is to use Static Var Compensator as was proposed in [3].

In this study, voltage disturbances were induced by a combination of reactor switching in the 330 kV network and network reconfiguration. The network reconfiguration was used for sustaining acceptable bus voltages on all network buses. The reactors were located at 330/110 kV substations tens of kilometres away from the measured 110/10 kV substations. The distance caused some attenuation of voltage deviations, but most of the relative voltage change induced in 330/110 kV substations was visible in 110/10 kV substations. Using reactor switching, it was possible to achieve voltage deviations up to a few per cent. The aim was to hold each voltage level for 5...10 min, as has been recommended in [2].

B. Measurement Data Pre-processing

Induced voltage disturbances were detected in measurement data by using sliding analysis window and averaging, similarly to [17]. The method uses the difference of mean values of two vectors with equal length (1).

$$\Delta V = \left| \frac{V_{old}/n - V_{new}/n}{V_{old}/n} \right| \cdot 100\% \quad (1)$$

where V_{old} and V_{new} are the sum of n old and n new samples, respectively, and n is the length of the averaging window.

The value of ΔV is compared with the event threshold value, and if ΔV is larger than the threshold value, the voltage difference indicates a voltage event. The first sample of the second vector is considered as the start of the event and the index of that sample is used for determining the time of the event. In this paper, to improve event detection, a secondary search was conducted in proximity of initially detected time value and the time with largest relative voltage change ΔV was recorded as the time of the event.

According to [5] and [8] small voltage changes of 0.5% can be used for load modelling. The same value was used in this study, so only voltage changes with $\Delta V \geq 0.5\%$ were considered as events. The averaging window length was 20 seconds in [17]. In this paper, n value corresponding to 10 seconds was used.

C. Load Model Estimation

Parameters of exponential and ZIP model were estimated. The exponential load model can be described by equations (2) and (3).

$$P = P_0(V/V_0)^{K_{pv}} \quad (2)$$

$$Q = Q_0(V/V_0)^{K_{qv}} \quad (3)$$

where P_0 and Q_0 are real and reactive power of the load at initial voltage V_0 respectively.

ZIP model can be described by (4) and (5). The ZIP model has three distinctive components: K_{pz} and K_{qz} with constant impedance (power proportional to the square of voltage); K_{pi}

and K_{qi} with constant current (power proportional to voltage); K_{pp} and K_{qq} with constant power (independent of voltage).

$$P = P_0(K_{pz}(V/V_0)^2 + K_{pi}(V/V_0) + K_{pp}) \quad (4)$$

where K_{pz} , K_{pi} , K_{pp} represent constant resistance, constant current and constant power type of real load component, respectively. V_0 corresponds to the initial voltage.

$$Q = Q_0(K_{qz}(V/V_0)^2 + K_{qi}(V/V_0) + K_{qq}) \quad (5)$$

where K_{qz} , K_{qi} , K_{qq} represent constant reactance, constant current and constant power type of reactive load component, respectively.

The load model estimation problem can be formulated based on minimisation of mean square error and expressed by (6). Least squares based load model estimation is a common solution for estimating load models from measurement data. It has been used for example in [5], [6], [18]. In [18] a comparison with Genetic Algorithm and Simulated Annealing is provided. Following equations are given for real power, reactive load models are estimated similarly.

$$\min MSE = \min \frac{1}{N} \sum_{i=1}^N (P_{modeli} - P_{measi})^2 \quad (6)$$

For estimating exponential load model parameters, following model equation and boundary conditions can be used for (6).

- $P_{modeli} = P_0(V_i/V_0)^{K_{pv}}$
- $-10.0 \leq K_{pv} \leq 10.0$
- $-10.0 \leq K_{qv} \leq 10.0$

For estimating ZIP load model parameters, following model equation and boundary conditions can be used for (6).

- $P_{modeli} = P_0(K_{pz}(V_i/V_0)^2 + K_{pi}(V_i/V_0) + K_{pp})$
- $K_{pz} + K_{pi} + K_{pp} = 1$
- $-10.0 \leq K_{pz} \leq 10.0$
- $-10.0 \leq K_{pi} \leq 10.0$
- $-10.0 \leq K_{pp} \leq 10.0$

D. Validation

Relatively small voltage disturbances (mostly $\leq 1\%$) were used for load model estimation. These voltage disturbances cause only small load deviations, often with comparable amplitude to the stochastic load variations. To validate the identified models, the modelling error is quantified by commonly used measures. Mean Square Error (MSE) (9) has been used in [18], typically the values were in the range $1 \cdot 10^{-5} \dots 10 \cdot 10^{-5}$. Normalized Mean Square Error (NMSE) (10) has been used in [19] and [22]. Alternatively, Mean Absolute Error (MAE) (7) can be used [21]. Normalized Mean Absolute Error (NMAE) (8) has been used in [6], [20], [21]. For all four measures of simulation error, the calculation is done based on measurement samples P_{measi} and modelled values P_{modeli} , where i is the index of the sample from 1... N . The reactive power modelling errors are calculated in the same way.

$$MAE = \frac{1}{N} \sum_{i=1}^N |P_{modeli} - P_{measi}| \quad (7)$$

According to Table II and Table III, the error normalization (MSE vs NMSE and MAE vs NMAE) has only a negligible impact on K_{pv} values. In Table II, the difference caused by normalization is below 0.05. In case of K_{qv} (Table III) the normalization of error has a larger impact, K_{qv} values differ by up to 0.22.

The identified load model voltage sensitivities in Table II differ in case of substation 1 'Cold Day' measurements over 0.4 units if absolute error (MAE, NMAE) and squared error (MSE, NMSE) based values are compared. Thus, in case of the analysed data, the impact of error type is larger than the impact of error normalisation. In Table II, the voltage sensitivities calculated using squared error (MSE and NMSE) based weighting are mostly lower than absolute error (MAE, NMAE) based values. The largest parameter values were obtained by mean value calculation, indicating that samples with high error had higher estimated load model parameter values. The median values were for all measurement periods lower than mean values. The differences caused by the choice of calculation methods were largest for daytime measurements of K_{pv} . In case of K_{qv} (Table III), the largest differences occur for substation 1 for 'Night' and 'Cold day' measurements.

D. Single Event Based Load Models and Identified Load Models

The main challenge faced during the analysis was the randomness of load: the natural load variations were large compared to the voltage changes. This caused large variations in estimated load model parameter values illustrated by box-plots Fig. 1, Fig. 2, Fig. 3 and Fig. 4.

In subsection III-C it was found that the differences between calculation methods were largest for daytime measurements of K_{pv} , and 'Night' and 'Cold day' measurements of K_{qv} at substation 1. According to Fig. 1, Fig. 2, Fig. 3 and Fig. 4, the mentioned daytime periods displayed a high variability of estimated event-based load model parameter values. Thus, the results indicate that the robustness of the calculation methods differs. Furthermore, in case of small number of samples, the weighted mean value calculation (method proposed in section II-E) may provide better results than averaging.

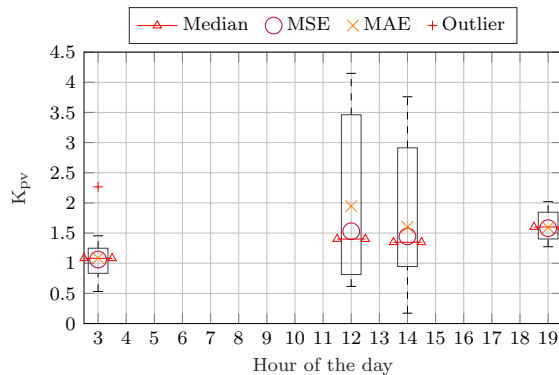


Fig. 1. Estimated real power exponent K_{pv} values of substation 1 and K_{qv} values identified by post-processing (using MSE and MAE for weights).

However, the downsides of using estimation error as the inverse of weight is that in case of extremely low error or zero values of power, numerical issues may occur. Some samples could obtain too high weights in comparison to other measured values, leading the calculated values away from the best estimate of the load model. A possible way to overcome these issues is to determine boundary values for the sample weights and validating the weight values during calculations. Too low or high values of determined weights could be replaced by boundary values.

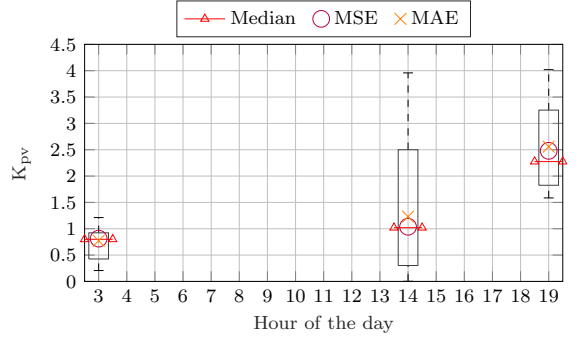


Fig. 2. Estimated real power exponent K_{pv} values of substation 2 and K_{qv} values identified by post-processing (using MSE and MAE for weights).

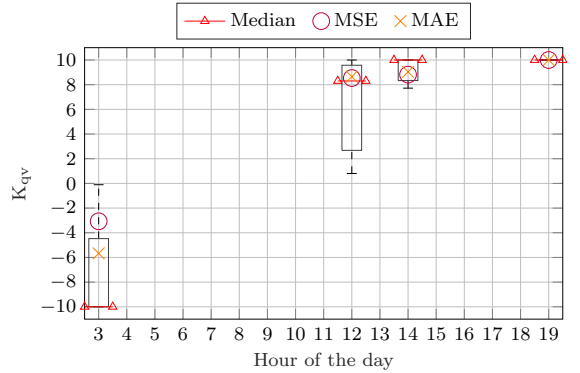


Fig. 3. Estimated reactive power exponent K_{qv} values of substation 1 and K_{qv} values identified by post-processing (using MSE and MAE for weights).

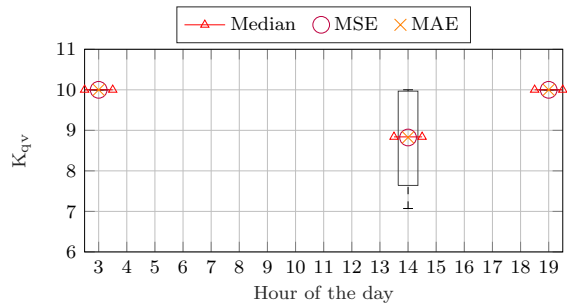


Fig. 4. Estimated reactive power exponent K_{qv} values of substation 2 and K_{qv} values identified by post-processing (using MSE and MAE for weights).

E. Identified Load Characteristics

Considering that Mean Square Error was used for defining the load model estimation problem, the post-processing results with MSE based weighting are given in the following Table IV and Table V. In addition to exponent values presented in previous subsection, ZIP model parameter values are presented. The ZIP model was also estimated for each event and for identifying ZIP load models for the day periods, the post processing method described in II-E was used.

TABLE IV
ESTIMATED REAL LOAD MODEL PARAMETERS

Substation	Time period	Exp. model		ZIP model	
		K_{pv}	K_{pz}	K_{pi}	K_{pp}
1	Cold day	1.53	1.12	-0.69	0.57
	Day	1.44	0.96	-0.49	0.53
	Evening	1.58	-0.16	1.89	-0.73
	Night	1.06	0.28	0.51	0.21
2	Day	1.04	0.77	-0.52	0.75
	Evening	2.48	-0.03	2.48	-1.45
	Night	0.81	0.58	-0.35	0.77

Table IV indicates an intra-day load model variability. Based on the identified load model parameter values in Table IV, the load real power has the largest parameter K_{pv} values during the evening and lowest values during the night. The K_{pv} value of 'Cold day' is higher than the value of 'Day'. Thus, the load model parameter K_{pv} is likely to have a temperature dependency.

The K_{qv} values in Table V are at evenings equal to the used boundary value of 10, indicating a possibly unsuitable load model structure. In addition, the 'Night' value of substation 1 differs significantly from the rest of the values, which may be caused by the low total reactive load during the night that was highly sensitive to random load changes. In Fig. 3 the event-based load model values have high variance, another indicator that the reliability of the identified 'Night' value of substation 1 is low.

TABLE V
ESTIMATED REACTIVE LOAD MODEL PARAMETERS

Substation	Time period	Exp. model		ZIP model	
		K_{qv}	K_{qz}	K_{qi}	K_{qq}
1	Cold day	8.54	7.80	-3.54	-3.26
	Day	8.81	6.13	-1.03	-4.10
	Evening	10.00	6.50	0.93	-6.43
	Night	-3.07	-2.11	-0.11	3.22
2	Day	8.82	4.58	0.21	-3.79
	Evening	10.00	6.40	1.29	-6.69
	Night	10.00	8.37	-0.62	-6.75

IV. CONCLUSION

The paper presented a novel method for post-processing event-based load model parameter values. It was found that

the results of the method depend on the used measure of error. The results also indicated that the normalization of the used error has smaller impact on the results than the type of error (absolute error or squared error) used. The method provided results that differ from commonly used average value calculation. Further work is required to properly assess the usability of the presented method and to determine suitable boundary values for the sample weighting.

The methodology and results of a conducted case study were presented. The results indicated that the voltage sensitivity of the measured load is temperature dependent and has highest real power parameter K_{pv} values during the evening and lowest during the night. The reactive load was found to be highly voltage dependent, the values of estimated reactive load model parameters were in some cases equal to the higher boundary value. Further measurements are required to determine a reliable load model for the reactive loads of the measured substations.

ACKNOWLEDGMENT

The authors would like to express their gratitude to the involved personnel of Elering (Estonian TSO). In addition, the authors would like to thank Uku Salumäe for helping with the measurements in the substation and technical support of the power quality monitors.

REFERENCES

- [1] A. J. Collin, J. L. Acosta, B. P. Hayes, and S. Z. Djokic, "Component-based aggregate load models for combined power flow and harmonic analysis," in *7th Mediterranean Conf. and Exhibition on Power Generation, Transmission, Distribution and Energy Conversion (MedPower 2010)*, Agia Napa, Cyprus, 2010, pp. 1-10.
- [2] L. M. Korunovic, D. P. Stojanovic, and J. V. Milanovic, "Identification of static load characteristics based on measurements in medium-voltage distribution network," *IET Generation, Transmission & Distribution*, vol. 2, no. 2, pp. 227-234, March 2008.
- [3] K. Q. Hua, A. Vahidnia, Y. Mishra, and G. Ledwich, "PMU measurement based dynamic load modelling using SVC devices in online environment," in *2015 IEEE PES Asia-Pacific Power and Energy Engineering Conf. (APPEEC)*, Brisbane, QLD, Australia, 2015, pp. 1-5.
- [4] L. M. Korunovic and D. P. Stojanovic, "The effects of normalization of static load characteristics," in *2009 IEEE Bucharest PowerTech*, Bucharest, Romania, 2009, pp. 1-6.
- [5] S. A. Arefifar and W. Xu, "Online tracking of voltage-dependent load parameters using ULTC created disturbances," *IEEE Trans. Power Systems*, vol. 28, no. 1, pp. 130-139, Feb. 2013.
- [6] M. Leinakse, T. Sarnet, T. Kangro, and J. Kilter, "First results on load model estimation using digital fault recorder measurements," in *16th International Symposium "Topical Problems in the Field of Electrical and Power Engineering" and "Doctoral School of Energy and Geotechnology III"*, Pärnu, Estonia, 2017, pp. 101-105.
- [7] H. Guo, K. Rudion, H. Abildgaard, P. Komarnicki, and Z. A. Styczynski, "Parameter estimation of dynamic load model using field measurement data performed by OLTC operation," in *2012 IEEE Power and Energy Society General Meeting*, San Diego, CA, USA, 2012, pp. 1-7.
- [8] W. Freitas and L. C. P. da Silva, "A discussion about load modeling by using voltage variations," in *2012 IEEE 15th Int. Conf. on Harmonics and Quality of Power*, Hong Kong, China, 2012, pp. 40-44.
- [9] M. Meldorf and J. Kilter, "Type models of electrical network load," *Oil Shale*, vol. 26, no. 3S, pp. 243-253, 2009.
- [10] M. Meldorf, Ü. Treufeldt, and J. Kilter, "Temperature dependency of electrical network load," *Oil Shale*, vol. 24, no. 2S, pp. 237-247, 2007.
- [11] M. Meldorf, T. Täht, and J. Kilter, "Stochasticity of electrical network load," *Oil Shale*, vol. 24, no. 2S, pp. 225-236, 2007.

- [12] C. A. Baone, S. Veda, Y. Pan, W. Premerlani, J. Dai, and A. Johnson, "Measurement based static load model identification," in *2015 IEEE Power & Energy Society General Meeting*, Denver, CO, USA, 2015, pp. 1-5.
- [13] E. Vaahedi, M. A. Fl-Kady, J. A. Libaque-Esaine, and V. F. Carvalho, "Load models for large-scale stability studies from end-user consumption," *IEEE Trans. Power Systems*, vol. 2, no. 4, pp. 864-870, Nov. 1987.
- [14] M. L. Coker and H. Kgasoane, "Load modeling," in *1999 IEEE Africon*, Cape Town, South Africa, 1999, vol. 2, pp. 663-668.
- [15] J. Marchgraber, E. Xypolytou, I. Lupandina, W. Gawlik, and M. Stifter, "Measurement-based determination of static load models in a low voltage grid," in *2016 IEEE PES Innovative Smart Grid Technologies Conf. Europe (ISGT-Europe)*, Ljubljana, Slovenia, 2016, pp. 1-6.
- [16] A. Arif, Z. Wang, J. Wang, B. Mather, H. Bashualdo, and D. Zhao, "Load modeling – a review," *IEEE Trans. Smart Grid*, vol. PP, no. 99, pp. 1-1.
- [17] I. R. Navarro, "Dynamic power system load – estimation of parameters from operational data," Ph.D. dissertation, Dept. Industrial Electrical Engineering and Automation, Lund Univ., Lund, Sweden, 2005.
- [18] Y. Zhu and J. V. Milanović, "Automatic identification of power system load models based on field measurements," *IEEE Trans. Power Systems*, vol. 33, no. 3, pp. 3162-3171, May 2018.
- [19] Y. Ge, A. J. Flueck, D. K. Kim, J. B. Ahn, J. D. Lee, and D. Y. Kwon, "Power system real-time event detection and associated data archival reduction based on synchrophasors," *IEEE Trans. Smart Grid*, vol. 6, no. 4, pp. 2088-2097, July 2015.
- [20] K. N. Hasan, J. V. Milanović, P. Turner, and V. Turnham, "A step-by-step data processing guideline for load model development based on field measurements," in *2015 IEEE Eindhoven PowerTech*, Eindhoven, Netherlands, 2015, pp. 1-6.
- [21] M. Leinakse and J. Kilter, "Conversion Error of Exponential to Second Order Polynomial ZIP Load Model Conversion," in *2018 IEEE International Conference on Environment and Electrical Engineering and 2018 IEEE Industrial and Commercial Power Systems Europe (EEEIC / I&CPS Europe)*, Palermo, Italy, 2018, in press.
- [22] Y. Ge, A. J. Flueck, D. K. Kim, J. B. Ahn, J. D. Lee, and D. Y. Kwon, "An event-oriented method for online load modeling based on synchrophasor data," *IEEE Trans. Smart Grid*, vol. 6, no. 4, pp. 2060-2068, July 2015.

Publication IV

M. Leinakse, P. Tani, and J. Kilter, "Impact of distributed generation on estimation of exponential load models," in *2019 IEEE Power & Energy Society General Meeting (PESGM)*, Atlanta, GA, USA, 2019, pp. 1–5, doi: 10.1109/PESGM40551.2019.8974014

©2019 IEEE. Reprinted with permission.

Impact of Distributed Generation on Estimation of Exponential Load Models

Madis Leinakse, Pärtel Tani, Jako Kilter

Department of Electrical Power Engineering and Mechatronics

Tallinn University of Technology

Tallinn, Estonia

madis.leinakse@ttu.ee

Abstract—This paper presents the results of a measurement-based load model estimation study, which was conducted in a distribution network with high penetration of distributed generation. The main goal of the study was to determine the impact of distributed generation on the estimation of exponential load models. The required voltage changes were induced using an on-load tap changer and measurements were taken using a power quality monitor. The exponential load models were estimated from transformer measurements (apparent load) and by combining power transformer measurement data with SCADA data (net load). Equations for conversion between apparent and net load model are presented and compared to load models estimated from measurement data.

Index Terms—distributed generation, exponential model, load modelling, static load models

I. INTRODUCTION

Three different methodologies are in use for load modelling: component-based, measurement-based and the combination of component-based and measurement-based. In case of the component-based load modelling approach, the aggregation of load component models is used to identify the model of the aggregated load. In case of measurement-based approach, measurement data is used for load model estimation. Typically, the load model estimation involves measurement data pre-processing (for example filtering), estimating the model, validating model and post-processing the results. In some cases, data analysis stages may be repeated if obtained results do not meet the required conditions. To estimate the voltage characteristics of the aggregated load by measurement-based approach, voltage changes need to occur. Either naturally occurring [1], [2] or induced [3]–[5] voltage changes can be used for measurement purposes. In this paper, an active measurement-based load modelling approach is used. The required voltage changes are induced by on-load tap changer switching and measurements are taken via power quality monitor (PQM) and SCADA system.

One way for modelling aggregated load, which includes wind turbines, is to use a composite load model that consists of static load model and an induction machine (or two in parallel) [6]–[8]. In [6] different configurations of composite load model are discussed and compared for modelling aggregated load considering distributed generation. In [7], [8] methods for the estimation of composite load model parameters are presented and analysed. Another way is to model the voltage

sensitivity of the aggregated load by static characteristics as was done in [9]. The mentioned paper focuses on load model estimation by the use of smart transformer. However, the impact of distributed generation on apparent voltage sensitivity of the load was discussed as well. In this paper, exponential load model, similarly to [9], is used for modelling aggregated load.

The introduction section of the paper is followed by four main sections. In section II, estimated load models and used measurement data processing methodology are explained. The conducted case study is described in section III. The results of the case study and discussion of the results is presented in section IV. The main results of the paper are summarised in section V.

II. THEORETICAL BACKGROUND

A. Measurement Data Pre-processing

The induced voltage changes were detected by using an algorithm described in [10], which was also used in [5]. The detection algorithm is based on comparison of average values of two sets of measurement data. The compared datasets with n samples are taken consecutively, average values of the datasets are calculated, and the voltage change is calculated using (1).

$$\Delta V = \left| \frac{V_{old}/n - V_{new}/n}{V_{old}/n} \right| \cdot 100\% \quad (1)$$

where V_{old} and V_{new} are the sum of n old and n new samples, respectively, and n is the length of the averaging window.

The value of ΔV is compared with the chosen event threshold value. If ΔV is larger than the threshold value, the voltage difference indicates a voltage event. The first sample of the second vector is considered as the start of the event. The index of that sample is used for determining the time of the event. According to [1] and [11] small voltage changes of 0.5% can be used for load modelling. In this study, on-load tap changer with 1.78% step was used, thus 1.5% was used as event threshold. The averaging window length of 20 seconds was used in [10]. In this paper, n value corresponding to 40 seconds was chosen based on event detection results.

B. Exponential Load Model

The exponential load model can be described by (2) and (3).

$$P_{EXP} = P_0(V/V_0)^{K_{pv}} \quad (2)$$

$$Q_{EXP} = Q_0(V/V_0)^{K_{qv}} \quad (3)$$

where P_0 and Q_0 are real and reactive power of the load at pre-event voltage V_0 respectively. K_{pv} and K_{qv} are exponents describing the voltage characteristics of the real and reactive power of the load.

C. Load Model Estimation

The load model estimation problem can be formulated based on minimisation of mean square error (5) and expressed by (4) [5]. The non-linear least squares (NLS) formulation of the problem is a common solution for load model estimation from measurement data. It has been used for example in [1], [2], [5], [12]. A comparison of NLS, Genetic Algorithm and Simulated Annealing is provided in [12]. Following equations are given for real power, reactive load models can be estimated similarly.

$$\min MSE = \min \frac{1}{N} \sum_{i=1}^N (P_{modeli} - P_{measi})^2 \quad (4)$$

For estimating exponential load model parameters, following model equation and boundary conditions can be used for (4).

- $P_{modeli} = P_0(V_i/V_0)^{K_{pv}}$
- $-10.0 \leq K_{pv} \leq 10.0$
- $-10.0 \leq K_{qv} \leq 10.0$

D. Estimation Error

The modelling error of the estimated characteristics is quantified by Mean Absolute Error (MAE) (5) and Mean Square Error (MSE) (6). Mean Absolute Error (MAE) (5) has been used in [13], [14] and MSE in [12]. The MSE values in [12] were in range $1 \cdot 10^{-5} \dots 10 \cdot 10^{-5}$.

For both measures of simulation error, the calculation is done based on measurement samples P_{measi} and modelled values P_{modeli} , where i is the index of the sample from $1 \dots N$.

$$MAE = \frac{1}{N} \sum_{i=1}^N |P_{modeli} - P_{measi}| \quad (5)$$

$$MSE = \frac{1}{N} \sum_{i=1}^N (P_{modeli} - P_{measi})^2 \quad (6)$$

E. Expected Impact of Distributed Generation

If the voltage and power changes are relatively small, the voltage sensitivity of the exponential load model for time instance t_k can be expressed by (7) [15].

$$K_p = \frac{\frac{P(t_k) - P(t_{k-1})}{P(t_{k-1})}}{\frac{V(t_k) - V(t_{k-1})}{V(t_{k-1})}} \quad (7)$$

where $V(t_k)$ and $P(t_k)$ are voltage and power measured at time t_k , and the previous samples are $V(t_{k-1})$ and $P(t_{k-1})$.

If a significant amount of distributed generation is connected to the load feeder, the apparent voltage sensitivity of the net load of the feeder differs from the load characteristic. The impact of distributed generation (DG) on the voltage sensitivity of net load was discussed in [9]. It was assumed that the DG is operating at unity power factor ($Q_G = 0$). Also, that the power generated by DG P_G is smaller than the load of the feeder P_L : $P_G < P_L$, thus the net load of the feeder was (8).

$$P_0 = P_L - P_G > 0 \quad (8)$$

The normalised voltage sensitivity $K_{pv,L}$ of load P_L was (9) and the active power of the DG was insensitive to voltage (considering its contribution to losses negligible), i.e., $K_{pv,G} = 0$.

$$K_{pv,L} = \frac{\Delta P_L / P_L}{\Delta V / V_0} \quad (9)$$

In such case, the net feeder load changed for a voltage disturbance ΔV as follows:

$$\Delta P = \Delta P_L = K_{pv,L}(\Delta V / V_0)P_L \quad (10)$$

Using (7), (9) and (10), the apparent feeder load sensitivity was determined to be (10) [9].

$$K_{pv} = \frac{\Delta P / P_0}{\Delta V / V_0} = K_{pv,L} \cdot \frac{P_L}{P_L - P_G} \quad (11)$$

From (11) it is possible to derive (12), which can be used for calculating voltage sensitivity of load $K_{p,L}$. If apparent voltage sensitivity K_p , load power P_L and generated power P_G are known.

$$K_{pv,L} = K_{pv} \cdot \frac{P_L - P_G}{P_L} \quad (12)$$

III. CASE STUDY

A. Studied Section of Distribution Network

The measurement-based case study was conducted in a distribution network section which supplies 13 755 customers. Based on average energy consumptions of March (of 2013...2015), the typical load division by customer categories is:

- Residential 33.2%
- Agricultural 2.3%
- Service and business 36.9%
- Industry 21.0%
- Public 6.6%

The average load of the customers, connected to the measured feeder, was during the measured period 7.4 MW. 6.7 MW of distributed generation is connected to the same feeder: 2 wind turbines (2,3 MW and 2,0 MW), and a 2,4 MW combined heat and power plant (CHP). The DG units are operated in fixed $\cos\phi$ mode.

B. Measurement Setup and Induced Voltage Changes

The measurement probes of the Power Quality Monitor (PQM) were connected to the voltage transformer (VT) of the section and to the current transformer (CT) of the transformer feeder. The load was around 100 A, thus the CT (2500/1) was under-loaded, which may have had a negative impact on the accuracy of current measurements. The PQM recorded three phase RMS values of voltage, active power and reactive power with sampling rate of 5 Hz (time-step 200 ms).

The voltage changes were induced for load model estimation by on-load tap changer (OLTC) switching. The used OLTC has 16 tap positions with 1.78% steps. During the study, voltage variations were limited by the DSO to 10.2 ... 10.8 kV. The voltage levels induced using OLTC for the study are shown in Fig. 1. At the beginning and at the end of the measurement period, the voltage was kept at normal level. During the measurement period, the voltage was switched to lower and higher level and each level was kept 10..15 minutes.

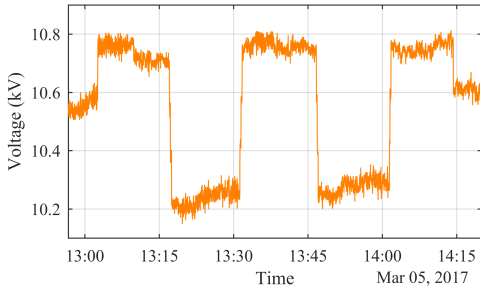


Fig. 1. Average RMS voltage at measured substation.

IV. RESULTS AND ANALYSIS

A. Measured Voltage and Power

The measurements were taken on March 5, 2017 on a windy afternoon in time range 12:30...14:30. Fig. 2 displays the voltage and feeder power measured by the Power Quality Monitor (PQM). The measured data indicates that the measured net load is not sufficient for fully understanding the processes taking place in the feeder.

The SCADA data was acquired for determining the generated power P_{Gen} of the distributed generation units and was plotted in Fig. 3. The P_{Gen} decreases and increases twice by around 2 MW. Based on Fig. 4, the P_{Gen} decreases occur 5...8 minutes after voltage increase, indicating the over-voltage protection of one wind turbine may be configured falsely. This theory is supported by the fact that, with a similar delay, voltage decreases caused restoration of same amount of generation capacity. Adding the generated power P_{Gen} to net load of the transformer P_{Tran} , the load P_{Load} is acquired. The load P_{Load} has peaks at the changes of P_{Gen} , which are caused by sampling rate mismatch: the SCADA data was with lower sampling rate than the PQM.

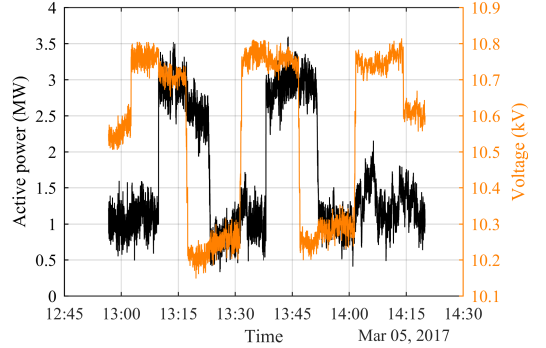


Fig. 2. Measured voltage and active power (at substation).

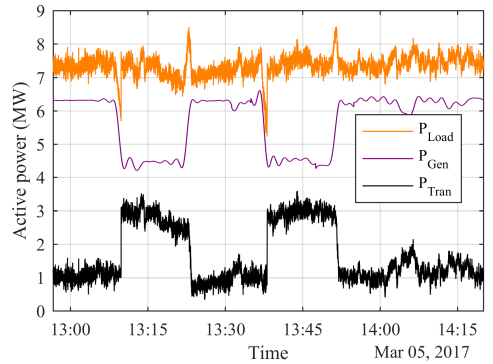


Fig. 3. Measured net load of the transformer P_{Tran} , total power of DG units P_{Gen} and calculated load P_{Load} .

The 6 voltage changing events are marked in Fig. 4 with vertical black lines. As the events are at a different time than the wind turbine switching events (rapid changes in P_{Gen}), the peaks in P_{Load} and rapid changes of P_{Gen} should not have a significant negative impact on the accuracy of load model estimation results.

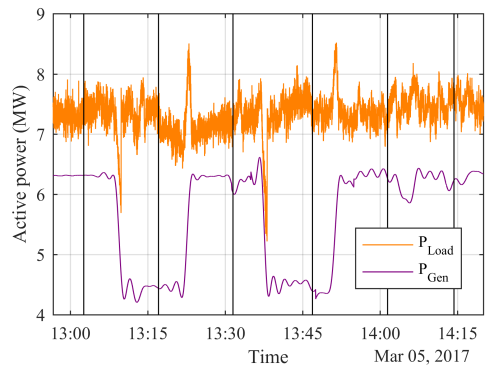


Fig. 4. Induced voltage events (marked by vertical black lines).

B. Estimated Load Characteristics

The parameters of exponential load models were estimated for each voltage event, both for load P_{Load} and net load P_{Tran} . The net load model represents aggregated model, which includes distribution generation. Fig. 5 shows that the net load has significantly higher voltage sensitivity than the actual load (without distributed generation). This results is logical as in both cases, a change in voltage would cause the load to increase or decrease by the same amount of power. However, in the presence of distributed generation, the net load value is decreased, which means a larger relative load change would be seen at the transformer.

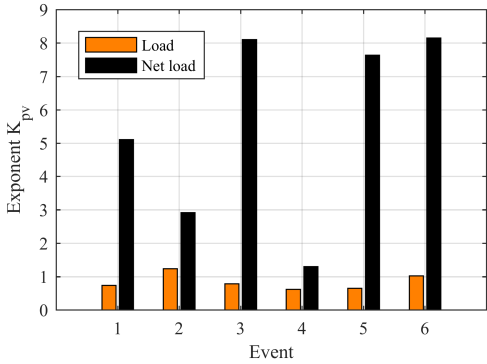


Fig. 5. Exponential load model of load and net load (includes load and distributed generation).

The numerical values of event based load model estimates are presented in Table I. The mean absolute modelling error (MAE) of the load is 4...10 times smaller than the modelling error of net load. The values of mean square error are comparable to [12].

TABLE I
ESTIMATED LOAD MODELS

Event	Load			Net load		
	$K_{pv,L}$	MSE ($\cdot 10^{-5}$)	MAE	$K_{pv,T}$	MSE ($\cdot 10^{-3}$)	MAE
1	0.74	17	0.011	5.11	19	0.105
2	1.24	10	0.008	2.92	1.9	0.034
3	0.79	14	0.009	8.11	14	0.093
4	0.62	9.9	0.008	1.30	1.3	0.030
5	0.65	8.1	0.008	7.64	11	0.084
6	1.03	4.7	0.006	8.15	3.5	0.046

In section II, equation (11) was presented for calculating the voltage sensitivity of net load from voltage sensitivity of load. In Fig. 6, the result of calculation with (11) is plotted. It is possible to notice that in case of events 1, 2 and 4, the calculated values are close to the value, which was estimated from measurement data. Event 1 was voltage rise from normal to high with high generation P_{Gen} . 2 and 4 had lower P_{Gen} level and voltage was decreased from high to low. Events 3, 5 and 6 had lower calculation accuracy, all three had higher

level of P_{Gen} . Thus, the accuracy of (11) may be lower if the penetration of distributed generation is higher.

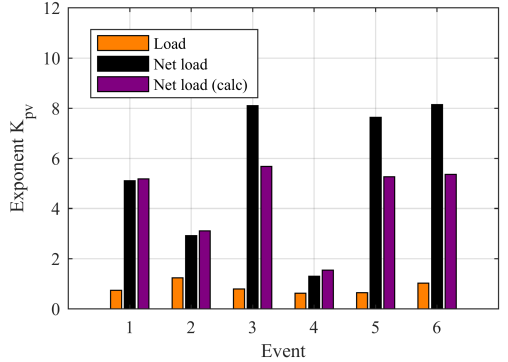


Fig. 6. Exponential load model of load and net load (includes load and distributed generation). Net load exponent K_{pv} (purple) calculated using (11) from load exponent (orange).

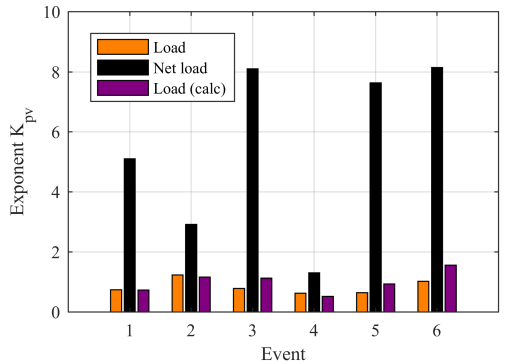


Fig. 7. Exponential load model of load and net load (includes load and distributed generation). Load exponent $K_{pv,L}$ (purple) calculated using (12) from estimated net load exponent (black).

Similarly, in section II (12) was presented for calculating the voltage sensitivity of load from the voltage sensitivity of the net load. In Fig. 7, the results of the calculation are shown. The accuracy of calculated values is similar to the previous calculation: parameters of events 1, 2 and 4 are close to the estimated values of parameters.

V. CONCLUSION

This paper presented the results of a measurement-based load modelling study that was conducted in a distribution network with a high penetration of distributed generation. It was shown that the distributed generation units increase the voltage sensitivity of the net load (aggregated load seen as the load of the transformer). It was found that the modelling accuracy of the net load is lower than the modelling accuracy of total load, if exponential model is used for modelling the aggregated load. The results of the study indicated that for

approximate assessment of the impact of distributed generation on exponential load model, equations (11) and (12) may be used.

REFERENCES

- [1] S. A. Arefifar and W. Xu, "Online tracking of voltage-dependent load parameters using ULTC created disturbances," *IEEE Trans. Power Systems*, vol. 28, no. 1, pp. 130-139, Feb. 2013. DOI: 10.1109/TPWRS.2012.2199336
- [2] M. Leinakse, T. Sarnet, T. Kangro, and J. Kilter, "First results on load model estimation using digital fault recorder measurements," in *16th International Symposium "Topical Problems in the Field of Electrical and Power Engineering" and "Doctoral School of Energy and Geotechnology III"*, Pärnu, Estonia, 2017, pp. 101-105.
- [3] L. M. Korunovic, D. P. Stojanovic, and J. V. Milanovic, "Identification of static load characteristics based on measurements in medium-voltage distribution network," *IET Generation, Transmission & Distribution*, vol. 2, no. 2, pp. 227-234, March 2008. DOI: 10.1049/iet-gtd:20070091
- [4] H. Guo, K. Rudion, H. Abildgaard, P. Komarnicki, and Z. A. Styczynski, "Parameter estimation of dynamic load model using field measurement data performed by OLTC operation," in *2012 IEEE Power and Energy Society General Meeting*, San Diego, CA, USA, 2012, pp. 1-7. DOI: 10.1109/PESGM.2012.6345563
- [5] M. Leinakse, H. Kiristaja, and J. Kilter, "Identification of intra-day variations of static load characteristics based on measurements in high voltage transmission network", in *2018 IEEE PES Innovative Smart Grid Technologies Conference Europe (ISGT-Europe)*, 2018. DOI: 10.1109/ISGTEurope.2018.8571712
- [6] W. Jili, H. Renmu and M. Jin, "Load modeling considering distributed generation," *2007 IEEE Lausanne Power Tech*, Lausanne, 2007, pp. 1072-1077. DOI: 10.1109/PCT.2007.4538464
- [7] J. Qian, X. Li and J. Hui, "Impact of wind generation on load modeling of distribution network," *2009 International Conference on Sustainable Power Generation and Supply*, Nanjing, 2009, pp. 1-5. DOI: 10.1109/SUPERGEN.2009.5348295
- [8] L. Rodríguez-García, S. Pérez-Londoño and J. Mora-Flórez, "A methodology for composite load modeling in power systems considering distributed generation," *2012 Sixth IEEE/PES Transmission and Distribution: Latin America Conference and Exposition (T&D-LA)*, Montevideo, 2012, pp. 1-7. DOI: 10.1109/TDC-LA.2012.6319122
- [9] G. De Carne, G. Buticchi, M. Liserre and C. Voumas, "Load control using sensitivity identification by means of smart transformer," in *IEEE Transactions on Smart Grid*, vol. 9, no. 4, pp. 2606-2615, July 2018. DOI: 10.1109/TSG.2016.2614846
- [10] I. R. Navarro, "Dynamic power system load – estimation of parameters from operational data," Ph.D. dissertation, Dept. Industrial Electrical Engineering and Automation, Lund Univ., Lund, Sweden, 2005.
- [11] W. Freitas and L. C. P. da Silva, "A discussion about load modeling by using voltage variations," in *2012 IEEE 15th Int. Conf. on Harmonics and Quality of Power*, Hong Kong, China, 2012, pp. 40-44. DOI: 10.1109/ICHQP.2012.6381271
- [12] Y. Zhu and J. V. Milanović, "Automatic identification of power system load models based on field measurements," *IEEE Trans. Power Systems*, vol. 33, no. 3, pp. 3162-3171, May 2018. DOI: 10.1109/TPWRS.2017.2763752
- [13] M. Leinakse and J. Kilter, "Conversion error of exponential to second order polynomial ZIP load model conversion," in *2018 IEEE International Conference on Environment and Electrical Engineering and 2018 IEEE Industrial and Commercial Power Systems Europe (EEEIC / I&CPS Europe)*, Palermo, Italy, 2018, pp. 1-5. DOI: 10.1109/EEEIC.2018.8493667
- [14] M. Leinakse and J. Kilter, "Conversion error of second order polynomial ZIP to exponential load model conversion," in *Mediterranean Conference on Power Generation, Transmission, Distribution and Energy Conversion (MEDPOWER 2018)*, Dubrovnik, Croatia, 2018, pp. 1-5. DOI: 10.1049/cp.2018.1882
- [15] G. De Carne, M. Liserre and C. Voumas, "On-Line Load Sensitivity Identification in LV Distribution Grids," in *IEEE Transactions on Power Systems*, vol. 32, no. 2, pp. 1570-1571, March 2017. DOI: 10.1109/TPWRS.2016.2581979

Publication V

M. Leinakse and J. Kilter, "Clustering of transmission system loads based on monthly load class energy consumptions," in *2020 21st International Scientific Conference on Electric Power Engineering (EPE)*, Prague, Czech Republic, Oct. 2020, pp. 1–6, doi: 10.1109/epe51172.2020.9269197

©2020 IEEE. Reprinted with permission.

Clustering of Transmission System Loads Based on Monthly Load Class Energy Consumptions

Madis Leinakse, Jako Kilter

Department of Electrical Power Engineering and Mechatronics

Tallinn University of Technology

Email: madis.leinakse@taltech.ee, jako.kilter@taltech.ee

Abstract—This paper presents an approach for clustering aggregated loads based on load class energy consumption time series, and choosing representative loads for each group. The described approach was applied in a transmission system load modelling study. The goal of the study was to choose representative loads for measurement-based modelling. The work was motivated by the limited number of available measurement devices and available personnel for data processing. The monthly energy consumption of each load class was known for each aggregated bus load. After measurement data pre-processing the larger loads were clustered using K-means algorithm, and smaller assigned to clusters. Representative loads were selected from each cluster.

Keywords—clustering; databases; data mining; energy consumption; load modeling, smart metering

I. INTRODUCTION

In power system calculations loads are typically modelled by aggregated bus loads. The parameter values of the aggregated load models are identified using measurements, survey results, literature, experience or have an unknown source [1], [2]. In general, there are three main ways for load modelling: measurement-based, component-based, and combined approach. In case of the measurement-based method load responses to naturally occurring [3], [4] or induced [5]–[7] voltage changes are analysed to estimate the aggregated load models. Typically, the load model estimation involves measurement data pre-processing, estimating the model, validating model and post-processing the results [8], [9]. In case of some distribution and transmission networks, the number of available measurement devices with sufficient measurement frequency may be limited. The procedure presented in this paper could be used for selecting the representative loads, which are modelled using measurements. The estimated models could be applied to the rest of the loads belonging to the same clusters, if the estimated models match the clustering results.

In case of the component-based load modelling, the aggregation of load component models is used to identify the model of the aggregated load. It is a convenient method for calculating load models of a large number of buses, when there is sufficient customer data and statistical data available. However, the component-based models should be validated by measurements to achieve the best results. In such case the

methodology could also be considered to be a combined approach: measurement-based and component-based method are both used. One possible method for validation is to first group substations based on load class compositions. Next, to choose a few representative substations from each group. Finally, to estimate the models of these loads from measurement data, and to compare the models estimated by different approaches. For easy comparison of some models (e.g. ZIP models), conversion of load models is reasonable [10], [11]. The results of the analysis could also help to identify load classification errors or confirm the classification logic. The selection and detailed analysis of representative loads would enable a more efficient use of measurement devices and manpower.

The previous paragraphs described how the clustering of aggregated loads and selecting representative loads for each group could be used when load modelling is conducted. In this study, the monthly energy consumptions of load classes were known for the aggregated loads, which were to be modelled. Thus, it was decided to use that data for clustering the bus loads. The clustering of substations by monthly energy consumptions is similar to grouping daily load profiles, which is used for customer classification and type profile identification. The main difference is the added dimension of load class composition: instead of one energy consumption value for each time instance, there are now several (five) load class contributions. In this paper it is shown how to take into account the load class composition information when clustering time series.

The clustering of time series of daily consumption (daily load profile grouping) has been done in [12], [13] using K-means clustering (Lloyds' algorithm) [14]. A more advanced approach is used in [15], [16], where the dynamic time warping is used, which is fundamentally similar to Lloyds' algorithm, but in addition allows for matching time shifted series. The K-means algorithm has also been applied to problems, which have parameters with different physical quantities. For example, in [17], [18] the K-means clustering was used for clustering wind power ramp events based on the parameters of ramp events (rise time, fall time, peak power).

The introduction section of the paper is followed by three main sections. In Section II, the measurement data processing procedure is presented and explained. In Section III, the data processing procedure presented in Section II is applied on measurement data, which covers 132 aggregated loads. The main results of the paper are summarised in Section IV.

This work was mainly funded by the Estonian TSO, Elering AS, with additional support of Tallinn City Council Scholarship.

II. DATA PROCESSING PROCEDURE & APPLIED METHODS

The data processing procedure was motivated by several factors. Firstly, the amount of customer data available for the TSO (DSO owns the end customer database) was highly limited. Secondly, the number of employees available for data processing was also limited. Thirdly, the available measurement devices were only sufficient for measuring only a fraction of the substations. The aim of the data processing procedure was to group (cluster) aggregated loads with similar time series of load class compositions, and to choose representative loads from each cluster. These substations would be analysed in more detail during the load modelling study. The selection of representative loads would enable a more efficient use of measurement resources, and employees.

A. Data Processing Procedure

The applied data processing procedure can be described by the following steps:

- 1) Data pre-processing.
- 2) Substations with the largest load and with medium load clustered using K-means algorithm.
- 3) Substations with the smallest load assigned to clusters with the closest centre.
- 4) Representative substations selected for each cluster.

B. Data Pre-Processing

1) *Measurement Data*: The monthly energy consumption data of load classes was provided by a distribution system operator, which classifies the consumers into 5 classes:

- Class 1: Residential
- Class 2: Agricultural
- Class 3: Commercial
- Class 4: Industrial
- Class 5: Public

The acquired meter data covered 33 months (from January 2013 to September 2015). The energy consumption of a substation, by load classes, is shown in Fig. 1. The years are marked with different markers (2013 by *, 2014 by O and 2015 by X), and the load classes with different colours. The figure indicates that the energy consumption of the substation has a seasonal pattern, and the pattern differs for load classes. Thus, the load class composition also changes each month.

2) *Decreasing Length of Time Series*: The input data includes 33 months, thus the first 9 months of the year have 3 values and last 3 months only 2 values. To even out the impact of months, a representative year (12 months of values) was calculated. The months of different years were matched and averaged to find the mean energy consumption for each month and load class.

3) *Normalising Load Class Composition Data*: The averaged monthly load class compositions were normalised to enable matching of substations with similar load class compositions. The normalisation was done by dividing each monthly average load class energy consumption with each month's total energy consumption. This was done separately for each

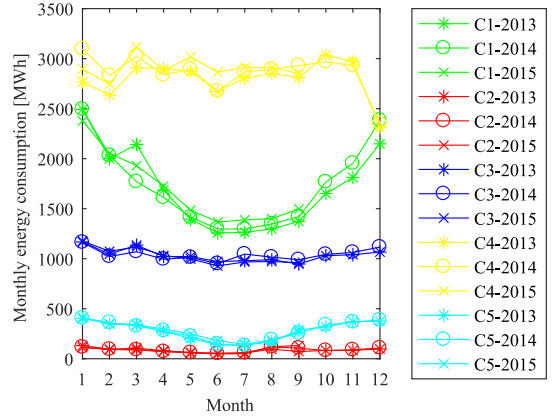


Fig. 1. Acquired monthly energy consumption data of a substation, disaggregated by load classes (C1...C5).

substation. The substation energy consumption data shown in Fig. 1 was calculated to Fig. 2.

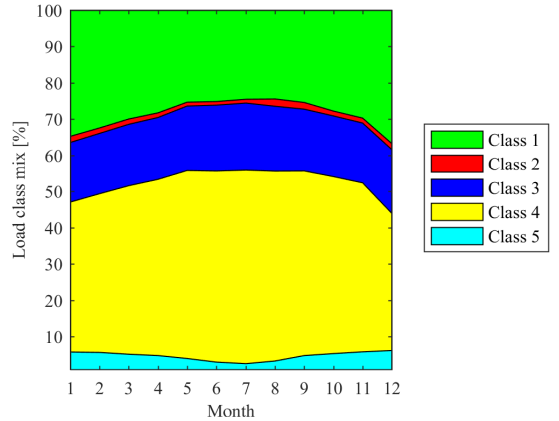


Fig. 2. Load class compositions of representative year after normalisation (values stacked).

C. K-means Clustering of Load Composition Time Series

1) *K-means Clustering Algorithm*: The K-means clustering algorithm, which is also known as Lloyd's algorithm [14], is used for classification of objects into groups (clusters) based on properties (attributes). In this paper, the substation loads are the objects and monthly load class compositions are the attributes. There are 5 classes and 12 monthly load class compositions, thus each load has 60 attributes.

The K-means algorithm is based on the minimisation of total squared Euclidean distance between the objects and centres of the assigned clusters. This objective can be written as (1), the steps of the K-means algorithm are explained in detail in [12].

$$\min(E) = \min \left(\sum_{i=1}^K \sum_{x \in C_i} d(x, z_i) \right) \quad (1)$$

where K is the number of clusters, z_i is the centre of cluster C_i , and $d(x, z_i)$ is the Euclidean squared distance between object x and cluster centre z_i .

The Euclidean distance squared $d(x, z_i)$ between object x with attributes x_1, x_2, \dots, x_n and centre of cluster z_1 with attributes $z_{1,1}, z_{1,2}, \dots, z_{1,n}$ is (2).

$$d(x, z_1) = (x_1 - z_{1,1})^2 + (x_2 - z_{1,2})^2 + \dots + (x_n - z_{1,n})^2 \quad (2)$$

Several methods are used for choosing the value of K , the number of clusters. [12] determined the analysed number of clusters by using equation $2 \leq K_{max} \leq \sqrt{m}$, where m is the number of objects in database. Next, the clustering was conducted for $K = 2 \dots K_{max}$, and based on Silhouette Global Index (SGI) the best solution was chosen. SGI is explained in the following point 2).

Another approach for choosing the value of K is based on the sum of squared Euclidean distance (SSE) plot. When the number of clusters increases, the SSE decreases, thus this plot is a diminishing plot and may look similar to an arm. The K value is chosen from the point of the figure, which resembles an elbow. That point usually represents where we start to have a diminishing return of increasing K [19].

2) *Evaluating Clustering Results by Silhouette Global Index*: The results of K-means clustering can be validated using Silhouette Global Index (SGI), which is one of the most used internal tests [12]. In case of SGI, the silhouette value s_i of object i is defined as (3).

$$s_i = (b_i - a_i) / \max(a_i, b_i) \quad (3)$$

where b_i is the minimum mean distance from object i to objects belonging to other clusters, minimised over clusters; a_i is the mean distance between object i and the other objects of the same cluster j .

The silhouette values of the objects s_i are averaged to find the local silhouette coefficient S_j (4), which describes cluster j .

$$S_j = (1/n_j) \sum_{i=1}^{n_j} n_j s_i \quad (4)$$

where n_j is the number of objects in cluster j .

The Silhouette Coefficient SC is calculated by averaging the local silhouette coefficients S_j (5) [12], [17], [20].

$$SC = 1/K \sum_{j=1}^K S_j \quad (5)$$

[21] proposed the following interpretation of silhouette coefficient SC values:

- ≤ 0.25 : No substantial structure has been found.
- $0.26 \dots 0.50$: The structure is weak and could be artificial.
- $0.51 \dots 0.70$: A reasonable structure has been found.
- $0.71 \dots 1.0$: A strong structure has been found.

The same interpretation has previously been used for example by [12], [17], [18].

D. Assigning Non-Clustered Loads to Existing Clusters

The smallest loads which were not in the clustered dataset were assigned to the cluster with the closest centroid (centre). The centroids of the clusters were calculated during the clustering process. Next, the total squared Euclidean distance of each (previously not clustered) load from each centroid of a cluster was calculated. The cluster with the smallest sum was assigned to the load.

E. Selecting Representative Loads

In order to validate the clustering results with measurements, the largest loads of each cluster were identified. Next, the sum of squared Euclidean distances was calculated for these largest loads, and the loads with smallest SSE were chosen as the representative loads. The larger loads were chosen as representative loads, because aggregated load behaviour of larger number of customers is closer to statistical than the behaviour of smaller number of customers. This means that the stochastic load variations of larger aggregated loads tend to be proportionally smaller than those of the smaller loads. Also, the larger loads are expected to have a larger impact on the transmission system modelling results, thus the accuracy of those load models may have a larger impact on network simulations.

III. CASE STUDY & RESULTS

A. Input Data & Pre-Processing

The measurement data provided by the distribution system operator covered 33 months. For each aggregated load, the monthly energy consumption of each load class was given. This data was averaged month-wise to obtain 12 month long time series. The time series were normalised by monthly total energy consumption. This way the sum of load classes was 100% for each month. 92 aggregated loads with highest energy consumption were taken from the whole dataset (132 loads) for clustering. These 92 loads consume 96% of total energy consumption of the analysed DSO. Rest of the loads (40) were assigned to the cluster with the closest centroid.

B. K-means Clustering and Selection of K

The K-means clustering was implemented using squared Euclidean distances $d(x, z_i)$ (2) as the measure of distance. The sum of squared Euclidean distances was minimised (1) by using MATLAB to acquire the results. The clustering was conducted for $K = 2 \dots 40$. For each value of K , 100 replications were done and the best solution was chosen.

The sum of squared Euclidean distances decreases with the increase of K , the total number of clusters. This characteristic is illustrated by Fig. 3. According to the figure, the sum decreases at a rapid rate until $K = 5$. After that point the returns of increasing K decrease. Due to the smoothness of the graph, it is impossible to clearly distinguish the elbow point. However, it can be detected that after $K = 15$, the sum decreases more slowly, compared to the proceeding part of the graph. Thus, the optimal number of clusters K should be between 5 and 15.

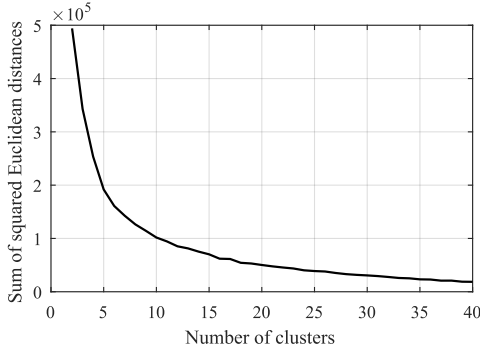


Fig. 3. Sum of squared Euclidean distance for different number of clusters

Next, the Silhouette Coefficient (SC) (5) was calculated. Fig. 4 displays the SC values for $K = 2...40$. According to the figure, increasing K over 15 has negligible impact on SC. This result matches the $K = 5...15$ range identified by analysing the sum of squared Euclidean distances. Taking into account both results, it is reasonable to choose a K value below 15.

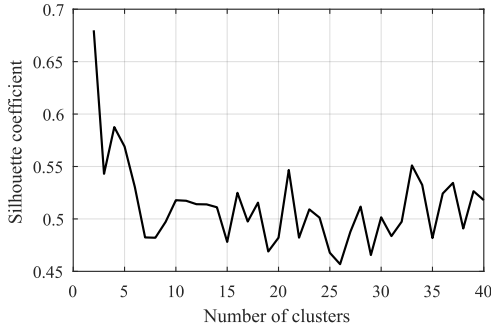


Fig. 4. Silhouette coefficient for different number of clusters K

Fig. 5 displays SC values for $K = 5...15$. The figure indicates that a reasonable structure ($SC = 0.51...0.70$) may have been found with 5, 6 and 10...14 clusters. Comparing the sum of squared Euclidean distances (Fig 3) at 5 and 10 clusters, it is clear that at 10 clusters the sum would be cut to nearly half. The difference between 10 and 14 clusters is significantly smaller, for this reason the number of clusters was chosen to be 10. At $K = 10$, $SC = 0.52$.

C. Clustering Results

When substations are clustered into 10 groups, it is possible to obtain silhouette values s_i (3) corresponding to Fig. 6. This result is satisfactory as all silhouette values are positive and several substation loads have high values.

However, once the smaller loads are assigned to existing clusters, the structure weakens. The value of SC drops from 0.52 to 0.42, which indicates a weak and possibly artificial structure. This weakening of cluster structure is also visible

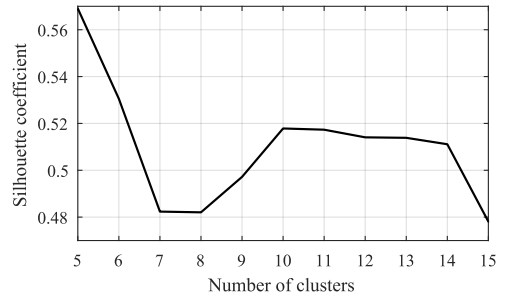


Fig. 5. Silhouette coefficient for 5...15 clusters

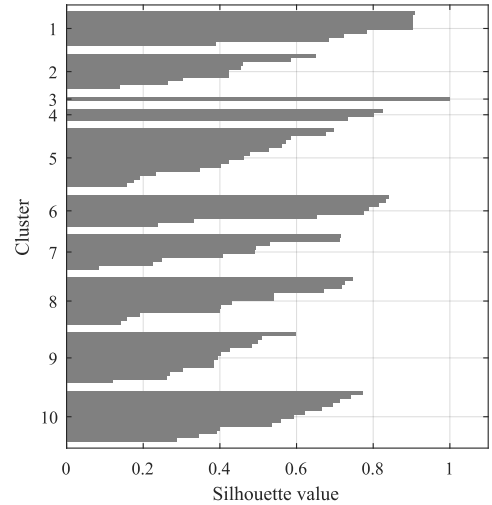


Fig. 6. Silhouette value of clustering results (92 largest loads).

in Fig. 7, where several loads have negative silhouette values. When all the 132 loads were clustered, instead of following the procedure with assigning smallest loads, the result was Fig. 8. The value of SC was 0.45 for that clustering, which is about 5% better result than the SC value after assigning smaller loads. Still, the SC is below 0.51, and the cluster structure is weak.

IV. CONCLUSION

This paper presented a procedure for grouping aggregated loads based on energy consumptions of load classes in Section II. In addition, the procedure involved identification of representative loads for each load cluster. The identified representative loads could be useful for selecting measurement locations or loads for analysis.

According to the Silhouette Global Index value, the clustering result of 92 largest loads had a reasonable structure. After assigning the smaller aggregated loads to the clusters with the

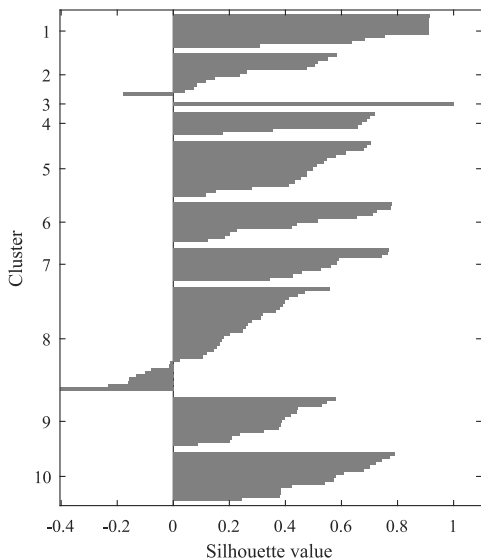


Fig. 7. Silhouette value after assigning smaller loads to closest cluster centres.

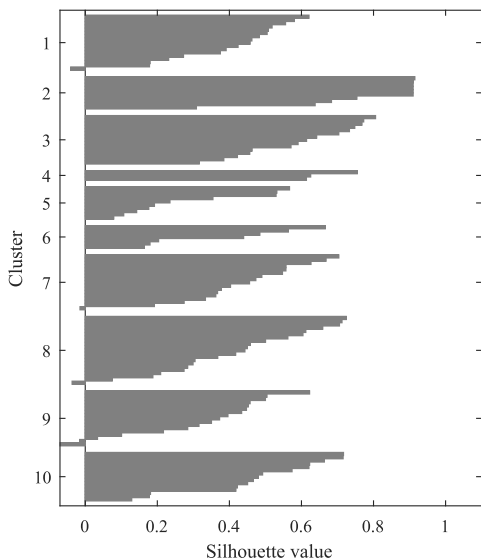


Fig. 8. Silhouette value when all 132 loads would be clustered instead of assigning smallest loads to closest centres.

closest centre, the Silhouette Coefficient decreased to 0.42, which indicates a weak and possibly artificial structure. When the clustering was done for all 132 loads, the best solution had a silhouette coefficient value of 0.45 (5% better than the result of assigning smallest loads). These results indicate that a better procedure could be the following: 1) data pre-processing as

described; 2) clustering of all loads; 3) filtering largest loads and calculating for each cluster the centre of largest loads (or even a weighted center, based on energy consumptions of loads); 4) choosing the representative loads as described in this paper. That way a better structure could be detected, and still the largest loads would have a higher impact on the selection of representative loads.

ACKNOWLEDGMENT

The authors would like to thank Elektrilevi OÜ, the Estonian DSO, and Elering, the Estonian TSO, for providing the load class composition data for the study.

REFERENCES

- [1] J. V. Milanovic, K. Yamashita, S. M. Villanueva, S. Z. Djokic, and L. M. Korunovic, "International industry practice on power system load modeling," *IEEE Transactions on Power Systems*, vol. 28, no. 3, pp. 3038–3046, Aug. 2013. DOI: 10.1109/TPWRS.2012.2231969
- [2] CIGRE Working Group C4.605: "Modelling and aggregation of loads in flexible power networks" (CIGRE, Feb. 2014)
- [3] S. A. Arefifar and W. Xu, "Online tracking of voltage-dependent load parameters using ULTC created disturbances," *IEEE Trans. Power Systems*, vol. 28, no. 1, pp. 130-139, Feb. 2013. DOI: 10.1109/tpwrs.2012.2199336
- [4] M. Leinakse, T. Sarnet, T. Kangro, and J. Kilter, "First results on load model estimation using digital fault recorder measurements," in *16th International Symposium "Topical Problems in the Field of Electrical and Power Engineering" and "Doctoral School of Energy and Geotechnology III"*, Pärnu, Estonia, 2017, pp. 101–105.
- [5] L. M. Korunovic, D. P. Stojanovic, and J. V. Milanovic, "Identification of static load characteristics based on measurements in medium-voltage distribution network," *IET Generation, Transmission & Distribution*, vol. 2, no. 2, pp. 227–234, March 2008. DOI: 10.1049/iet-gtd:20070091
- [6] M. Leinakse, P. Tani, and J. Kilter, "Impact of Distributed Generation on Estimation of Exponential Load Models," in *2019 IEEE Power & Energy Society General Meeting (PESGM)*, Atlanta, GA, USA, 2019, pp. 1-5. DOI: 10.1109/PESGM40551.2019.8974014
- [7] H. Guo, K. Rudion, H. Abildgaard, P. Komarnicki, and Z. A. Styczynski, "Parameter estimation of dynamic load model using field measurement data performed by OLTC operation," in *2012 IEEE Power and Energy Society General Meeting*, San Diego, CA, USA, 2012, pp. 1-7. DOI: 10.1109/pesgm.2012.6345563
- [8] M. Leinakse, H. Kiristaja, and J. Kilter, "Identification of intra-day variations of static load characteristics based on measurements in high voltage transmission network", in *2018 IEEE PES Innovative Smart Grid Technologies Conference Europe (ISGT-Europe)*, 2018. DOI: 10.1109/ISGTEurope.2018.8571712
- [9] K. N. Hasan, J. V. Milanović, P. Turner, and V. Turnham, "A step-by-step data processing guideline for load model development based on field measurements," in *2015 IEEE Eindhoven PowerTech*, Eindhoven, Netherlands, 2015, pp. 1-6. DOI: 10.1109/PTC.2015.7232307
- [10] M. Leinakse and J. Kilter, "Conversion error of second order polynomial ZIP to exponential load model conversion," in *Mediterranean Conference on Power Generation, Transmission, Distribution and Energy Conversion (MEDPOWER 2018)*, Dubrovnik, Croatia, 2018, pp. 1-5. DOI: 10.1049/cp.2018.1882
- [11] M. Leinakse and J. Kilter, "Exponential to ZIP and ZIP to Exponential Load Model Conversion: Methods and Error", *IET Generation, Transmission & Distribution*, to be published.
- [12] G. Grigoraş, F. Scarlatache, and G. Cârţină, "Load estimation for distribution systems using clustering techniques," in *13th International Conference on Optimization of Electrical and Electronic Equipment (OPTIM)*, Brasov, Romania, 2012, pp. 301-306. DOI: 10.1109/OPTIM.2012.6231789
- [13] J. E. Parra, F. L. Quilumba, and H. N. Arcos, "Customers' demand clustering analysis — A case study using smart meter data," in *2016 IEEE PES Transmission & Distribution Conference and Exposition-Latin America (PES T&D-LA)*, Morelia, Mexico, 2016, pp. 1–7. DOI: 10.1109/TDC-LA.2016.7805685

- [14] S. P. Lloyd, "Least Squares Quantization in PCM," *IEEE Transactions on Information Theory*, vol. 28, pp. 129–137, 1982. DOI: 10.1109/TIT.1982.1056489
- [15] M. Grabner, Z. Bregar, Š. Ivanjko, and L. Valenčič, "Improved model for the spatial load forecasting of the Slovenian distribution network," *CIREN - Open Access Proceedings Journal*, vol. 2017, no. 1, pp. 2354–2357, 10 2017. DOI: 10.1049/oap-cired.2017.1020
- [16] M. Grabner, A. Souvent, B. Blažič, and A. Košir, "Statistical Load Time Series Analysis for the Demand Side Management," in *2018 IEEE PES Innovative Smart Grid Technologies Conference Europe (ISGT-Europe)*, Sarajevo, Bosnia and Herzegovina, 2018, pp. 1–6. DOI: 10.1109/ISGTEurope.2018.8571845
- [17] S. Mishra, M. Leinakse, and I. Palu, "Wind power variation identification using ramping behavior analysis," *Energy Procedia*, vol. 141, pp. 565–571, 2017. DOI: 10.1016/j.egypro.2017.11.075
- [18] S. Mishra, M. Leinakse, I. Palu, and J. Kilter, "Ramping Behaviour Analysis of Wind Farms," in *2018 IEEE International Conference on Environment and Electrical Engineering and 2018 IEEE Industrial and Commercial Power Systems Europe (EEEIC / I&CPS Europe)*, Palermo, Italy, 2018, pp. 1–5. DOI: 10.1109/EEEIC.2018.8493720
- [19] R. Gove, "Using the elbow method to determine the optimal number of clusters for k-means clustering," Dec. 26, 2017. [Online]. Available: <https://bl.ocks.org/rpgove/0060ff3b656618e9136b> [Accessed: Feb. 9, 2020].
- [20] P. J. Rousseeuw, "Silhouettes: a Graphical Aid to the Interpretation and Validation of Cluster Analysis," *Journal of Computational Applied Mathematics*, vol. 20, pp. 53–65, 1987. DOI: 10.1016/0377-0427(87)90125-7
- [21] L. Kaufman and P.J. Rousseeuw, *Finding Groups in Data: An Introduction to Cluster Analysis*. Hoboken, NJ: John Wiley & Sons, Inc., 1990. DOI: 10.1002/9780470316801

Publication VI

M. Leinakse and J. Kilter, "Exponential to ZIP and ZIP to exponential load model conversion: Methods and error," *IET Generation, Transmission & Distribution*, vol. 15, no. 2, pp. 177–193, 2021, doi: 10.1049/gtd2.12002

Exponential to ZIP and ZIP to exponential load model conversion: Methods and error

Madis Leinakse  | Jako Kilter 

Department of Electrical Power Engineering and Mechatronics, Tallinn University of Technology, Tallinn, Estonia

Correspondence

Madis Leinakse, Department of Electrical Power Engineering and Mechatronics, Tallinn University of Technology, Ehitajate tee 5, 19086 Tallinn, Estonia.
Email: madis.leinakse@taltech.ee

Funding information

Tallinn City Council

Abstract

This paper presents several methods for performing two types of static load model conversion: exponential to ZIP & ZIP to exponential model conversion. In general, these conversions are inaccurate due to non-equivalence of exponential and ZIP (second-order polynomial) models. A numerical analysis is conducted using generated datasets of load models to analyse the error and to compare the accuracy of the presented methods. The results of the analysis indicate that the optimal selection of conversion method depends on a number of factors, including normalisation of load models, ZIP model type (accurate or constrained) and expected use of the converted model. In addition, a case study is conducted to analyse the impact of conversion error on load flow results. The results of the case study indicate that a significant difference in load flow results can occur when the load models are converted. Recommendations for conversion method selection are given in the discussion section of the paper.

1 | INTRODUCTION

In the context of this paper, (static) load models are considered to be equations describing static voltage characteristics of the loads. An overview of existing load models is given in [1] and [2]. According to survey results presented in [3] and [4], the most common static load models are constant power, constant current and constant impedance model, which are followed by exponential and polynomial (i.e. ZIP) load model. In real-world applications, exponential and (second-order) polynomial load model are commonly used [5], and are standard models used for dynamic studies in established stability programs (e.g. PSS/E, PSLE, TSAT and ETMSP packages) [6]. Similarity of PSS/E and PSCAD load models to exponential and polynomial load model is discussed in [7, 8], where [9] and [10] are used as main references. In addition to usage in load modelling, exponential and ZIP model are used for assessing the potential of conservation voltage reduction (CVR) [11–14].

The parallel use of exponential and ZIP model causes in some cases the need for load model conversion [3, 8, 15, 16]. Firstly, load model conversion may be required when an existing power system model is used for constructing the system

model for another software, and the load models of the software packages differ [8]. For conducting some power system model conversions, commercial tools are available (e.g. PSS®E-PSCAD Network Data Conversion Module, E-TRAN Runtime Library for PSCAD). Secondly, the exponential to ZIP model conversion can be used for simplifying the load model aggregation stage in component-based load modelling.

The ZIP models of load components can be accurately aggregated by calculating weighted sum of ZIP models as is done in [17–19]. When the known models of some load components are in exponential form, these models need to be converted to ZIP models to calculate the aggregated load model (using weighted sum). Thirdly, the conversion of ZIP models to exponential models is useful for comparing load models [3, 16], and plotting load model changes in time [19, 21]. In case of load model comparison and plotting, the exponential model is preferred due to smaller number of parameters: the exponential voltage characteristic is described by one parameter, while ZIP model has three parameters, in addition to common initial/nominal power and voltage parameters.

The load model conversion methods are rarely described and the conversion error is commonly neglected [8]. Still, an

This is an open access article under the terms of the [Creative Commons Attribution License](https://creativecommons.org/licenses/by/4.0/), which permits use, distribution and reproduction in any medium, provided the original work is properly cited.

© 2020 The Authors. *IET Generation, Transmission & Distribution* published by John Wiley & Sons Ltd on behalf of The Institution of Engineering and Technology

analytical method for exponential to ZIP model conversion is described in [22] and is analysed in [8]. Analytical solution of the method is presented in Section 3.3.1 and is denoted as ‘Analytical method AM1’. A second method for conducting the same conversion is presented and analysed in [8]. The method is described in Section 3.3.2 and is denoted as ‘Analytical method AM2’. In addition, a new formulation of method AM2 is presented for converting exponential models to constrained ZIP models. In case of constrained ZIP model, the parameter values are limited to range 0...1. In Section 3.3.3, an equivalent equation system for ‘Analytical method AM3’ [8] is presented and some derivation errors present in [8] are corrected. In [16] methods for second-order polynomial (i.e. ZIP) to exponential load model conversion are described and analysed. The analytical method described in [16], and in Section 3.2, is used for conversion from ZIP model to exponential model in [3, 16, 19]. The descriptions of optimisation-based methods presented in [8, 16] are generalised in Section 3.1 for handling different load model approximation situations. The optimisation-based conversion is used to provide a benchmark for evaluating the performance of other methods. The conversion methods for both conversion directions are presented to give a comprehensive overview of this load model conversion pair.

In case of load model conversion, the main aim is to minimise the conversion error to approximate the original load characteristic as well as possible. It is assumed that the input model is accurate. The conversion between exponential and ZIP load model is, in the general case, not accurate. Exceptions are load models with constant impedance, constant current and constant power, which have equivalent exponential and ZIP models. Numerical analysis is used for analysing the conversion error that occurs when presented conversion methods are used. It is shown that the load model conversion error depends on the input load model parameter values, used method, chosen voltage and the voltage sensitivity of the characteristic. When the converted load model is used in a power system model, the conversion error leads to a shift in power flow results. This shift can lead to inaccurate power system analysis results, which may lead to wrong decisions. The impact of conversion error on power flow results is illustrated by a case study.

The paper is divided into eight sections. The introduction is followed by Section 2, where exponential and ZIP load model are described. In addition, in Subsection 2.2, measures of conversion error are defined. In Section 3, methods for conversion are presented. The load model conversion error of the presented methods is analysed in two sections: Section 4 and Section 5. The results are divided between the sections based on conversion direction: Section 4 deals with ZIP to exponential conversion and Section 5 with exponential to ZIP conversion. The impact of load model conversion on load flow results is analysed in Section 6. Finally, the main results of the study are discussed and summarised in Section 7 and Section 8.

2 | LOAD MODELS AND CONVERSION ERROR

2.1 | Exponential and ZIP load model

In case of second-order polynomial (i.e. ZIP) and exponential load model, the models can be defined using the nominal value of voltage and power [8, 16, 20, 23] or initial values [1, 21, 23, 24]. The load models are generalised by using base voltage v_b , base active power P_b and base reactive power Q_b .

2.1.1 | Second-order polynomial (ZIP) load model

The second-order polynomial load model, also known as a ZIP model, can be described by (1) subject to (2). Reactive load is represented by similar equations (3) and (4).

$$P_{ZIP} = P_b \cdot \left[K_Z \cdot (v/v_b)^2 + K_I \cdot (v/v_b) + K_P \right], \quad (1)$$

$$K_Z + K_I + K_P = 1, \quad (2)$$

$$Q_{ZIP} = Q_b \cdot \left[K_{Z,Q} \cdot (v/v_b)^2 + K_{I,Q} \cdot (v/v_b) + K_{Q,Q} \right], \quad (3)$$

$$K_{Z,Q} + K_{I,Q} + K_{Q,Q} = 1, \quad (4)$$

where P_b and Q_b are active and reactive load, respectively, at base voltage v_b . Voltage v is the load bus voltage in SI units. K_Z, K_I, K_P and $K_{Z,Q}, K_{I,Q}, K_{Q,Q}$ are parameters describing the voltage dependence of the active and reactive loads, respectively.

The values of ZIP model parameters (K_Z, K_I and K_P) may in some cases be limited to range 0...1, and such a ZIP model is called a ‘constrained ZIP model’ [4, 16]. Without these constraints the model is considered to be an ‘accurate ZIP model’ [4, 16].

2.1.2 | Exponential load model

The exponential load model can be described by (5), reactive load is represented by a similar Equation (6).

$$P_{EXP} = P_b \cdot (v/v_b)^{K_{EXP}}, \quad (5)$$

$$Q_{EXP} = Q_b \cdot (v/v_b)^{K_{EXP,Q}}, \quad (6)$$

where P_b and Q_b are active and reactive load, respectively, at base voltage v_b . Voltage v is the load bus voltage in SI units. K_{EXP} and $K_{EXP,Q}$ are exponential parameters describing the voltage dependence of the active and reactive loads, respectively.

2.2 | Measures of conversion error

In Section 2.1.1 it is shown that the ZIP model of active power voltage characteristic P_{ZIP} (1) is mathematically similar to reactive load characteristic Q_{ZIP} (3). Next, it is shown in Section 2.1.2 that the exponential model P_{EXP} (5) and Q_{EXP} (6) are similar. Due to mathematical similarity of active and reactive load model, following equations are only given for active load, but also apply for reactive load models.

In case of load model conversion, the input voltage characteristic P_{IN} is assumed to be accurate and estimated model P_{OUT} inaccurate. Depending on conversion direction and converted model, P_{IN} and P_{OUT} may stand for P_{ZIP} (1), Q_{ZIP} (3), P_{EXP} (5) or Q_{EXP} (6).

The difference ε_i (7) between the accurate voltage-power characteristic P_{IN} and converted characteristic P_{OUT} at voltage $V_i = v_i/v_b$ is considered to be conversion error at voltage V_i .

$$\varepsilon_i = P_{IN}(V_i) - P_{OUT}(V_i). \quad (7)$$

The relative conversion error at voltage V_i is defined as η_i (8).

$$\eta_i = \frac{P_{IN}(V_i) - P_{OUT}(V_i)}{P_{IN}(V_i)}. \quad (8)$$

The values of ε_i and η_i are used for analysing the direction of the conversion error. In analysis steps, where the accuracy difference of methods is more important than the error direction, the absolute values of ε_i and η_i are used.

To quantify the conversion error across voltage range $V_i \in \{V_1 \dots V_N\}$ ($i, N \in \mathbb{N}$) the mean absolute error (MAE) (9) and normalised mean absolute error (NMAE) (10) are used. MAE describes the mean magnitude of conversion error ε_i (7) and NMAE the mean magnitude of relative conversion error η_i (8).

$$MAE = \frac{1}{N} \sum_{i=1}^N |P_{IN}(V_i) - P_{OUT}(V_i)|, \quad (9)$$

$$NMAE = \frac{1}{N} \sum_{i=1}^N \left| \frac{P_{IN}(V_i) - P_{OUT}(V_i)}{P_{IN}(V_i)} \right|. \quad (10)$$

Voltage range 0.8...1.2 p.u. is used for MAE and NMAE calculation range $V_1 \dots V_N$, similarly to [7, 8, 16], for result comparability. This range corresponds to voltages where exponential PSCAD load models behave as exponential model and the PSS/E ZIP load model behaves as a ZIP model (assuming the value of PSS/E setting parameter PQBRAK to have value 0.8 p.u. or lower) [7, 8].

3 | METHODS FOR LOAD MODEL CONVERSION

This paper focuses on the load model conversion from generic ZIP load model to generic exponential load model. The input load models are assumed to be accurate. The goal of the conversion is to approximate the input load model by another model as accurately as possible. In case of analytical methods presented in Section 3.2 and Section 3.3, the same base values should be used for input and output model to achieve best accuracy. Conversion of models with base value mismatch is discussed in Section 3.1. The specifics of PSS/E and PSCAD load models that have to be taken into account when converting the models of these software packages are discussed in [7, 8]. In the following sections of the paper, equations are given only for the active load component. The reactive component of the load has mathematically similar equations.

In Section 3, the following load model conversion methods are described:

- Non-linear least squares–based error minimisation methods ‘NLS abs’ (12) and ‘NLS rel’ (13) are presented in Section 3.1. These methods are flexible, can handle both conversion directions and different application needs.
- Analytical method for ZIP to exponential model conversion is presented in Section 3.2.
- Three analytical methods for exponential to ZIP model conversion are presented in Section 3.3:
 - (1) Analytical method ‘AM1’ in Section 3.3.1
 - (2) Analytical method ‘AM2’ in Section 3.3.2
 - (3) Analytical method ‘AM3’ in Section 3.3.3

This notation of methods corresponds to names used in [8, 16] for easier comparison of results.

3.1 | Using non-linear least squares optimisation for load model conversion

The aim of load model conversion is to minimise the mismatch between the input and output models. This goal can be written as a non-linear least squares optimisation problem, which is a common approach for approximation of static load characteristics from measurement data. In case of non-linear least squares, the square of error is minimised (11).

$$\min \sum_{i=1}^N [\psi_i]^2. \quad (11)$$

If the conversion error ψ_i in (11) is represented by absolute conversion error ε_i (7), the model conversion problem can be formulated by (12). In following sections of the paper, the

minimisation of squared absolute error is denoted by NLS abs.

$$\min \sum_{i=1}^N [P_{IN}(V_i) - P_{OUT}(V_i)]^2, \quad (12)$$

where V_i is normalised voltage v/v_b .

If instead of conversion error ε_i , the relative conversion error η_i (8) is used as ψ_i in (11), the objective function (13) is obtained. In the following sections of this paper, the non-linear least squares optimisation of relative error is denoted by NLS rel.

$$\min \sum_{i=1}^N \left[\frac{P_{IN}(V_i) - P_{OUT}(V_i)}{P_{IN}(V_i)} \right]^2. \quad (13)$$

In the case of exponential to ZIP model conversion, the optimisation problem is subject to $K_Z + K_I + K_P = 1$ (2) or $K_{Z,Q} + K_{I,Q} + K_{Q} = 1$ (4), depending if active or reactive load characteristics are converted. To obtain parameter values for a constrained ZIP model, the non-linear least squares method is subject to bounds $0 \leq K_Z \leq 1$, $0 \leq K_I \leq 1$ and $0 \leq K_P \leq 1$ or in case of reactive load model $0 \leq K_{Z,Q} \leq 1$, $0 \leq K_{I,Q} \leq 1$ and $0 \leq K_Q \leq 1$.

If the base power and voltage of input model and output model differ, it can be taken into account by using different value of P_b and v_b in the equation of P_{IN} and P_{OUT} in (12) and (13). When P_{ZIP} and P_{EXP} use the same voltage and power normalisation bases, P_b and v_b , the optimisation problem (12) can be simplified to Equation (14).

$$\min \sum_{i=1}^N [(K_Z \cdot (V_i)^2 + K_I \cdot (V_i) + K_P) - (V_i)^{K_{Exp}}]^2. \quad (14)$$

3.2 | Analytical method for ZIP to exponential model conversion

ZIP models are converted in [3, 4, 19] to exponential models by Equation (15). In Section 2.1.1 and Section 2.1.2 it is shown that the active power voltage characteristics P_{EXP} (5) and P_{ZIP} (1) are mathematically similar to reactive load characteristics Q_{EXP} (6) and Q_{ZIP} (3), respectively. Due to mathematical similarity of active and reactive load model, (15) also applies for reactive load models.

$$K_{Exp} \approx \frac{2 \cdot K_Z + 1 \cdot K_I + 0 \cdot K_P}{K_Z + K_I + K_P}. \quad (15)$$

3.3 | Analytical methods for exponential to ZIP model conversion

The exponential load models can be converted to ZIP models by several analytical methods, described in Section 3.3.1, Section 3.3.2 and Section 3.3.3, or by previously described non-linear least squares optimisation, described in Section 3.1. First

two analytical methods, AM1 (Section 3.3.1) and AM2 (Section 3.3.2) are suitable for exponential to constrained ZIP model conversion. Analytical method AM2 (Section 3.3.2) and AM3 (Section 3.3.3) are also suitable for exponential to accurate ZIP model conversion.

3.3.1 | Analytical method AM1

Analytical method AM1 is presented in [22] by a set of rules and equations, which are reformulated in [8]. The suitable equation or set of parameter values is chosen based on the value of the exponent K_{Exp} . For exponent $K_{Exp} \leq 0.5$, a constant power model is used (16). A constant current model is used when $K_{Exp} < 1.0$ (17). In exponent K_{Exp} value range $1 \dots 2$, the values of ZIP model parameters are calculated using (18) [8], which is the analytical solution of the equation system presented in [22]. A constant admittance model is used if the value of exponent K_{Exp} is larger than 2 (19).

$$K_{Exp} < 0.5 \rightarrow \begin{cases} K_Z = 0 \\ K_I = 0 \\ K_P = 1 \end{cases} \quad (16)$$

$$0.5 \leq K_{Exp} \leq 1.0 \rightarrow \begin{cases} K_Z = 0 \\ K_I = 1 \\ K_P = 0 \end{cases} \quad (17)$$

$$1.0 < K_{Exp} < 2.0 \rightarrow \begin{cases} K_Z = K_{Exp} - 1 \\ K_I = 2 - K_{Exp} \\ K_P = 0 \end{cases} \quad (18)$$

$$K_{Exp} \geq 2.0 \rightarrow \begin{cases} K_Z = 1 \\ K_I = 0 \\ K_P = 0 \end{cases} \quad (19)$$

3.3.2 | Analytical method AM2

An improved version of conversion method AM1, described in Section 3.3.1, is proposed in [8] and denoted as analytical method AM2. AM2 is based on AM1. Equations (16) and (17) are replaced by a more accurate Equation (20). Equation (19) is replaced by (21), extending the K_{Exp} range of (18).

In case of $K_{Exp} = 0$ and $1.0 \leq K_{Exp} \leq 2.0$, the conversion results of method AM1 and method AM2 are equivalent [8].

$$K_{Exp} \leq 1 \rightarrow \begin{cases} K_Z = 0 \\ K_I = K_{Exp} \\ K_P = 1 - K_{Exp} \end{cases} \quad (20)$$

$$K_{Exp} > 1 \rightarrow \begin{cases} K_Z = K_{Exp} - 1 \\ K_I = 2 - K_{Exp} \\ K_P = 0 \end{cases} \quad (21)$$

The values of ZIP model parameters K_Z , K_I and K_P can be limited to the range $0 \dots 1$ for converting exponential models to constrained ZIP model by implementing the following changes to the equation system described by (20) and (21):

- (1) For negative values of K_{Exp} ($K_{Exp} < 0$), (22) should be used instead of (20) to avoid negative values of K_I and $K_P > 1$. Thus, (20) should be limited to $0 \leq K_{Exp} \leq 1$, deriving (23).
- (2) Equation (21) should be limited to $1 < K_{Exp} < 2$, deriving (24), because $K_{Exp} \geq 2$ would otherwise lead to $K_Z > 1$. When $K_{Exp} \geq 2$, (25) should be used.

These modifications would lead to a similar method to analytical method AM1 in case $K_{Exp} < 0$ or $K_{Exp} \geq 1$. Thus, in case of constrained ZIP model, the improvements of method AM2 would only have an effect when $0 \leq K_{Exp} < 1$.

$$K_{Exp} \leq 0 \rightarrow \begin{cases} K_Z = 0 \\ K_I = 0 \\ K_P = 1 \end{cases} \quad (22)$$

$$0 \leq K_{Exp} \leq 1 \rightarrow \begin{cases} K_Z = 0 \\ K_I = K_{Exp} \\ K_P = 1 - K_{Exp} \end{cases} \quad (23)$$

$$1 < K_{Exp} < 2 \rightarrow \begin{cases} K_Z = K_{Exp} - 1 \\ K_I = 2 - K_{Exp} \\ K_P = 0 \end{cases} \quad (24)$$

$$K_{Exp} \geq 2.0 \rightarrow \begin{cases} K_Z = 1 \\ K_I = 0 \\ K_P = 0 \end{cases} \quad (25)$$

3.3.3 | Analytical method AM3

The exponential (5) and polynomial (1) load models are equivalent at base voltage v_b , because if $v/v_b = 1$, then $P = P_b$. At intersections of the load characteristics, the load equations have equivalent values $P_{ZIP} = P_{Exp}$:

$$P_b \cdot \left[K_Z \cdot \left(\frac{v}{v_b} \right)^2 + K_I \cdot \left(\frac{v}{v_b} \right) + K_P \right] = P_b \cdot \left(\frac{v}{v_b} \right)^{K_{Exp}}, \quad (26)$$

$$K_Z \cdot V^2 + K_I \cdot V + K_P = V^{K_{Exp}}. \quad (27)$$

Replacing K_P in (27) with $1 - K_Z - K_I$ and simplifying the equations leads to derivation of (28).

$$K_Z \cdot (V + 1) + K_I = \frac{V^{K_{Exp}} - 1}{V - 1}. \quad (28)$$

Equation (28) includes two unknowns: K_Z and K_I and has $0 \dots \infty$ solutions. To limit the number of solutions to $0 \dots 1$, it is assumed that two additional intersections of ZIP and exponential characteristics exist at voltages $V_1 = v_1/v_b$ and $V_2 = v_2/v_b$. This assumption is supported by the conversion error analysis results presented in [8]. Using the assumption, (29) is derived.

$$\begin{cases} K_Z \cdot (V_1 + 1) + K_I = \frac{(V_1)^{K_{Exp}} - 1}{V_1 - 1} \\ K_Z \cdot (V_2 + 1) + K_I = \frac{(V_2)^{K_{Exp}} - 1}{V_2 - 1} \end{cases}, \quad (29)$$

where V_1 and V_2 are in p.u., normalised with base voltage v_b .

The solution of equation system (29) is (30) [8]. The value of K_P can be calculated from values of K_Z and K_I using Equation (31).

$$\begin{bmatrix} K_Z \\ K_I \end{bmatrix} = \frac{1}{V_1 - V_2} \cdot \begin{bmatrix} 1 & -1 \\ -V_2 - 1 & V_1 + 1 \end{bmatrix} \begin{bmatrix} \frac{V_1^{K_{Exp}} - 1}{V_1 - 1} \\ \frac{V_2^{K_{Exp}} - 1}{V_2 - 1} \end{bmatrix}, \quad (30)$$

$$K_P = 1 - K_Z - K_I. \quad (31)$$

Equations (30) and (31) can be written as an equation system (32).

$$\begin{cases} K_Z = \frac{1}{V_1 - V_2} \cdot \left[\frac{V_1^{K_{Exp}} - 1}{V_1 - 1} - \frac{V_2^{K_{Exp}} - 1}{V_2 - 1} \right] \\ K_I = \frac{1}{V_1 - V_2} \cdot \left[(-V_2 - 1) \cdot \frac{V_1^{K_{Exp}} - 1}{V_1 - 1} \right. \\ \quad \left. + (V_1 + 1) \cdot \frac{V_2^{K_{Exp}} - 1}{V_2 - 1} \right] \\ K_P = 1 - K_Z - K_I \end{cases} \quad (32)$$

4 | RESULTS (1/2): ZIP TO EXPONENTIAL MODEL CONVERSION

This results section complements the results presented in [16], where the absolute error of conversion ε_i and MAE are analysed. In this section, the focus is on relative conversion error η_i and NMAE.

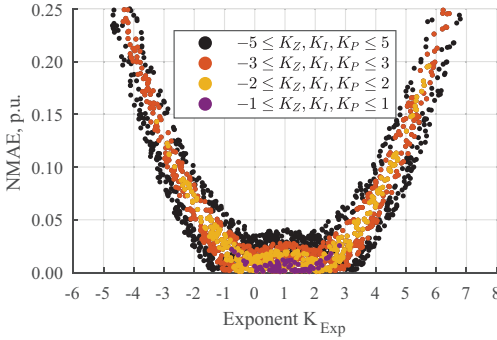


FIGURE 1 Impact of ZIP model parameter constraints on the normalised mean absolute error (NMAE) of conversion. Load model converted using method NLS rel. Plotted subsets filtered based on ZIP load model parameter ranges $-1\dots1$, $-2\dots2$, $-3\dots3$ and $-5\dots5$

4.1 | (ZIP to Exp) input models and notation of methods

A new smaller set of ZIP models (around 16,000) was generated to test repeatability of results presented in [16], where 30,000 models are used. Firstly, two vectors with 100,000 values $-25\dots25$ were generated. The random values are generated with uniform distribution. Next, the third ZIP model parameter was calculated by subtracting the two generated vectors from a vector of ones to fulfil ZIP model property (2). ZIP models with extremely high voltage sensitivity ($abs(K_{Exp}) > 8$) were detected based on exponential load model calculated by analytical method presented in Section 3.2 and removed from the input model dataset. During plotting, the set is further decreased to increase the readability of the figures.

ZIP to exponential load model conversion is conducted using three different methods:

- (1) Analytical: analytical method described in Section 3.2 by (15).
- (2) NLS abs: conversion method based on minimisation of squared absolute error described in Section 3.1 by (12).
- (3) NLS rel: conversion method based on minimisation of squared relative error described in Section 3.1 by (13).

4.2 | (ZIP to Exp) impact of zip model parameter values on conversion error

Figure 2 describes the impact of ZIP model (input load model) parameter values K_Z, K_I, K_P on the NMAE (10) of conversion. ZIP models with NLS rel determined exponent K_{Exp} values $-5 \leq K_{Exp} \leq 5$ are shown. NLS rel determined exponent K_{Exp} values $-3 \leq K_{Exp} \leq 3$ and constrained ZIP models are indicated with different colours.

The highest conversion error (maximum value in Figure 2) occurs if ZIP load model parameter K_Z has a large negative value while K_I has a large positive value. In such cases, based on

the $\Delta NMAE$ subfigures, the NLS rel method is able to decrease the NMAE value by less than 10%, compared to the analytical method. The figure also indicates the gain to be proportional to absolute values of ZIP load model parameter K_Z, K_I, K_P values, higher $\Delta NMAE$ occurs at higher absolute values of K_Z, K_I and K_P .

In Figure 2, the conversion error of constrained ZIP models with $0 \leq K_Z, K_I, K_P \leq 1$, which corresponds to $0 \leq K_{Exp} \leq 2$, is negligibly small compared to the errors of models with more relaxed constraints. For example, $-3 \leq K_{Exp} \leq 3$ or $-5 \leq K_{Exp} \leq 5$. Figure 1 illustrates the dependence between NMAE, exponent K_{Exp} and constraints of ZIP model parameters K_Z, K_I and K_P . The model conversion is conducted using NLS rel method. Based on Figure 1, the larger the ZIP model parameter value limits, the larger the variability of NMAE of conversion and the larger the maximum values of NMAE.

4.3 | (ZIP to Exp) estimated exponential model and conversion error

The exponent K_{Exp} values obtained by the use of analytical, NLS rel and NLS abs method differ significantly, as shown by Figure 3 and Figure 4. The smallest difference occurs in Figure 3 when $K_{Exp} \approx -0.5$ and in Figure 4 when $K_{Exp} \approx 0$. In [8] the K_{Exp} of analytical and NLS abs method is shown to have highest similarity when $K_{Exp} \approx 0.5$. The three different values of K_{Exp} and non-linearity of the figures indicate conversion result dependence on conversion method.

Figure 5 displays the NMAE (10) of ZIP to exponential model conversion. NMAE values of ZIP models with analytical K_{Exp} values $-5 \leq K_{Exp} \leq 5$ are shown. According to Figure 5, the conversion error displays a significant variation for all K_{Exp} values. Thus, it is not possible to assign a specific NMAE value for each calculated K_{Exp} value. However, it is possible to notice that the lowest maximum values of NMAE occur in K_{Exp} range $-2\dots3$. In Figure 6, NMAE is plotted for NLS rel converted models with $K_{Exp} -5 \leq K_{Exp} \leq 5$. In Figure 6 the NMAE values are significantly smaller than in Figure 5. Still, the NMAE values can be high (0.3 p.u.) even when the models have K_{Exp} values near 0. The input models with high NMAE were previously found to have large negative K_Z values and large positive values of K_I . Figure 2 illustrates the relation between ZIP model parameter values and NMAE values.

The NMAE value difference of analytical and NLS rel method $\Delta NMAE$ (33) is plotted in Figure 7. ZIP models with NLS rel determined K_{Exp} values $-5 \leq K_{Exp} \leq 5$ are shown, similarly to Figure 6. In Figure 7, a positive value of $\Delta NMAE$ would indicate that the NMAE value of analytical method is larger than NLS rel and the NLS rel method is more accurate based on this measure of accuracy. The $\Delta NMAE$ values in Figure 7 are small, thus in case of these models, $-5 \leq K_{Exp} \leq 5$, the usage of NLS rel method does not significantly increase the conversion accuracy compared to the analytical method.

$$\Delta NMAE = NMAE_{Analytical} - NMAE_{NLSrel}. \quad (33)$$

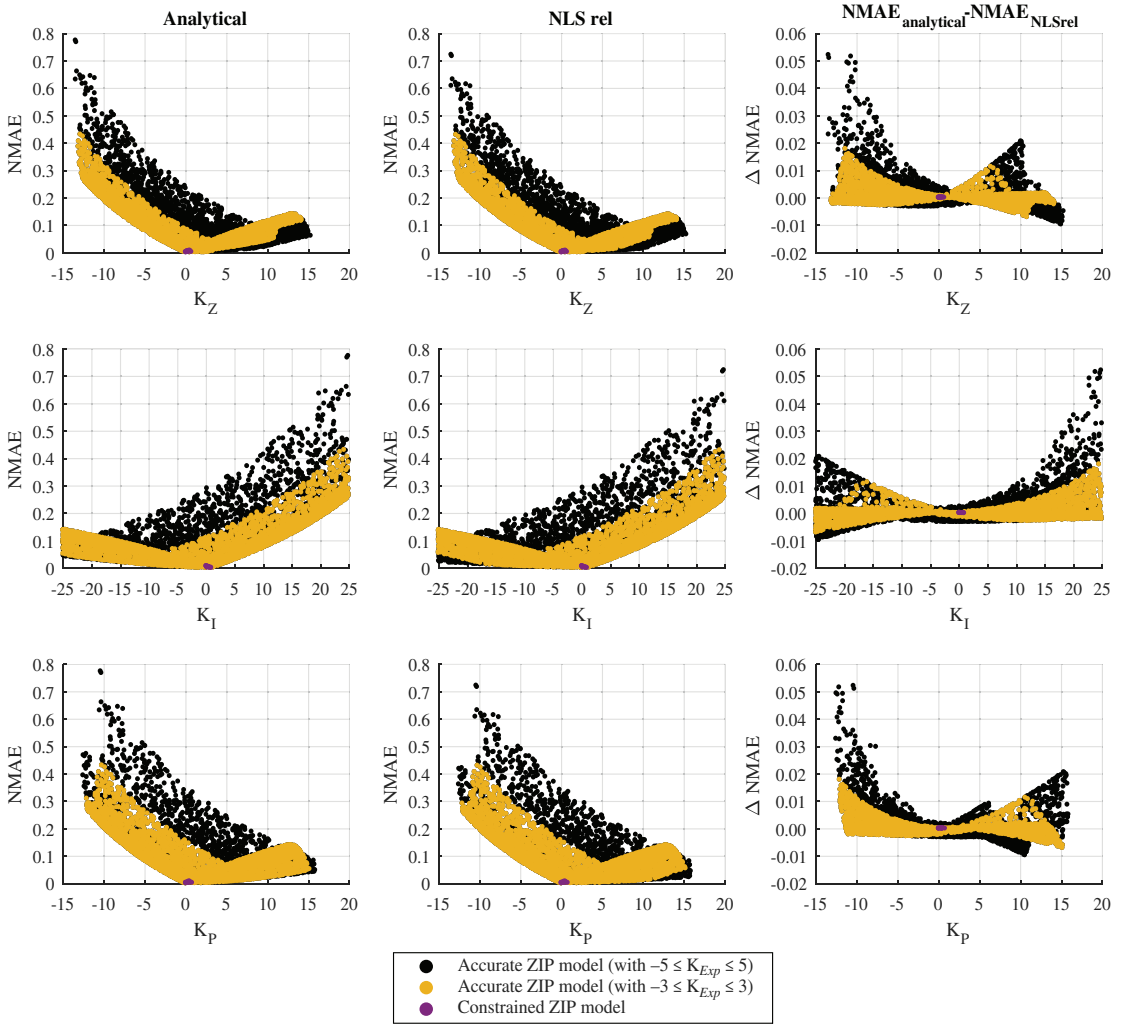


FIGURE 2 Normalised mean absolute error (NMAE) dependence on ZIP model parameters K_Z , K_I and K_p

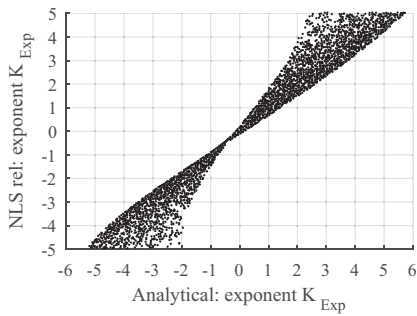


FIGURE 3 Calculated exponent K_{Exp} values of analytical and NLS rel method

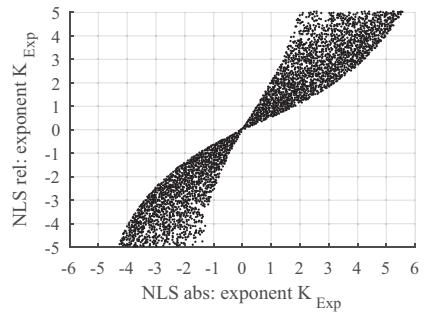


FIGURE 4 Calculated exponent K_{Exp} values of NLS abs and NLS rel method

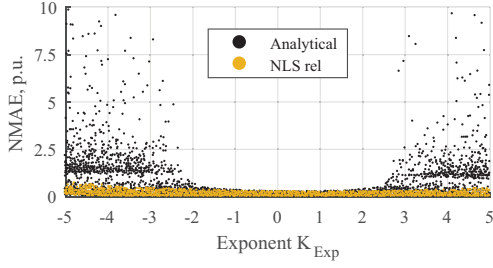


FIGURE 5 Relation between the calculated model exponent value K_{Exp} and the normalised mean absolute error (NMAE) of the load characteristic

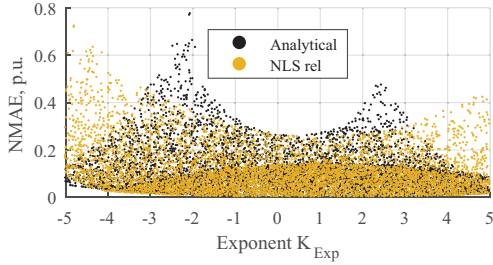


FIGURE 6 Relation between the calculated model exponent value K_{Exp} and the normalised mean absolute error (NMAE) of the load characteristic. Filtered based on NLS rel estimated $-5 \leq K_{Exp} \leq 5$

4.4 | (ZIP to Exp) voltage dependence of conversion error

The relative load model conversion error η_i (8) depends on voltage. The voltage dependence of conversion error of the analytical method is shown in Figure 8, and NLS rel in Figure 9. ZIP models with NLS rel determined K_{Exp} values $-5 \leq K_{Exp} \leq 5$ are shown. According to Figures 8 and 9, the conversion error of both analysed methods, NLS rel and analytical, is lowest near nominal voltage. This is an expected result, as near nominal volt-

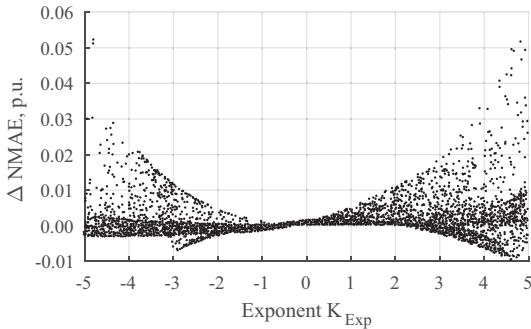


FIGURE 7 Relation between the exponent value K_{Exp} of NLS rel method and mean absolute error decrease $\Delta NMAE$ compared to the analytical method

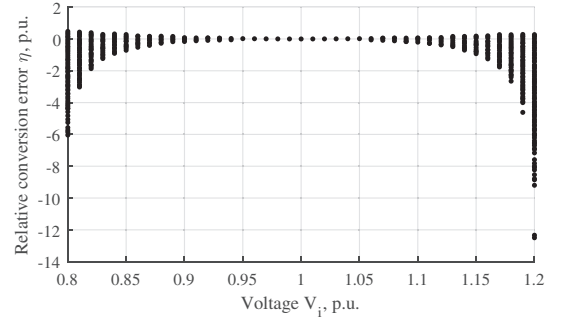


FIGURE 8 Voltage dependence of relative error of analytical conversion method

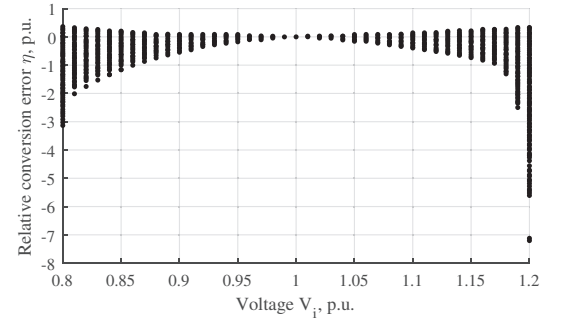


FIGURE 9 Voltage dependence of relative error of NLS rel conversion method

age, the load is close to nominal as well, independent of load model parameter values. Both methods display largest relative conversion errors η at higher voltages. To analyse the difference between Figure 8 and Figure 9, $\Delta\eta_i$ is plotted in Figure 10. $\Delta\eta_i$ is the difference between the relative conversion error of analytical and NLS rel conversion methods, defined by (34). The absolute values of relative conversion error are used to detect which conversion result is closer to the accurate voltage-power

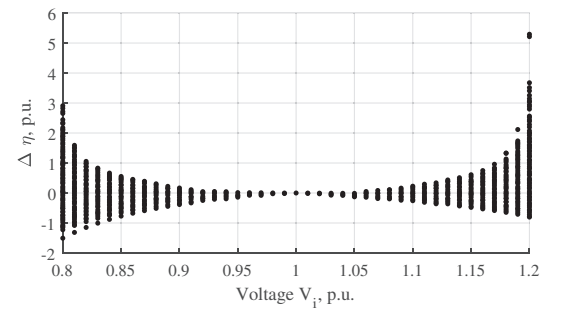


FIGURE 10 Relation between voltage V_i and conversion error decrease $\Delta\eta_i$ when NLS rel is used instead of analytical method

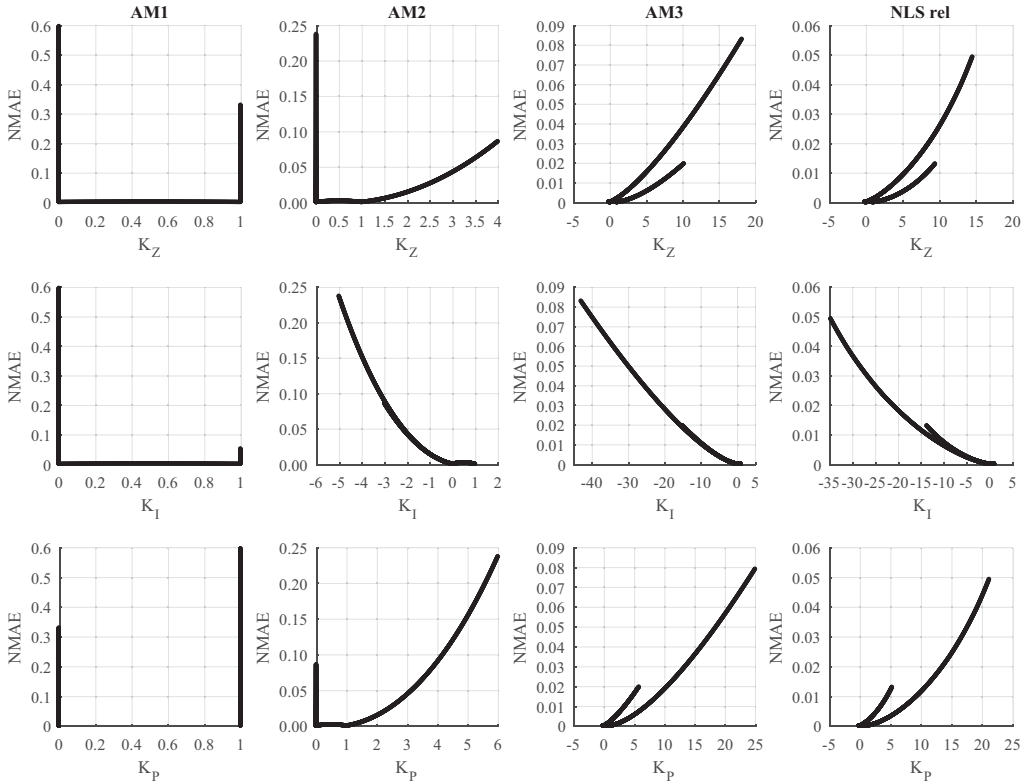


FIGURE 11 Normalised mean absolute error (NMAE) dependence on ZIP model parameters K_Z , K_I and K_P and conversion method

characteristic at voltage V_i .

$$\Delta\eta_i = |\eta_{i,Analytical}| - |\eta_{i,NL_Abs}|. \quad (34)$$

Figure 10 indicates that the gains of using one method instead of the other can provide significant accuracy gains. However, neither method displays constantly lower absolute value of η .

5 | RESULTS (2/2): EXPONENTIAL TO ZIP MODEL CONVERSION

In this section, the relative conversion error η_i (8) and NMAE (10) of exponential to ZIP load model conversion are analysed. These error measures are chosen for comparability to previous Section 4.

5.1 | (Exp to ZIP) input models and notation of methods

The set of exponential load models for load model conversion error analysis was calculated using 0.005 step size and value

range $-5 \dots 5$. This led to a dataset of 2001 exponent values with even distribution.

Exponential load models are converted to ZIP load models by using five different methods:

- (1) AM1: analytical method described in Section 3.3.1
- (2) AM2: analytical method described in Section 3.3.2
- (3) AM3: analytical method described in Section 3.3.3
- (4) NLS abs: optimisation of squared conversion error described by (12) in Section 3.1
- (5) NLS rel: optimisation of squared relative error described by (13) in Section 3.1

5.2 | (Exp to ZIP) impact of exponential model parameter values on conversion error

The NMAE (10) was calculated for each converted load model using the same voltage range as was used for model conversion, from 0.8 to 1.2 p.u. In total, 2001 NMAE values were obtained for each conversion method. The results were plotted in Figure 12. According to the figure, the normalised mean conversion error (NMAE) of positive K_{Exp} value is smaller

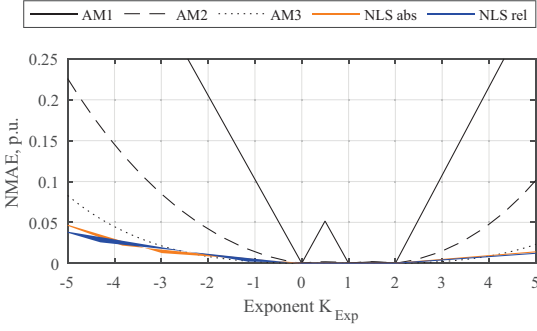


FIGURE 12 Impact of input load model exponent value K_{Exp} on the mean absolute value of relative error of conversion. [[8], redrawn with new dataset]

than the error of negative K_{Exp} value with equivalent absolute value. The model conversion error is approximately symmetrical for $K_{Exp} = 1$, except for analytical method AM1 in range $K_{Exp} = (0 \dots 1)$. AM1 has a local peak at $K_{Exp} = 0.5$, at the boundary of (16) and (17).

At $K_{Exp} = 1$, conversion is error-less for all methods, because the exponential model is equivalent to the constant current component of the ZIP model. Similar error-less conversion takes place for $K_{Exp} = 0$ and $K_{Exp} = 2$.

Figure 12 clearly indicates that analytical method AM1 has the worst performance and other methods should be used instead. Analytical methods AM2 and AM3 display comparable NMAE values to NLS abs and NLS rel method when $0 \leq K_{Exp} \leq 2$. Outside that K_{Exp} range, the analytical method AM3 and non-linear least squares methods (NLS abs and NLS rel) display significantly lower conversion error than analytical methods AM1 and AM2.

5.3 | (Exp to ZIP) estimated zip model and conversion error

Figure 11 describes the NMAE (10) dependence of estimated ZIP model parameter values K_Z, K_I, K_P . According to Figure 11, the NMAE values of analytical method AM1 are highest when K_Z, K_I or K_P are equal to 0 or 1. Based on the figure, analytical method AM2 parameters are limited to $K_Z \geq 0, K_P \geq 0, K_I \leq 1$, which is in accordance with (20), (21) and (22). The K_Z, K_I and K_P NMAE characteristics are similar for analytical method AM3 and non-linear least squares relative error minimisation method NLS rel. The highest conversion error (maximum value in Figure 11) occurs if ZIP load model parameter K_Z and K_P have a large positive value while K_I has a large negative value.

5.4 | (Exp to ZIP) voltage dependence of conversion error

The exponential load models are converted to ZIP models using voltage range from 0.8 to 1.2 p.u. with 0.01 p.u. voltage step.

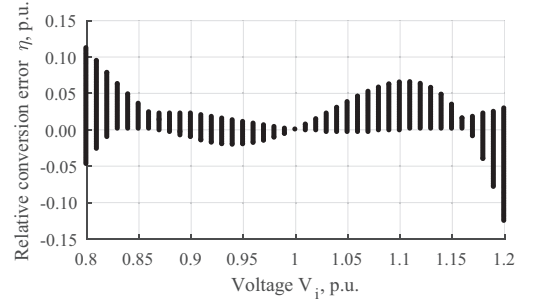


FIGURE 13 Voltage dependence of relative error of NLS rel method

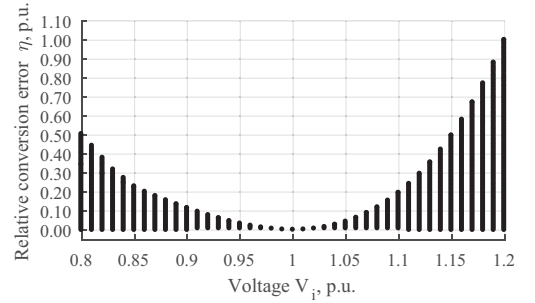


FIGURE 14 Voltage dependence of relative error of analytical method AM2

Relative conversion error (8) is calculated for NLS rel, analytical method AM2 and analytical conversion method AM3. The voltage dependence of the methods is plotted in Figures 13, 14 and 16, respectively.

The voltage dependence of relative conversion error of NLS rel method shown in Figure 13 indicates the existence of three intersection points of exponential and ZIP characteristics: first in voltage range 0.83...0.90 p.u., second at nominal voltage and third in voltage range 1.12...1.18 p.u. The intersection points are indicated by zero value of η_i . Such intersections are also observed in [8] and were used for deriving analytical method AM3. The intersections occur within the optimisation region, between voltages 0.8 and 1.2 p.u., near the boundary values 0.8 p.u. and 1.2 p.u.

According to Figure 14 the relative error of analytical method AM2 is unidirectional and smallest near base voltage. The positive sign of relative conversion error (8), indicates that the ZIP characteristic calculated by AM2 typically underestimates the load compared to the exponential input characteristic.

The relative conversion error difference of analytical and NLS rel method $\Delta\eta_i$ (35) is plotted in Figure 15 and indicates that NLS rel method has lower relative error across the whole voltage range than analytical method AM2. The accuracy gain offered by the NLS rel method is significant, in the same range

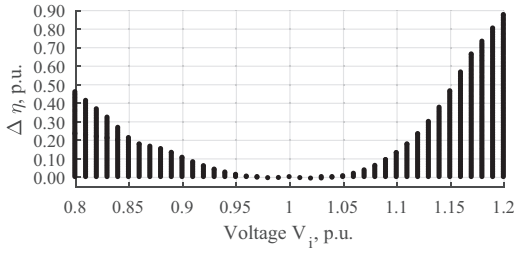


FIGURE 15 Relation between voltage V_i and conversion error decrease $\Delta\eta_i$ when NLS rel is used instead of analytical method AM2

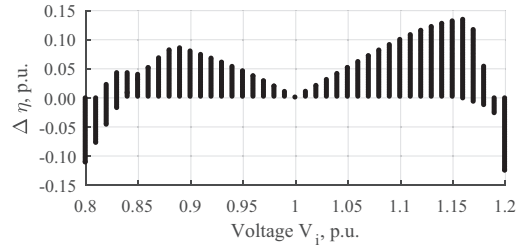


FIGURE 17 Relation between voltage V_i and conversion error decrease $\Delta\eta_i$ when NLS rel is used instead of analytical method AM3

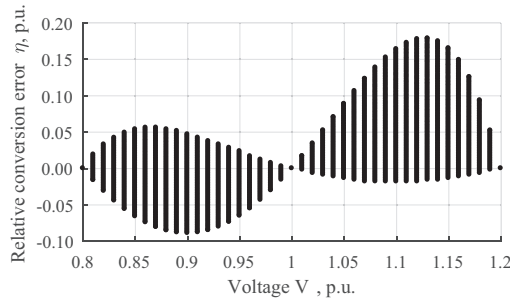


FIGURE 16 Voltage dependence of relative error of analytical method AM3

as whole error of method AM2.

$$\Delta\eta_i = |\eta_{i,Analytical}| - |\eta_{i,NL_Sab}|. \quad (35)$$

The voltage dependence of relative error of analytical method AM3 shown in Figure 16 indicates the existence of three intersection points of exponential and ZIP characteristic: first at 0.80 p.u., second at nominal voltage and third in voltage range 1.20 p.u. The intersection points are indicated by zero value of η_i . Using the range boundary values 0.8 p.u. and 1.2 p.u. as V_1 and V_2 in (30), the lowest relative conversion error will occur at the voltage boundaries. The intersection points of exponential and ZIP characteristic were used for deriving analytical method AM3, thus the existence of these intersections corresponds to the expectations.

The relative error difference of analytical and NLS rel method $\Delta\eta_i$ (35) is plotted in Figure 17. The figure indicates, usage of NLS rel instead of analytical method AM3 could provide a relative error decrease in voltage range 0.83...1.16 p.u. and increase outside that range.

6 | CASE STUDY

In previous sections of the paper it is shown that the conversion between exponential and ZIP load models involves an error: load model conversion error. The load model conversion error

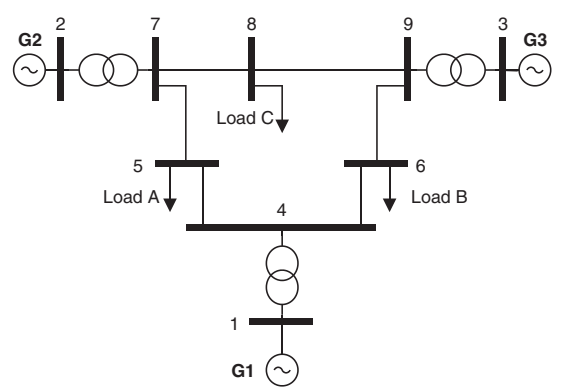


FIGURE 18 Nine-bus power system

describes the mismatch between the original and the converted voltage characteristic. In order to analyse the impact of conversion error on load flow results, a case study of a small power system is conducted. DigSILENT PowerFactory is used for conducting the load flow calculations of the nine-bus power system [25] shown in Figure 18.

DigSILENT PowerFactory is used for conducting the calculations due to the included load model *General Load* [26], which can accurately represent the ZIP model (Section 2.1.1) and the exponential model (Section 2.1.2). The mathematical model of *General Load* corresponds to (36). The model of the reactive load is similar. When *General Load* is used as a ZIP model, exponents e_a , e_b and e_c are assigned values 0, 1 and 2. This way the polynomial equation (36) becomes a second-order polynomial, similar to the ZIP models (1) and (3). However, when *General Load* is used as an exponential load model, the value of two coefficients (among a , b and c) are set to 0, and the value of the third is set to 1. The exponent corresponding to the coefficient with value 1 is used as the exponent of the exponential model.

$$\begin{cases} P_{GL} = P_o \cdot \left[a \cdot \left(\frac{v}{v_o} \right)^{e_a} + b \cdot \left(\frac{v}{v_o} \right)^{e_b} + c \cdot \left(\frac{v}{v_o} \right)^{e_c} \right] \\ a + b + c = 1 \end{cases} \quad (36)$$

TABLE 1 Nine-bus system generator setpoints in original model, and after increasing generator bus voltages (after modification)

Gen.	Bus	Original nine-bus model			After modification		
		P (MW)	Q (Mvar)	V (p.u.)	P (MW)	Q (Mvar)	V (p.u.)
G1	1	71.60	26.78	1.040	71.06	12.32	1.090
G2	2	163.00	6.70	1.025	163.00	1.00	1.088
G3	3	85.00	-10.90	1.025	85.00	-15.00	1.089

TABLE 2 Nine-bus system loads

Load	Bus	P (MW)	Q (Mvar)
A	5	125.00	50.00
B	6	90.00	30.00
C	8	100.00	35.00

where P_o is active power of the load at voltage v_o , both defined as *Operating Point* values in DIGSILENT PowerFactory; a , b and c are coefficients of the polynomial equation; e_a , e_b and e_c are exponents of the polynomial equation.

The nine-bus power system (Figure 18) includes three generators (Table 1), which are connected to the 1st, 2nd and 3rd bus. The 1st bus, where generator G1 is connected, is modelled as a slack bus. Generators G2 and G3 are modelled as PQ buses. Previously, the voltage dependence of conversion error was illustrated by Figures 8, 9, 13 and 14. According to the figures, the load model conversion error tends to increase with voltage. To increase the impact of conversion error, the voltage of the power system was increased by modifying generator bus settings. In the original model generator G1 is operated at 1.04 p.u. voltage [25, 27]. To increase the impact of load model conversion error in the study, the voltage of generator G1 was increased to 1.09 p.u. In addition, the reactive power references of generator G2 and generator G3 were increased compared to the original model to achieve similar voltages on all the generator buses (when loads are modelled by constant power). The same generator settings were used for all simulations.

The nine-bus power system (Figure 18) includes three loads (Table 2), which are located at the 5th bus (Load A), 6th bus (Load B) and 8th bus (Load C). In the original nine-bus system, the loads are modelled by constant power model.

In this study, the constant power model is replaced by exponential or ZIP models depending on the analysis scenario. The selected 'accurate' exponential and ZIP models are given in Table 3. The exponential models of the table are used in the base case for analysing the impact of exponential to ZIP model conversions. Next, the exponential models are converted to ZIP models with different conversion methods, and power flow calculations are conducted with the ZIP models, obtained by converting selected exponential models to ZIP models. The selected ZIP models (Table 3) are used when calculating power flow for analysing the impact of ZIP to exponential conversion error. Again, the ZIP models are converted to exponen-

TABLE 3 Selected exponential and ZIP load models

Load	Exponential				ZIP			
	K_P	K_Q	$K_{Z,P}$	$K_{I,P}$	K_P	$K_{Z,Q}$	$K_{I,Q}$	K_Q
A	1.33	2.47	5.68	-9.89	5.21	-5.77	9.86	-3.09
B	0.67	1.35	-4.70	9.49	-3.79	-11.39	24.48	-12.09
C	-1.35	-2.47	-4.18	9.98	-4.80	-5.66	8.93	-2.27

TABLE 4 NMAE when chosen exponential models are converted to ZIP models

Load	AM1		AM2		AM3		NLS rel	
	P	Q	P	Q	P	Q	P	Q
A	0.16%	4.88%	0.16%	0.51%	0.01%	0.06%	0.01%	0.03%
B	3.39%	0.16%	0.16%	0.16%	0.01%	0.01%	0.01%	0.01%
C	13.82%	25.36%	2.22%	6.03%	0.36%	1.34%	0.20%	0.71%

tial models with different methods to illustrate the impact of method selection.

For exponential to ZIP model conversions, the exponential models are chosen based on the results of an international survey [3]. The mean load model of the international survey is used for Load A and the maximum values of load model parameters for Load B. Load C is assigned negative voltage sensitivities, which are chosen to match the two largest exponent values of Load A and Load B.

The ZIP models for ZIP to exponential model conversion are selected with realistic voltage sensitivities (values comparable to load models presented in [17]) and high conversion errors. The active load models with corresponding voltage sensitivity 0...2, and reactive models with voltage sensitivity -3...3 are analysed. Most of the chosen ZIP models have a high $K_{I,P}$ and $K_{I,Q}$ value. Active load model of Load A is chosen with a negative $K_{I,P}$ value, and reactive load model of Load B with high $K_{I,Q}$ value. The rest of the ZIP load models are chosen with $K_{I,P}$ and $K_{I,Q}$ close to 10 from the previously generated set of ZIP load models.

6.1 | Results of case study: Exponential to ZIP model conversion

The chosen 'accurate' exponential load models (Table 3, columns 2 & 3) were converted to ZIP models by four different methods: AM1, AM2, AM3 and NLS rel. The same voltage range (0.8 to 1.2 p.u.) is used for the conversion and error calculation as in previous sections of the paper for clarity. The conversion error would depend on the selected conversion method, as shown in Table 4. The least accurate results would be obtained by AM1 and the most accurate by NLS rel. The models converted by these two methods were chosen for simulations to illustrate the impact of conversion method.

TABLE 5 Selected exponential load models and ZIP models acquired by model conversion (using methods AM1 and NLS rel)

Conversion method	Load	ZIP model of P			ZIP model of Q		
		$K_{Z,P}$	$K_{I,P}$	K_P	$K_{Z,Q}$	$K_{I,Q}$	K_Q
AM1	A	0.33	0.67	0.00	1.00	0.00	0.00
	B	0.00	1.00	0.00	0.35	0.65	0.00
	C	0.00	0.00	1.00	0.00	0.00	1.00
NLS rel	A	0.22	0.89	-0.11	1.81	-1.14	0.33
	B	-0.11	0.89	0.22	0.24	0.87	-0.11
	C	1.62	-4.63	4.01	4.37	-11.37	7.99

The ZIP models acquired by exponential to ZIP model conversion are shown in Table 5. The table clearly illustrates the limited conversion capability of method AM1: it converts exponential models to constrained ZIP models, thus causing large conversion errors for models with negative exponents (models of Load C, indicated by high NMAE values in Table 4). Method NLS rel uses unconstrained ZIP model, which enables it to approximate the exponential load model by ZIP models with lower NMAE.

The use of least accurate conversion method AM1 (Table 6, upper section) leads to three to four times higher relative voltage magnitude error compared to the results of NLS rel (Table 6, lower section). In case of both simulations with the ZIP models, the error is highest for Bus 8, where Load C is connected. This is in accordance with the previous analysis results of conversion error.

The load modelling errors caused by load model conversion (Table 6) do not match with the NMAE values (Table 4). The NMAE describes the mean absolute value of relative conversion error, which is voltage dependant. The load bus voltage of the load flow results differs. Table 7 shows how the relative conversion error is affected by the voltage used in calculations. The relative conversion errors are calculated at three different voltages for each load model:

TABLE 7 Relative conversion error η of AM1 and NLS rel converted models at different voltages. Voltages based on: V_{Exp} – load flow with exponential models; V_{AM1} – load flow with ZIP models from AM1; V_{NLSrel} – load flow with ZIP models from NLS rel; V_{LF} – load flow corresponding to model

Load	P/Q	AM1 load model			NLS rel load model		
		V_{Exp}	V_{AM1}	V_{LF}	V_{Exp}	V_{NLSrel}	V_{LF}
A	P	0.03%	0.02%	-0.99%	0.00%	0.00%	0.05%
	Q	-2.43%	-2.08%	-3.90%	0.03%	0.03%	0.12%
B	P	2.34%	2.04%	1.45%	-0.10%	-0.10%	-0.07%
	Q	0.06%	0.04%	-1.13%	0.09%	0.09%	0.16%
C	P	12.07%	9.11%	12.07%	-0.27%	-0.27%	-0.41%
	Q	23.19%	17.29%	23.19%	-1.06%	-1.07%	-1.31%

- (1) V_{Exp} – voltages based on load flow with exponential models
- (2) V_{AM1} – voltages based on load flow with ZIP models from AM1
- (3) V_{NLSrel} – voltages based on load flow with ZIP models from NLS rel
- (4) V_{LF} – accurate load calculated based on the load flow with exponential models, converted load calculated based on load flow with AM1 or NLS rel converted load models.

The conversion error in column V_{LF} (Table 7) matches well the load modelling error shown in Table 6. The small differences are caused by numerical inaccuracies of calculation. The conversion errors calculated based on single load flow results (V_{Exp} , V_{AM1} and V_{NLSrel}) differ from the V_{LF} , but in this case study have a similar scale. For example, V_{Exp} , V_{AM1} and V_{NLSrel} around 20% corresponds to a load modelling error around 20%. These results suggest that the calculated load model conversion error at load flow voltages could indicate the scale of the impact. If the values are small, the impact of the conversion error of load flow results is low.

TABLE 6 Relative error η of simulation with ZIP models acquired by using conversion methods AM1 and NLS rel

Conv. meth.	Bus	Voltage magn.	Voltage angle	P gen.	Q gen.	P load	Q load
AM1	1	–	–	14.35%	50.57%	–	–
	2	-1.68%	-6.70%	0.00%	0.00%	–	–
	3	-1.61%	-15.89%	0.00%	0.00%	–	–
	5	-0.76%	13.46%	–	–	-0.99%	-3.90%
	6	-0.87%	16.67%	–	–	1.44%	-1.12%
	8	-1.97%	-100.00%	–	–	12.07%	23.20%
NLS rel	1	–	–	-0.30%	-2.62%	–	–
	2	0.09%	0.00%	0.00%	0.00%	–	–
	3	0.00%	0.23%	0.00%	0.00%	–	–
	5	0.04%	-0.26%	–	–	0.05%	0.14%
	6	0.04%	-0.58%	–	–	0.03%	0.06%
	8	0.10%	2.97%	–	–	-0.37%	-1.16%

TABLE 8 NMAE when chosen ZIP models converted to exponential models using analytical method (AM) and NLS rel

Load	AM		NLS rel	
	P	Q	P	Q
A	6.82%	14.82%	6.72%	14.99%
B	7.43%	30.94%	7.38%	29.16%
C	8.07%	20.28%	7.87%	20.56%

TABLE 9 Converted exponential models from AM and NLS rel

Load	AM		NLS rel	
	K_P	K_Q	K_P	K_Q
A	1.48	-1.69	1.25	-1.99
B	0.09	1.69	0.15	2.94
C	1.61	-2.39	1.91	-3.00

6.2 | Results of case study: ZIP to exponential model conversion

The chosen ‘accurate’ ZIP load models (Table 3, columns 4 to 9) were converted to exponential models by two different methods: analytical and NLS rel. The same voltage range (0.8 to 1.2 p.u.) is used for the conversion and error calculation as in previous sections of the paper for clarity. The NMAE difference of the two methods is negligible in Table 8.

However, when the converted models (Table 9) are compared, significant differences may be observed. All converted models differ, largest difference is over 1, smallest 0.06.

The simulation with chosen ZIP load models is used as an accurate result for error calculation. Both conversion methods lead to a similar voltage magnitude error (Table 10) $-3.5 \dots -2.2\%$. Considering the similar conversion error results shown in Table 8, this is an expected result. The voltage angle error of most buses is significantly lower with NLS rel method (compared to AM).

The load modelling errors caused by load model conversion (Table 10) do not match with the NMAE values (Table 8). The NMAE describes the mean absolute value of relative conversion error, which is voltage dependant. The load bus voltage of the load flow results differs. Table 11 shows how the relative conversion error is affected by the voltage used in calculations. The relative conversion errors are calculated at three different voltages for each load model:

- (1) V_{ZIP} – voltages based on load flow with ZIP models
- (2) V_{AM} – voltages based on load flow with exponential models from analytical method
- (3) V_{NLSrel} – voltages based on load flow with exponential models from NLS rel
- (4) V_{LF} – accurate load calculated based on the load flow with ZIP models, converted load calculated based on load flow with analytical or NLS rel converted load models.

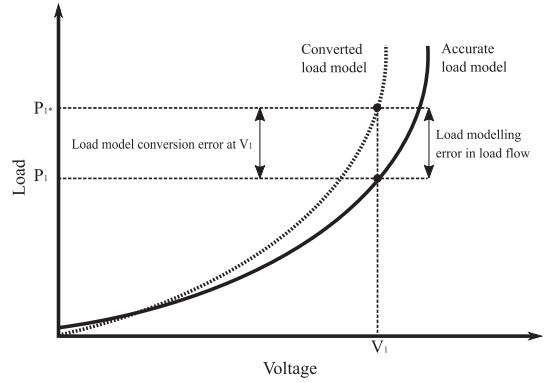


FIGURE 19 Conversion error and load modelling error in load flow results when the load bus voltage is not affected by the load model replacement. With accurate load model the load operates at voltage V_1 and consumes P_1 . With converted load model the load operates at voltage V_1 and consumes P_{1*}

The conversion error in column V_{LF} (Table 11) matches well the load modelling error shown in Table 10. The small differences are caused by numerical inaccuracies of calculation. The conversion errors calculated based on single load flow results (V_{Exp} , V_{AM} and V_{NLSrel}) differ from the V_{LF} , but in this case study have a similar scale. For example, V_{Exp} , V_{AM} and V_{NLSrel} around 20% corresponds to a load modelling error around 20%. These results suggest that the calculated load model conversion error at load flow voltages could indicate the scale of the impact. If the values are small, the impact of the conversion error of load flow results is low.

7 | DISCUSSION

7.1 | Conversion error and load modelling error in load flow

In Section 6 load flow calculations are conducted with chosen load models and converted load models. The acquired load flow results differ, and the calculated conversion error describes the observed changes of load flow results only partially. In this subsection, the relation between conversion error and load flow error is discussed.

When replacing the load models in the system model has only negligible effect on the load bus voltages, the load modelling error in load flow corresponds to the load model conversion error. This situation is illustrated by Figure 19, where the load bus voltage is assumed to be V_1 in both load flows (with chosen and converted load model), and depending on the load model, the load flow converges at load P_1 or P_{1*} . As the load is operating at the same voltage in both load flow results, the load modelling error matches the load model conversion error (calculated at V_1).

In the conducted case study, the replacing of load models caused a change in calculated load bus voltages. This situation is

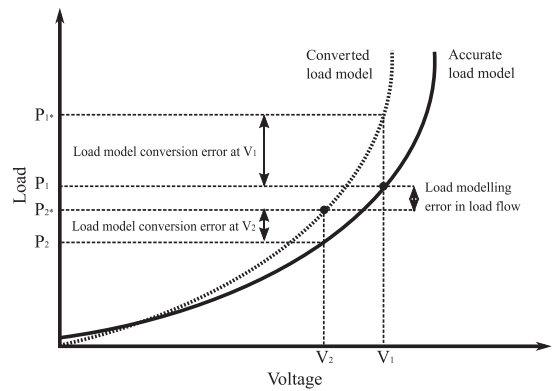
TABLE 10 Relative error η of simulation with exponential models acquired by using analytical conversion (AM) and method NLS rel

Conv. meth.	Bus	Voltage magn.	Voltage angle	P gen.	Q gen.	P load	Q load
AM	1	–	–	–3.72%	–105.02%	–	–
	2	–3.20%	19.51%	0.00%	0.00%	–	–
	3	–3.19%	40.34%	0.00%	0.00%	–	–
	5	–2.23%	–6.49%	–	–	–7.39%	13.90%
	6	–2.23%	1.53%	–	–	5.60%	9.21%
	8	–3.51%	–12.00%	–	–	2.05%	45.21%
NLS rel	1	–	–	–2.06%	–108.23%	–	–
	2	–3.12%	13.97%	0.00%	0.00%	–	–
	3	–3.19%	21.01%	0.00%	0.00%	–	–
	5	–2.16%	–5.44%	–	–	–8.81%	11.31%
	6	–2.45%	3.94%	–	–	6.08%	20.03%
	8	–3.47%	0.40%	–	–	5.15%	36.68%

TABLE 11 Relative conversion error η of AM and NLS rel converted models at different voltages. Voltages based on: V_{ZIP} – load flow with chosen ZIP models; V_{AM} – load flow with exponential models from AM; V_{NLSrel} – load flow with exponential models from NLSrel; V_{LF} – load flow corresponding to model

Load	P/Q	AM load model			NLS rel load model		
		V_{ZIP}	V_{AM}	V_{LF}	V_{ZIP}	V_{NLSrel}	V_{LF}
A	P	–4.27%	–2.53%	–7.41%	–6.29%	–4.16%	–8.81%
	Q	9.63%	5.03%	13.89%	6.60%	2.92%	11.33%
B	P	5.77%	3.36%	5.56%	6.46%	3.68%	6.07%
	Q	13.47%	7.94%	9.22%	29.20%	18.63%	20.10%
C	P	8.14%	4.26%	2.07%	12.48%	7.36%	5.13%
	Q	33.30%	13.68%	45.21%	23.03%	7.32%	36.78%

illustrated by Figure 20. Using the accurate load model, the load operates at voltage V_1 and consumes P_1 . When the accurate load characteristic (black line) is converted to dashed characteristic, the load flow converges at load bus voltage V_2 . The load consumes P_{2*} based on the converted load model and bus voltage. This means that the operation point of the load has shifted due to load model conversion from $P_1 V_1$ to $P_{2*} V_2$. The conversion error is defined as the difference of two characteristics at a specific voltage. This means that the difference between P_1 and P_{1*} corresponds to load model conversion error at V_1 . Similarly, the difference between P_2 and P_{2*} corresponds to conversion error at V_2 . Both of these values differ from load modelling error, which is the difference between P_1 and P_{2*} . The load modelling error can only be caused by load model conversion if conversion error exists, thus the conversion error affects the load modelling error in load flow. The voltage change caused by the model replacement is dependent on the network model. In the case study, the load model conversion error at voltage V_1 and V_2 has a similar scale as the load modelling error in load flow. It is possible that in realistic power system models, the load models replacement has a limited effect on the bus voltages, and

**FIGURE 20** Conversion error and load modelling error in load flow when change of load characteristics causes bus voltage to change. Conversion error and load modelling error in load flow results when the load bus voltage is affected by the load model replacement. With accurate load model the load operates at voltage V_1 and consumes P_1 . With converted load model the load operates at voltage V_2 and consumes P_{2*}

the result applies in most cases. In future research, this hypothesis could be tested by simulating additional network models. Another possible direction for future research is sensitivity analysis: the sensitivity of load flow results to load conversion error could be analysed.

7.2 | Recommendations for choosing load model conversion method

7.2.1 | ZIP model to exponential model conversion

Three methods were presented for converting ZIP models to exponential models:

- (1) Analytical: analytical method described in Section 3.2
- (2) NLS abs: conversion method based on minimisation of total squared absolute error described in Section 3.1
- (3) NLS rel: conversion method based on minimisation of total squared relative error described in Section 3.1

When ZIP models with expected exponential model $-3 \leq K_{Exp} \leq 3$ are converted, the NMAE of NLS rel and analytical method are similar and the analytical method may be a better choice due to simplicity. This conclusion is supported by the case study results, where the converted load models are in range $-3 \leq K_{Exp} \leq 3$. In the case study, the voltage magnitude errors of load flow calculations are similar for both conversion methods. However, the voltage angle errors and load modelling error of the case study are contradicting: analytical method has mostly lower load modelling error, while NLS rel has lower voltage angle error. The use of NLS rel and NLS abs is reasonable when models with extreme voltage characteristics are converted or additional flexibility is needed. For example, for handling model base value mismatch on non-symmetrical voltage range of conversion. The choice between NLS rel and NLS abs should be done based on selected measure of error: NLS rel is better at minimising relative conversion error and NLS abs more suitable for minimising non-normalised conversion error.

7.2.2 | Exponential model to ZIP model conversion

Five methods were presented for converting exponential models to ZIP models:

- (1) AM1: analytical method described in Section 3.3.1, suitable for converting exponential models to constrained ZIP models, use of method not recommended
- (2) AM2: proposed method described in Section 3.3.2, suitable for converting exponential models to accurate and constrained ZIP models
- (3) AM3: proposed method described in Section 3.3.3, suitable for converting exponential models to accurate ZIP models
- (4) NLS abs: optimisation of squared conversion error described in Section 3.1
- (5) NLS rel: optimisation of squared relative error described in Section 3.1

The accuracy and flexibility of non-linear least squares optimisation, described in Section 3.1, methods NLS abs and NLS rel, are the highest. When models with extreme voltage characteristics are converted or additional flexibility is needed, e.g. for handling model base value mismatch or non-symmetrical voltage range of conversion, the use of NLS rel or NLS abs method is recommended.

First two analytical methods, AM1 (Section 3.3.1) and AM2 (Section 3.3.2) are suitable for exponential to constrained ZIP model conversion. AM2 has higher conversion accuracy than AM1, thus it should be used instead of AM1 when constrained ZIP models are desired. Analytical methods AM2 (Sec-

tion 3.3.2) and AM3 (Section 3.3.3) are suitable for exponential to accurate ZIP model conversion. If the exponent of exponential model is $0 \leq K_{Exp} \leq 2$, the accuracy of AM2 and AM3 is similar, either method can be chosen. However, outside the previously defined K_{Exp} range, analytical method AM3 and non-linear least squares methods (NLS abs and NLS rel) display significantly lower conversion error than analytical methods AM1 and AM2. Thus, in such cases analytical method AM3 is recommended over AM1 and AM2.

8 | CONCLUSION

This paper described several methods for ZIP to exponential and exponential to ZIP load model conversion. For comparing the accuracy of the methods, a ZIP model dataset and an exponential model dataset were generated. The generated datasets were converted using the presented methods. The relative conversion error and the NMAE were calculated for the converted models. The conversion errors were plotted and analysed. It was shown that the conversion error depends on the method, voltage and parameter values of the load models. Recommendations for load model conversion method selection based on load model conversion error are given in Section 7. A case study (Section 6) was conducted to illustrate the impact of load model conversion on load flow results. The results of the case study indicate that load model conversion can cause a significant change in load flow results.

ACKNOWLEDGEMENTS

The authors would like to thank all the anonymous reviewers, who have taken the time to read the drafts of this paper and have given insightful feedback. Thanks to their contributions, this paper was improved significantly compared to the initial submission. The authors are grateful to Guido Andreesen and Kaur Tuttelberg for proofreading and proposing corrections. The authors would also like to thank Henry Kapp and Hendrik Kiristaja for their contributions, which were instrumental for developing the conversion methods. This publication was partially funded by Tallinn City Council Scholarship.

ORCID

Madis Leinakse  <https://orcid.org/0000-0003-0364-5405>
 Jako Kilter  <https://orcid.org/0000-0003-4985-857X>

REFERENCES

1. Price, W.W., et al.: Bibliography on load models for power flow and dynamic performance simulation, IEEE Trans. Power Syst. 10, 523–538 (1995) <https://doi.org/10.1109/59.373979>
2. Arif, A., et al.: Load modeling: a review. IEEE Trans. Smart Grid 9(6), 5986–5999 (2018) <https://doi.org/10.1109/TSG.2017.2700436>
3. Milanovic, J.V., et al.: International industry practice on power system load modeling, IEEE Trans. Power Syst. 28(3), 3038–3046 (2013) <https://doi.org/10.1109/TPWRS.2012.2231969>
4. CIGRE Working Group C4.605: Modelling and aggregation of loads in flexible power networks (566) (Feb. 2014). ISBN: 978-2-85873-261-6. <https://e-cigre.org/publication/566-modelling-and-aggregation-of-loads-in-flexible-power-networks>

5. EPRI, Palo Alto, CA, and Public Service Company of New Mexico, Albuquerque, NM: Advanced Load Modeling (2002) 1007318. <https://www.epri.com/research/products/1007318>
6. EPRI, Palo Alto, CA: Measurement-Based Load Modeling (2006) 1014402. <https://www.epri.com/research/products/1014402>
7. Leinakse, M., et al.: Preliminary study on comparative load modelling in PSS/E and PSCAD. In: 17th International Symposium 'Topical Problems in the Field of Electrical and Power Engineering' and 'Doctoral School of Energy and Geotechnology III', Kuressaare, Estonia, 197–199 (2018)
8. Leinakse, M., Kilter, J.: Conversion error of exponential to second order polynomial ZIP load model conversion. In: 2018 IEEE International Conference on Environment and Electrical Engineering and 2018 IEEE Industrial and Commercial Power Systems Europe (EEEIC/I&CPS Europe), Palermo, Italy, 1–5 (2018) <https://doi.org/10.1109/iecec.2018.8493667>
9. Siemens PTI: PSS@E 34 Program Operation Manual (2015)
10. Manitoba HVDC Research Centre: PSCAD User's Guide v4.6.0 (2015)
11. Hossain, M.S., et al.: Comparison of the ZIP load model and the exponential load model for CVR factor evaluation. In: 2017 IEEE Power & Energy Society General Meeting, Chicago, IL, USA, 1–5 (2017) <https://doi.org/10.1109/PESGM.2017.8274490>
12. Diaz-Aguilo, M., et al.: Field-validated load model for the analysis of CVR in distribution secondary networks: energy conservation. IEEE Trans. Power Delivery. 28(4), 2428–2436 (2013) <https://doi.org/10.1109/TPWRD.2013.2271095>
13. Carne, G., et al.: Load control using sensitivity identification by means of smart transformer. IEEE Trans. Smart Grid. 9(4), 2606–2615 (2018) <https://doi.org/10.1109/TSG.2016.2614846>
14. Carne, G., et al.: On-line load sensitivity identification in LV distribution grids. IEEE Trans. Power Syst. 32(2), 1570–1571 (2017) <https://doi.org/10.1109/TPWRS.2016.2581979>
15. Ravindra, H., et al.: Conversion of PSS@E models into RSCAD models: lessons learned. In: IECON 2014–40th Annual Conference of the IEEE Industrial Electronics Society, Dallas, TX, 3743–3749 (2014) <https://doi.org/10.1109/IECON.2014.7049057>
16. Leinakse, M., Kilter, J.: Conversion error of second order polynomial ZIP to exponential load model conversion. In: Mediterranean Conference on Power Generation, Transmission, Distribution and Energy Conversion (MEDPOWER 2018), Dubrovnik, Croatia, 1–5 (2018) <https://doi.org/10.1049/cp.2018.1882>
17. Korunović, L.M., et al.: Recommended parameter values and ranges of most frequently used static load models. IEEE Trans. Power Syst. 33(6), 5923–5934 (2018) <https://doi.org/10.1109/TPWRS.2018.2834725>
18. Asres, M.W., et al.: Non-intrusive load composition estimation from aggregate ZIP load models using machine learning. Int. J. Electr. Power Energy Syst. 105, 191–200 (2019) <https://doi.org/10.1016/j.ijepes.2018.08.016>
19. Collin, A.J., et al.: Development of low-voltage load models for the residential load sector. IEEE Trans. Power Syst. 29(5), 2180–2188 (2014) <https://doi.org/10.1109/TPWRS.2014.2301949>
20. Kheradmandi, M., Feuillet, R.: Using voltage control for reducing standing phase angle in power system restoration. Electr. Power Syst. Res. 146, 9–16 (2017) <https://doi.org/10.1016/j.epsr.2017.01.006>
21. Leinakse, M., et al.: Identification of intra-day variations of static load characteristics based on measurements in high-voltage transmission network. In: 2018 IEEE PES Innovative Smart Grid Technologies Conference Europe (ISGT-Europe), Sarajevo, Bosnia and Herzegovina, 1–6 (2018) <https://doi.org/10.1109/isgtEurope.2018.8571712>
22. Zhang, J., et al.: Electric load model based on aggregation algorithm. In: 2009 Asia-Pacific Power and Energy Engineering Conf., Wuhan, China, 1–4 (2009) <https://doi.org/10.1109/APPEEC.2009.4918324>
23. Korunovic, L.M., Stojanovic, D.P.: The effects of normalization of static load characteristics. In: 2009 IEEE Bucharest PowerTech, Bucharest, Romania, 227–234 (2009) <https://doi.org/10.1109/PTC.2009.5281826>
24. Leinakse, M., et al.: Impact of distributed generation on estimation of exponential load models. In: 2019 IEEE Power & Energy Society General Meeting (PESGM), Atlanta, GA, USA, 1–5 (2019) <https://doi.org/10.1109/PESGM40551.2019.8974014>
25. Anderson, P., Fouad, A.: Power System Control and Stability, 1. Iowa State University Press, Iowa (1977)
26. DIgSILENT: DIgSILENT PowerFactory 2017: Technical Reference Documentation General Load, ElmLod, TypLod (2017)
27. DIgSILENT: DIgSILENT PowerFactory 2017: Nine-bus System (2017)
28. Korunovic, L.M., et al.: Identification of static load characteristics based on measurements in medium-voltage distribution network, IET Gener. Transm. Distrib. 2(2), 227–234 (2008) <https://doi.org/10.1049/iet-gtd:20070091>

How to cite this article: Leinakse M, Kilter J. Exponential to ZIP and ZIP to exponential load model conversion: Methods and error. *IET Gener Transm Dis.* 2020;1–17. <https://doi.org/10.1049/gtd2.12002>

Publication VII

M. Leinakse and J. Kilter, "Processing and filtering digital fault recorder events for load model estimation," in *2021 IEEE PES Innovative Smart Grid Technologies Europe (ISGT Europe)*, Espoo, Finland, Oct. 2021, pp. 01–05, doi: 10.1109/isgteurope52324.2021.9640026

©2021 IEEE. Reprinted with permission.

Processing and Filtering Digital Fault Recorder Events for Load Model Estimation

Madis Leinakse

*Dept. of Electrical Power Engineering and Mechatronics
Tallinn University of Technology
Tallinn, Estonia*

0000-0003-0364-5405

Jako Kilter

*Dept. of Electrical Power Engineering and Mechatronics
Tallinn University of Technology
Tallinn, Estonia*

0000-0003-4985-857X

Abstract—This paper focuses on the data post-processing stage of the measurement-based load modelling. Exponential load models are estimated from DFR (Digital Fault Recorder) measured events. The least squares algorithm is used for model estimation. The acquired set of models is used for investigating how the distribution of estimated values depends on the event filtering. Filtering based on voltage and current unbalance ratio, residual voltage of disturbance, voltage deviation, and estimated load model parameter values is analysed. In addition, two different methods for calculating representative model from a set of event based values are compared. One of the analysed methods is found to be less sensitive to event filtering.

Index Terms—exponential model, load modelling, static load models

I. INTRODUCTION

There are three main approaches for estimating the load model of an aggregated bus load. Firstly, the component-based approach, which involves identification of load component models and composition. The load components can be load classes (residential, industrial), device types (boiler, incandescent lamp, washing machine). The load component models are defined as a sum of basic models (e.g. ZIP model, induction motor model). The total consumption is disaggregated to determine the contributions of the components, and by aggregation the bus load is derived. Secondly, measurement-based approach, where the load models are estimated based on measurement data. Thirdly, combined approach, which involves a combination of the first two methods. In this study the measurement-based approach is implemented.

The measurement-based load modelling typically involves several data processing stages: 1) data collection, 2) data pre-processing, 3) load model estimation (may include load model selection), 4) model validation. Different measurement systems can be used for acquiring the data: Digital Fault Recorder (DFR) [1]–[3], SCADA [4], [5], Phasor Measurement Unit (PMU) [6]–[10], Power Quality (PQ) Monitor [11]–[13]. The DFR data was used in this study due to the available historical database, and coverage of the measurement system (large number of aggregated loads measurable by this system). The pre-processing can involve filtering [14], [16],

DFT-based signal processing [15], rms value calculation [3], positive sequence component calculation [16], event selection for load model estimation [15]. In this paper the impact of event selection is discussed and analysed based on a case study. The load model estimation is commonly done by using least squares estimation (used for example in [16]–[18]). Alternatively, Genetic Algorithm [16], [19], and Simulated Annealing [16], improved particle swarm optimization (IPSO) [20] and others have been implemented by different authors. The least squares minimisation was used in this study as the estimation algorithm improvement is not a goal of this paper and this method works well. In the fourth stage, validation, the estimated model is used for event simulation and results are compared to measured data, or compared to historical events [15]. In this study, the estimation error was calculated for the models to assess the goodness of fit. After the estimation of load models based on events, there can be a significant number of load models. Which one to use as the representative value? Several different approaches are used in this kind of situation: common approach is mean value calculation [6], [14], [16], [21]–[23], it is also possible to calculate a weighted mean [24] or estimate a load model using several events [10]. In this paper, the mean and error weighted mean value have been used, and were compared.

The introduction section of this paper is followed by three sections. In Section II the used data processing methods are presented and explained. In Section III the results of the conducted case study are presented. The main results of the paper are summarised in Section IV.

II. METHODS

A. Case Study

In this case study DFR data was acquired from a historical database. The data is from years 2018-2020. Data from 1 substation is used. The used DFR is event based: 250 ms of data is recorded pre-triggering and 5 seconds after. 1 kHz sampling rate is used for recording instantaneous values of voltage and current. All other values are derived from these measured values. Sliding window algorithm using discrete Fourier transform is used for obtaining phasor domain quantities. The exponent K_{pv} and K_{qv} of exponential load model (Section II-B is estimated for each recorded event using

least squares estimation (Section II-C). The estimation error is quantified by Mean Square Error (MSE) (4) and Mean Absolute Error (MAE) (9). The possibly bad events (from load model estimation perspective) are detected using methods discussed in Section II-D. In addition, the sets of estimated load models (sets of K_{pv} and K_{qv} values) are processed using methods described in Section II-E. The results are presented in Section IV.

B. Exponential Load Model

The exponential load model can be described by (1) and (2).

$$P_{EXP} = P_0(V/V_0)^{K_{pv}} \quad (1)$$

$$Q_{EXP} = Q_0(V/V_0)^{K_{qv}} \quad (2)$$

where P_0 and Q_0 are real and reactive power of the load at pre-event voltage V_0 respectively. K_{pv} and K_{qv} are exponents describing the voltage characteristics of the real and reactive power of the load.

C. Load Model Estimation

Exponential load models (1) and (2) are estimated by using the commonly used least squares estimation, which has been used for example in [3], [12], [16], [18], [28], [29].

$$\min MSE = \min \frac{1}{N} \sum_{i=1}^N (P_{model_i} - P_{meas_i})^2 \quad (3)$$

For estimating exponential load model parameters, the following model equation and boundary conditions can be used for (3).

$$MSE = \frac{1}{N} \sum_{i=1}^N (P_{model_i} - P_{meas_i})^2 \quad (4)$$

- $P_{model_i} = P_0(V_i/V_0)^{K_{pv}}$
- $-10.0 \leq K_{pv} \leq 10.0$
- $-10.0 \leq K_{qv} \leq 10.0$

D. Methods for Assessing Event Suitability

Different requirements for events that can be used for load model estimation are described and used in the literature. In this paper, several approaches are implemented and the detected events are compared.

According to [15] a suitable event for load model estimation should have voltage and current unbalance below 10%. In this study maximum value of negative and zero sequence unbalance ratio is calculated for each recorded event. The negative sequence unbalance ratio u_2 (5) is defined in [26] as the ratio between negative sequence component U_2 and the positive sequence component U_1 . Similarly, [26] defines the zero sequence unbalance ratio u_0 (6) by the ratio of zero component U_0 , and the positive sequence component U_1 .

$$u_2 = \frac{U_2}{U_1} \cdot 100\% \quad (5)$$

$$u_0 = \frac{U_0}{U_1} \cdot 100\% \quad (6)$$

In [15] the event is required to take place upstream or on an adjacent feeder. In [23] the direction of voltage and power change is used for detecting load disturbances. [23] expressed this condition as $sign(\Delta V) \cdot sign(\Delta P) > 0$. This idea could be implemented in several ways. Firstly, the $\Delta V \cdot \Delta P > 0$ could be used instead of sign functions. Secondly, the opposing direction of voltage and load change would lead to estimation of negative value of active power exponent K_{pv} . Based on the survey results presented in [27] the used minimum values of active power parameter np (here denoted as K_{pv} and load change would lead to estimation of negative value of active power exponent K_{pv}) are 0. In [30] a few loads displayed a K_{pv} value of -0.01. When analysing aggregated loads, occurrence of negative values should be highly unlikely. In conclusion, the negative values of K_{pv} could provide similar results to using equation $\Delta V \cdot \Delta P > 0$ or $sign(\Delta V) \cdot sign(\Delta P) > 0$. In this study, the negative K_{pv} value detection was implemented as filter F1.

In [15] the suitable event is required to have a sufficient drop in voltage (10% or more). [23] and [31] claim that voltage changes of 0.5% are sufficient for load model estimation. The difference between maximum and minimum measured voltage ΔV was calculated for each event to analyse the impact of depth of voltage drop. In the filter F6 ΔV value 5% was implemented.

In [15] the event is required not to be a voltage interruption. To detect interruptions, the minimum value of rms voltage was measured. An interruption is defined in [32] by rms voltage drop below 5%, [26] mentions a threshold of 5% or 10%. Actually, at voltages below 85% of nominal voltage load devices self-disconnect from the grid [25]. For this reason, actually the minimum voltage threshold for load model estimation can be set much higher. For example at 80% of nominal voltage, which was implemented in this study.

E. Post-Processing Estimated Values

In order to calculate a representative value from a set of load model parameter values, several methods can be used. The most common approach is to average the values, as has been done in [6], [14], [16], [21]–[23]. Extreme values of load models can significantly affect the results when the number of averaged samples is relatively small. Alternatively to the common approach, [10] uses a multi-curve identification process, where the measurement data of several events is used for identifying a load model.

In [24] the idea of calculating estimation error weighted average was proposed. In case of that approach a weighted mean value K (7) is calculated from M event-based parameter values K_i , adding weight w_i to each estimated value.

$$K = \frac{\sum_{i=1}^M (w_i \cdot K_i)}{\sum_{i=1}^M w_i} \quad (7)$$

The inverse of error ε_i is used as the weight w_i and (8) is obtained. The values of MSE (4) are used in this study as the values of ε_i .

$$K = \frac{\sum_{i=1}^M (K_i/\varepsilon_i)}{\sum_{i=1}^M (1/\varepsilon_i)} \quad (8)$$

In this paper two measures of error are used for quantifying the goodness of fit of estimation: MSE (4) and Mean Absolute Error (MAE) (9)

$$MAE = \frac{1}{N} \sum_{i=1}^N |P_{model_i} - P_{meas_i}| \quad (9)$$

III. RESULTS

A. Unfiltered Events

Firstly, the load models are estimated for all DFR recorded events (1843 in total). The histograms of estimated K_{pv} and K_{qv} values are shown in Fig. 1. In the figure there is a high estimated value count at value -10 and 10. This is caused by the used boundary values of load model parameter estimation (marked by blue lines in Fig. 1): -10 and 10 were used as boundary values in load model estimation phase. The exponent K_{pv} is at the boundary value for 1279 and K_{qv} for 1557 times. From these 1105 are common events. When the boundary values are removed from the set of estimated parameter values, Fig. 2 is acquired. Compared to Fig. 1, the new histogram Fig. 2 is closer to the normal distribution, and it is apparent that the boundary values acted as outlier.

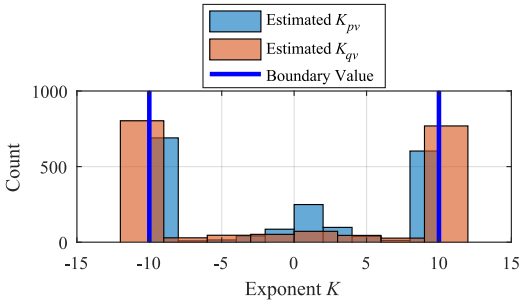


Fig. 1. Estimated exponential parameter K_{pv} and K_{qv} when load models are estimated for all measured events, blue lines mark the boundary values used in estimation.

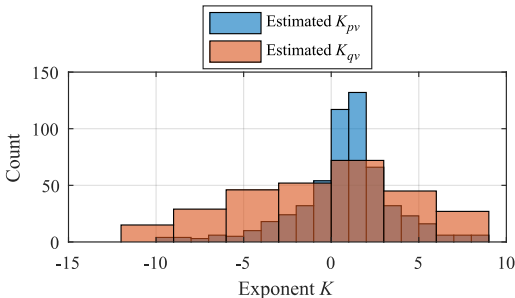


Fig. 2. Estimated exponential parameter K_{pv} and K_{qv} when load models are estimated for all measured events and results at boundary values are removed.

The sets of estimated parameter values were fitted to normal distribution (with 95% confidence), and the mean μ and the standard deviation σ were calculated (shown in Tab. I). The estimated Probability Density Functions (PDF) are shown in Fig. 3 and Fig. 4.

TABLE I
MEAN VALUE μ AND STANDARD DEVIATION σ OF NORMAL DISTRIBUTION FIT (WITH 95% CONFIDENCE), MSE WEIGHTED MEAN VALUE μ_{MSE} AND MAE WEIGHTED MEAN VALUE μ_{MAE} BASED ON ALL MEASURED EVENTS, EXCEPT BOUNDARY VALUES

Exp Model Parameter	Avg., μ	Std. Dev., σ	MAE Weight. Avg., μ_{MSE}	MSE Weight. Avg., μ_{MAE}
K_{pv}	0.792	2.854	0.927	0.782
K_{qv}	-0.448	4.857	0.176	1.034

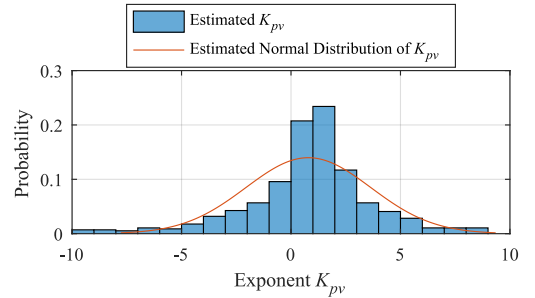


Fig. 3. Estimated exponential parameter K_{pv} when load models are estimated for all measured events and results at boundary values are removed.

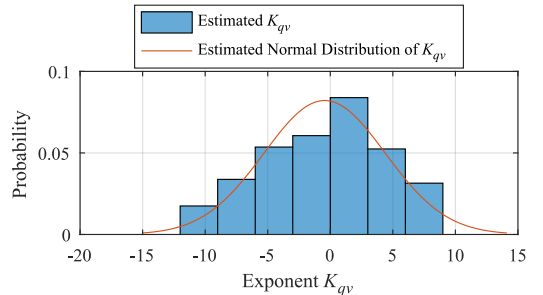


Fig. 4. Estimated exponential parameter K_{qv} when load models are estimated for all measured events and results at boundary values are removed.

B. Event Filtering

In Section II several approaches for detecting possibly unsuitable events were described, nine different event filters were implemented based on the discussions. To analyse how many events would be filtered out by a filter and how many events are detected by several filters Tab. II was constructed. In the table, the diagonal elements indicate the number of events that would be filtered out if only that filter would be used. The rest of the numbers of the table illustrate how many common events would be flagged by two different filters. The following denotation is used in Tab. II:

- F1 - negative value of K_{pv}
- F2 - negative sequence ratio of voltage over 10%
- F3 - zero sequence ratio of voltage over 10%
- F4 - negative sequence ratio of current over 10%
- F5 - zero sequence ratio of current over 10%
- F6 - ΔV below 5%
- F7 - rms voltage drops below 80% of nominal
- F8 - value of K_{pv} is at a boundary
- F9 - value of K_{qv} is at a boundary

According to Tab. II the largest number of events are flagged by boundary condition filters F8 and F9. Most of the events detected by F8 are also detected by F4 and F5, which are based on current unbalance (F4 checks for maximum value of negative sequence ratio and F5 zero sequence ratio). This means that most of the boundary events of K_{pv} could be detected by current unbalance filter. In case of K_{qv} boundary values (filter F9), roughly 2/3 of flagged events were detected by the same current unbalance filters (F4 and F5). The detected events of F4 and F5 are mostly common, F5 can detect only 5 events, that were undetected by F4. The voltage unbalance filter F2 and F3 only detect a small number of events that were also detected by the current unbalance filters. In conclusion, the voltage unbalance ratio filters (F2, F3) and large voltage drop detection (F7) were with lowest sensitivity and were covered by the current unbalance detection. Thus, these filters can be considered to be redundant.

TABLE II
NUMBER OF UNSUITABLE EVENTS DETECTED BY FILTER^a

	F1	F2	F3	F4	F5	F6	F7	F8	F9
F1	842								
F2	19	65							
F3	11	40	40						
F4	728	65	40	1428					
F5	602	64	40	1257	1264				
F6	769	11	11	1193	1070	1576			
F7	18	56	40	58	55	11	58		
F8	682	18	10	1266	1144	1155	13	1279	
F9	736	11	7	1183	1025	1421	11	1105	1557

^a Explanation of event filter F1...F9 in text.

C. Estimated Load Models After Event Filtering

Based on the histograms of estimated values, filter F1 was disabled, as it caused distortion in the data distribution: when negative K_{pv} were removed, the symmetry of the values weakened, which could cause erroneous shift of mean value. Thus, if the mean value of a set of load models is used, filter F1 may need to be omitted for acquiring proper results. Filters F2...F9 were implemented, the load model parameter sets were fitted to normal distribution, PDF of K_{pv} and K_{qv} is shown in Fig. 5 and Fig. 6, respectively.

Based on the calculated load model values (Tab. III), the calculated mean value of K_{pv} increased, and the standard deviation decreased from 2.854 to 2.498. This indicates that the accuracy of mean value of K_{pv} could have improved as a result of the filtering. Contradictory is the standard deviation σ of K_{qv} , which increased from 4.857 to 5.148. The filtering

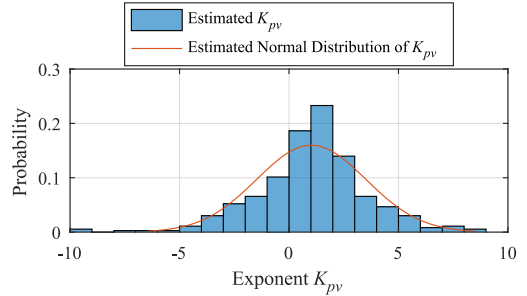


Fig. 5. Estimated exponential parameter K_{pv} when load models are estimated for filtered events.

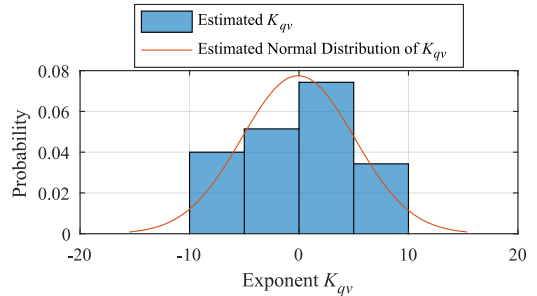


Fig. 6. Estimated exponential parameter K_{qv} when load models are estimated for filtered events.

had lowest impact on the weighted mean value that was calculated using MSE based weighting. The K_{qv} values of error weighted sums differ significantly from the calculated mean. Considering the results, the accuracy of the K_{qv} values is possibly with low accuracy, and the values can not be used for estimating a reliable value.

TABLE III
MEAN VALUE μ AND STANDARD DEVIATION σ OF NORMAL DISTRIBUTION FIT (WITH 95% CONFIDENCE), MSE WEIGHTED MEAN VALUE μ_{MSE} AND MAE WEIGHTED MEAN VALUE μ_{MAE} BASED ON FILTERED EVENTS

Exp Model Parameter	Avg., μ	Std. Dev., σ	MAE Weight. Avg., μ_{MAE}	MSE Weight. Avg., μ_{MSE}
K_{pv}	1.018	2.498	0.889	0.763
K_{qv}	-0.078	5.148	0.272	0.964

IV. CONCLUSION

In this paper several methods for unsuitable event detection, and post-processing estimated values are presented. The presented approaches are compared based on a set of DFR measurement data, which covers 3 years and includes 1843 events. Nine different event filters were implemented for unsuitable event detection (and flagging). The filters are based on voltage and current unbalance ratio, residual voltage of disturbance, voltage deviation, and estimated load model parameter values. The implemented filters were compared and it was found that the current unbalance ratio based filtering is able to detect all the same events as were detected by

voltage unbalance, and many more. Furthermore, the negative sequence current ratio based filtering is able to detect almost all the zero-sequence current ratio filter detected events, and all the interruptions. MSE error weighted averaging was found to be less sensitive to event filtering than basic averaging.

REFERENCES

- [1] S. Sheng, K. K. Li, W. L. Chan, Z. Xiangjun and L. Xinran, "Using substation automation information for electric power load modeling and predictive maintenance of circuit breaker," *INDIN '05. 2005 3rd IEEE International Conference on Industrial Informatics*, 2005., Perth, WA, Australia, 2005, pp. 546–551, doi: 10.1109/INDIN.2005.1560435.
- [2] A. Abdelaziz, M. Badr, and A. Younes, "Dynamic load modeling of an Egyptian primary distribution system using neural networks," *International Journal of Electrical Power & Energy Systems*, vol. 29, no. 9, pp. 637 – 649, 2007. doi: <https://doi.org/10.1016/j.ijepes.2006.09.006>.
- [3] M. Leinakse, T. Sarnet, T. Kangro, and J. Kilter, "First results on load model estimation using digital fault recorder measurements," in *16th International Symposium "Topical Problems in the Field of Electrical and Power Engineering" and "Doctoral School of Energy and Geotechnology III"*, Pärnu, Estonia, 2017, pp. 101–105.
- [4] A. Gulakhmadov et al., "A Statistical-Based Approach to Load Model Parameter Identification," in *IEEE Access*, vol. 9, pp. 66915–66928, 2021, doi: 10.1109/ACCESS.2021.3076690.
- [5] M. Leinakse and J. Kilter, "Clustering of transmission system loads based on monthly load class energy consumptions," in *2020 21st International Scientific Conference on Electric Power Engineering (EPE)*, Prague, Czech Republic: IEEE, oct 2020, pp. 1–6. doi: 10.1109/epe51172.2020.9269197
- [6] Y. Ge, A. J. Flueck, D.-K. Kim, J.-B. Ahn, J.-D. Lee, and D.-Y. Kwon, "Power system real-time event detection and associated data archival reduction based on synchrophasors," *IEEE Transactions on Smart Grid*, vol. 6, no. 4, pp. 2088–2097, jul 2015. doi: 10.1109/tsg.2014.2383693
- [7] K. Q. Hua, A. Vahidnia, Y. Mishra, and G. Ledwich, "PMU measurement based dynamic load modeling using SVC devices in online environment," in *2015 IEEE PES Asia-Pacific Power and Energy Engineering Conference (APPEEC)*, Brisbane, QLD, Australia, nov 2015, pp. 1–5.
- [8] X. Zhang, C. Lu, J. Lin, Y. Wang, J. Wang, H. Huang, and Y. Su, "Experimental measurement of PMU error distribution and its impact on load model identification," in *2016 IEEE Power and Energy Society General Meeting (PESGM)*, jul 2016. doi: 10.1109/pesgm.2016.7741069
- [9] X. Wang, "Estimating dynamic load parameters from ambient PMU measurements," in *2017 IEEE Power & Energy Society General Meeting*, jul 2017. doi: 10.1109/pesgm.2017.8273913
- [10] D. Han, J. Ma, R. mu He, and Z. yang Dong, "A real application of measurement-based load modeling in large-scale power grids and its validation," *IEEE Transactions on Power Systems*, vol. 24, no. 4, pp. 1756–1764, nov 2009. doi: 10.1109/tpwrs.2009.2030298
- [11] "Measurement-based load modeling, 1014402," EPRI, Palo Alto, CA, Tech. Rep., 2006.
- [12] M. Leinakse, P. Tani, and J. Kilter, "Impact of distributed generation on estimation of exponential load models," in *2019 IEEE Power & Energy Society General Meeting (PESGM)*, Atlanta, GA, USA, 2019, pp. 1–5. doi: 10.1109/PESGM40551.2019.8974014
- [13] M. Leinakse, G. Andreessen, P. Tani, and J. Kilter, "Estimation of exponential and ZIP load model of aggregated load with distributed generation," in *2021 IEEE 62nd International Scientific Conference on Power and Electrical Engineering of Riga Technical University (RTUCON)*, Riga, Latvia, 2021, in press.
- [14] K. N. Hasan, J. V. Milanovic, P. Turner, and V. Turnham, "A step-by-step data processing guideline for load model development based on field measurements," in *2015 IEEE Eindhoven PowerTech*, Eindhoven, Netherlands, jun 2015, pp. 1–6. doi: 10.1109/ptc.2015.7232307
- [15] Z. Dong, A. Borghetti, K. Yamashita, A. Gaikwad, P. Pourbeik, and J. Milanovic, "Cigre wg c4.065 recommendations on measurement based and component based load modelling practice," in *CIGRE SC C4 Colloquium: Fusion of Lightning Research and Practice for Power System in the Future*, Hakodate, Japan, Oct. 2012.
- [16] Y. Zhu and J. V. Milanovic, "Automatic identification of power system load models based on field measurements," *IEEE Transactions on Power Systems*, vol. 33, no. 3, pp. 3162–3171, may 2018.
- [17] M. Leinakse and J. Kilter, "Exponential to ZIP and ZIP to exponential load model conversion: Methods and error," *IET Generation, Transmission & Distribution*, vol. 15, no. 2, pp. 177–193, 2021. doi: 10.1049/gtd2.12002
- [18] "Advanced load modeling, 1007318," EPRI, Palo Alto, CA, and Public Service Company of New Mexico, Albuquerque, NM, Tech. Rep., 2002.
- [19] P. Zhang and H. Bai, "Derivation of load model parameters using improved genetic algorithm," in *2008 Third International Conference on Electric Utility Deregulation and Restructuring and Power Technologies*, apr 2008. doi: 10.1109/drpt.2008.4523547
- [20] P. Regulski, D. S. Vilchis-Rodriguez, S. Djurovic, and V. Terzija, "Estimation of composite load model parameters using an improved particle swarm optimization method," *IEEE Transactions on Power Delivery*, vol. 30, no. 2, pp. 553–560, apr 2015. doi: 10.1109/tpwrd.2014.2301219
- [21] J. Marchgraber, E. Xypolytou, I. Lupandina, W. Gawlik, and M. Stifter, "Measurement-based determination of static load models in a low voltage grid," in *2016 IEEE PES Innovative Smart Grid Technologies Conference Europe (ISGT-Europe)*, Ljubljana, Slovenia, oct 2016, pp. 1–6. doi: 10.1109/isgt-europe.2016.7856297
- [22] L. M. Korunovic and D. P. Stojanovic, "The effects of normalization of static load characteristics," in *2009 IEEE Bucharest PowerTech*, Bucharest, Romania, jun 2009, pp. 227–234.
- [23] S. A. Arefifar and W. Xu, "Online tracking of voltage-dependent load parameters using ULTC created disturbances," *IEEE Transactions on Power Systems*, vol. 28, no. 1, pp. 130–139, feb 2013.
- [24] M. Leinakse, H. Kiristaja, and J. Kilter, "Identification of intra-day variations of static load characteristics based on measurements in high-voltage transmission network," in *2018 IEEE PES Innovative Smart Grid Technologies Conference Europe (ISGT Europe 2018)*, Sarajevo, Bosnia-Herzegovina, 2018, pp. 1–6. doi: 10.1109/ISGT-Europe.2018.8571712
- [25] CIGRE Working Group C4.605: "Modelling and aggregation of loads in flexible power networks" (CIGRE, Feb. 2014)
- [26] European standard EN 61000-4-30:2015. Electromagnetic compatibility (EMC) - Part 4-30: Testing and measurement techniques - Power quality measurement methods
- [27] J. V. Milanovic, K. Yamashita, S. M. Villanueva, S. Z. Djokic, and L. M. Korunovic, "International industry practice on power system load modeling," *IEEE Transactions on Power Systems*, vol. 28, no. 3, pp. 3038–3046, aug 2013. doi: 10.1109/tpwrs.2012.2231969
- [28] M. Leinakse and J. Kilter, "Conversion error of exponential to second order polynomial ZIP load model conversion," in *2018 IEEE International Conference on Environment and Electrical Engineering and 2018 IEEE Industrial and Commercial Power Systems Europe (EEEIC / I&CPS Europe)*, Palermo, Italy, jun 2018, pp. 1–5. doi: 10.1109/eeeic.2018.8493667
- [29] M. Leinakse and J. Kilter, "Conversion error of second order polynomial ZIP to exponential load model conversion," in *Mediterranean Conference on Power Generation, Transmission, Distribution and Energy Conversion (MedPower 2018)*, Dubrovnik, Croatia, 2018, pp. 1-5. doi: 10.1049/cp.2018.1882
- [30] L. Korunovic, J. V. Milanovic, S. Z. Djokic, K. Yamashita, S. Martinez-Villanueva, and S. Sterpu, "Recommended parameter values and ranges of most frequently used static load models," *IEEE Transactions on Power Systems*, pp. 1–1, 2018. doi: 10.1109/tpwrs.2018.2834725
- [31] W. Freitas and L. C. P. da Silva, "A discussion about load modeling by using voltage variations," in *2012 IEEE 15th International Conference on Harmonics and Quality of Power*, Hong Kong, China, jun 2012, pp. 40–44. doi: 10.1109/ichqp.2012.6381271
- [32] European standard EN 50160:2010+A1+A2+A3:2019. Voltage characteristics of electricity supplied by public electricity networks

Publication VIII

M. Leinakse, G. Andreesen, P. Tani, and J. Kilter, "Estimation of exponential and ZIP load model of aggregated load with distributed generation," in *2021 IEEE 62nd International Scientific Conference on Power and Electrical Engineering of Riga Technical University (RTU CON)*, Riga, Latvia, 2021, to be published

©2021 IEEE. Reprinted with permission.

Estimation of Exponential and ZIP Load Model of Aggregated Load with Distributed Generation

Madis Leinakse, Guido Andreesen, Pärtel Tani, Jako Kilter
Department of Electrical Power Engineering and Mechatronics
Tallinn University of Technology
Tallinn, Estonia
madis.leinakse@taltech.ee

Abstract—The voltage dependence of loads plays a major role when the conservation voltage reduction (CVR) is analysed or implemented. This dependence is affected by the amount of distributed generation (DG) included among the load of the aggregated bulk supply point. In this paper, the impact of DG on estimated values of exponential load model and ZIP load model (second order polynomial load model) is analysed based on a measurement-based case study. A new equation is presented for assessing the impact of DG penetration level on the ZIP model of the aggregated load (with DG). Additionally, the modelling accuracy of ZIP and exponential model is compared and the exponential model is shown to provide a better accuracy than the ZIP model for modelling this type of loads. The case study was conducted in a distribution network with significant amount of DG. An on-load tap changer was used for inducing the voltage changes. Both, exponential load models and ZIP load models, were estimated from measurement data for transformer load and aggregated load excluding the DG.

Keywords—conservation voltage reduction (CVR); distributed generation; exponential load model; load modelling; static load models; ZIP model

I. INTRODUCTION

The use of renewable energy sources has increased for over a decade, each year more power is generated by centralised and distributed units powered by renewable sources. In European Union, the increasing use of DG is supported by the long-term goal of EU to become climate neutral by 2050 [1], and in shorter term by the Energy Performance of Buildings Directive (2010/31/EU). The directive required all the new buildings to be nearly zero-energy buildings (NZEB) from the end of 2020 [2]. Many recently built NZEB are mounted with local photovoltaic (PV) generation to meet the NZEB requirements. Mentioned aspects enlarge the amount of DG connected to the distribution network. In most cases, the DG units influence and change the demand variability at the bulk supply points of the power grid [3] due to weather dependent intermittent generation [4]. Therefore, it creates new challenges for grid operation [5]. One resource for increasing flexibility is the voltage dependence of loads. By controlling the supply voltage of the loads, it is possible to affect the operation points of the loads and to decrease the load of the system. Load control by voltage regulation is known as Conservation Voltage Reduction (CVR). A detailed review of CVR implementation aspects is given in [6]. The load reduction through CVR (CVR

factor) depends highly on the voltage characteristic of the load [3], [7] (load composition in [8]). The load composition of bus loads can also be used for grouping aggregated loads into type groups [9]. Furthermore, load reduction is affected by generated active power of the DG units [3], [7], [10], and the reactive power control of the DG [11].

In [3] the net feeder load sensitivity (to voltage) is used to estimate the effectiveness of CVR. The load sensitivity, CVR factor (power/energy change divided by voltage change), is approximately equivalent to the exponent of an exponential load model [3], [12]. The CVR is quantified in [3], [12], [13] by an exponential load model, and in [13], [14] the ZIP model is used. The ZIP and exponential load models, and the conversions between the models are described and analysed in [15]–[17]. Based on the results of [13], the modelling accuracy of the ZIP load model could be higher than accuracy of exponential model. In this paper, the exponential and a ZIP load model are both estimated for feeder load, which includes high amount of DG. The accuracy of the models is compared.

In [3] the effect of DG on net voltage sensitivity of aggregated load is analysed and demonstrated with a real time digital simulator. The numerical aspects of the derived equations are discussed in [18]. Similarly to [19], [20], the DG units are assumed to operate as constant power sources. The mathematical derivations of [3] were further developed and applied in measurement-based case study [21]. In the study [21] the impact of DG on estimation of exponential load models of aggregated loads is analysed. The results of the case study indicate that the linearisation based derivations give reasonable analytical results in a small distribution network with high penetration of DG (60...80%). In [21] the DG units are connected relatively close to the substation and other network configurations are not analysed.

In this paper a new mathematical equation is presented for assessing the impact of DG penetration on the estimated values of ZIP load model. The authors of this paper has been unable to find similar equation in the literature. Furthermore, case study results are analysed to compare the accuracy of the presented equation with the equation presented in [3]. In addition, the results of the analytical equations are compared to load models, which are estimated directly from the measured data. The presented equation provides a quick and simple way to assess how the apparent ZIP load characteristic is affected

by the penetration level of DG.

The introduction section of this paper is followed by four main sections. In Section II, estimated ZIP and used exponential load model are described. Additionally, the used measurement data processing methodology is introduced. A new equation is presented for calculating the ZIP load model of an aggregate of load and DG. The conducted case study is described in Section III. The results of the case study and discussion of the results is presented in Section IV. The main results of the paper are summarised in Section V.

II. THEORETICAL BACKGROUND

A. Measurement Data Pre-processing

The voltage events are detected by the same algorithm as is used in [21]–[23]. The averages of two consecutive sets of n samples are used for calculating the voltage change (1). In [22] the averaging window length of 20 seconds is used. However, in this paper, n value corresponding to 40 seconds is chosen based on event detection results. The same value is used in [21].

$$\Delta V = \left| \frac{V_{old}/n - V_{new}/n}{V_{old}/n} \right| \cdot 100\% \quad (1)$$

where V_{old} and V_{new} are the sum of n old and n new samples, respectively, and n is the length of the averaging window.

Next, the calculated values of ΔV are compared to a chosen event threshold value. According to [24] and [25] voltage changes of 0.5% can be used for load model estimation. In this case study, on-load tap changer (OLTC) with 1.78% step was used. For this reason, 1.5% voltage threshold is suitable for induced event detection. An event is detected if ΔV is larger than the threshold value. The start of the detected event is the first sample of the second vector V_{new} .

B. Exponential Load Model and Second Order Polynomial (ZIP) Load Model

The exponential load model is described by static characteristic (2).

$$P_{EXP} = P_0(V/V_0)^{K_{pv}} \quad (2)$$

where P_0 is load at pre-event voltage V_0 . Exponent K_{pv} describes the static voltage characteristic of the load.

The second order polynomial load model, ZIP load model, can be described by (3). The ZIP models include three components: K_{pz} with power proportional to the square of voltage (constant impedance); K_{pi} with power proportional to voltage (constant current); K_{pp} with constant power (independent of voltage).

$$P = P_0(K_{pz}(V/V_0)^2 + K_{pi}(V/V_0) + K_{pp}) \quad (3)$$

where V_0 corresponds to the initial voltage and P_0 to initial load power.

C. Load Model Estimation

The load model estimation is conducted by minimising the mean square error (5) between estimated ZIP model P_{model} and measured data P_{meas} . The minimisation problem is formulated by objective (4). The described non-linear least squares (NLS) formulation of the estimation problem is a common solution. It is used for example in [21], [23], [24], [26]–[28]. The performance of the NLS algorithm is compared with Genetic Algorithm and Simulated Annealing in [28], where it is shown that the NLS algorithm provides lower computational load and good solutions compared to the other 2 algorithms.

$$\min MSE = \min \frac{1}{N} \sum_{i=1}^N (P_{model_i} - P_{meas_i})^2 \quad (4)$$

The following model equation and boundary conditions are used for (4).

- $P_{model_i} = P_0(K_{pz}(V_i/V_0)^2 + K_{pi}(V_i/V_0) + K_{pp})$
- $K_{pz} + K_{pi} + K_{pp} = 1$
- $-20.0 \leq K_{pz} \leq 20.0$
- $-20.0 \leq K_{pi} \leq 20.0$
- $-20.0 \leq K_{pp} \leq 20.0$

D. Estimation Error

In paper [21] the estimation error is quantified by Mean Absolute Error (MAE) (5) and Mean Square Error (MSE) (6). To enable error comparison of the two papers, the same measures of error are used in this paper. In case of both, MAE and MSE, the error calculation is done based on measurement samples P_{meas_i} and modelled values P_{model_i} , where i is the index of the sample from 1... N .

$$MAE = \frac{1}{N} \sum_{i=1}^N |P_{model_i} - P_{meas_i}| \quad (5)$$

$$MSE = \frac{1}{N} \sum_{i=1}^N (P_{model_i} - P_{meas_i})^2 \quad (6)$$

E. Expected Impact of Distributed Generation on Voltage Sensitivity

The DG connected to the feeder decreases the power supplied by the transformer P_T and the pre-event load of the transformer P_{T0} . When a voltage change takes place, the load P_{T0} reacts and obtains value P_T . Assuming the impact of DG on losses to be negligible and voltage changes to be relatively small, the load response can be approximated by the voltage sensitivity of the load. In case of ZIP model (3), the voltage sensitivity of the load is (7) [29].

$$\frac{dP}{dV} = 2 \cdot K_{pz} + K_{pi} \quad (7)$$

In papers [3], [12] equations are derived for approximating the impact of DG on apparent aggregated exponential load model. The exponent of the load model K_{pv} (approximately

equivalent to voltage sensitivity of the load [3], [12]) is determined to be (8).

$$K_{pv} = \frac{\Delta P/P_0}{\Delta V/V_0} = K_{pv,L} \cdot \frac{P_L}{P_L - P_G} \quad (8)$$

where $K_{pv,L}$ is voltage sensitivity/exponent of the load model (without DG), P_L is the load power, and P_G is the total output power of the DG.

Applying a similar approach on (7), it is possible to derive (9). This equation has multiple solutions. In this paper, solution given by (10) is applied and error is calculated.

$$2 \cdot K_{pz,T} + K_{pi,T} = \frac{P_L}{P_L - P_G} \cdot (2 \cdot K_{pz,L} + K_{pi,L}) \quad (9)$$

$$\begin{cases} K_{pz,T} = \frac{P_L}{P_L - P_G} \cdot K_{pz,L} \\ K_{pi,T} = \frac{P_L}{P_L - P_G} \cdot K_{pi,L} \\ K_{pp,T} = 1 - K_{pi,T} - K_{pz,T} \end{cases} \quad (10)$$

If the penetration level of DG is described by factor $\beta = P_G/P_L$ (used in [30]), the fraction $(P_L)/(P_L - P_G)$ in (8), (9), (10) may also be replaced by fraction $1/(1 - \beta)$.

III. CASE STUDY

A. Measured Distribution Network and Measurement System

A power quality monitor (PQM) was installed at a medium voltage substation to measure three phase RMS values of voltage, active power and reactive power with a sampling rate of 5 Hz (time-step 200 ms). The measurement probes were connected to the voltage transformer (VT) of the measured section and to the current transformer (CT) of the transformer feeder. In addition, the SCADA measurements were used for obtaining the output power of the distributed generation units.

The measured distribution network feeders supply 13 755 customers, which consumed during the measured period on average 7.4 MW. The load consisted mainly from residential (1/3), commercial (1/3) customers, and industrial (1/5) customers. There is 6.7 MW of DG connected to the feeders: 2 wind turbines (2.0 MW and 2.3 MW) and a 2.4 MW combined heat and power plant (CHP). The DG units were operated in fixed $\cos\phi$ mode.

B. Induced Voltage Changes

An OLTC was used for inducing 6 voltage changes that were used for load model estimation by measurement-based approach. The used OLTC has 16 tap positions with 1.78% steps. During the study, the voltage was kept in range 10.2 ... 10.8 kV to stay within boundaries set by the DSO. Fig. 1 displays the induced voltage changes (induced changes are marked in the figure by numbers from 1 to 6). Normal voltage level is used at the beginning and end of the study. The 1st and the 6th voltage change correspond to one tap position change, and the 2nd to 5th change to three taps. After switching the OLTC, the voltage levels were held for 10...15 minutes to detect possible longer term dynamics of load responses.

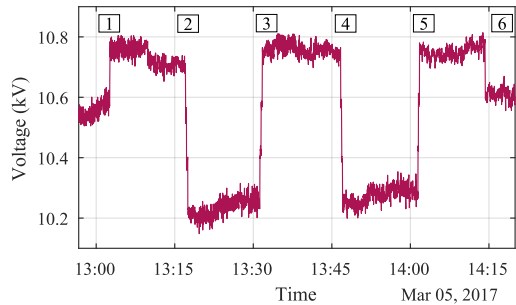


Fig. 1. Average RMS voltage at measured substation.

C. Measured Power

Fig. 2 displays the measured power values. The induced voltage events are marked on the figure with numbers from 1 to 6. In addition to the induced voltage changes introduced in Section III-B, one of the wind turbines reacted to the voltage changes with time delay, causing changes in generated power. The wind turbine responses are marked in Fig. 2 by letters *a*, *b*, *c*, and *d*. At *a* and *c* (Fig. 2) the wind turbine disconnects, and reconnects at *b* and *d*. This causes similar power changes with opposite direction in the transformer load P_{Tran} . The load power P_{Load} includes peaks near the changes of the total output of generators P_{Gen} (marked in Fig. 2 by *a*, *b*, *c*, and *d*) due to sampling rate mismatch of the SCADA (lower sampling rate) and PQM (higher sampling rate) measurements.

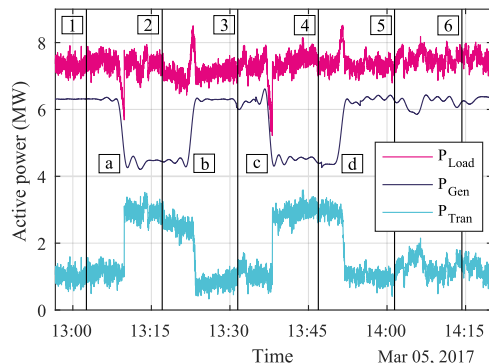


Fig. 2. Power consumed by the consumers and losses P_{Load} , load of the transformer P_{Tran} and total generated power P_{Gen} .

IV. RESULTS AND ANALYSIS

The load models of the connected load (consumed by consumers and system losses), and aggregated transformer load (includes connected load and distributed generation) were estimated for each induced voltage disturbance. The estimated ZIP models, and event modelling error of the estimated model are presented in Table I. According to the estimation error values (MAE and MSE), the models have a better fit for event 1, 5, and 6, compared to events 2...4. Mostly (in case of 5 out

TABLE I
ESTIMATED ZIP LOAD MODELS

Event	Load					Transformer Load				
	$K_{pz,L}$	$K_{pi,L}$	$K_{pp,L}$	MSE ($\cdot 10^{-3}$)	MAE	$K_{pz,T}$	$K_{pi,T}$	$K_{pp,T}$	MSE ($\cdot 10^{-2}$)	MAE
1	0.38	-0.02	0.65	0.19	0.010	4.31	-3.40	0.09	1.87	0.10
2	-8.32	17.66	-8.33	32.43	0.122	-8.69	20.00	-10.31	4.82	0.16
3	4.71	-8.77	5.06	7.85	0.074	-5.36	20.00	-13.64	10.03	0.26
4	10.49	-20.00	10.51	40.50	0.170	10.83	-20.00	10.17	3.76	0.16
5	1.32	-2.05	1.73	0.30	0.014	-2.46	13.61	-10.15	6.67	0.20
6	2.07	-3.09	2.02	0.17	0.011	4.61	-1.44	-2.17	0.47	0.05

of 6 events), the purely load fitted better with ZIP model than the measured transformer load.

In [21] the same measurement data was analysed and exponential load models were estimated based on each event. Table II depicts the acquired results. Compared to the estimated ZIP models shown in Table I more consistent estimation errors can be observed in Table II. The estimated models of the 1st event have nearly identical estimation error, while the largest differences occur for events 2...4. Mostly, the estimation error of estimated ZIP models is higher in Table I than estimation error of exponential models in Table II. All the MSE values and 10 out of 12 MAE values are higher for ZIP models compared to exponential models. These results indicate a better fit of estimated exponential models compared to the estimated ZIP models. This result is contradicting to the results of [13], where it was found that ZIP models could be more accurate.

TABLE II
ESTIMATED EXPONENTIAL LOAD MODELS [21]

Event	Load			Transformer Load		
	$K_{pv,L}$	MSE ($\cdot 10^{-5}$)	MAE	$K_{pv,T}$	MSE ($\cdot 10^{-3}$)	MAE
1	0.74	17	0.011	5.11	19	0.105
2	1.24	10	0.008	2.92	1.9	0.034
3	0.79	14	0.009	8.11	14	0.093
4	0.62	9.9	0.008	1.30	1.3	0.030
5	0.65	8.1	0.008	7.64	11	0.084
6	1.03	4.7	0.006	8.15	3.5	0.046

The estimated models of the 1st event have nearly identical estimation error in Table I and Table II. This means that both ZIP and exponential model should be able to model this voltage change with similar accuracy. As the load models have similar fit, this event is valuable for comparing how well (8) and (10) can predict the apparent transformer load, based on the load model of the aggregate of the connected loads and the total output power of the DG units. The calculated transformer load models (calculated by using (8) and (10)) display a similar estimation error in Table III. Furthermore, the event modelling error is comparable to the estimated transformer load model errors of Table I and Table II. This indicates that (8) and (10) can be used for assessing the impact of DG on exponential and ZIP model, respectively. However, the rest of the errors of calculated ZIP load models in Table III indicate that the

result is as good as the estimated models of the connected loads (without DG): if the estimated load models have high error (as in case of 2nd to 4th event), the calculated value based on these will also have a high modelling error. The errors of exponential load model have more consistent values also in Table III, all with comparable errors to the estimated load models of transformer load (Table II).

TABLE III
TRANSFORMER LOAD MODELLING BY CALCULATED LOAD MODEL
(BASED ON DG PENETRATION AND THE MODEL OF THE CONNECTED LOAD)

Event	ZIP		Exponential	
	MSE	MAE	MSE	MAE
1	0.020	0.11	0.019	0.11
2	0.286	0.36	0.002	0.03
3	1.156	0.76	0.018	0.10
4	0.160	0.35	0.001	0.03
5	0.019	0.11	0.015	0.10
6	0.004	0.05	0.004	0.05

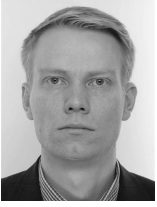
V. CONCLUSION

This paper presented the results of a case study, which was conducted in a medium voltage distribution system with high penetration of distributed generation. The objective of the case study was to assess how the penetration of DG affects the estimated static load models of the aggregate load of the transformer. Voltage disturbances were induced by on-load tap changer to estimate the load models for the bus load by measurement-based load modelling approach. The load models were estimated for both, the aggregate of the connected loads (consumers and system losses) and transformer load (combination of aggregated loads and distributed generation). The estimation error of exponential and ZIP model was compared. The exponential load model displayed lower and more consistent estimation error than the ZIP model. Thus, in this case study the exponential load model was more suitable for modelling the loads. An equation was presented in this paper for describing the impact of DG on the ZIP load model (which describes an aggregated load that includes DG). The transformer net load models were calculated by using the presented equation, load model of the aggregated load (sum of consumers and system losses),

and the output of DG. The calculated values of the load models displayed similar accuracy to the estimated models. Thus, the derived equation was suitable for describing the impact of DG on ZIP load models. Similar results were achieved for equation that can be used for calculating the exponential load model of transformer load (that includes DG).

REFERENCES

- [1] European Commission. (2019, Jul.) Going climate-neutral by 2050: A strategic long-term vision for a prosperous, modern, competitive and climate-neutral eu economy.
- [2] European Commission. Nearly zero-energy buildings. [Online]. Available: <https://ec.europa.eu/energy/en/topics/energy-efficiency/buildings/nearly-zero-energy-buildings>
- [3] G. D. Carne, G. Buticchi, M. Liserre, and C. Vournas, "Load control using sensitivity identification by means of smart transformer," *IEEE Transactions on Smart Grid*, vol. 9, no. 4, pp. 2606–2615, jul 2018. doi: 10.1109/tsg.2016.2614846
- [4] S. Mishra, M. Leinakse, I. Palu, and J. Kilter, "Ramping behaviour analysis of wind farms," in *2018 IEEE International Conference on Environment and Electrical Engineering and 2018 IEEE Industrial and Commercial Power Systems Europe (IEEEIC / I&CPS Europe)*, Palermo, Italy, 2018, pp. 1–5. doi: 10.1109/ieeic.2018.8493720
- [5] Z. Wang, J. Wang, B. Chen, M. M. Begovic, and Y. He, "MPC-based voltage/var optimization for distribution circuits with distributed generators and exponential load models," *IEEE Transactions on Smart Grid*, vol. 5, no. 5, pp. 2412–2420, sep 2014. doi: 10.1109/tsg.2014.2329842
- [6] Z. Wang and J. Wang, "Review on implementation and assessment of conservation voltage reduction," *IEEE Transactions on Power Systems*, vol. 29, no. 3, pp. 1306–1315, may 2014. doi: 10.1109/tpwrs.2013.2288518
- [7] T. Lawanson, R. Karandeh, V. Cecchi, and A. Kling, "Impacts of distributed energy resources and load models on conservation voltage reduction," in *2018 Clemson University Power Systems Conference (PSC)*, Charleston, SC, USA, 2018, pp. 1–6. doi: 10.1109/psc.2018.8664059
- [8] Z. Wang and J. Wang, "Time-varying stochastic assessment of conservation voltage reduction based on load modeling," *IEEE Transactions on Power Systems*, vol. 29, no. 5, pp. 2321–2328, sep 2014. doi: 10.1109/tpwrs.2014.2304641
- [9] M. Leinakse and J. Kilter, "Clustering of transmission system loads based on monthly load class energy consumptions," in *2020 21st International Scientific Conference on Electric Power Engineering (EPE)*, Prague, Czech Republic, 2020, pp. 1–6. doi: 10.1109/epe51172.2020.9269197
- [10] T. Masuta, S. Asano, and N. H. Viet, "Applicability of conservation voltage reduction to distribution networks with photovoltaic generation considering various load characteristics," in *2017 IEEE International Conference on Industrial and Information Systems (ICIIS)*, Peradeniya, Sri Lanka, 2017, pp. 1–6. doi: 10.1109/iciifs.2017.8300333
- [11] D. A. Quijano and A. P. Feltrin, "Assessment of conservation voltage reduction effects in networks with distributed generators," in *2015 IEEE PES Innovative Smart Grid Technologies Latin America (ISGT LATAM)*, Montevideo, Uruguay, 2015, pp. 393–398. doi: 10.1109/isg-la.2015.7381188
- [12] G. D. Carne, M. Liserre, and C. Vournas, "On-line load sensitivity identification in LV distribution grids," *IEEE Transactions on Power Systems*, vol. 32, no. 2, pp. 1570–1571, mar 2017. doi: 10.1109/tpwrs.2016.2581979
- [13] M. S. Hossain, H. M. M. Maruf, and B. Chowdhury, "Comparison of the ZIP load model and the exponential load model for CVR factor evaluation," in *2017 IEEE Power & Energy Society General Meeting*, Chicago, IL, USA, 2017, pp. 1–5. doi: 10.1109/pesgm.2017.8274490
- [14] M. Diaz-Aguilo, J. Sandraz, R. Macwan, F. de Leon, D. Czarkowski, C. Comack, and D. Wang, "Field-validated load model for the analysis of CVR in distribution secondary networks: Energy conservation," *IEEE Transactions on Power Delivery*, vol. 28, no. 4, pp. 2428–2436, oct 2013. doi: 10.1109/tpwrd.2013.2271095
- [15] M. Leinakse, H. Kapp, and J. Kilter, "Preliminary study on comparative load modelling in PSS/E and PSCAD," in *17th International Symposium "Topical Problems in the Field of Electrical and Power Engineering" and "Doctoral School of Energy and Geotechnology III"*, Kuressaare, Estonia, 2018, pp. 197–199.
- [16] M. Leinakse and J. Kilter, "Conversion error of second order polynomial ZIP to exponential load model conversion," in *Mediterranean Conference on Power Generation, Transmission, Distribution and Energy Conversion (MedPower 2018)*, Dubrovnik, Croatia, 2018. doi: 10.1049/cp.2018.1882
- [17] M. Leinakse and J. Kilter, "Exponential to ZIP and ZIP to exponential load model conversion: Methods and error," *IET Generation, Transmission & Distribution*, vol. 15, no. 2, pp. 177–193, 2021. doi: 10.1049/gtd2.12002
- [18] M. Leinakse, "Modelling aggregated load with distributed generation by exponential load model," in *2021 IEEE 62nd International Scientific Conference on Power and Electrical Engineering of Riga Technical University (RTUCON)*, Riga, Latvia, 2021, in press.
- [19] K. C. Fagen, "Distribution efficiency voltage optimization supports lowest cost new resource," in *IEEE PES General Meeting*, Providence, RI, USA, jul 2010, pp. 1–6. doi: 10.1109/pes.2010.5590142
- [20] B. Hayes and K. Tomsovic, "Conservation voltage reduction in secondary distribution networks with distributed generation and electric vehicle charging loads," in *2018 5th International Conference on Electric Power and Energy Conversion Systems (EPECS)*, Kitakyushu, Japan, apr 2018, pp. 1–6. doi: 10.1109/epecs.2018.8443502
- [21] M. Leinakse, P. Tani, and J. Kilter, "Impact of distributed generation on estimation of exponential load models," in *2019 IEEE Power & Energy Society General Meeting (PESGM)*, Atlanta, GA, USA, 2019, pp. 1–5. doi: 10.1109/PESGM40551.2019.8974014
- [22] I. R. Navarro, "Dynamic power system load – estimation of parameters from operational data," Ph.D. dissertation, Dept. Industrial Electrical Engineering and Automation, Lund Univ., Lund, Sweden, 2005.
- [23] M. Leinakse, H. Kiristajta, and J. Kilter, "Identification of intra-day variations of static load characteristics based on measurements in high-voltage transmission network," in *2018 IEEE PES Innovative Smart Grid Technologies Conference Europe (ISGT Europe 2018)*, Sarajevo, Bosnia-Herzegovina, 2018, pp. 1–6. doi: 10.1109/ISGTEurope.2018.8571712
- [24] S. A. Arefifar and W. Xu, "Online tracking of voltage-dependent load parameters using ULTC created disturbances," *IEEE Transactions on Power Systems*, vol. 28, no. 1, pp. 130–139, feb 2013. doi: 10.1109/tpwrs.2012.2199336
- [25] W. Freitas and L. C. P. da Silva, "A discussion about load modeling by using voltage variations," in *2012 IEEE 15th International Conference on Harmonics and Quality of Power*, Hong Kong, China, jun 2012, pp. 40–44. doi: 10.1109/ichqp.2012.6381271
- [26] M. Leinakse, T. Sarnet, T. Kangro, and J. Kilter, "First results on load model estimation using digital fault recorder measurements," in *16th International Symposium "Topical Problems in the Field of Electrical and Power Engineering" and "Doctoral School of Energy and Geotechnology III"*, Pärnu, Estonia, 2017, pp. 101–105.
- [27] M. Leinakse and J. Kilter, "Processing and filtering digital fault recorder events for load model estimation," in *2021 IEEE PES Innovative Smart Grid Technologies Conference Europe (ISGT Europe 2021)*, Espoo, Finland, 2021, pp. 1–5, in press.
- [28] Y. Zhu and J. V. Milanovic, "Automatic identification of power system load models based on field measurements," *IEEE Transactions on Power Systems*, vol. 33, no. 3, pp. 3162–3171, may 2018. doi: 10.1109/tpwrs.2017.2763752
- [29] Tushar, S. Pandey, A. K. Srivastava, P. Markham, and M. Patel, "Online estimation of steady-state load models considering data anomalies," *IEEE Transactions on Industry Applications*, vol. 54, no. 1, pp. 712–721, jan 2018. doi: 10.1109/tia.2017.2753719
- [30] M. Leinakse, "Thoughts on impact of distributed generation on estimation of exponential load models," in *19th International Symposium "Topical Problems in the Field of Electrical and Power Engineering" and "Doctoral School of Energy and Geotechnology III"*, Tartu, Estonia, 2020, pp. 161–162.



Madis Leinakse, the presenter, received his B.Sc. degree in electrical power engineering from Tallinn University of Technology (TalTech), Tallinn, Estonia, in 2012. He received M.Sc. degree in electrical engineering from KTH Royal Institute of Technology, Stockholm, Sweden, and M.Sc. degree in smart grids and buildings from Grenoble Institute of Technology (Grenoble INP), Grenoble, France, in 2015. Currently he is working as a junior researcher and pursuing his PhD degree at Department of Electrical Power Engineering and Mechatronics of

TalTech.

His main research interests include load modelling and power system measurement data processing.

Curriculum Vitae

Personal data

Name	Madis Leinakse
Date of birth	29 April 1989
Place of birth	Rakvere, Estonia
Nationality	Estonian
E-mail	madis.leinakse@taltech.ee

Education

Period	Description
2015 — 2022	Tallinn University of Technology, Electrical Power Engineering, PhD
2015 — 2021	Tallinn University of Technology, Estonian Centre for Engineering Pedagogy, Engineering Education Training according to IGIP Curriculum
2014 — 2015	Grenoble Institute of Technology (Grenoble INP), Smart Grids and Buildings (<i>Réseaux et Bâtiments Intelligents</i>), MSc
2013 — 2015	KTH Royal Institute of Technology, Smart Electrical Networks and Systems, MSc
2008 — 2012	Tallinn University of Technology, Electrical Power Engineering, BSc (<i>Cum Laude</i>)

Professional employment

Period	Description
2017 — 2022	Tallinn University of Technology, School of Engineering, Department of Electrical Power Engineering and Mechatronics, Junior Researcher
2016 — 2017	Tallinn University of Technology, Faculty of Power Engineering, Department of Electrical Power Engineering, Junior Researcher
2015 — 2016	Tallinn University of Technology, Faculty of Power Engineering, Department of Electrical Power Engineering, Engineer
2015 — 2015	Laboratoire de Génie Electrique de Grenoble (G2Elab), Trainee
2011 — 2013	ABB AS, Pre-Sales Support Engineer
2011 — 2011	ABB AS, Final Control
2010 — 2010	Eesti Energia Võrguehitus AS, Power Grid Development Specialist Trainee

Honours, awards and scholarships

Year	Description
2021	Dora Plus short-term mobility scholarship for participating on conference "2021 IEEE PES Innovative Smart Grid Technologies Conference Europe (ISGT Europe)", Haridus- ja Noorteamet
2020	Dora Plus short-term mobility scholarship for participating on conference "21st International Scientific Conference on Electric Power Engineering 2020 (EPE 2020)", Haridus- ja Noorteamet
2019	City Council Scholarship, City of Tallinn
2019	Dora Plus short-term mobility scholarship for participating on conference "2019 Power & Energy Society General Meeting (PESGM)", SA Archimedes
2018	Dora Plus short-term mobility scholarship for participating on conference "2018

- IEEE PES Innovative Smart Grid Technologies Conference Europe (ISGT Europe)", SA Archimedes
- 2018 Dora Plus short-term mobility scholarship for participating on conference "2018 IEEE International Conference on Environment and Electrical Engineering and 2018 IEEE Industrial and Commercial Power Systems Europe (IEEEIC / I&CPS Europe)", SA Archimedes
- 2018 Dora Plus short-term mobility scholarship for participating in DTU CEE summer school "Modern Optimization in Energy", SA Archimedes
- 2017 Madis Leinakse, Supervisor of Henry Kapp's BSc thesis "Comparative load modelling with PSCAD and PSS/E", which won 3rd prize (among Natural Sciences and Engineering BSc theses) at Estonian National Contest for University Students, Estonian Research Council
- 2017 TTÜ Development Fund, Mati Jostov scholarship
- 2017 Best Presenter Award in Electrical Power Engineering, 16th International Symposium "Topical Problems in the Field of Electrical and Power Engineering"
- 2016 Jaan Poska Scholarship, City of Tallinn
- 2013 Excellence Scholarship, European Institute of Innovation and Technology
- 2010 ABB AS Bachelor's Scholarship, ABB AS & TTÜ Development Fund

Defended theses

- "Development of distribution system state estimator algorithms," M.Sc. thesis, ENSE3, Grenoble INP, Grenoble, France, 2015. Supervisors Dr. Selle Toure and Prof. Raphael Caire.
- "Elektrienergia kvaliteedi mõõtmine analüsaatoriga Chauvin Arnoux C.A 8352" (Analysis of electrical power quality with electrical network analysis instrument Chauvin Arnoux C.A 8352), Dept. Electrical Power Engineering, Tallinn University of Technology, 2012. Supervisor Jaan Niitsoo.

Papers and technical reports published during PhD studies:

1. Ü. Treufeldt, M. Leinakse, U. Salumäe, T. Sarnet, M. Meldorf, J. Kilter, A. Reinson, and I. Drovtar, "Eesti elektrisüsteemi ülekandevõrgu koormuste staatilised ja dünaamilised karakteristikud. Uurimistöö 1.1-4/2015/227 / Lep 15066 I etapi lõpparuanne," Tallinn University of Technology, Tech. Rep., 2015, (In Estonian)
2. Ü. Treufeldt, M. Leinakse, U. Salumäe, T. Sarnet, M. Meldorf, J. Kilter, A. Reinson, I. Matjas, and K. Krusell, "Eesti elektrisüsteemi ülekandevõrgu koormuste staatilised ja dünaamilised karakteristikud. Uurimistöö 1.1-4/2015/227 / Lep 15066 II etapi lõpparuanne," Tallinn University of Technology, Tech. Rep., 2016, (In Estonian)
3. M. Leinakse, T. Sarnet, T. Kangro, and J. Kilter, "First results on load model estimation using digital fault recorder measurements," in *16th International Symposium "Topical Problems in the Field of Electrical and Power Engineering" and "Doctoral School of Energy and Geotechnology III"*, Pärnu, Estonia, 2017, pp. 101–105
4. Ü. Treufeldt, M. Meldorf, M. Leinakse, T. Sarnet, U. Salumäe, J. Kilter, and A. Reinson, "Eesti elektrisüsteemi ülekandevõrgu koormuste staatilised ja dünaamilised karakteristikud. Uurimistöö 1.1-4/2015/227 / Lep 15066 lõpparuanne," Tallinn University of Technology, Tech. Rep., 2017, (In Estonian)

5. S. Mishra, M. Leinakse, and I. Palu, "Wind power variation identification using ramping behavior analysis," *Energy Procedia*, vol. 141, pp. 565–571, 2017, doi: 10.1016/j.egypro.2017.11.075
6. M. Leinakse, H. Kapp, and J. Kilter, "Preliminary study on comparative load modelling in PSS/E and PSCAD," in *17th International Symposium "Topical Problems in the Field of Electrical and Power Engineering" and "Doctoral School of Energy and Geotechnology III"*, Kuressaare, Estonia, 2018, pp. 197–199
7. I. Palu, M. Leinakse, Ü. Treufeldt, M. Meldorf, T. Sarnet, J. Šuvalova, K. Kull, U. Salumäe, A. Avingu, and T. Trummal, "Reaktiivvõimsuse kompenseerimine Eesti elektrisüsteemis. Iep 17056 lõpparuanne," Tallinn University of Technology, Tech. Rep., 2018, (In Estonian)
8. M. Leinakse and J. Kilter, "Conversion error of exponential to second order polynomial ZIP load model conversion," in *2018 IEEE International Conference on Environment and Electrical Engineering and 2018 IEEE Industrial and Commercial Power Systems Europe (EEEIC / I&CPS Europe)*, Palermo, Italy, Jun. 2018, pp. 1–5, doi: 10.1109/eeeic.2018.8493667
9. S. Mishra, M. Leinakse, I. Palu, and J. Kilter, "Ramping behaviour analysis of wind farms," in *2018 IEEE International Conference on Environment and Electrical Engineering and 2018 IEEE Industrial and Commercial Power Systems Europe (EEEIC / I&CPS Europe)*, Palermo, Italy, Jun. 2018, pp. 1–5, doi: 10.1109/eeeic.2018.8493720
10. M. Leinakse, H. Kiristaja, and J. Kilter, "Identification of intra-day variations of static load characteristics based on measurements in high-voltage transmission network," in *2018 IEEE PES Innovative Smart Grid Technologies Conference Europe (ISGT Europe 2018)*, Sarajevo, Bosnia-Herzegovina, 2018, pp. 1–6, doi: 10.1109/ISGTEurope.2018.8571712
11. M. Leinakse and J. Kilter, "Conversion error of second order polynomial ZIP to exponential load model conversion," in *Mediterranean Conference on Power Generation, Transmission, Distribution and Energy Conversion (MedPower 2018)*, Dubrovnik, Croatia, 2018, doi: 10.1049/cp.2018.1882
12. M. Leinakse, "Thoughts on conversion of static load models," in *18th International Symposium "Topical Problems in the Field of Electrical and Power Engineering" and "Doctoral School of Energy and Geotechnology III"*, Toila, Estonia, 2019, pp. 187–188
13. M. Leinakse, P. Tani, and J. Kilter, "Impact of distributed generation on estimation of exponential load models," in *2019 IEEE Power & Energy Society General Meeting (PESGM)*, Atlanta, GA, USA, 2019, pp. 1–5, doi: 10.1109/PESGM40551.2019.8974014
14. M. Leinakse, "Thoughts on impact of distributed generation on estimation of exponential load models," in *19th International Symposium "Topical Problems in the Field of Electrical and Power Engineering" and "Doctoral School of Energy and Geotechnology III"*, Tartu, Estonia, 2020, pp. 161–162
15. M. Leinakse and J. Kilter, "Clustering of transmission system loads based on monthly load class energy consumptions," in *2020 21st International Scientific Conference on Electric Power Engineering (EPE)*, Prague, Czech Republic, Oct. 2020, pp. 1–6, doi: 10.1109/epe51172.2020.9269197

16. M. Leinakse and J. Kilter, "Exponential to ZIP and ZIP to exponential load model conversion: Methods and error," *IET Generation, Transmission & Distribution*, vol. 15, no. 2, pp. 177–193, 2021, doi: 10.1049/gtd2.12002
17. M. Leinakse and J. Kilter, "Processing and filtering digital fault recorder events for load model estimation," in *2021 IEEE PES Innovative Smart Grid Technologies Europe (ISGT Europe)*, Espoo, Finland, Oct. 2021, pp. 01–05, doi: 10.1109/isgteurope52324.2021.9640026
18. M. Leinakse, G. Andreesen, P. Tani, and J. Kilter, "Estimation of exponential and ZIP load model of aggregated load with distributed generation," in *2021 IEEE 62nd International Scientific Conference on Power and Electrical Engineering of Riga Technical University (RTUCON)*, Riga, Latvia, 2021, to be published
19. M. Leinakse, "Modelling aggregated load with distributed generation by exponential load model," in *2021 IEEE 62nd International Scientific Conference on Power and Electrical Engineering of Riga Technical University (RTUCON)*, Riga, Latvia, 2021, to be published
20. S. Mishra, C. Bordin, M. Leinakse, F. Wen, R. Howlett, and I. Palu, *Handbook of Smart Energy Systems*. Springer Nature, 2022, ch. Scope and overview of virtual power plants with integrated energy systems, to be published

BSc theses supervised during PhD studies:

- S. Rõigas, "Modelling of aggregated commercial and public services loads with PSCAD," B.Sc. thesis, Dept. Electrical Power Engineering and Mechatronics, Tallinn University of Technology, 2017, (In Estonian).
- H. Kapp, "Comparative load modelling with PSCAD and PSS/E," B.Sc. thesis, Tallinn University of Technology, 2017, (In Estonian).
- H. Kiristaja, "Identification of intra-day variations of static load characteristics," B.Sc. thesis, Dept. Electrical Power Engineering and Mechatronics, Tallinn University of Technology, 2018, (In Estonian).
- T. Pihlak, "Determining frequency of rapid voltage changes in continuous measurement data," B.Sc. thesis, Dept. Electrical Power Engineering and Mechatronics, Tallinn University of Technology, 2020, (In Estonian).
- I. Nigul, "Development of test system for ACX580-07 frequency converters," B.Sc. thesis, Dept. Electrical Power Engineering and Mechatronics, Tallinn University of Technology, 2021, (In Estonian).

MSc theses supervised during PhD studies:

- R. Aavik, "Modelling of induction motors in PSCAD network calculations," M.Sc. thesis, Dept. Electrical Power Engineering and Mechatronics, Tallinn University of Technology, 2017, (In Estonian).
- E. Karin, "Modelling of voltage characteristics of domestic load components in PSCAD," M.Sc. thesis, Dept. Electrical Power Engineering and Mechatronics, Tallinn University of Technology, 2017, (In Estonian).

- S. Sorts, "Researching frequency dependence of Estonian electrical system load classes," M.Sc. thesis, Dept. Electrical Power Engineering and Mechatronics, Tallinn University of Technology, 2017, (In Estonian).
- P. Tani, "Influence of distributed generation on the aggregated load models of the bus loads," M.Sc. thesis, Dept. Electrical Power Engineering and Mechatronics, Tallinn University of Technology, 2017, (In Estonian).

Elulookirjeldus

1. Isikuandmed

Nimi	Madis Leinakse
Sünniaeg	29.04.1989
Sünnikoht	Rakvere, Eesti
Kodakondsus	Eesti
E-post	madis.leinakse@taltech.ee

Haridus

Periood	Kirjeldus
2015 — 2022	Tallinna Tehnikaülikool, Inseneriteaduskond, Elektroenergeetika, Filosoofiadoktor
2015 — 2021	Tallinna Tehnikaülikool, Eesti Inseneripedagoogika keskus, Inseneripedagoogika täiendusõppekava õppejõududele
2014 — 2015	Grenoble Polütehniline Instituut (Grenoble INP), Targad võrgud ja hooned (<i>Réseaux et Bâtiments Intelligents</i>), Tehnikateaduse magister
2013 — 2015	Rootsi Kuninglik Tehnikaülikool (KTH), Targad elektrivõrgud ja süsteemid (<i>Smart Electrical Networks and Systems</i>), Tehnikateaduse magister
2008 — 2012	Tallinna Tehnikaülikool, Energeetika teaduskond, Elektroenergeetika, Tehnikateaduse bakalaureus (<i>Cum Laude</i>)

Teenistuskäik

Periood	Kirjeldus
2017 — 2022	Tallinna Tehnikaülikool, Inseneriteaduskond, Elektroenergeetika ja mehhatroonika instituut, Nooremteadur
2016 — 2017	Tallinna Tehnikaülikool, Energeetikateaduskond, Elektroenergeetika instituut, Energiasüsteemide õppetool, Nooremteadur
2015 — 2016	Tallinna Tehnikaülikool, Energeetikateaduskond, Elektroenergeetika instituut, Energiasüsteemide õppetool, Insener
2015 — 2015	Laboratoire de Génie Electrique de Grenoble (G2Elab) , Praktikant
2011 — 2013	ABB AS, Müügieelse tugiteenuse insener
2011 — 2011	ABB AS, Lõppkontroll
2010 — 2010	Eesti Energia Võrguehitus AS, Võrguarengu spetsialist

Teaduspreemiad, tunnustused ja stipendiumid

Aasta Kirjeldus

- 2021 Dora Pluss lühiajalise õpirände toetus osalemiseks konverentsil "2021 IEEE PES Innovative Smart Grid Technologies Conference Europe (ISGT Europe)", Haridus- ja Noorteamet
- 2020 Dora Pluss lühiajalise õpirände toetus osalemiseks konverentsil "21st International Scientific Conference on Electric Power Engineering 2020 (EPE 2020)",

Haridus- ja Noorteamet

- 2019 Raestipendium, Tallinna Linnavalitsus
- 2019 Dora Pluss lühiajalise õpirände toetus osalemiseks konverentsil "2019 IEEE Power & Energy Society General Meeting (PESGM)", SA Archimedes
- 2018 Dora Pluss lühiajalise õpirände toetus osalemiseks konverentsil "2018 IEEE PES Innovative Smart Grid Technologies Conference Europe (ISGT Europe)", SA Archimedes
- 2018 Dora Pluss lühiajalise õpirände toetus osalemiseks konverentsil "2018 IEEE International Conference on Environment and Electrical Engineering and 2018 IEEE Industrial and Commercial Power Systems Europe (IEEEIC / I&CPS Europe)", SA Archimedes
- 2018 Dora Pluss lühiajalise õpirände toetus osalemiseks DTU CEE suvekoolis "Modern Optimization in Energy", SA Archimedes
- 2017 Eesti Teadusagentuuri üliõpilaste teadustööde konkursi 3. preemia (loodusteaduste ja tehnika valdkonnas rakenduskõrgharidus ja bakalaureuseõppe üliõpilaste astmes) saanud Henry Kapp'i bakalaureusetöö „Koormuste modelleerimise erinevused tarkvarades PSCAD ja PSS/E” juhendaja
- 2017 Mati Jostovi nimeline stipendium, TTÜ Arengufond
- 2017 Parim elektroenergeetika ettekanne, 16. Rahvusvaheline sümposium "Topical Problems in the Field of Electrical and Power Engineering"
- 2016 Elering AS stipendium
- 2016 Jaan Poska nimeline stipendium, Tallinna Linnavalitsus
- 2013 Euroopa Innovatsiooni- ja Tehnoloogiainstituudi tasemeõppe stipendium
- 2010 ABB AS bakalaureuseõppe stipendium, TTÜ Arengufond / ABB AS

Kaitstud lõputööd

- "Development of distribution system state estimator algorithms (Jaotusvõrgu talitusparameetrite estimateerimisalgoritmide arendamine)," Magistritöö, ENSE3, Grenoble INP, Grenoble, Prantsusmaa, 2015. Juhendajad Dr. Selle Toure ja Prof. Raphael Caire.
- "Elektrienergia kvaliteedi mõõtmise analüsaatoriga Chauvin Arnoux C.A 8352," Bakalaureusetöö, Elektroenergeetika instituut, Tallinna Tehnikaülikool, Tallinn, Eesti, 2012. Juhendaja Jaan Niitsoo.

Doktoriõpingute käigus juhendatud bakalaureusetööd:

- S. Rõigas, "Äri ja avaliku teeninduse sektori agregeeritud koormuste modelleerimine tarkvaras PSCAD," Bakalaureusetöö, Tallinna Tehnikaülikool, 2017.
- H. Kapp, "Koormuste modelleerimise erinevused tarkvarades PSCAD ja PSS/E," Bakalaureusetöö, Tallinna Tehnikaülikool, 2017.
- H. Kiristaja, "Koormuse staatiliste pingekarakteristikute ööpäeva-sisese muutlikkuse katseline määramine," Bakalaureusetöö, Tallinna Tehnikaülikool, 2018.
- T. Pihlak, "Kiirete pingemuutuste esinemissageduse määramine pidevmõõteandmetes," Bakalaureusetöö, Tallinna Tehnikaülikool, 2020.
- I. Nigul, "ACX580-07 sagedusmuundurite testsüsteemi arendamine," Bakalaureusetöö, Tallinna Tehnikaülikool, 2021.

Doktoriõpingute käigus juhendatud magistritööd:

- R. Aavik, "Asünkroonmootorite modelleerimine PSCAD tarkvara võrguarvutustes," Magistritöö, Tallinna Tehnikaülikool, 2017.
- E. Karin, "Kodutarbijate tüüpkoormusseadmete pingekarakteristikute modelleerimine tarkvaraga PSCAD," Magistritöö, Tallinna Tehnikaülikool, 2017.
- S. Sorts, "Eesti elektrisüsteemi põhivõrgu koormusklasside sagedussõltuvuste uurimine," Magistritöö, Tallinna Tehnikaülikool, 2017.
- P. Tani, "Hajatootjate mõju agregeeritud sõlmekoormustele," Magistritöö, Tallinna Tehnikaülikool, 2017.

Teadustegevus

Teadusartiklite, konverentsiteeside ja konverentsiettekannete loetelu on esitatud ingliskeelse elulookirjelduse juures.

ISSN 2585-6901 (PDF)
ISBN 978-9949-83-793-9 (PDF)